Intra-crystalline amino acids in deep-sea corals: a first look at organic skeletal controls

Lydia Crampton

MSc (by research)

University of York

Environment and Geography

March 2025

Abstract

Deep-sea corals are found in oceans around the world. However, there are emerging environmental challenges, like ocean acidification and climate change, that could threaten deep-sea corals. Previous research into deep-sea corals and how they respond to environmental change has been focused on biogeographic habitat mapping and paleoclimate work, exploring their environmental history using their skeletal remains. Most of this research has focused on inorganic geochemistry – including dating and trace metal and isotopic compositions. Despite the potential importance of biomineralisation in calcifying corals, there is no existing information on the amino acid composition of deep-sea corals.

This study is the first analysis of amino acids in deep-sea corals, helping to fill this knowledge gap. Using ultra-high-performance liquid chromatography (UHPLC), intra-crystalline amino acids were extracted from two groups of deep-sea corals - stylasterids and Scleractinia. One hundred and thirty-six deep-sea corals were analysed from eight locations. First, the analytical and preparative reproducibility were assessed. Then the internal heterogeneity was established, showing that some coral tips have lower total hydrolysable amino acid concentration (THAA) than branch sections. Overall, high levels of acidic amino acids (such as aspartic acid and glutamic acid) support previous findings of coral acid-rich proteins found within shallow water corals. Amino acid differences were observed between stylasterid and scleractinian corals, with further differences between aragonitic and calcitic stylasterid corals.

The new amino acid data was also compared to co-located hydrographic data, (aragonite saturation, pH, dissolved inorganic carbon, temperature and salinity). This comparison indicated that coral amino acids may be influenced by some environmental conditions. Two clear correlations were found: (i) THAA increased with decreasing pH within the scleractinian coral (*Caryophyllia),* and (ii), the percentage of aspartic acid was higher in stylasterid corals living in water that was undersaturated in aragonite compared to saturated conditions.

Together, these are the first THAA data from deep-sea corals and show variations of amino acids between genera, mineralogies and correlations with environmental parameters.

Declaration

I declare that the work presented within this thesis is original work of which I am the sole author. This work has not previously been presented for a degree or other qualifications at the University of York or elsewhere. All sources of information are acknowledged as references.

Acknowledgements

I want to start by thanking Professor Laura Robinson and Professor Kirsty Penkman for giving me the opportunity to submerge myself in this new challenge. You have both given me guidance, support and advice that I will hold onto way after this project. As well as a new insight into how research is a passion built from a core desire to continuously educate and inspire, something you both radiate. My love for the deep sea has grown tenfold and I will never stop telling people about the work I have done to explore this mysterious environment and what you both did to help me achieve this.

Thank you also to deep-sea coral icons: Joe, Ana, James and Jess, who allowed me to ask all the questions I needed to try to piece things together. Especially Joe for picking, from my experimental requests, a great selection of beautiful corals. Thanks for access to specimens from the Muséum National d'Histoire Naturelle (MNHN, Paris) was funded by a SYNTHESYS+ grant awarded to James Kershaw, facilitated by Magalie Castelin (Cnidaria curator) and Jonathan Blettery (SYNTHESYS+). MNHN Paris specimens were obtained during research cruise SPANBIOS, organised by the MNHN and the Institut de Recherche pour le Développement as part of the Tropical Deep-Sea Benthos program. We are grateful to the cruise leader, Sarah Samadi. Daniela Pica provided taxonomic identifications for these samples. Gerald R. Hoff, Meredith Everett and Peter Etnoyer are acknowledged for providing samples from the NOAA Alaska Deep-sea Coral and Sponge Initiative, which were collected during cruises F/V Alaska Provider 201601 and F/V Alaskan Leader 202001. Rachel Wilborn and Gerald R. Hoff identified these specimens. Thanks also to SAERI and Darwin Plus funds involving the South Atlantic Environment Research institute (SAERI) and British Antarctic Survey (BAS) for the four coral specimens from the Burdwood Bank. Thank you to Narissa Bax for the CITES organisation and for providing the specimens for study in the UK, and for the species identifications. Thank you also to the Falkland Islands Fisheries Department for providing bycatch samples.

I also definitely need to thank Ellie for letting me pester you with amino questions while I learned this new field. Furthermore, I would like to thank my parents, my aunt and my nan for always having the ability to believe in me even when I did not do so myself. The interest you all showed in my work always made me feel like I had achieved something extraordinary each and every day. Ruben, you, too, deserve acknowledgement for your unfaltering support, something that I would have struggled without this year. You really

are the kindest person I know. Finally, to Freya, who would make me laugh no matter what my day had been like and is the best friend anyone could ask for.

Just remember, even when the chromatogram is blank, aminos are out there!
– Myself during the first run of deep-sea corals.

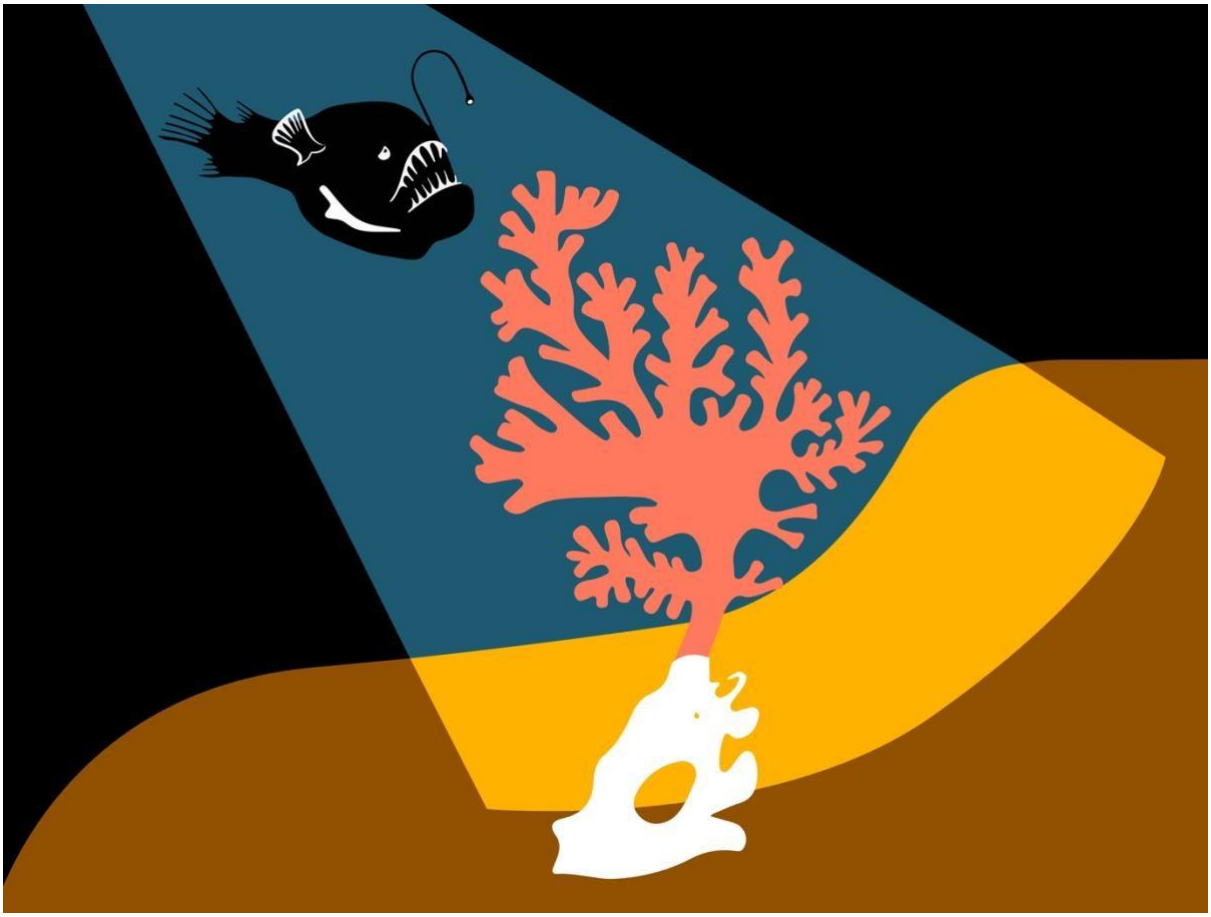

Art piece commissioned from Hannah Grahamslaw

Table of Contents

1 Chapter - 1 Introduction

1.1 Deep-sea Corals

Deep-sea corals (also often referred to as cold-water corals) are a varied group of animals that live in and below the mesopelagic zone located at 200m (below sea level) (Robinson *et al*, 2010). Deep-sea corals are defined as animals that fit within the grouping of the Cnidarian classes Anthozoa and Hydrozoa. They produce either calcium carbonate (aragonitic or calcitic) secretions forming a continuous skeleton or as multiple, usually microscopic, individual sclerites. Some have a black, proteinaceous axis, although no proteinaceous corals were sampled within this study. The description of deep-sea corals was aquired from descriptions found in Cairns (2007). They differ from shallow-water corals as they do not require sunlight or warm tropical water. Possessing no symbiotic relationship with algae to produce food, deep-sea corals are reliant on 'marine snow'. Marine snow is an accumulation of dead marine organisms, faecal matter and other organic and inorganic material that is produced by surface water plankton and subsequently falls through the water column to deeper levels (Alldredge *et al*, 1988).

There are challenges for calcifying corals to live in certain areas - such as in low oxygen minimum zones and in areas that are undersaturated with respect to aragonite. However, deep-sea corals have been observed across the global oceans even within these areas (Brooke *et al*., 2013, Li *et al*., 2023, Stewart *et al*., 2022). One of the major focuses of the research is understanding how these corals can live
within these zones and to begin understanding the inorganic biomineralising mechanisms of deep-sea coral skeletons. Organic biomolecules (including proteins) have also been shown to be a crucial part of biomineralisation. The interaction between organic molecules and calcium carbonate secretion highlights the importance of biological control involved in deep-sea coral survival, but to date, very few studies of the protein composition of deep-sea coral skeletons have been undertaken.

With rapid environmental change caused by anthropogenic factors, it is more crucial than ever to understand how these corals will be impacted. Anthropogenic climate change first made its mark from the Industrial Revolution, where more fossil fuels were being burned to sustain new technology and machinery (Martinez, 2005). This burning of fossil fuels added more greenhouse gases to the atmosphere, changing its chemical composition. In turn the oceans chemical composition also changed, leading to a process of ocean acidification,

causing pressures for the biomineralisation of calcium carbonate producing animals, like coral (Höök and Tang, 2013). The IPCC (intergovernmental pannel on climate change) report that has looked at the impacts for global warming above 1.5°C5oc in 2019, has indicated that even if temperatures are restrained to this 1.5°C 5oc limit, 70-90% of shallow water reefs will be lost (IPCC, 2019) This prediction only includes tropical shallow water corals, so what will the impact be to deep-water species?

Two contrasting deep-sea carbonate-producing coral groups are therefore targeted within this study, Scleractinia corals (section 1.2) and *Stylasteridae* (section 1.3). The correlation of the two different corals is shown within figure 1.1 (Chapter 1, page 9).

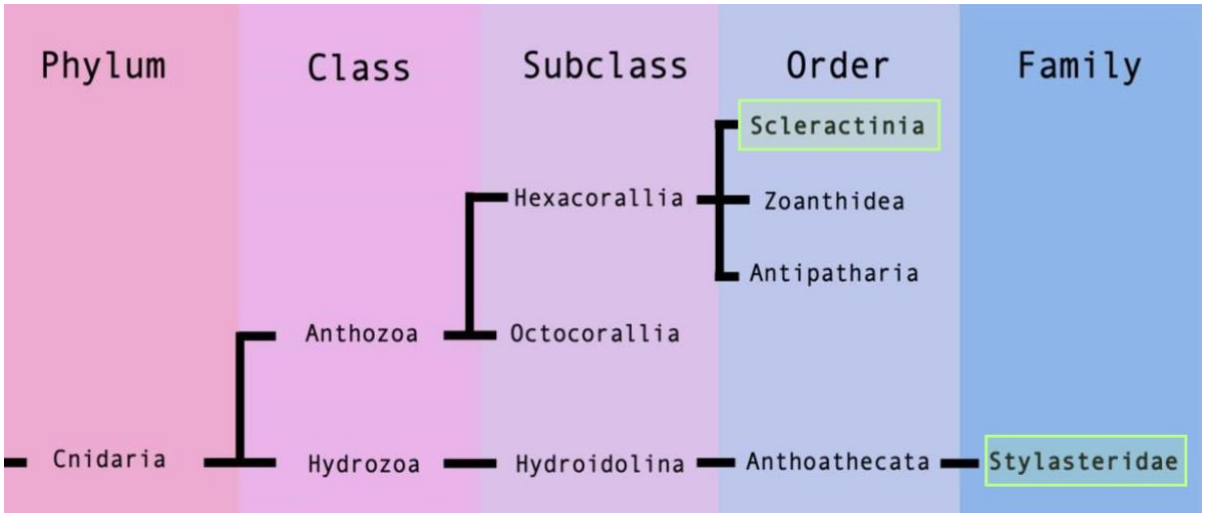

Figure 1.1, A targeted phylogenetic tree showing the relationship between stylasterid corals and scleractinian corals, following the relationship shown in Cairns (2007).

1.2 Scleractinian corals

Scleractinian corals live on deep-sea seamounts, along continental slopes and ocean canyons or plateaus across the world; they can form ecologically and biologically important reefs or gardens (Bo *et al.*, 2015). All are protected by CITES, (the convention on International Trade in Endangered Species of Wild Fauna and Flora), designed to stop animals and plants from being exploited (Bruckner, 2001). They are a particularly important taxa due to the biodiversity that comes along with the corals growing there, due to them being vulnerable marine ecosystems (Parker, Penney and Clark, 2009).

The growth rates of Scleractinia are slow, 0.2 – 1.25mm/a within *Solenosmilia variabilis*,
(e.g. Fallon, Thresher and Adkins, 2013, and Tracey et al., 2024) and within *Desmophyllum dianthus* a growth rate of 0.5 – 2mm/a (Adkins *et al.*, 2004, and Risk et al., 2002). These rates are much slower than their shallow-water reef-

forming counterparts like *Montastrea annularis* which has growth rates of 0.4-1.2cm/a (Hubbard and Scaturo, 1985, and Carricart-Ganivet, 2004).

Most cold-water Scleractinia corals precipitate aragonite (discussed below) with the exception of *Paraconotrochus antarcticus* (Stolarski *et al.*, 2020). However, within this study, only aragonite cold-water Scleractinia corals were used for observations. They include *Caryophyllia, Enallopsammia, Lophelia, Desmophyllum, Flabellum, and Vaughanella*.

The aragonite saturation horizon is the depth at which aragonite across the oceans transitions from being saturated to undersaturated. It forms the boundary at which aragonite (a form of calcium carbonate) will either dissolve or not (Hicks et al., 2025). This is crucial for animals that biomineralise with aragonite calcium carbonate, as they often will not be able to live successfully within undersaturated calcium carbonate water (Zheng and Cao, 2014). The aragonite saturation horizon changes by ocean region. Further oceanographic factors such as temperature, dissolved inorganic carbon and pressure all contribute to how deep the aragonite saturation horizon is found within these areas, and therefore how deep the aragonitic calcium carbonate-producing animals are found (Sun et al., 2021). The aragonite saturation state will shallow across the world due to climate change; for example, it is even predicted that the Southern oceans will become completely undersaturated by the end of the twenty-first century (Negrete-García et al., 2019). This shoaling of the aragonite saturation horizon has also been seen recently in the Bay of Bengal, where the shoaling reached $6.3 \pm 5\ m\ yr^{-1}$, (Sridevi and Sarma, 2024).

Despite their aragonite skeletons, deep-sea scleractinian coral have been found well below the aragonite saturation horizon, as well as in low-oxygen waters. For example, six reefs were discovered on an expedition to the northwestern Hawaiian Islands where the aragonite saturation state was as low as 0.71 (Baco *et al.*, 2017). There have been many studies conducted on cold water scleractinian corals to test their resilience to many environmental factors including aragonite saturation. Guinotte et al. (2006), began to suggest the implications of anthropogenic climate change would impact cold water scleractinia corals due to a prediction of 70% of the water where they are found to become undersaturated by 2099. A more recent study by Stewart et al. (2022) on scleractinia resilience has seen that within the calcifying fluid of these corals, they are able to upregulate the pH internally to help them biomineralise. This adaptation may be advantageous to these corals when further anthropogenic climate change takes place.

An experiment conducted by Hennige et al. (2015) over a 12-month period observed that *Lophelia pertusa,* physiologically adapted to an increased amount of pCO_2, however the structure of the aragonite crystals within the coral became weaker the further along the study went. A study later conducted by Farfan et al.

(2018), on *Lophelia pertusa,* collected from the Gulf of Mexico, observed that the mineralogy of these corals (using x-ray diffraction) showed a positive correlation between the increase of aragonite in the natural seawater to the increase in size of skeletal crystals. Further supporting the idea that these corals have stronger mineralogies in more saturated water and although can help sustain their growth processes by adaptation, may still be susceptible to anthropogenic climate change.

1.3 Stylasterid corals

The Stylasteridae family, also known as lace corals, and often shortened to stylasterids, are globally distributed and can be found from the polar regions to the tropics (Maggioni *et al*, 2022). Deep-sea stylasterids are typically found on seamounts or areas with submarine ridges, specifically away from coastal areas (Aspects *et al*, 1992). Expeditions have discovered deep-sea Stylasteridae corals from all over the world with a high numbers of species being observed within the waters of Indonesia and the Caribbean (Cairns, 2011).

Stylasterids are unusual as some can biomineralise different polymorphs of calcium carbonate: aragonite, high-Mg calcite or both. As stylasterid can precipitate both high-Mg calcite and aragonite, this could allow them to have a mechanism for resilience to surrounding environmental change. High-Mg calcite is less soluble than aragonite in modern seawater, so having a potential 'choice' of polymorph could mean that stylasterid corals have a route to biomineralize in undersaturated waters (Stewart *et al*., 2022). The mineralogy difference occurs even within a single genus, as seen in Figure 1.2, chapter 1, page 11. This leads to the possibility that stylasterid corals could be more resilient to changes caused by anthropogenic climate change, depending on the biological controls of the species.

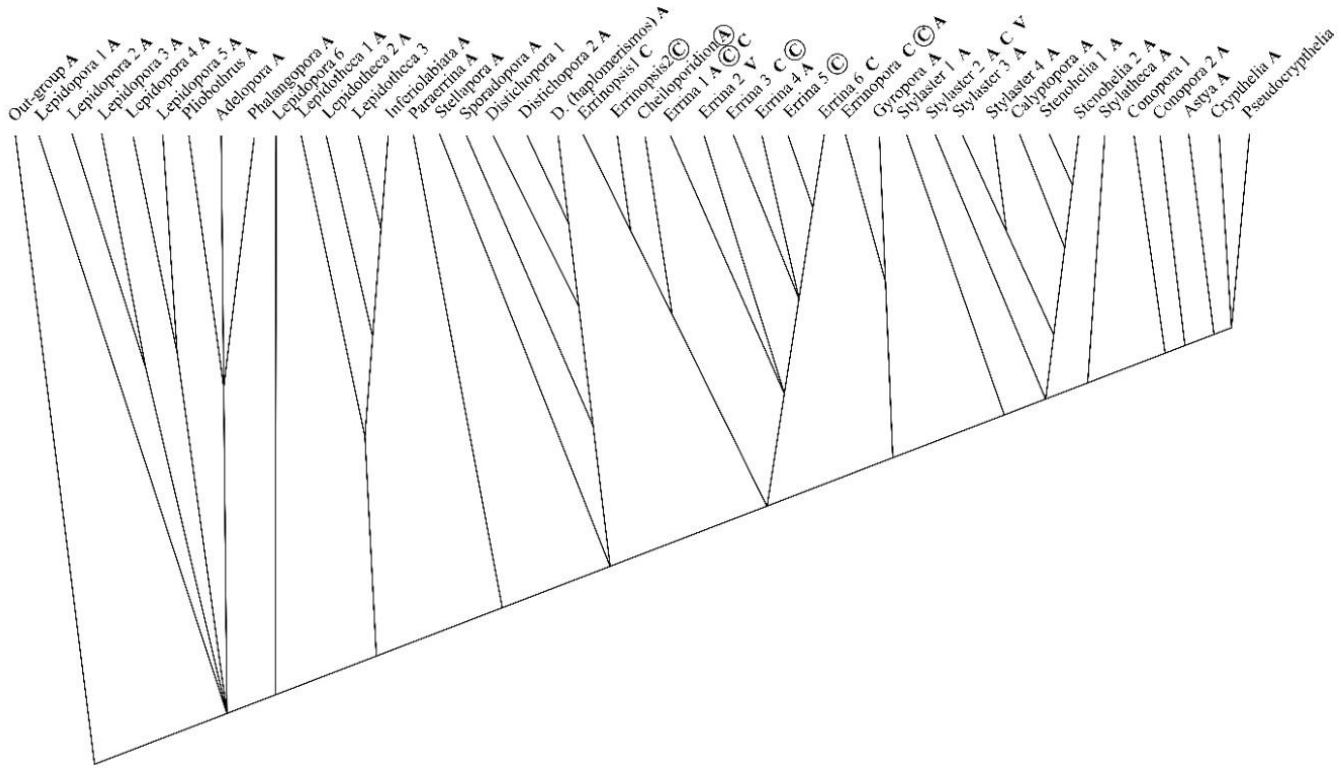

Figure 1.2, *Cladogram of stylasterid genera taken from (Samperiz. A, 2018) showing the distribution of the calcium carbonate polymorph secreted by the genus of stylasterid corals (modified from Cairns and MacIntyre (1992)).* ***A****, 100% aragonite;* ***C,*** *100% calcite;* ***(C)****, primarily aragonite with some calcite;* ***(A)****, primarily calcite with some aragonite;* ***V****, coexisting polymorphs of variable percentage. Note that this cladogram was based on Cairns* (1984)*, and it was ordered based on apparent morphological complexity. Further morphological research has shown that morphological characters exhibit high variability and are influenced by parallel evolution and therefore making them unreliable indicators of relationships between the taxa (Puce et al., 2016).*

1.4 Biomineralisation in coral

It is crucial that we understand the process of biomineralisation of deep-sea corals to help understand how they can live within conditions where we would presume them to be vulnerable. Within this study, for the first time, we take a look at potential biological controls in the form of amino acids within the two different deep-sea coral groups, stylasterids and Scleractinia. It is known that some hard corals form calcium carbonate within the organic matrix of the coral (Tambutté *et al*., 2007); this is proposed to be2007), which controlled by proteins that are high in acidic amino acids (Puverel *et al*., 2005).

It is thought that the process of producing skeletal material that is applicable in scleractinian corals starts by a secretion of the proteoglycan matrix where the minerals are secreted. The second process is deemed the “thickening stage”, produced by fibers in the ectodermal region indicating a biochemically driven process (Cuif and Dauphin, 2005). This is further supported by Von Euw *et al* (2017), who found that mineral precipitation within skeletogenesis in stony corals

is controlled by a biological process, driven by coral acid-rich proteins. Scleractinia corals also have the ability to upregulate the pH of their calcifying fluid to further aid biomineralisation in harsh environments (McCulloch *et al.*, 2012). The ability to not be restricted by external environmental factors (at least over particular ranges) is beneficial when considering the implications climate change could have. However, it is energy-demanding and therefore still makes these corals vulnerable (Gagnon *et al.*, 2021).

Biomineralisation within stylasterid corals differs from scleractinian corals, as they have not been observed to modify the pH of external seawater within their calcifying regions and are predicted to be more reliant on organic molecule controls (Stewart *et al*, 2022). Exposure to external seawater conditions while biomineralising could make stylasterids vulnerable to potential climate change implications. The exact process of biomineralisation within stylasterid corals is poorly understood, although is thought to also have a potential two-step biomineralisation process like Scleractinia corals. This includes the first stage of fast initial skeleton construction, then slower development of skeletal material infilling towards the centre of the coral (Cuif and Dauphin, 2005).

1.5 Climate change and the deep sea:

Ocean acidification is caused by an increased concentration of CO_2 within the atmosphere dissolving into the ocean. As a result the equilibrium of dissolved carbon dioxide ($CO_{2\,(aq)}$) within the ocean from atmospheric drawdown begins to form a chain equilibrium reaction, following Henrys law:

$$, CO_2\,(g) \rightleftharpoons CO_2\,(aq)$$

Once the CO_2 is dissolved into the seawater (forming hydrated co2) it reversibly reacts with water to form carbonic acid (H_2CO_3):

$$CO_2\,(aq) + H_2O \rightleftharpoons H_2CO_3 \text{ (Feely and Doney, 2011)}$$

Carbonic acid can further dissociates into bicarbonate (HCO_3^-) and then carbonate (CO_3^{2-}) ions:

$$, H_2CO_3 \rightleftharpoons HCO_3- + H+$$

$$HCO_3^- \rightleftharpoons CO_3^{2-} + H^+$$

Both dissociation reactions also form hydrogen ions (H^+), making the ocean more acidic. Hydrogen ions can also react with carbonate ions to form more bicarbonate. pH is projected to decrease by a factor of 0.4 by 2100 within global surface waters (Findlay and Turley, 2021). This dissolved carbon dioxide is a consequence of a build-up in the atmosphere caused by anthropogenic pressures like industrialisation (Hansen and Stone, 2015). Furthermore, carbon dioxide creates a greenhouse effect, retaining heat, which also increases global sea temperatures (IPCC, 2021). Warming of the oceans will impact deep-sea

coral distribution as they have limited tolerance to warmer waters (Anderson et al., 2022). This reduction of available carbonate ions for marine calcifying organisms to biomineralise means they would not be expected to be found in lower pH conditions or areas with lower carbonate ions (Turley, Roberts and Guinotte, 2007).

Warming oceans and ocean acidification cause bleaching in shallow-water tropical corals (Hoegh-Guldberg *et al.*, 2007). Bleaching is when the symbiotic relationship of the coral and a form of algae known as zooxanthellae, is disrupted due to the zooxanthellae leaving the body of the shallow water corals. A bleached coral is vulnerable to starvation if it cannot replace the algae or are exposed to extended periods of warm temperatures (Jones, 2008). However, knowledge of the impact on ocean acidification on deep-sea corals is more limited. Deeper in the water column there is typically less food available, and the carbonate chemistry (carbonate saturation, pH) conditions are less favourable for calcification (Thresher *et al.*, 2011). Ocean acidification is projected to bring further carbonate undersaturation, stretching the entire Southern Ocean and subarctic Pacific Ocean by 2030 (Hauri, Friedrich and Timmermann, 2015).

Calcium carbonate organisms, such as hard coral, found in the diverse habitats of the ocean are likely to be particularly vulnerable to pH change as the skeletons found within them will degrade and dissolve in more acidic conditions (Leung, Zhang and Connell, 2022). A study conducted on *Lophelia* by Hennige et al. (2014), showed decreasing maintenance of the calcification used to keep the skeleton strong, happened when exposed to increases of CO_2, with direct correlation to pH. Further experiments on *Lophelia* by Brooke et al. (2013), have seen a higher mortality rate at higher temperatures even after 24 hours. Both experiments indicating the vulnerability of one genus of deep-sea corals to different climate change variables. Corals within the shallow and deep oceans are currently, and will be increasingly, impacted by ocean acidification (Hoegh-Guldberg *et al.*, 2007, Andersson and Gledhill, 2013, Anthony *et al.*, 2011).

1.6 Coral acid-rich proteins

The understanding that there is a level of biochemical control within the process of biomineralisation indicates that proteins will play a role in this process (Falini, Fermani and Goffredo, 2015). It is known that coral acid-rich proteins (CARPs) within certain corals regulate the formation of crystal nucleation and therefore the calcium carbonate needed for skeletal growth (Mass. T, *et al* 2013). CARPs within scleractinian coral have been seen in corals living both above and below the aragonite saturation horizon (Laipnik *et al.*, 2020). The CARP grouping of proteins individually have different amino acid sequences but are characterised by their high levels of aspartic acid and glutamic acid (Mass *et al*, 2013). Zaquin

et al. (2021), identified a core set of proteins that are used by shallow water scleractinian corals to biomineralise, including aspartic acid-rich proteins.

As yet, there is no knowledge of what proteins are being used within deep-sea Scleractinia, or in stylasterid corals, because there have been no public measurements. However, Laipnik (2020), observed that Mg-calcite increased with CARP3 concentration when grown on an *E.coli* petri dish, but aragonite was not precipitated in low quantities of Mg by CARP3. CARP3 is a coral acid-rich protein high in aspartic/glutamic acid, which plays a key role in the up-regulationupregulation of aragonite material in the process of biomineralisation. CARP3 specifically has been seen to alter the pathways used for crystalisation *in vitro*, helping to determine the process of biomineralisation (Mass.T, 2020). This study supports the idea that biological controls must play a larger role than water chemistry alone (Stewart *et al*, 2022).

1.7 Amino Acids

Amino acids are the building blocks of proteins (Sanger, 1952) and therefore CARPs. Amino acid compositions in shallow water coral skeletons have previously been measured (e.g. Mitterer, 1976; Itzgerald and Szmant, 1997; Nyberg *et al*, 2001; Cristina Castillo Alvarez *et al*.,2024), and in some cases found to alter with environmental conditions (Gupta et al., 2006). However, there is little information on amino acid composition within deep-sea coral skeletons (Luo, Chen and Jia, 2024., Shen *et al*., 2021) particularly on a global scale. In 2021, six CARPs were characterised and had been found to have sequences with over 100 amino acids within them (Mummadisetti *et al*, 2021).

Amino acid analysis provides initial information on whether proteins are being used within coral skeletons and which amino acids predominate. Reverse-phase ultra-high-performance liquid chromatography (RP-UHPLC) will be used to find the first insight into which proteins are being used within deep-sea corals. Where protein sequences are known, the amino acid compositions can be compared to their amino acid sequences to determine which is present. Metabolic reactions are linked to amino acids as they form the basis of proteins and enzymes, which catalyse chemical reactions linked to growth (Aguilar *et al*., 2019).

1.8 Thesis Aims

This thesis focuses on the ability to measure skeletal amino acids from deep-sea corals and identify any variability of the amino acids across genera.

This study was developed to bring new insight into the skeletal amino acids of two different deep-sea coral groups. Then, comparing to environmental data to determine if deep-sea coral biological controls dominate biomineralisation. If so, could this be making them less susceptible to external factors, including climate

change? Or do environmental factors dominate the biomineralisation process? This will help us understand the potential link between amino acid concentrations/profiles and environmental data, potentially another variable used to predict future climate challenges for deep-sea corals.

This study, therefore, has three objectives:

Objective 1: Analyse deep-sea coral skeletal amino acids by RP-UHPLC and quantify sources of variability (Chapters 2 and 3)

Objective 2: Test if the skeletal amino acid composition is influenced by taxa (hypothesis 1) or mineralogy (hypothesis 2), (Chapter 4).

Objective 3: Test whether key external environmental parameters influence the skeletal amino acid composition (hypothesis 3, chapter 5)

1.8.1 Hypotheses:

Hypothesis 1. Corals of different Genera will have different amino acids.

It has been seen throughout skeletal amino acid research on corals that there are differences between the proteins and amino acids of different coral taxa and genera. Mitterer (1976) recorded the differences between several scleractinian and alcyonarian coral skeletons and also concluded that they were all dominated by aspartic acid. Therefore, it is hypothesised that deep-sea corals would also have different amino acid concentrations. Yet they could also still be dominated by aspartic acid or other acidic amino acids.

Hypothesis 2. Corals with different mineralogies will have different amino acids due to protein differences.

Conci *et al*. (2020) undertook research on scleractinian corals and octocorals with a summary that there is little overlap between the proteins seen in aragonite and calcite skeletons, therefore, the amino acids must also be different. From this, it could be inferred that there could also be differences in amino acids in deep-sea stylasterid corals precipitating different mineralogies.

Hypothesis 3. The environment will have an impact on skeletal amino acid levels

Previous amino acid analysis on shallow water corals of unpublished data by Tomiak et al. (2013) has indicated that within shallow water corals THAA increases with decreasing pH, therefore this finding should be tested on deep-sea corals. The mole%Asx (the molar percentage of aspartic acid, calculated by the amount of aspartic acid against the total amount of amino acids in a sample multiplied by 100) has been recorded to have seasonal fluctuations within the skeletons of *Porites* corals, therefore reflecting the biological activity of the coral's skeletal growth in response to environmental factors over time (Gupta, Suzuki and Kawahata, 2006). Sogin *et al*. (2016), also found that *Pocillopora damicornis* was having metabolic reactions to external environmental factors (ocean acidification and temperature changes).

2 Chapter 2 -Materials and Methods

2.1 Materials

One hundred and thirty-six individual deep-sea stylasterid and Scleractinia coral samples were analysed within this study (Table 1, Chapter 2, page 18). The samples were selected for the quality and quantity of skeletal material available. Samples with an undamaged structure and a large quantity of skeletal material were chosen. To assess a wide range of hydrographical variance, samples from a variety of depths were included (Table 1, Chapter 2, page 18). The deep-sea coral samples were also selected to include a range of genera that had previously been (or are currently being) analysed for their inorganic compositions (e.g. Kershaw 2023, Stewart *et al*. 2020, Samperiz *et al*. 2020, Robinson *et al*. 2014, Anagnostou *et al*. 2011). Inorganic geochemistry data provides information about how corals are reacting to environmental changes; this information is retained in their skeletal material. Furthermore, this understanding of how corals have previously responded to environmental parameters will help us to further understand how the corals will respond to future challenges caused by climate change.

This study only focused on amino acid composition and concentration data using modern coral samples only. Three shallow-water *Porites* corals from Thailand and Hawaii were also analysed for comparison. These samples had been previously run for unpublished amino acid data, (Hewitt, T. 2018. Amino acids in biomineralisation of coral: investigating and comparing the artificial protein degradation of *Pocillopora eydouxi* with *Porites* sp. fossil data. Unpublished BSc dissertation, University of York). Published *Porites* amino acid data previously analysed within the lab can be found by Hendy et al. (2012). Although there is little research conducted on the amino acid data of deep-sea corals, there has been research conducted on shallow-water corals making them great for comparison purposes.

Sampling location	No of Samples (Individual corals)	Genera	Depth range (m)
South Orkney	6	*Errina sp.*	522-1000
	2	*Inferiolabiata sp*	522- 735
	1	*Conopora sp.*	726
	3	*Stylaster sp.*	522 - 726
Equatorial Atlantic	8	*Enallopsammia sp.*	862 - 1482
	2	*Flabellum sp.*	703 - 780
	7	*Caryophyllia sp.*	621 - 1498
	3	*Errina sp.*	431 - 826
	3	*Adelopora sp.*	739 - 1175
	3	*Stylaster sp.*	339 - 2809
New Caledonia	3	*Stylaster sp.*	201 – 424.5
	1	*Stephanohelia*	425
Drake Passage	5	*Flabellum sp.*	334 - 1419
	1	*Desmophyllum sp.*	1862
	6	*Stylaster sp.*	715 - 1879
	7	*Errinopsis sp.*	334 - 1879
	3	*Errina sp.*	130 - 770
	1	*Cheiloporidion sp.*	316
North Pacific	3	*Stylaster sp.*	140- 270
	2	*Errionopora sp.*	78-161
Burwood Bank	1	*Conopora sp*	352.72
	1	*Stylaster sp*	707.52
	2	*Cheiloporidion*	1182.5 - 1506
North Atlantic	2	*Stylaster sp*	820 - 845
	5	*Caryophyllia sp*	1710 - 2683
	3	*Vaughanella sp*	1047 - 1216
	6	*Desmophyllum sp*	794 - 2149
	8	*Flabellum sp*	1673 - 1826
	6	*Lophelia sp*	746 - 1144
Galapagos	20	*Stylaster sp*	213.46 – 1090.17
	7	*Crypthelia sp*	543.95 – 960.92
	4	*Lepidotheca*	297.23 – 715.48
	1	*Unknown*	510.13

Table 1: Coral samples used throughout the study with their locations, genus and depth ranges. Purple highlighted genus indicates scleractinian corals.

2.2 Sample collection period

Samples were taken across the world from different cruises. The cruises were conducted the following locations, including: the Drake-Passage, Equatorial Atlantic, Alaska and the Galapagos Islands (Anteco, (2016), Geoscience, (2025), British Oceanographic Data Centre, (2025), Armstrong and Masetti (2016), Fischer, C.S.J. and Fischer, J., (2001), Sands, *et al* (2018), Samadi (2021), British Oceanographic Data Centre (2013), Howell *et al* (2016), Dalziel *et al* (2025), Hendry, *et al* (2017), Robert *et al* (2023) Marine-geo.org, 2023). The 136 deep-sea coral samples were collected from around the world between 2011 and 2023, as seen in Figure 2.1, chapter 2, page 19.

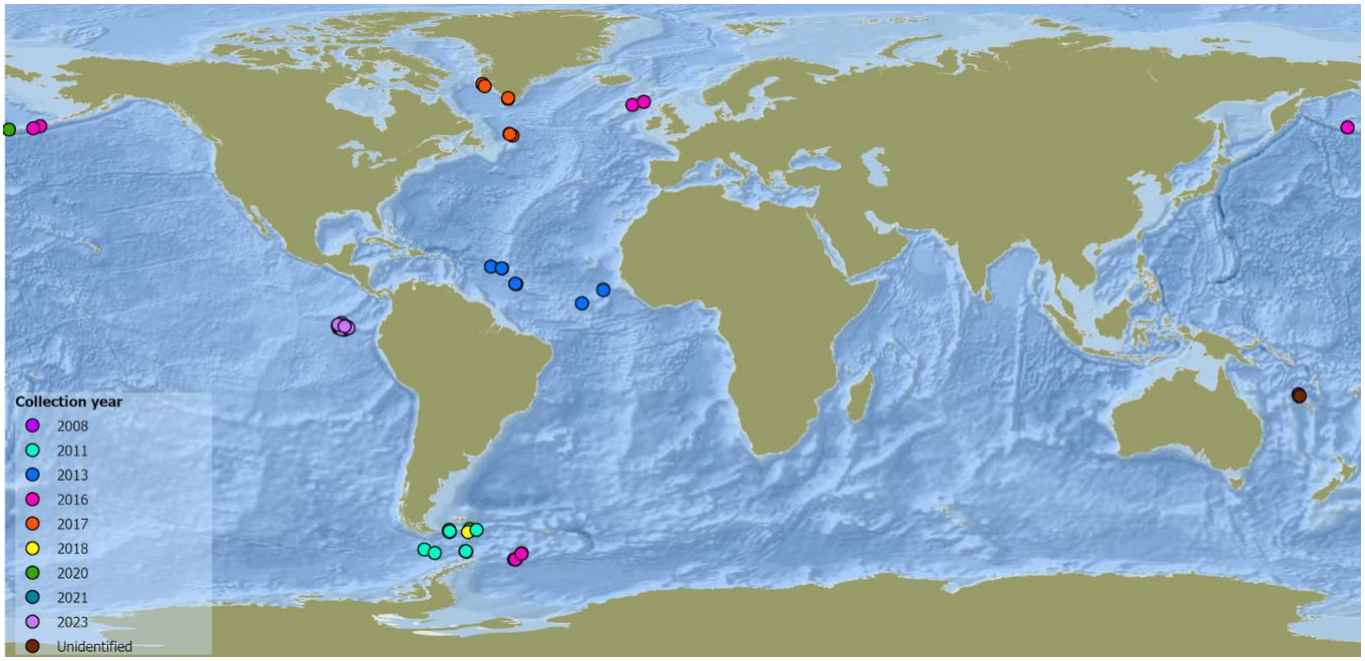

Figure 2.1 Global Distribution of cruise years from where samples used within this study. Further cruise data can be seen in table 2, below.

Cruise Name	Ship name	Year of collection	Sample Quantity
JR15005	RRS James Clark Ross	2016	12
LMG0802	R/V Laurence M. Gould	2008	1
JC094	RRS James Cook	2013	26
201601	F/V Alaska Provider	2016	4
202001	F/V Alaskan Leader	2020	1
JR19002	RRS James Clark Ross	2020	2
JR18003	RRS James Clark Ross	2018	1
Spanbios	R/V Alis	2021	2
NBP1103	R/V Nathaniel B. Palmer	2011	19
Unknown, longline fishing	Unknown, longline fishing	2011	1
JC136	RRS James Cook	2016	2
NBP0805	R/V Nathaniel B. Palmer	2008	3
DY081	RRS Discovery	2017	28
AT5009	R/V Atlantis	2023	28
FKt230918	R/V Falkor	2023	4
Unidentified	Unidentified	Unidentified	2

Table 2: Cruises from which samples have been taken throughout the study with the year of collection, sample quantity and ship name. The two unidentified samples are sampled from the collection stored at the MNHM.

2.3 Chiral amino acid analysis

This study used a revised technique of chiral amino acid analyses, which has previously been used to extract amino acids within shallow-water coral skeletons for geochronology (Hendy *et al.*, 2012). This approach first requires the isolation of the intra-crystalline skeletal amino acids through a bleaching treatment. The visualisation of intra-crystalline proteins is shown below in Figure 2.4, chapter 2, page 21. All samples were then hydrolysed to obtain the THAA, with analysis of the chiral amino acid composition using RP-HPLC (reverse-phase high-performance liquid chromatography). The revision used in this study was the use of UHPLC (ultra-high performance liquid chromatography) following the method developed by Crisp (2013). UHPLC has a faster analysis period than RP-HPLC and higher resolution.

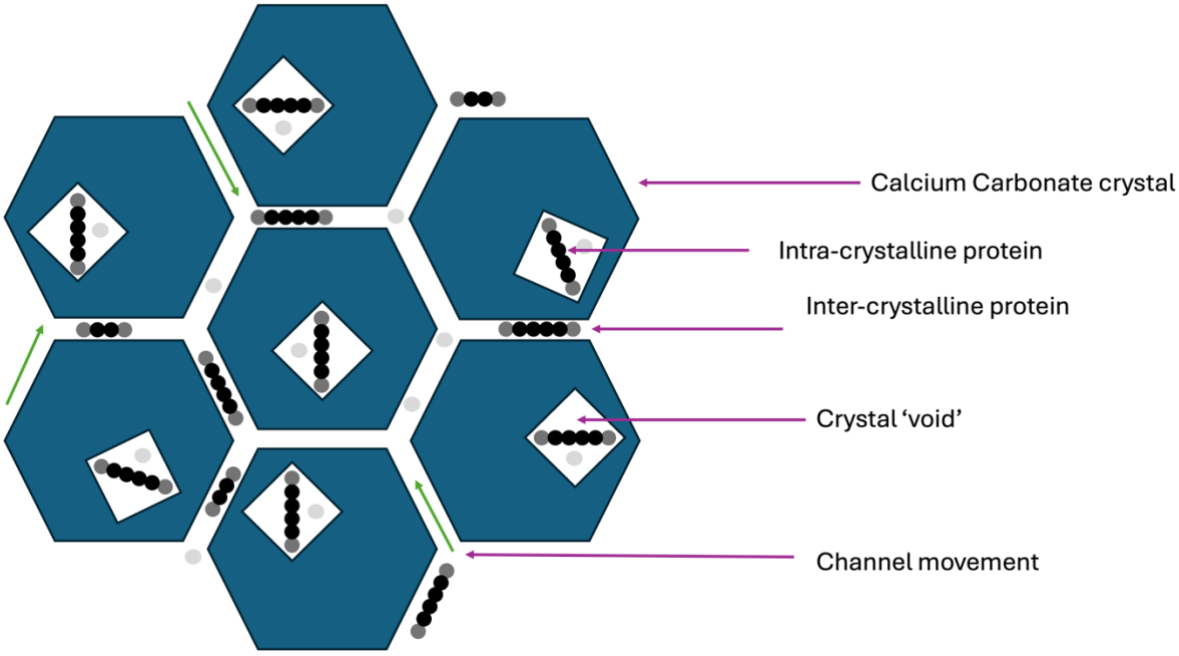

Figure 2.4, Visualisation of the intra-crystalline proteins and where they are found in retrospect to the calcium carbonate structure.

Name	Three letter code	One letter code
Glycine	Gly	G
Alanine	Ala	A
Serine	Ser	S
Threonine	Thr	T
Valine	Val	V
Leucine	Leu	L
Isoleucine	Ile	I
Methionine	Met	M
Proline	Pro	P
Phenylalanine	Phe	F
Tyrosine	Tyr	Y
Aspartic Acid	Asp	D
Glutamic Acid	Glu	E
Asparagine	Asn	N
Histidine	His	H
Lysine	Lys	K
Arginine	Arg	R

Table 3: Amino acids three letter and one letter codes of the amino acids found within this study. Aspartic acid and Asparagine within this method are combined.

2.4 Sampling techniques

Within this study, there were different sampling techniques used to understand if amino acids could be extracted from deep-sea coral (initial) and the variability in the sample itself (analytical). Then also the variation of the preparation of a sample (preparative) and the material itself (internal heterogeneity). All four replication approaches were conducted on stylasterid samples (a stylasterid coral diagram indicates what the whole coral would have looked like, Figure 2.2, chapter 2, page 23), the initial, analytical, preparative and internal heterogeneity (explained and visualised below in Table 4, Chapter 2, page 23/24). For the Scleractinia samples, the initial sampling technique was used, and internal heterogeneity samples were also measured.

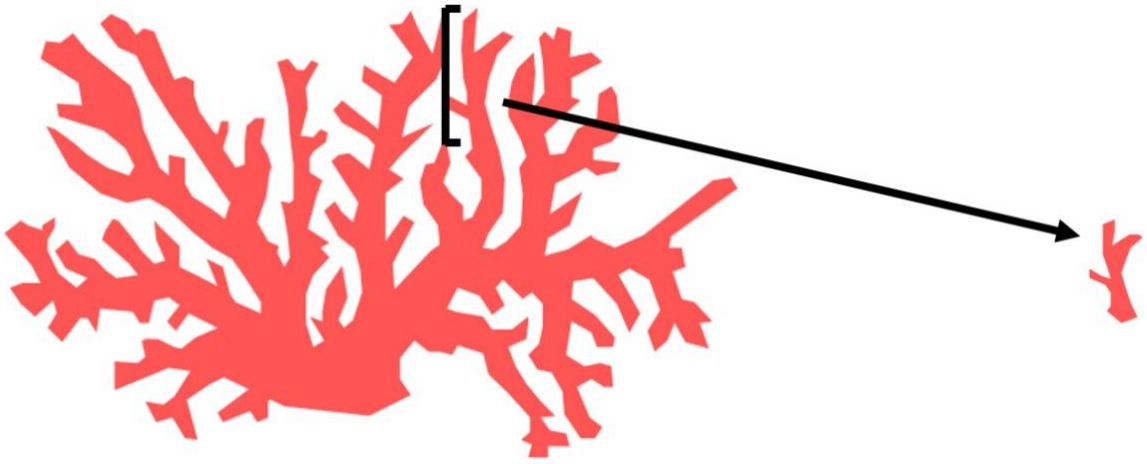

Figure 2.2: Diagram of a stylasterid coral indicating an example of where a sample such as those used within this study could be taken from the main body of the coral.

Replication tests	Description
Initial Sample	A subsample that was taken from an original piece of coral, randomly.
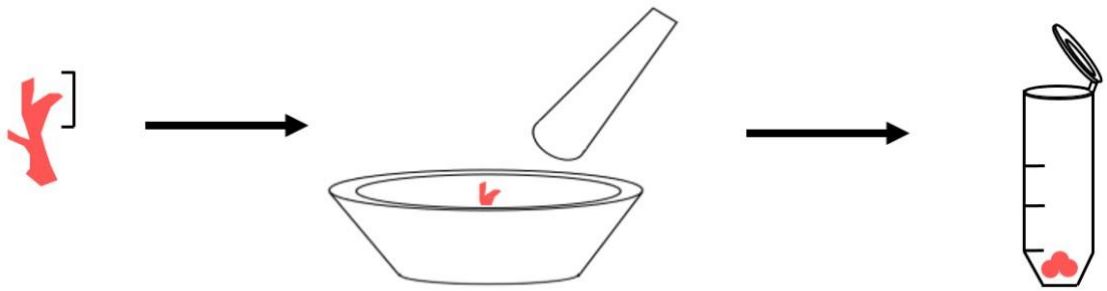	
Analytical Replicate	A sample that has been taken from the initial, bleached, hydrolysed and rehydrated vial. Then reinjected on the UHPLC multiple times individually.

Preparative Replicate	A single piece of coral powdered to form a homogenous powder. This powder is then distributed into multiple vials and then treated as an individual sample. Where it is then bleached, hydrolysed and rehydrated.

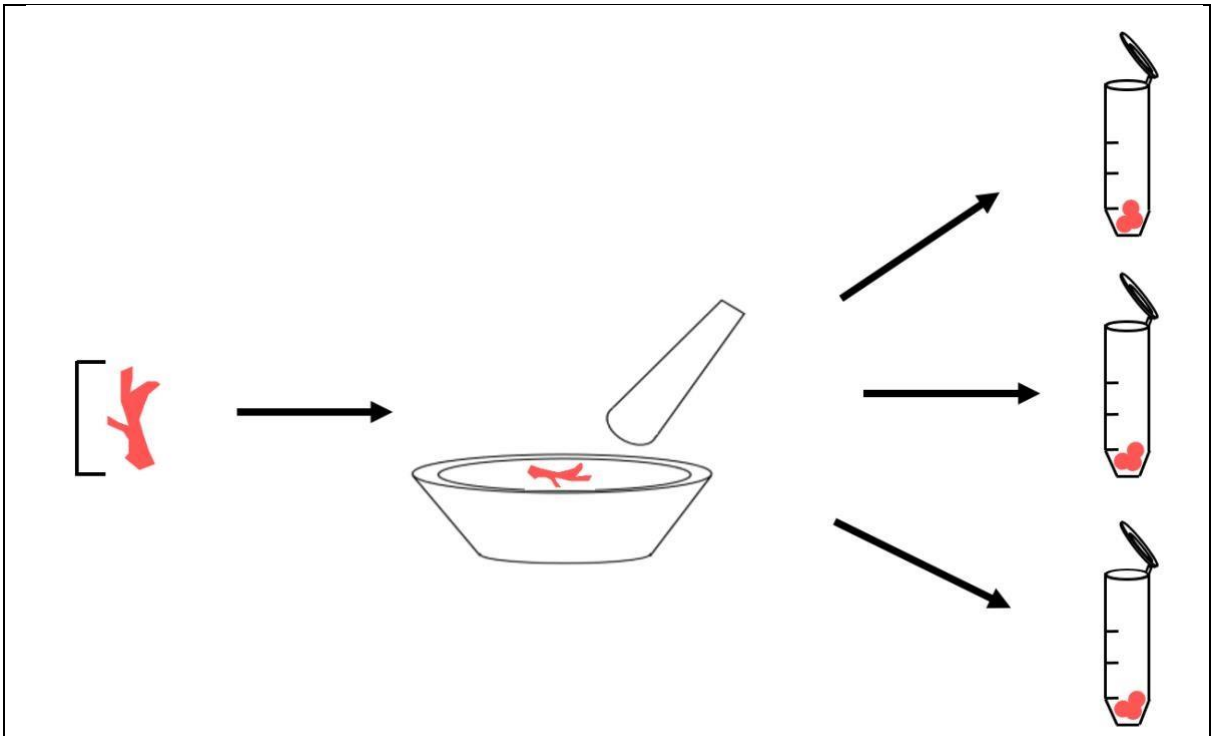

Internal Heterogeneity Sample	A sample taken from different parts of the initial sample following growth within the branch of a coral, including the tip of the branch (stylasterids only). The sample is powdered, bleached, hydrolysed and rehydrated.

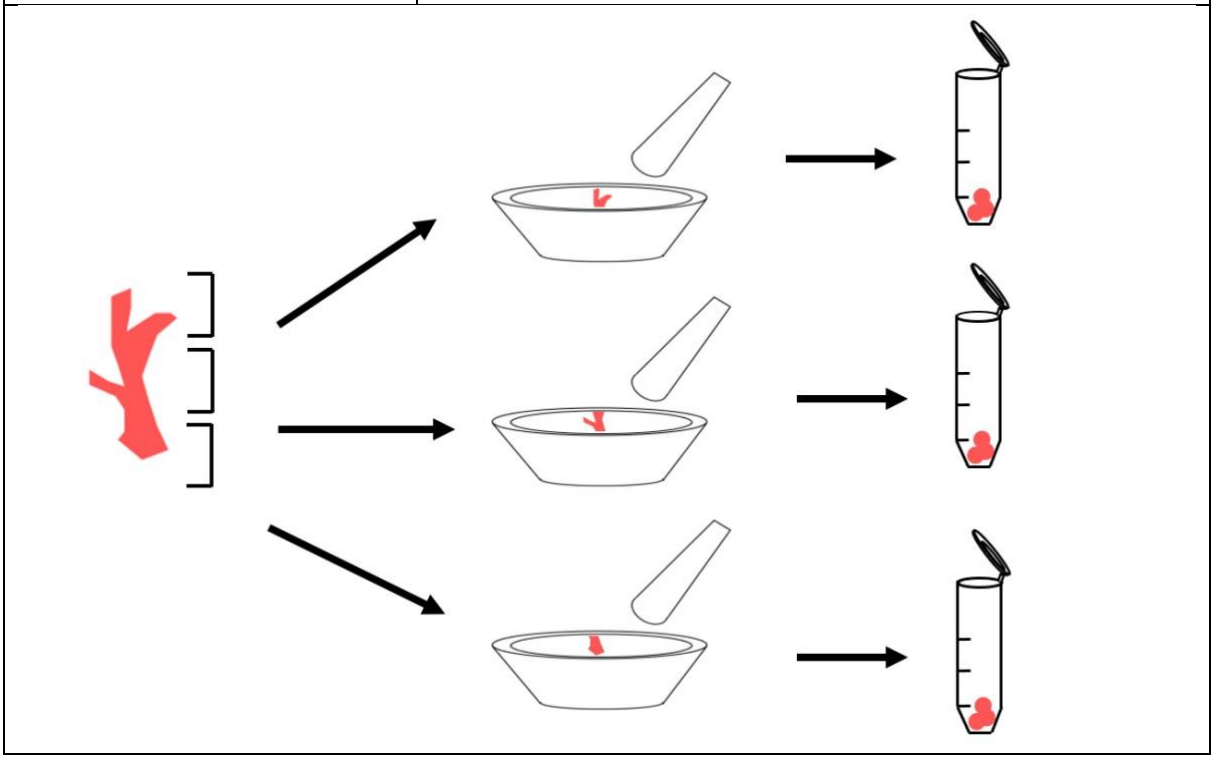

Table 4: Replication tests used on deep-sea corals within the study

To test internal heterogeneity, subsamples from 20 single corals were taken, including segmented branches with no tips and branches with multiple tips. Where possible, subsampling followed a linear progression of the newest growth to the oldest growth (Figure 2.3, chapter 2, page 25).

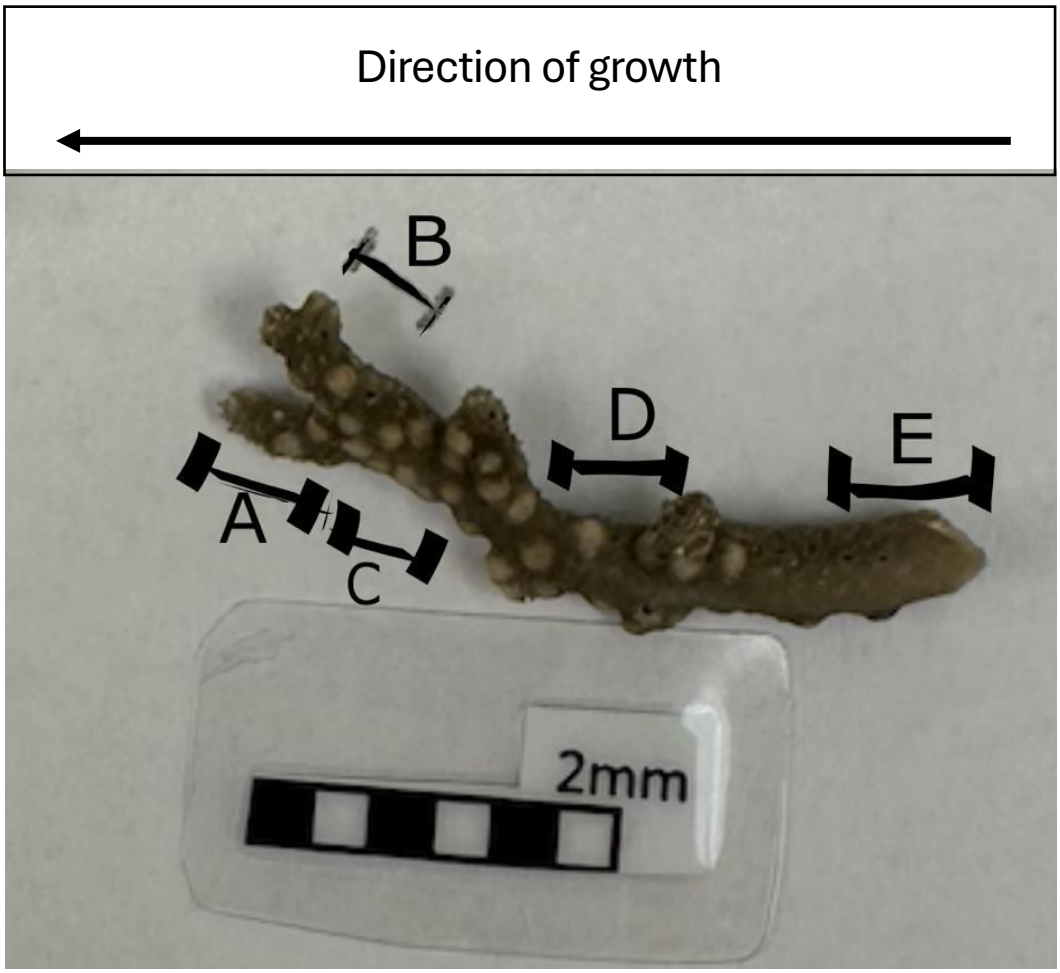

Figure 2.3: Sample FKt230918_S0588_Ev14_01, a Galapagos stylasterid: Lepidotheca macropora used for internal heterogeneity sampling.

2.5 Isolation of intra-crystalline fraction

The modern deep-sea coral samples within this study were prepared following the methods of Penkman *et al*. (2008). It had previously been observed within a *Porites* coral study that the optimum bleach treatment for corals is 12% NaOCl for a 48-hour period on powdered samples at a ratio of 50 µL/mg of sample (Hendy *et al*., 2012). This length of time and concentration of NaOCl removes the maximum amount of inter-crystalline proteins whilst also minimising induced racemisation (changes to the amount of L to D isomers).

Each sample used within this study was broken into smaller pieces, except for internal heterogeneity samples, which were drilled for precision of subsampling. They are then powdered as fine as possible using an agate pestle and mortar. Then ~20 mg of each was weighed accurately into a sterile plastic 2 mL microcentrifuge tube (Fisher brand), and then bleached for 48 hours using 12% NaOCl. After the 48-hour bleaching period, the bleach was removed as precisely as possible, using a pipette, aiming not to take any powder during the removal. The bleached powder is then rinsed with 500 µL of purified water and placed into a centrifuge. The water, like the bleach, is then carefully removed aiming not to uptake any sample within the pipette tip. This water wash is repeated 6 times, and then finally rinsed with methanol to evaporate any remaining water, the methanol was removed after 10 minutes. Due to the quantity, it is better to remove than leave to evaporate, speeding up the process.

2.6 RP-UHPLC analysis

Before any analysis is undertaken on the RP-UHPLC, the intra-crystalline proteins must be broken down into their amino acids. As these are modern samples, little natural peptide bond hydrolysis would have occurred (Johnson and Miller, 1997). Therefore, this is undertaken in the lab, through the use of concentrated mineral acid that is heated to a high temperature. This is the THAA fraction.

A fraction of the bleached powder was weighed accurately into a sterile 2 mL glass vial (Wheaton) treated with 7 M hydrochloric acid (HCl), at a ratio of 50:1, under N_2 at 110℃ for 24 hours. This breaks the peptide-bound amino acids, leading to the yield of THAA. Samples were then placed into a centrifugal evaporator to dry and then rehydrated using L-homo-arginine (LhArg) as an internal standard.

Fluorescence detection on the RP-UHPLC was used to analyse the amino acid compositions of each sample using the method developed by Crisp (2013) based on the original HPLC method of Kaufman and Manley (1998). The method by Crisp (2013) results in the separation of 14 amino acid L and D isomers. To separate the amino acids, a 2 µL sample was injected into RP-UHPLC using an adapted method from Crisp (2013) detailed in Conti *et al*. (2024). The sample was

mixed online with 2.2 µL of derivatising reagent (260 mM n-iso-l-butyryl L-cysteine (IBLC), 170 mM ophthaldialdehyde (OPA) in 1 M potassium borate buffer, adjusted to pH 10.4 with KOH pellets). Separation of the amino acids was carried out on an Agilent Eclipse Plus C18 column (4.6×100 mm, 1.8 µm particle size) using a gradient solution of sodium acetate buffer (solvent A; 23 mM sodium acetate tri-hydrate, 1.5 mM sodium azide, 1.3 µM EDTA, adjusted to pH 6.00 ± 0.01 with 10% acetic acid and sodium hydroxide) and methanol and acetonitrile (solvent B, at a ratio of 92.5: 7.5). Asparagine and glutamine undergo rapid, irreversible deamination during hydrolysis, so it is impossible to distinguish between them using this approach (Hill, 1965). Therefore, aspartic acid and asparagine are reported jointly as Asx and glutamic acid and glutamine as Glx. This method has been visualised within Figure 2.4, chapter 2, pages 28-33.

2.7 Visual representation of the method section through schematics

Step 1: Bleaching

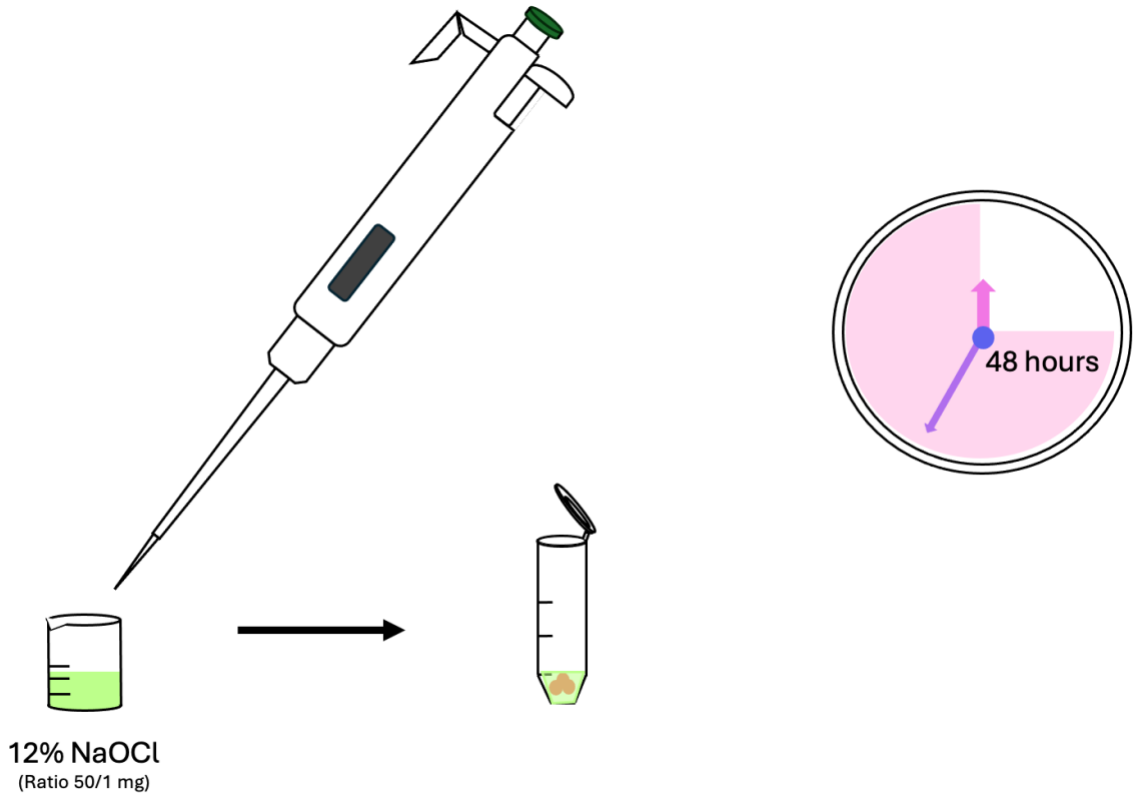

Step 2: Removing Bleach

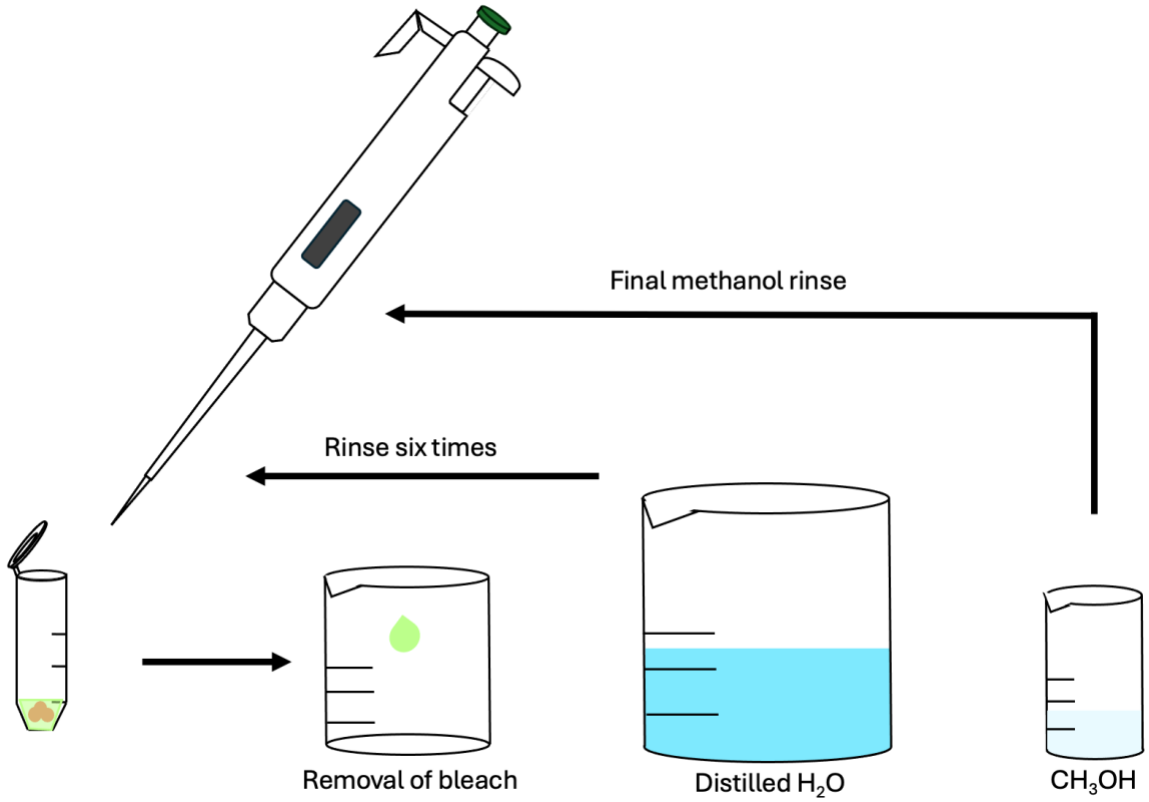

Step 3: Transfer of Material

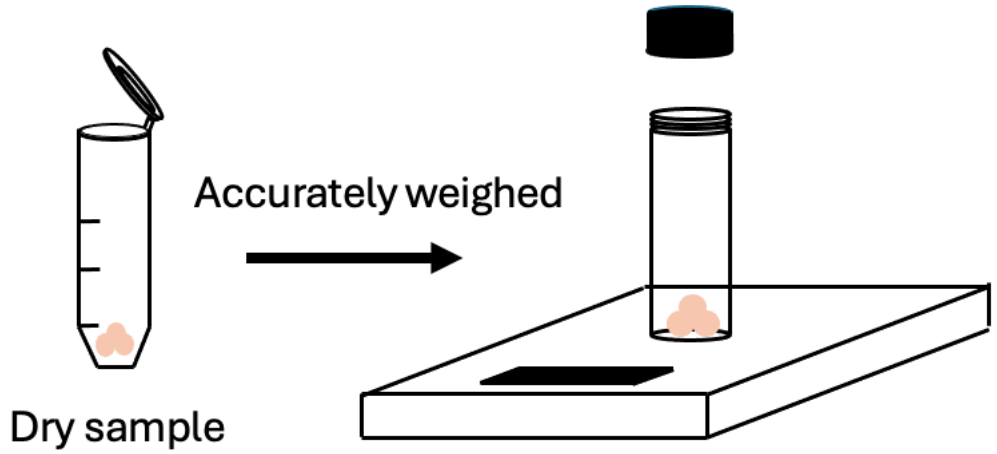

Step 4: HCl addition

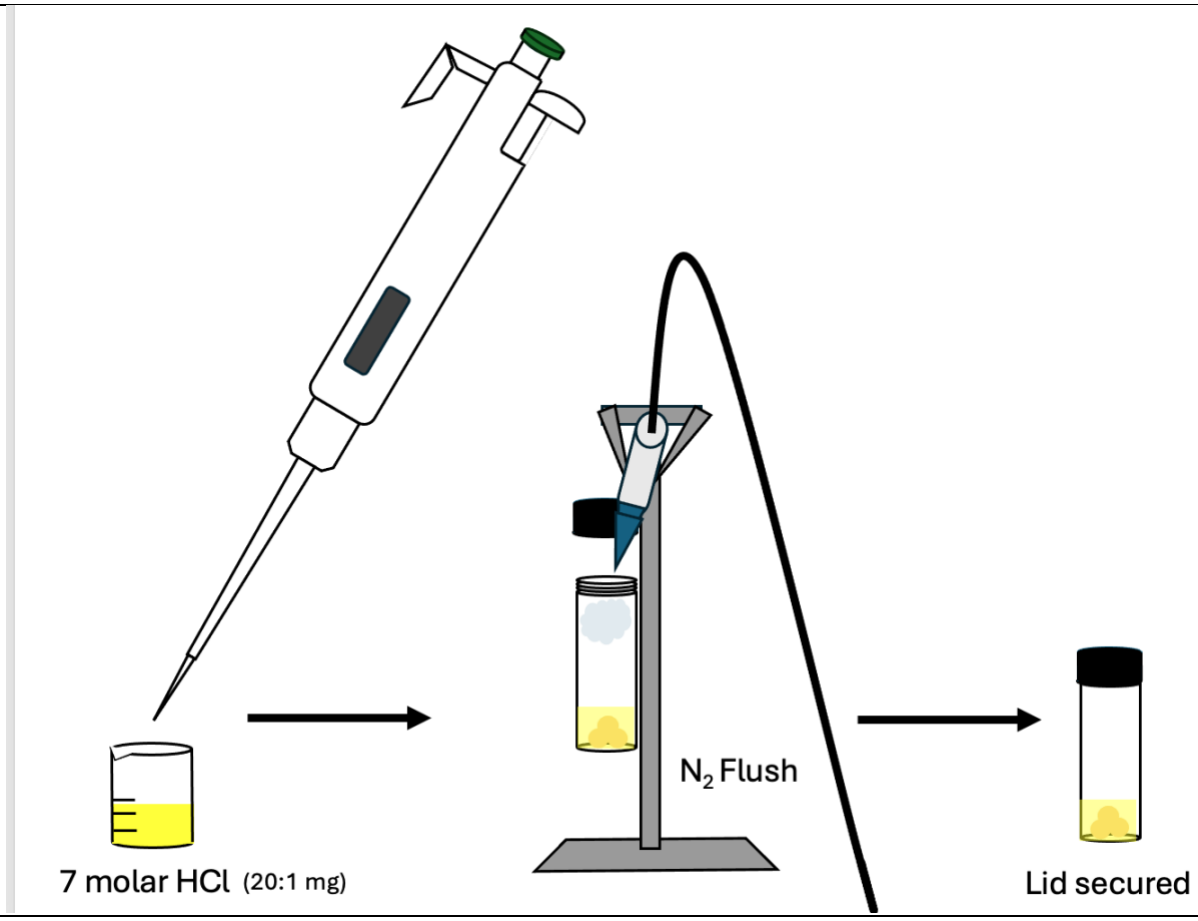

Step 5: Hydrolysis

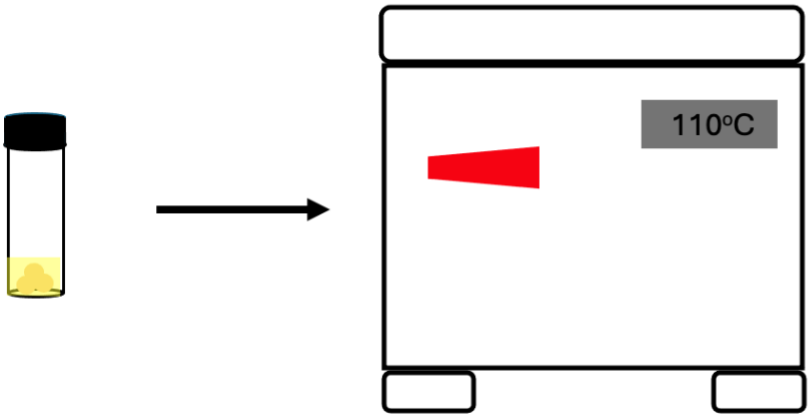

Step 6: Drying samples

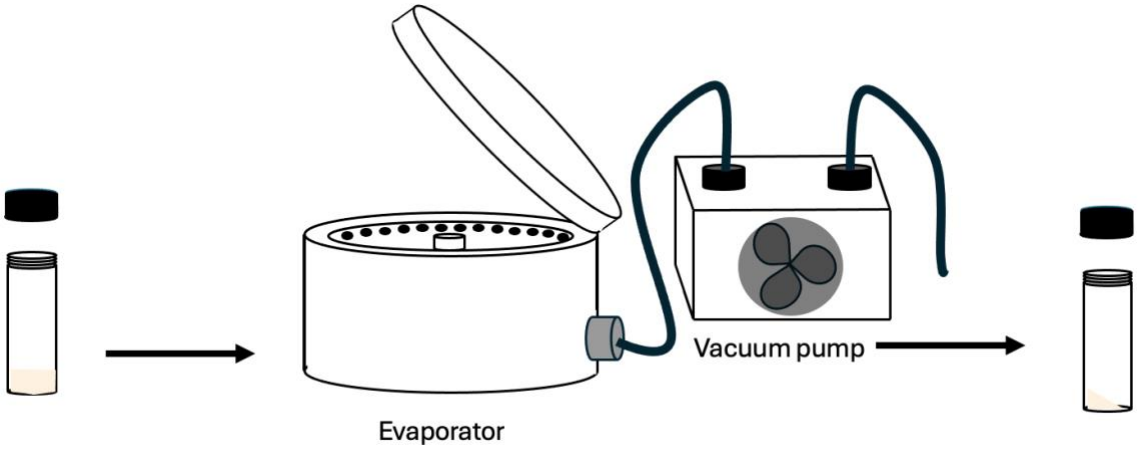

Step 7: Rehydration

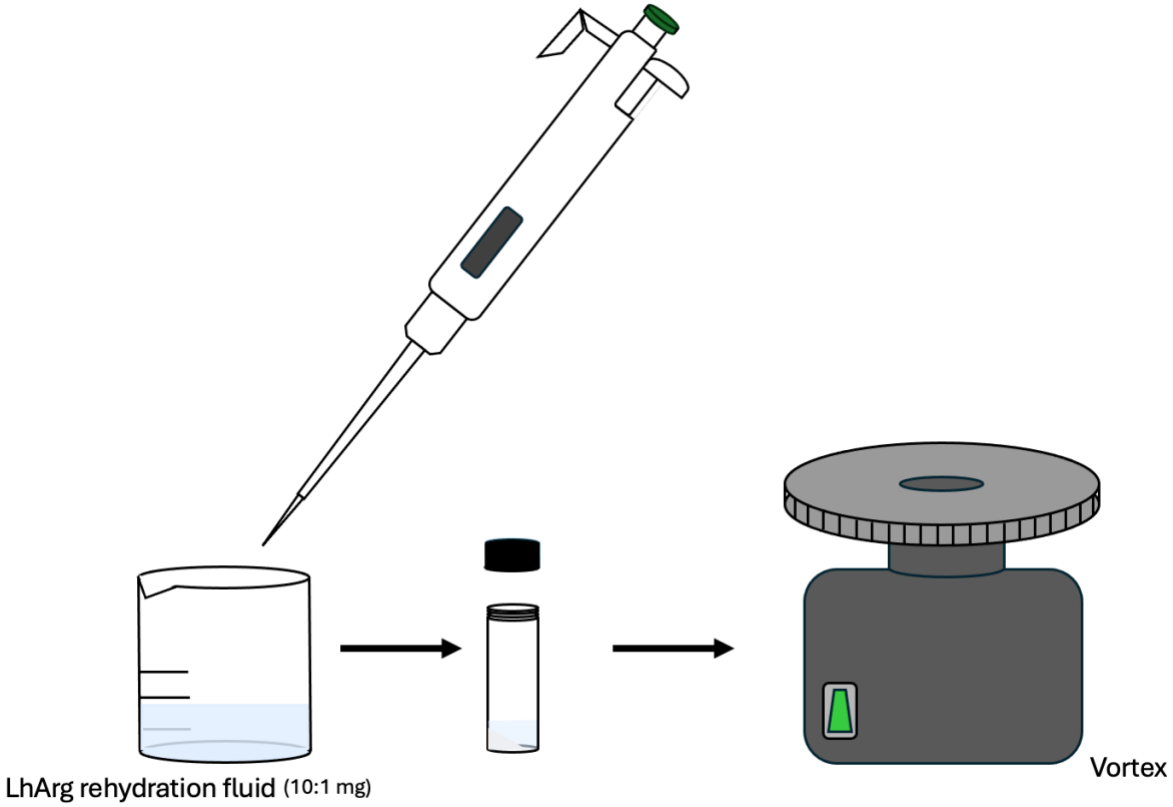

Step 8: Transfer of material

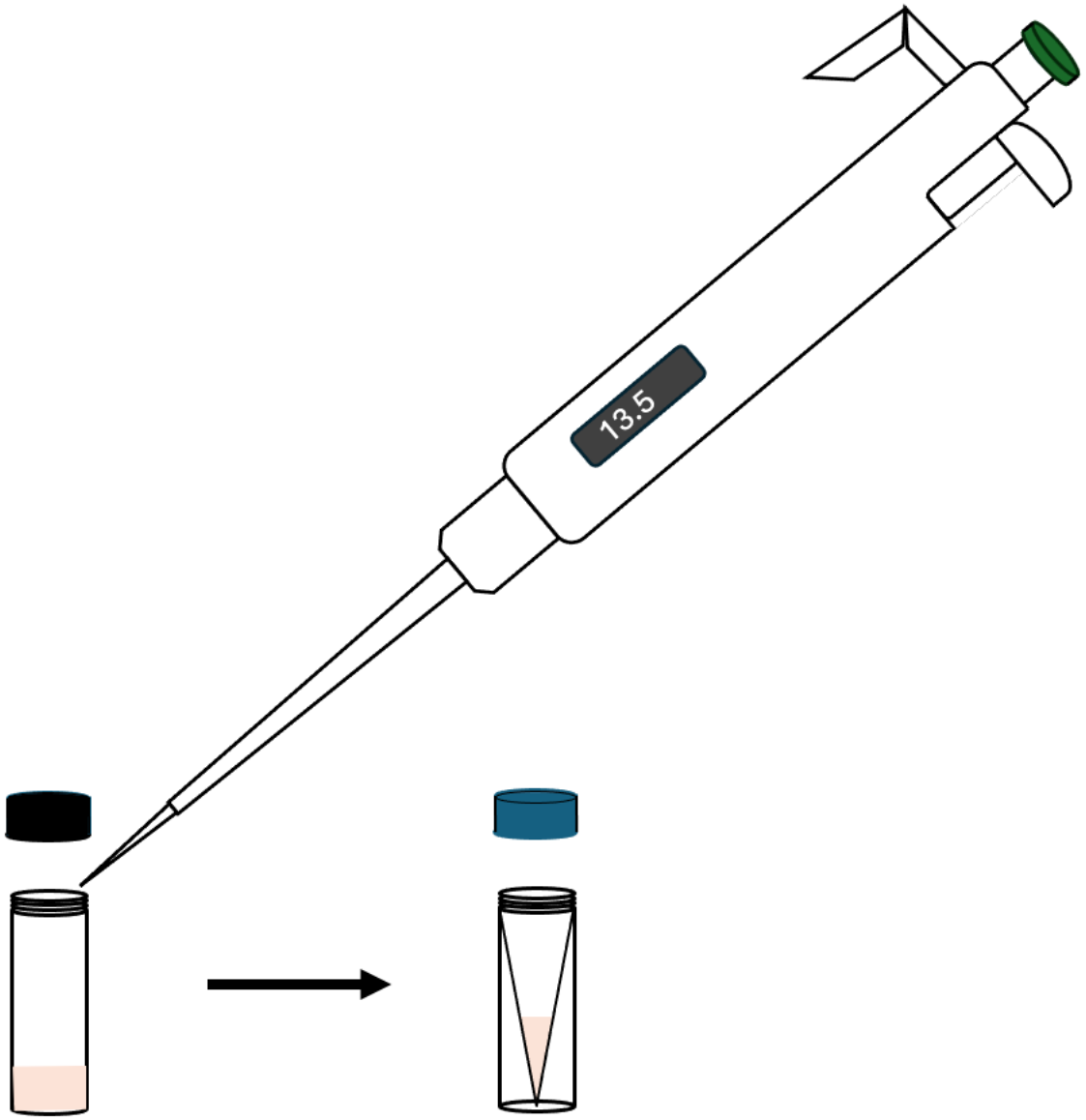

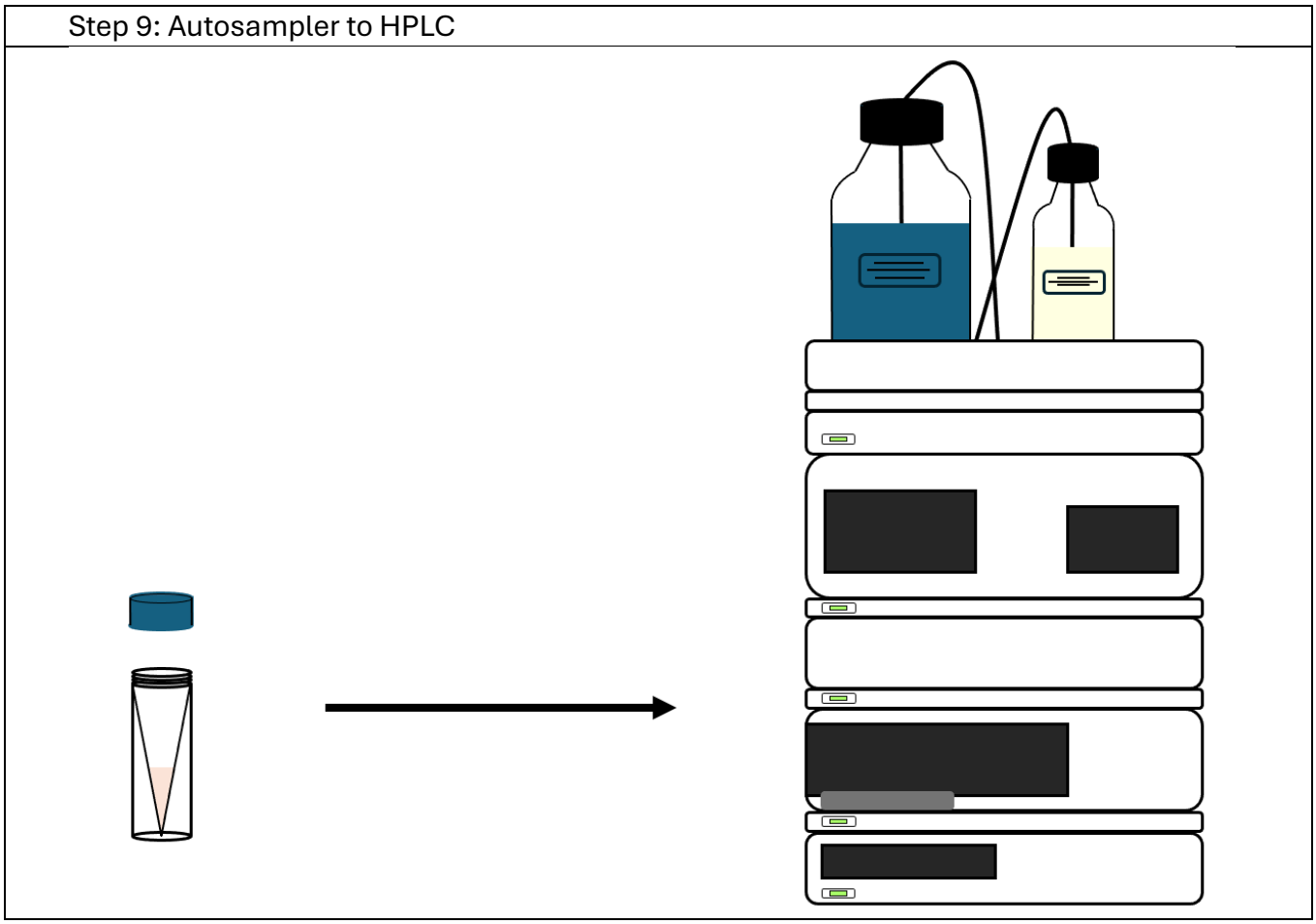

Figure 2.4: Method schematic detailing the process used within this study for amino acid analysis. Broken down into nine steps following the bleaching, hydrolysis and further steps described in sections 2.5 and 2.6.

3 Chapter 3 – Results: Analysing amino acids within deep-sea coral

The methods chapter (2) outlined how the analyses were undertaken. In this results chapter, there are five main objectives:

1. To identify if (and how well) chiral amino acid analysis can be undertaken on deep-sea coral skeletons using a small (n=9) initial sample set.
2. Determine amino acid composition by undertaking analysis of an extended sample set n =136
3. Assess preparative and analytical replication of the analytical approach
4. Assess internal heterogeneity within a subset of corals
5. Compare replicate results

3.1 Initial Sample Set

To determine if amino acids could be measured within the skeletal material of deep-sea corals, 18 stylasterid samples were chosen spanning a range of depths and species (Table 5, chapter 3, page 35) to test the detectability of amino acids within skeletal material. In addition, three *Porites* coral skeletons that had previously provided successful unpublished data, (Hewitt, T. 2018. Amino acids in biomineralisation of coral: investigating and comparing the artificial protein degradation of *Pocillopora eydouxi* with *Porites* sp. fossil data. Unpublished BSc dissertation, University of York) were analysed. A large range was found in amino acid variability between different genera. The *Porites* data was only used for standard comparison and training purposes; the data was not used further within this study. No previous UHPLC work was conducted on these samples. The initial samples selected were used for hydrolysis and free samples, meaning 2 molar HCl was added rather than 7m HCl. Only two Porites corals were used within the initial hydrolysed sample set, and three in the free sample set.

Sample (Shortened sample names)	NEAAR Number	Genus	Type
3352 (T1)	17232bH*	Stylaster	Deep-sea
3404 (T2)	17233bH*	Stylaster	Deep-sea
ErrNabk	17234bH*	*Errinopora*	Deep-sea
Ean1	17235bH*	Errina	Deep-sea
Ela844	17236bH*	Errina	Deep-sea
Ea141ak	17237bH*	Errina	Deep-sea
Egr2421	17238bH*	Errina	Deep-sea
TH ThPoloPB3	17240bH*	Porites	Shallow
TH HaPoT302-R3	17241bH*	Porites	Shallow

Table 5, Initial samples run, all bleached and hydrolysed. Porites corals were used as a standard for comparison as a training data set and no further analysis was conducted on them.

Within the initial sample run, the first hydrolysed sample run failed, as shown in Figure 3.1, chapter 3, page 36, and a chromatogram of a standard showing where peaks should have been seen, Figure 3.2, chapter 3, page 36 . There were insufficiently well-defined peaks for almost all amino acids in the samples. In turn, there were also low internal standard levels within these samples (LhArg), and therefore, it was clear that there had been peak suppression from an unknown cause. To test that this was not a machine error, the same failed sample (Vials) within the initial samples were tested on a different machine. A HPLC instead of the UHPLC. This also tested if an air bubble had become trapped within the autosampler vial, preventing the uptake of the sample. The results came back very similar to those before. Indicating that there had been an issue within the sample or preparation, instead of the machine. The samples were then re-prepared and run on the UHPLC; the issue was no longer visible on the chromatographs. There was no indication of the reason for the first failed runs, and therefore, we have no idea what the issue was caused by. Quality control of blank samples and internal standards helped indicate an issue with results and determine that there was most likely no issue with material but potential chemical mix up or strength issue. Although there were no other issues in the lab so this si still undetermined. After these method development samples, it was established that the method is appropriate for deep-sea corals, returning measurements that could be used to determine the THAA (pmol/mg), amino acid concentrations (pmol/mg) and percentage of amino acids.

Sample Info : 3352A(Tl)-Species:Stylaster sp.-Location:New Caledonia-Depth:346.5-
Bleach info:Bleached 48h, Free

Additional Info : Peak(s) manually integrated

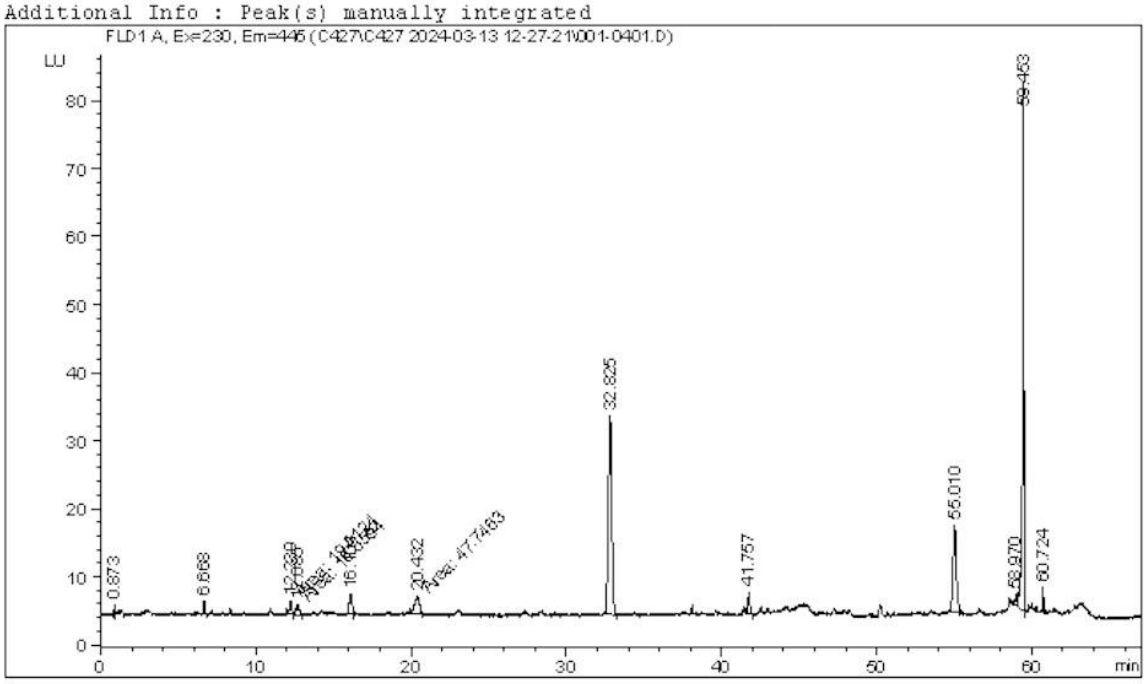

Figure 3.1, A failed chromatogram, showing low to no peaks and low internal standard (LhArg).

Sample Info : 0.5 std - 1 in 20 L-hArg - p:19/01/24, al: 19/01/24

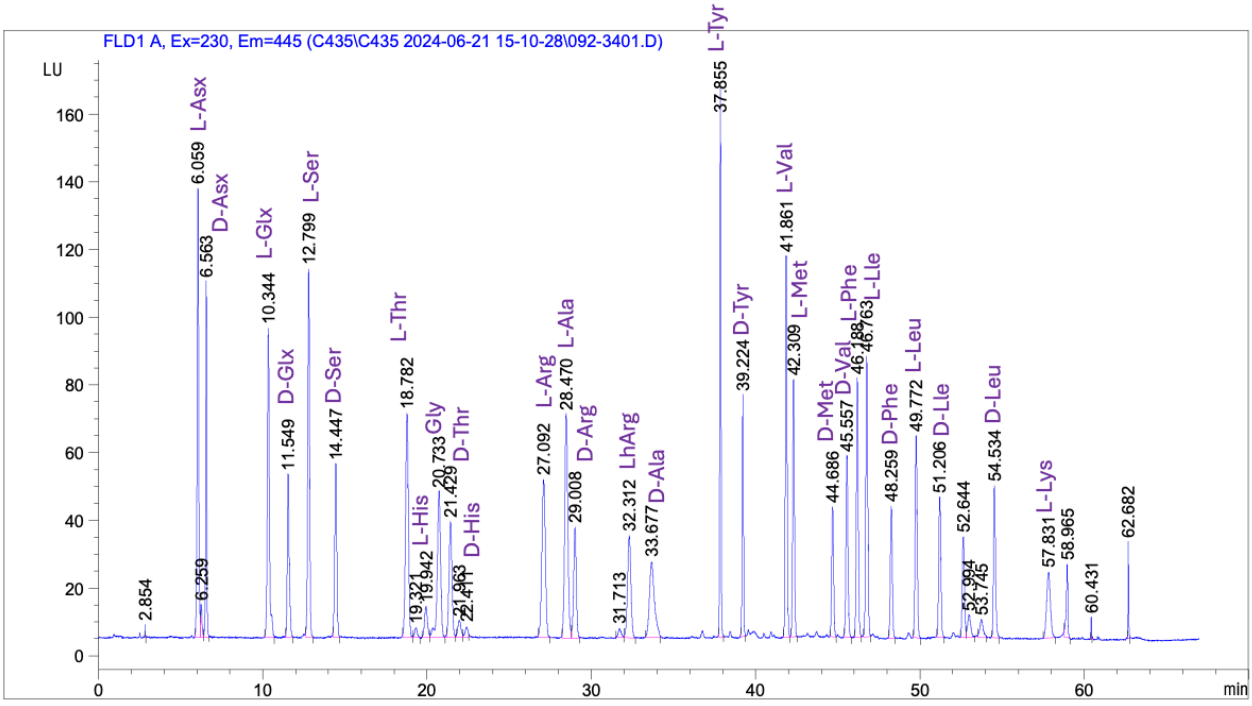

Figure 3.2, A standard 0.5 sample to show where peaks of amino acids could have been seen.

3.2 Extended Sample Set

Having demonstrated that amino acids could be measured within stylasterid coral skeletons, the study was extended to scleractinian corals and a wider range of
stylasterid corals. In total 85 stylasterid corals and 51 Scleractinia corals were analysed (Table 1, chapter 2, page 18). The amino acid composition in all samples was dominated by L-Asx, a combination of aspartic acid and asparagine, then followed by other acidic amino acids. These high results of Asx and acidic amino acids are in line with previous research that has been conducted on shallow water corals, (Mitterer, 1976). Acidic amino acids are an indication that CARPs and SAARPs (Coral acid-rich proteins and skeletal aspartic acid-rich proteins) are present and important within the skeletal material of the coral (Mass *et al*., 2013).

Once amino acids had been extracted from the skeletal material of stylasterid coral and scleractinian coral, knowing the variability of the replication for these samples was the next priority. This was to understand where the largest variability could be coming from within a sample. Sixteen stylasterid corals and five scleractinian corals had replication tests undertaken on them (Table 6, chapter 3, page 38).

Sample	Genus	Analytical replicate (Original sample)	Preparative replicate	Internal heterogeneity
Stylasterid				
FKt230918_S0588_Ev14_01	*Lepidotheca*	3	6	5
Egr2426	*Errina*	3	5	6
StyBrcc	*Stylaster*	3	7	4
Sdefg	*Stylaster*	3		4
ErrNabi	*Errinopora*	3	8	4
JC094-B0548-Hydls/m-001 to 019Eal48aq	*Errina*	3		4
JR15005-Ev113-2429-Il29bd	*Inferiolabiata*	3		4
NBP1103-DH22-Stc1-01-Sde22aw	*Stylaster*	3		4
NBP1103-DH39-St-2-02-Ebo02	*Errina*	3		3
ErrNabk	*Errinopora*	4	12	
AT5009_B0246_Dive5161_Ev012_001	*Stylaster*	3		4
AT5009_B1616_Dive5174_Ev008_001	*Lepidotheca*	3		3
JR15005-Ev39-784-Il39be	*Inferiolabiata*	3		2
JC094-B0480-Hydls(f)-001-Sty80an	*Stylaster*	3		3
Adp88	*Adelopora*	3		4
JC094-F0184-Hydlm-001-Eal001	*Errina*	3		3
Scleractinia				
DY081-031-ROV333-Ev032-201-583Loph	*Lophelia*	3		3
JC094-42-VEM-ROV233-ARM79B0089-Enall-00	*Enallopsammia*	3		2
DY081-031-ROV333-Ev033-201-570Loph	*Lophelia*	3		3
JC094-21-EBB-ROV228-ARM33B0027-Enall-001	*Enallopsammia*	3		2
JC094-15-EBA-ROV227-SLP46B0018-Carlm-001	*Caryophyllia*	3		3

Table 6: Samples and the amount and type of replication methods undertaken on them, with stylasterid corals and scleractinian corals separated.

3.3 Analytical replicates

Analytical replicates were completed for 21 of the samples (16 stylasterid & 5 Scleractinia) seen in Table 6, chapter 3, page 38. Analytical replication used the rehydrated (prepared and bleached) samples, which were injected on the UHPLC at different times or runs. The analytical samples within this study were reinjected three times, leading to a total of three replicates, as seen in Table 6, chapter 3, page 38. The [THAA], [Asx] and % Asx have been highlighted for completing analysis. As L-Asx is the most dominant amino acid seen within all the corals, and [THAA] has been analysed throughout, the graphs for all other concentrations and percentages of amino acids can be found within the appendix.

The analytical replication of these samples showed that the average [THAA] replication error of stylasterid corals is ~4% with a range of 1.12 – 8.57%. The analytical replication of [THAA] error for Scleractinia corals is ~1.6%, with a range of 1.08 – 5.77% (Coefficient of variation analytical tables found in section 7.1.1). This has been calculated from the average of the coefficient of variance for stylasterids and Scleractinia individually using [THAA] results. For the Asx concentration, the average error for stylasterid corals is 3% with a range of 0.25-6.13 and for scleractinian 0.6% with a range of 0.37-0.76. Within the % Asx, the average error for stylasterid corals is 4% with a range of 1.25-11.4, within scleractinian corals, the average error is 1.81 with a range of 0.42 – 3.08.

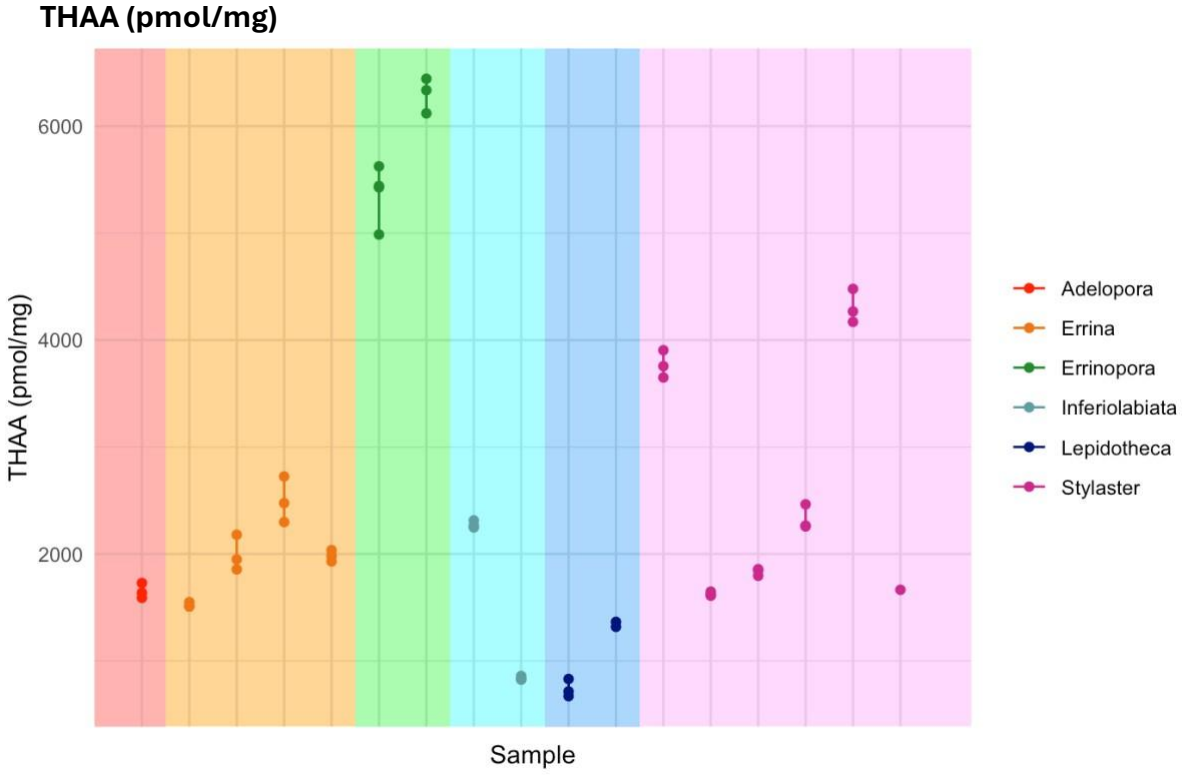

Figure 3.2, The genus of stylasterid analytical replicates against THAA (pmol/mg), showing the range of analytical variability of THAA (pmol/mg) within samples. The range of THAA (pmol/mg) coefficient of variance is from 1.12-8.57 with an average of 4.07.

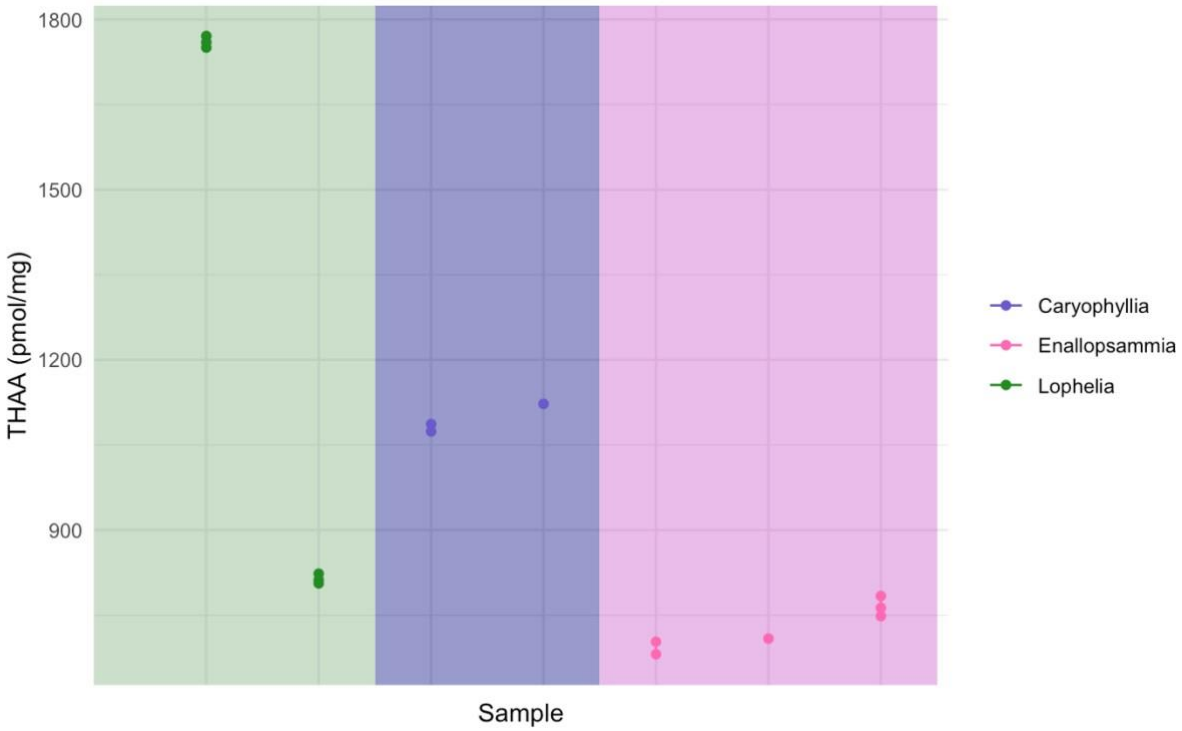

Figure 3.3, The genus of Scleractinia analytical replicates against THAA (pmol/mg), showing the range of analytical variability of THAA (pmol/mg) within samples. The range of THAA (pmol/mg) coefficient of variance is from 1.08 – 5.77 with an average of 1.67.

Asx Concentration

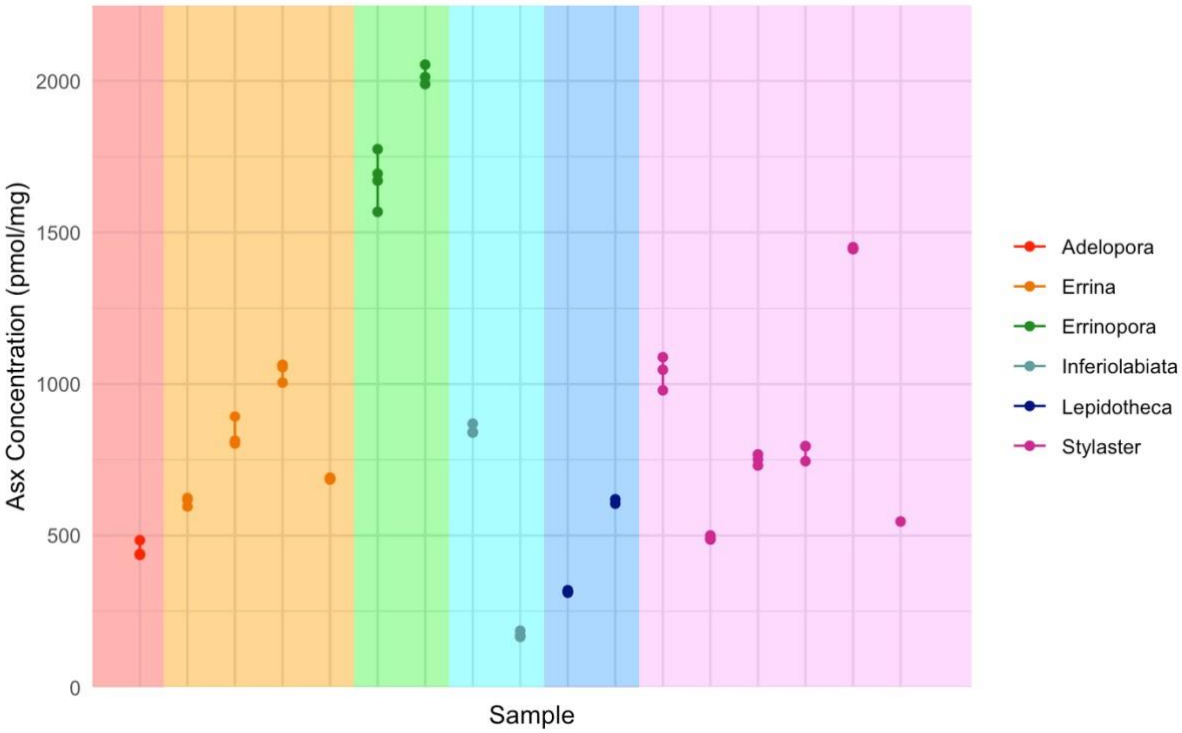

Figure 3.4, The genus of stylasterid analytical replicates against Asx concentration (pmol/mg), showing the range of analytical variability of Asx concentration (pmol/mg)

within samples. The Asx concentration (pmol/mg) coefficient of variance range is from 0.25 – 6.13 with an average of 3.02.

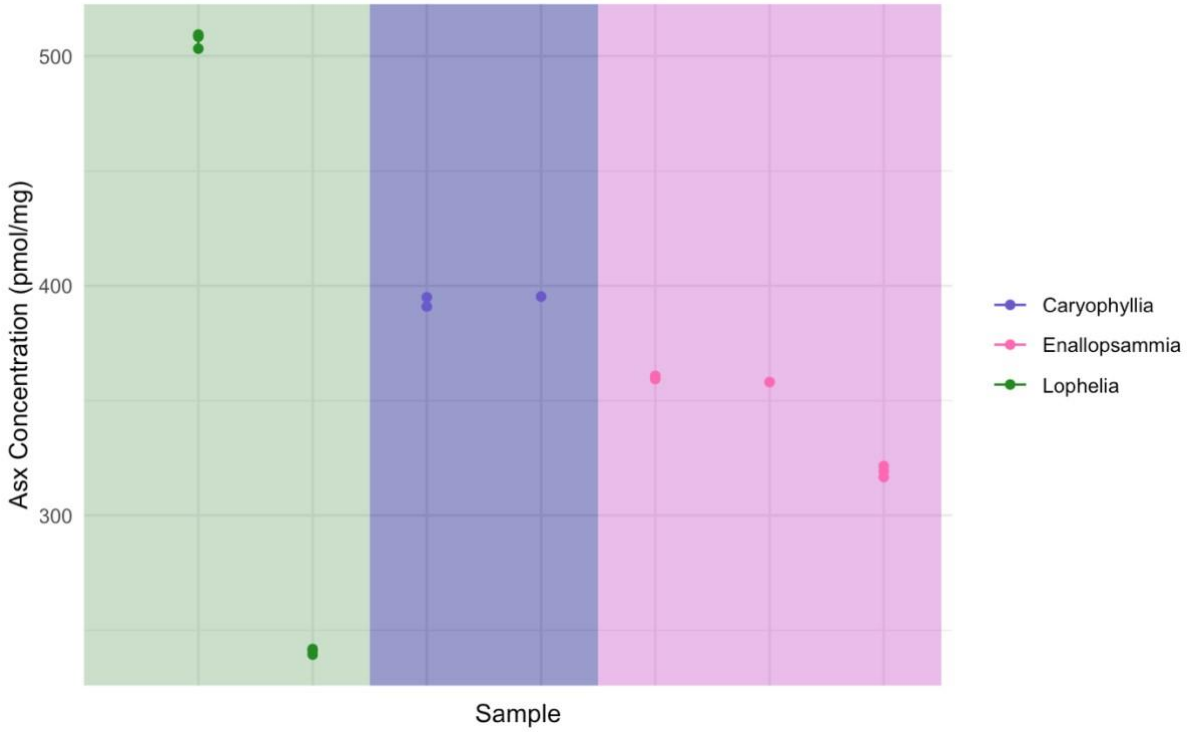

Figure 3.5, The genus of Scleractinia analytical replicates against Asx concentration (pmol/mg), showing the range of analytical variability of Asx concentration (pmol/mg) within samples. The Asx concentration (pmol/mg) coefficient of variance is from 0.37 – 0.76 with an average of 0.58.

Percentage of Asx:

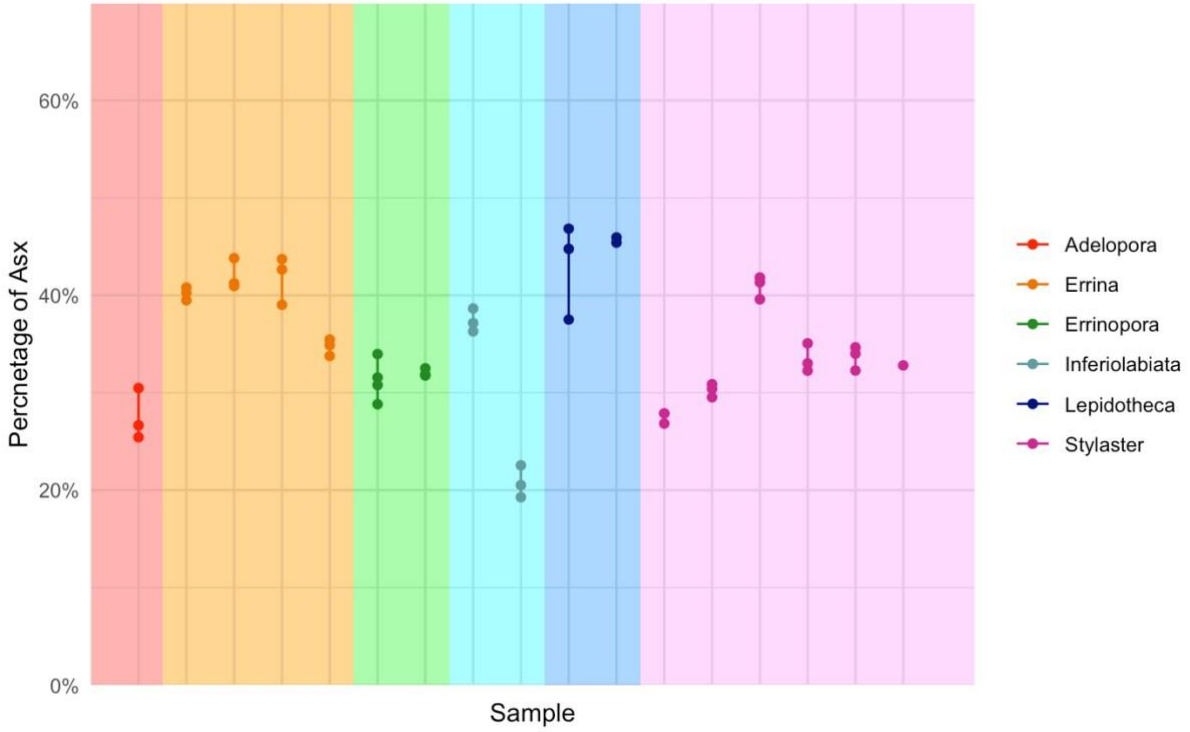

Figure 3.6, The genus of stylasterid analytical replicates against the percentage of Asx, showing the range of analytical variability of the percentage of Asx within samples. The percentage of Asx coefficient of variance range is from 1.25 – 11.4 with an average of 4.41%.

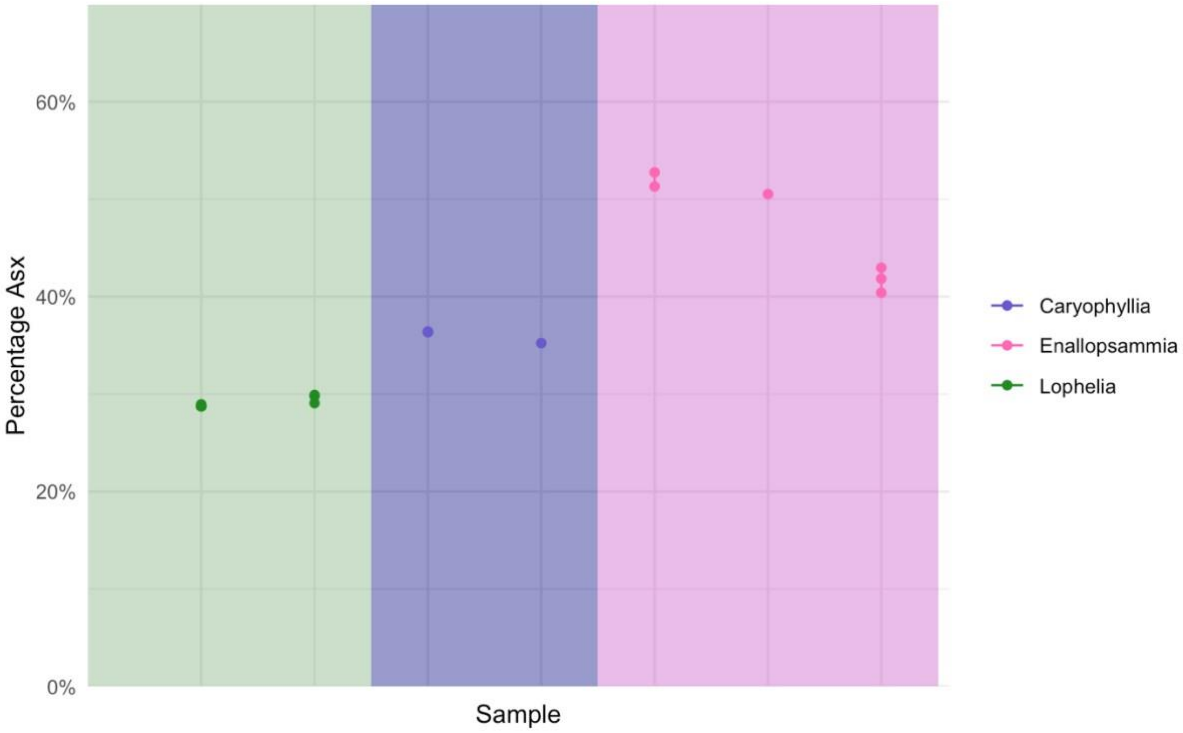

Figure 3.7, The genus of Scleractinia analytical replicates against the percentage of Asx showing the range of analytical variability of percentage of Asx within samples. The percentage of Asx coefficient of variance range is from 0.42-3.08 with an average of 1.81.

3.4 Preparation Replicates

Five corals were used to undertake preparation replicate analysis (Table 6, chapter 3, page 38); they cover a range of locations, depths and species. In total 42 preparation replicates were undertaken in order to assess the reproducibility variation of a sample. ErrNabi and ErrNabk are the same species of coral (*Errinopora nanneca*) that consistently produced the highest concentrations of Asx, and therefore, were both used to ensure there was consistency throughout both samples of coral. No scleractinian coral samples were used to conduct the preparation replication as there was a limited quantity of samples and therefore, the internal heterogeneity was prioritised.

Preparation replicates for each sample came from a single piece of coral that was then powdered by pestle and mortar and then portioned into multiple different plastic microcentrifuge vials for the bleaching step (Sec 2.3). This was then processed separately for the rest of the preparative & analytical procedure (Sec 2.3). Coral samples were all different sizes, and therefore, it was possible to

extract more powder from some than others. Corals with larger material quantities were selected for preparation replicates to produce a larger number of samples to complete the preparation replication. The amount of powder ranged from having enough material to have between five to 14 vials of the coral samples.

The preparative variability [THAA] within stylasterid corals has an average of 7.53 pmol/mg with a range of 1.23-8.85 pmol/mg, for the Asx concentration, the average is 7.26 pmol/mg with a range of 4.74-11.4 pmol/mg (tables of coefficient of variance results found in section 7.1.2). Within the percentage of Asx, the average error is 2.69 with a range of 1.25-4.6.

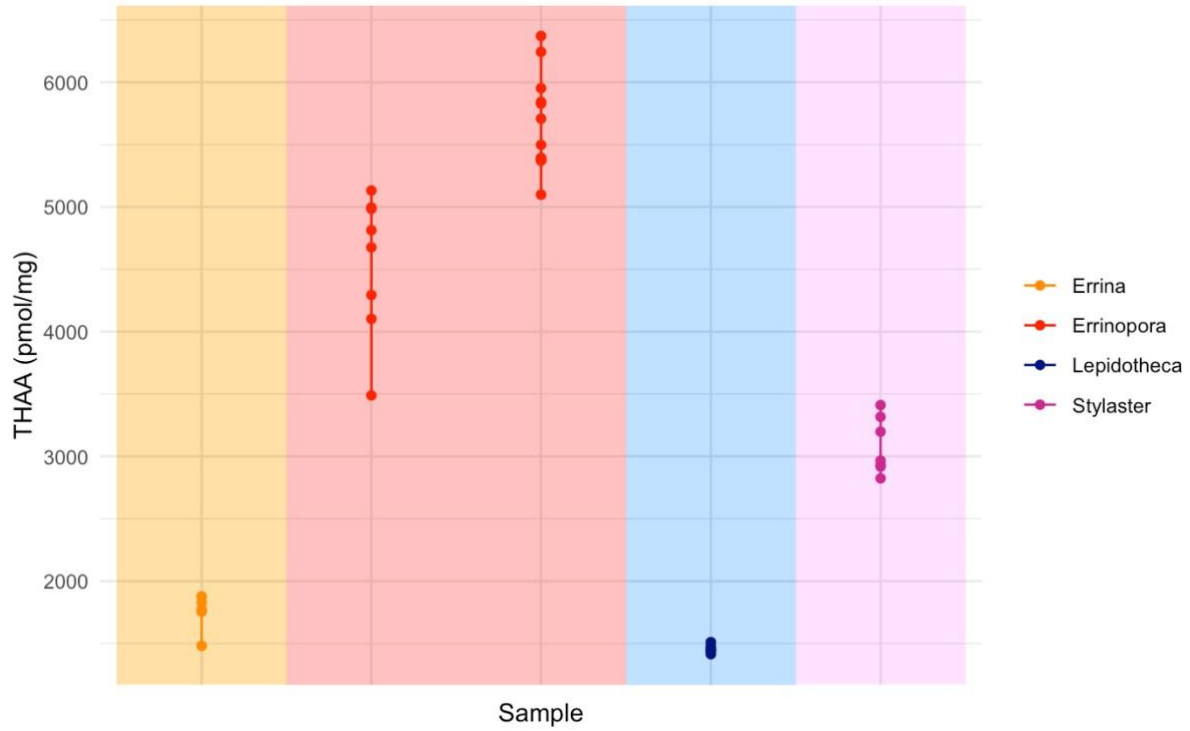

Figure 3.8, The genus of stylasterid preparative replicates against THAA (pmol/mg), showing the range of preparative variability of THAA (pmol/mg) within samples.

Asx Concentration:

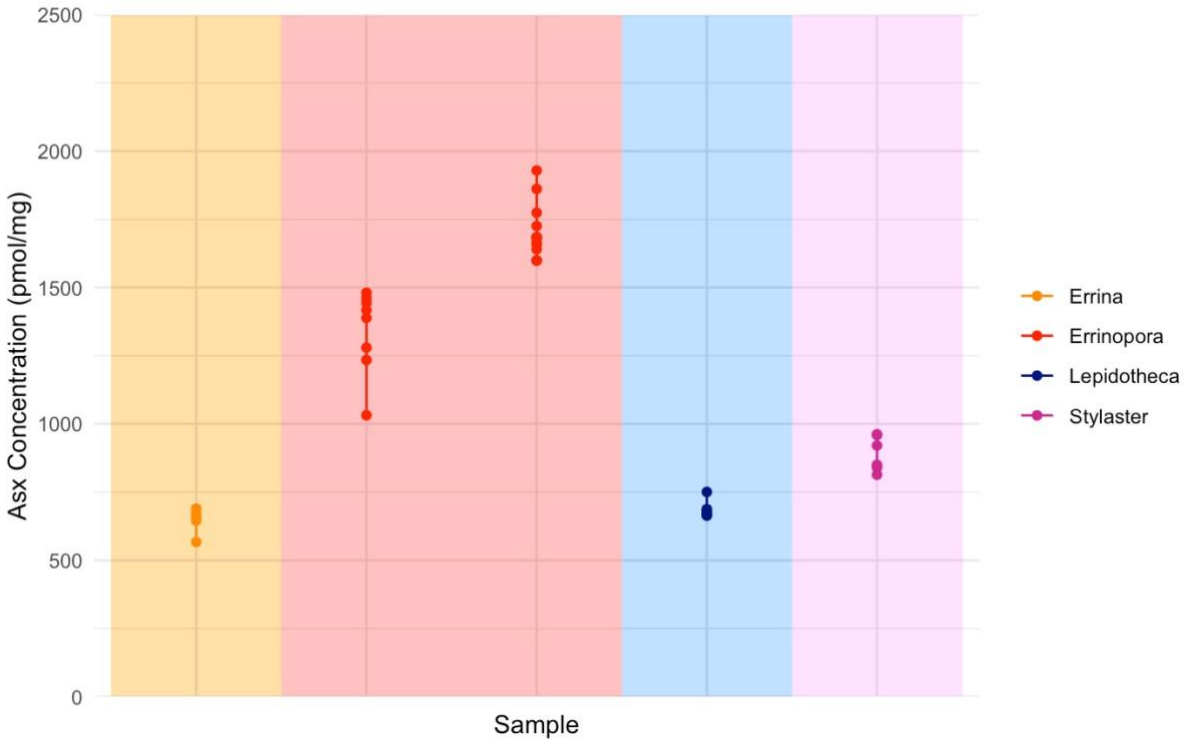

Figure 3.9, The genus of stylasterid preparative replicates against Asx concentration (pmol/mg), showing the range of preparative variability of Asx concentration (pmol/mg) within samples.

Percentage of Asx:

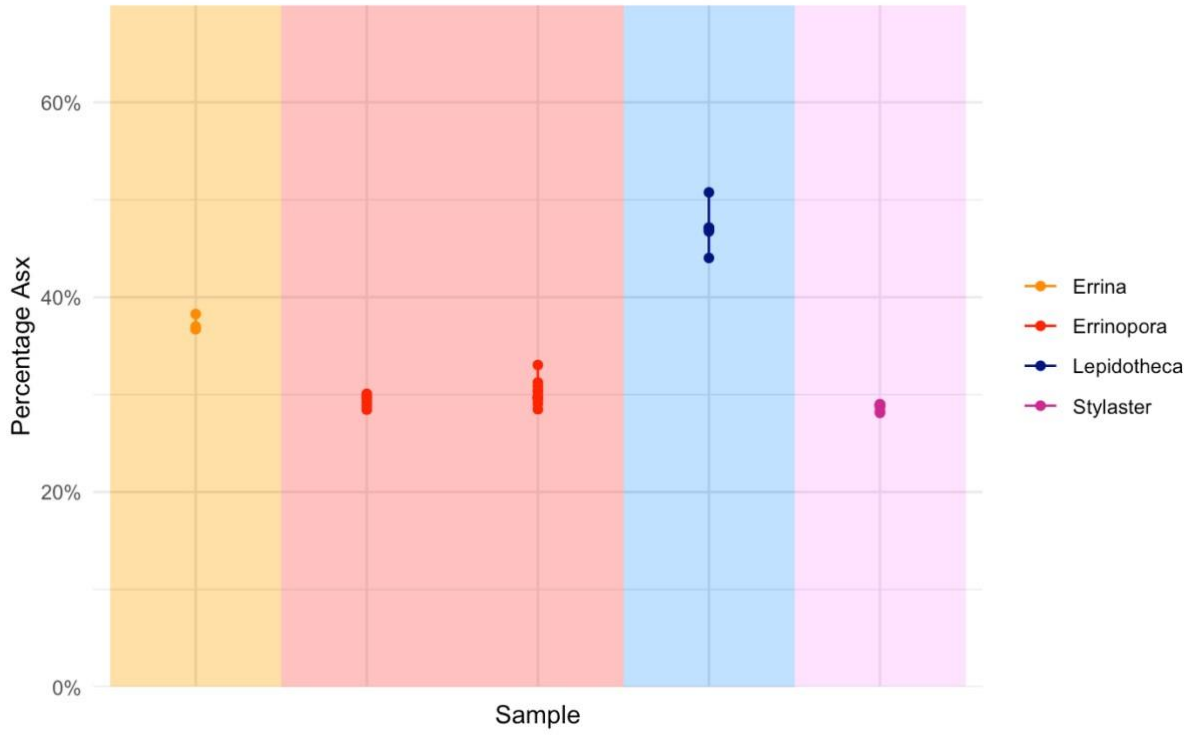

Figure 3.10, The genus of stylasterid preparative replicates against the percentage of Asx, showing the range of preparative variability of the percentage of Asx within samples.

Two samples were removed from the analysis as outliers due to results that were skewing the data from peak malformation or error. As the peak was malformed it was creating a larger result for that particular amino acid and therefore this altered the overall concentrations of the other amino acids. This is often caused by inorganic material being detected within the fluorescence detector. These samples were ErrNabi 1 and FKt230918_S0588_Ev14_01 4.

Knowing the variability between the analytical replication and the preparative replication it can be determined that the variation of the preparative replicability is larger than the analytical. Therefore, it can be determined that some variation is coming from the coral skeletal material. This was then tested by looking at the internal heterogeneity of the samples.

3.5 Internal Heterogeneity

Internal heterogeneity analysis was conducted on 15 of the 16 samples, where analytical replicability was also assessed. This was to understand how variable the amino acids are within the skeletal material of the corals. ErrNabk was not tested for internal heterogeneity, as the sample was split vertically down the centre, and it was, therefore not possible to identify the detailed structure of the branch.

Internal heterogeneity was assessed on four Stylasterid samples that had sufficient linear structure from the tip to the end of the branch. The location of where the initial coral samples were taken was not recorded and, therefore, will range for all tip-to-branch corals and has not been included. The internal heterogeneity covered a range of variables: the linearity of branches, the difference in amino acid of branches moving away from the main body of the coral colony and also branches with new growths that have tips. Therefore, the testing of the branches has the potential to demonstrate any similarities in amino acid composition between similar anatomic structures throughout the coral.

3.5.1 Stylasterid coral

The different branch structures of stylasterid corals can include multiple tips, axial branches and proximal branches that can fork away from the main body of the coral colony. Axial branches have tip structures at the end of them. However, it is not always clear if that tip from the axial branch is a continuous new growth for the coral or a growth that had stopped growing, and the tip was no longer forming a new part of the coral skeleton. This could be important as the differences in the amino acid compositions and total concentration of amino acids (pmol/mg) could vary between new growths and dead tips. A diagram of the branch structure is seen in Figure 3.11, chapter 3, page 46.

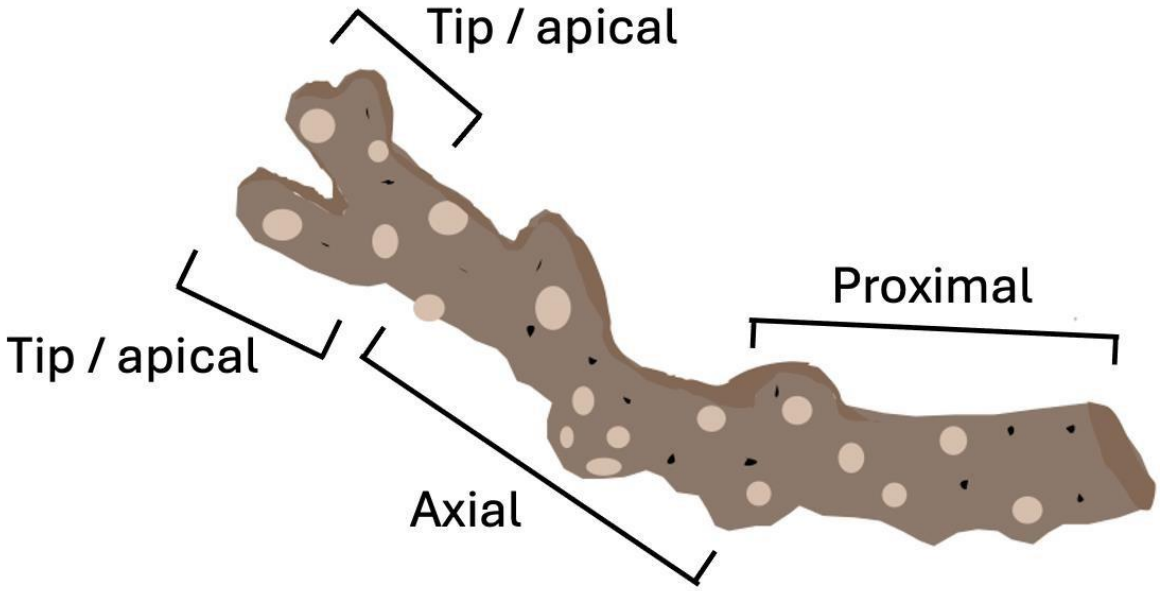

Figure 3.11: Tip to branch schematic stylasterid coral, indicating how sections of the branch are defined. Branches that have been split more than the axial and proximal sections will be below the proximal section and described as lower.

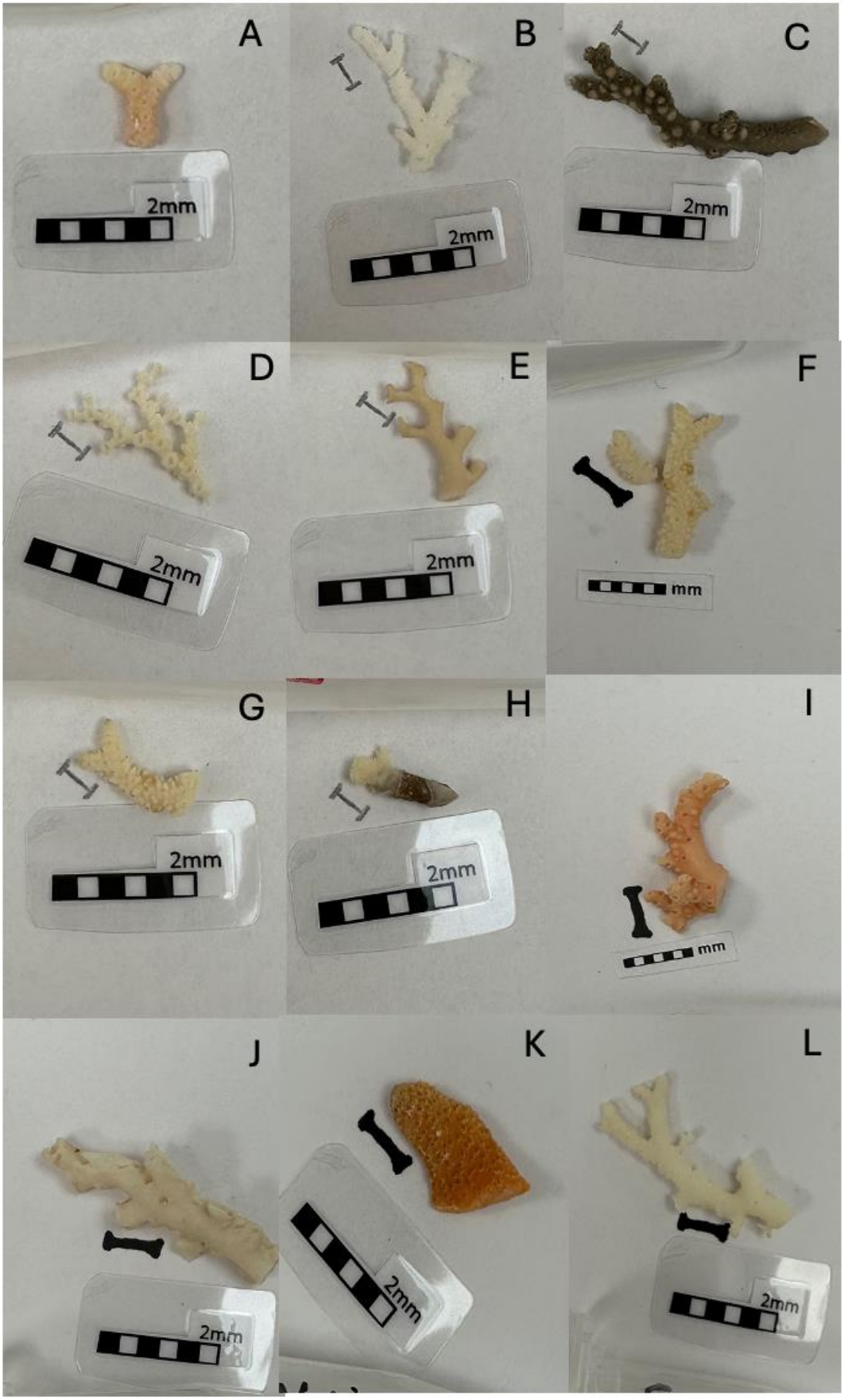

Figure 3.12: Images of the stylasterid corals used for internal heterogeneity tip-to-branch testing, ordered left to right to match Table A.10 (found in appendix). The drawn I bar indicates areas of targeted selection, in no specific image order.

For 8 out of 12 stylasterid samples, the tip was lower in total hydrolysed amino acid and Asx concentrations (figures 3.13, 3.14, chapter 3, pages 48/49). This difference in concentrations is larger than the assessed preparative reproducibility of the method (~18% vs 7.5%),
(coefficient of variance tables can be found in appendix section 7.1.3). It is also seen in Figure 3.13 that the branch sub-samples further towards where the centre of the coral would be, often increase in total hydrolysed amino acids and Asx concentrations.

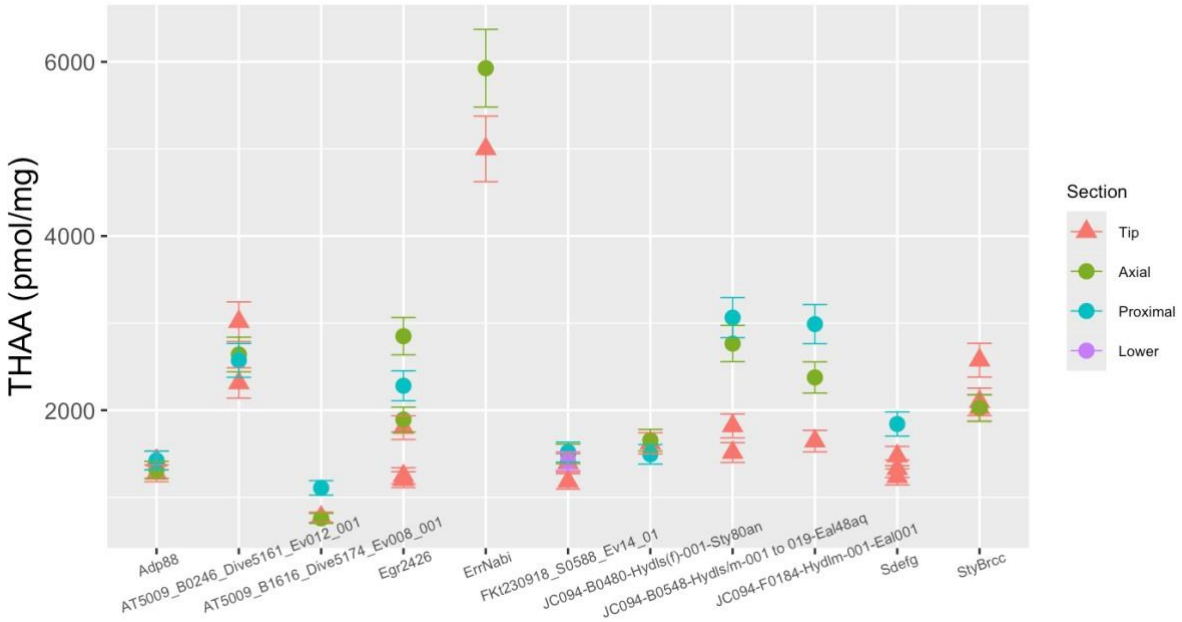

Figure 3.13: Internal Heterogeneity [THAA] stylasterid samples; error bars indicate the 7.5% preparative variability average across samples. Colours and shapes indicate the section of one branch being sampled from Axial being closest to the tip and Proximal / Lower being the furthest away, lower sections distinguish larger coral samples. .

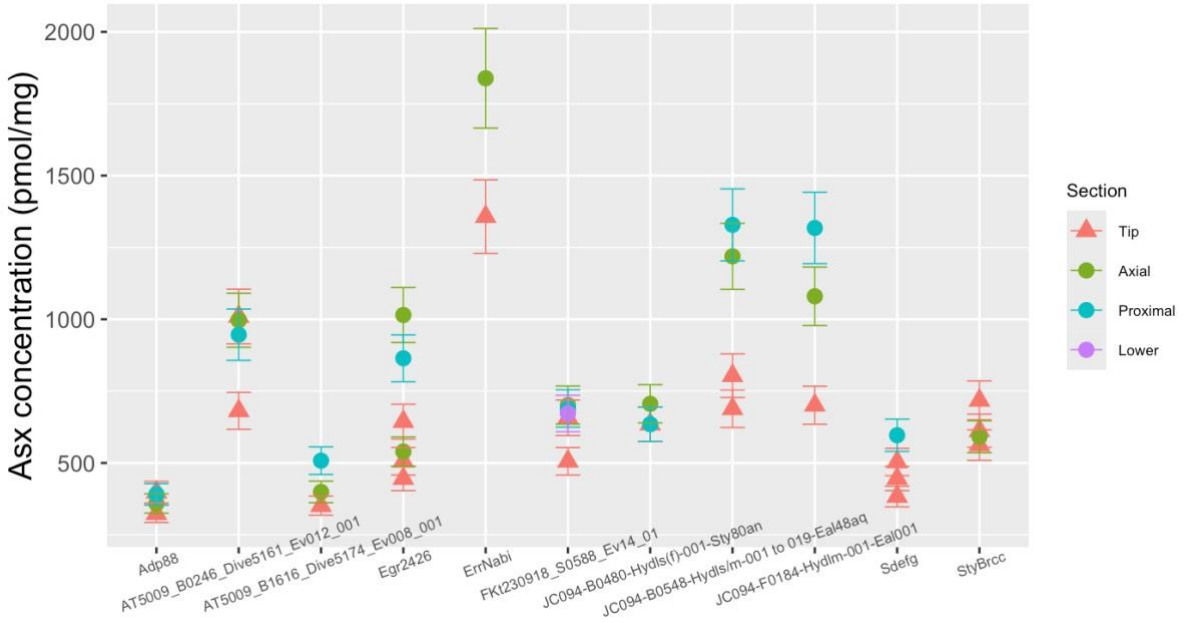

Figure 3.14: Internal Heterogeneity Asx concentration (pmol/mg) *stylasterid samples; error bars indicate the 7.5% preparative variability average across samples.* Colours and shapes *indicate the section of one branch being sampled from* Axial *being closest to the tip and* Proximal / Lower *being the furthest away.*

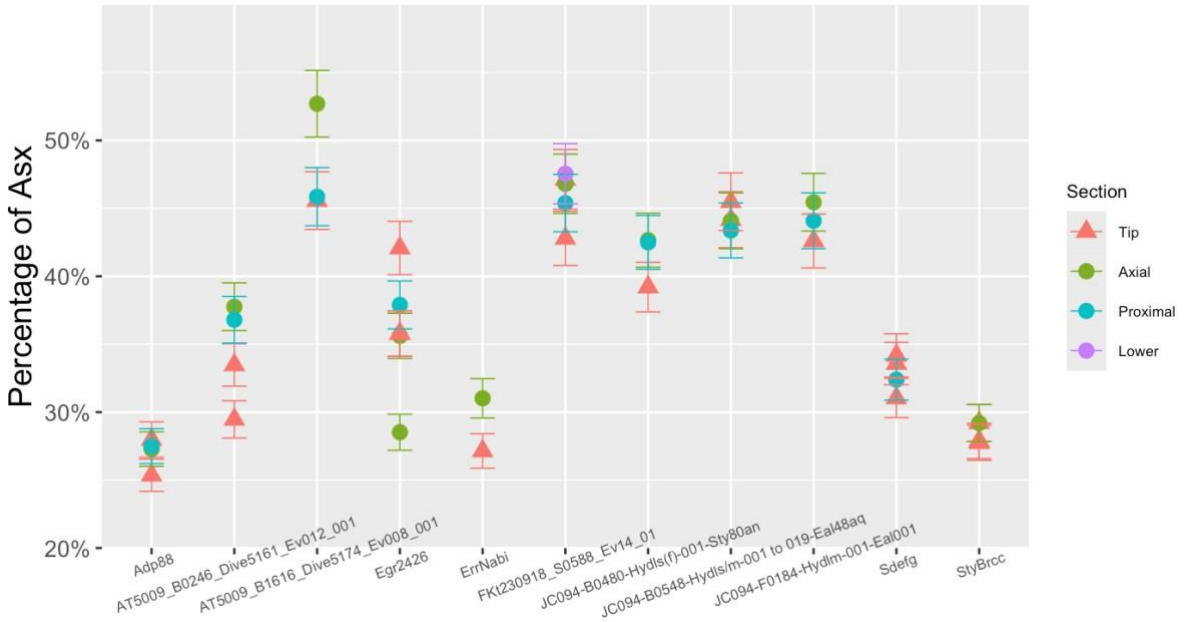

Figure 3.15: Internal Heterogeneity percentage of Asx stylasterid samples; error bars indicate the 7.5% preparative variability average across samples. Colours and shapes indicate the section of one branch being sampled from Axial being closest to the tip and Proximal / Lower, being the furthest away.

There are three exceptions to the increasing [THAA] and Asx concentrations from tip to base patterns (Fig. 3.13). StyBrcc is a sample that has all tips and a small amount of branched material, if not only the beginning. However, has still been included as the sample shows the variation of THAA (pmol/mg) within different

tips of the same coral. AT5009_B0246_Dive5161_Ev012_001 follows the pattern of lower concentrations in the tip to branches other than one sample (AT5009_B0246_Dive5161_Ev012_001), which introduces the question: have some tips stopped growing, and therefore the THAA are higher? Or could this be a defence mechanism while growing, due to environmental changes? It has been identified that shallow-water corals will grow slower when reacting to environmental changes, as studied by the research conducted by Shinn E.A, (1966). Furthermore, it has been identified that there is a general trend of decreasing total concentration of amino acids over the past 100 years within *Montastraea faveolata* (Nyberg *et al,* 2001). This general trend seen in shallow water corals is important as stylasterid corals are known to be able to live to 100 years (King, Rosenheim and James, 2024) as the decrease could be an indication of the small values seen within this study where tips are lower in THAA (pmol/mg) than the majority of branch material. If the corals are able to adapt to their environment the tips of the coral, the newly formed skeletal material, would be predicted to be different to older skeletal material. A variation in amino acids within the internal heterogeneity could be influencing results.

Within linear branches, there is still some (~5-34%) variation between each subsample taken. The coefficient of variance for the tip-to-branch average is ~18% and the linear branch coefficient of variance is 11.6%. It was expected that the linear branch would be less than the tip-to-branch samples, this is a similar testing process to the internal heterogeneity replication method. The difference between these replication methods, is that linear replication uses unrecorded sampling (due to the structure of the material being very similar) and the internal heterogeneity branch testing is recorded sections.

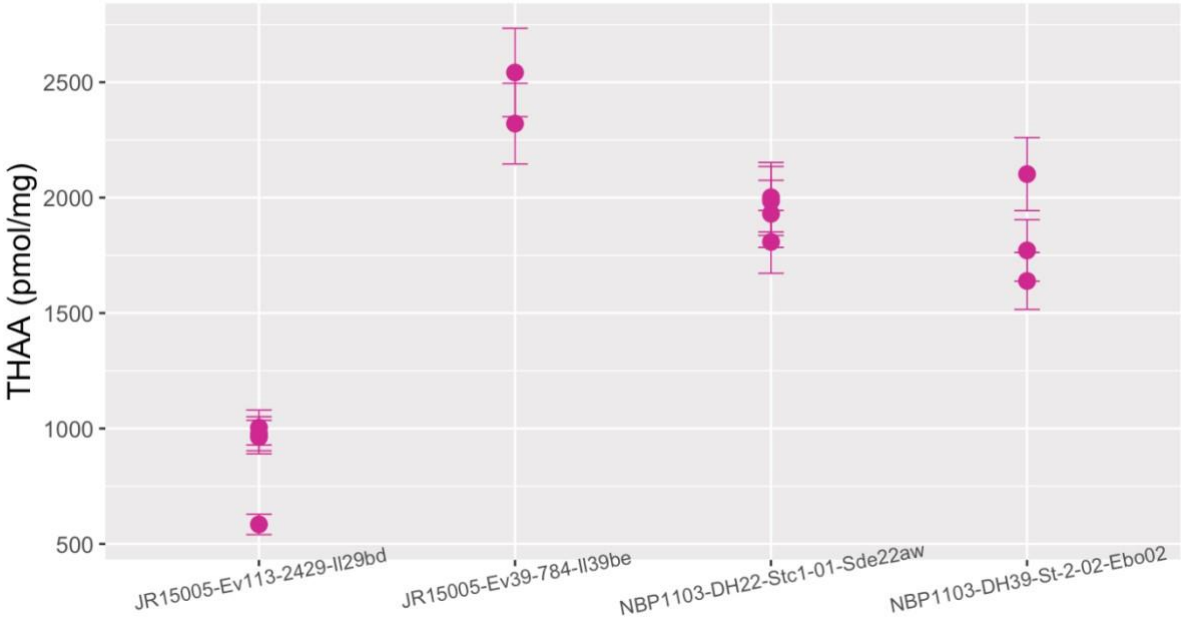

Figure 3.16 Internal Heterogeneity [THAA] of linear Branches (all Stylasterids) with 7.5% preparative error bars

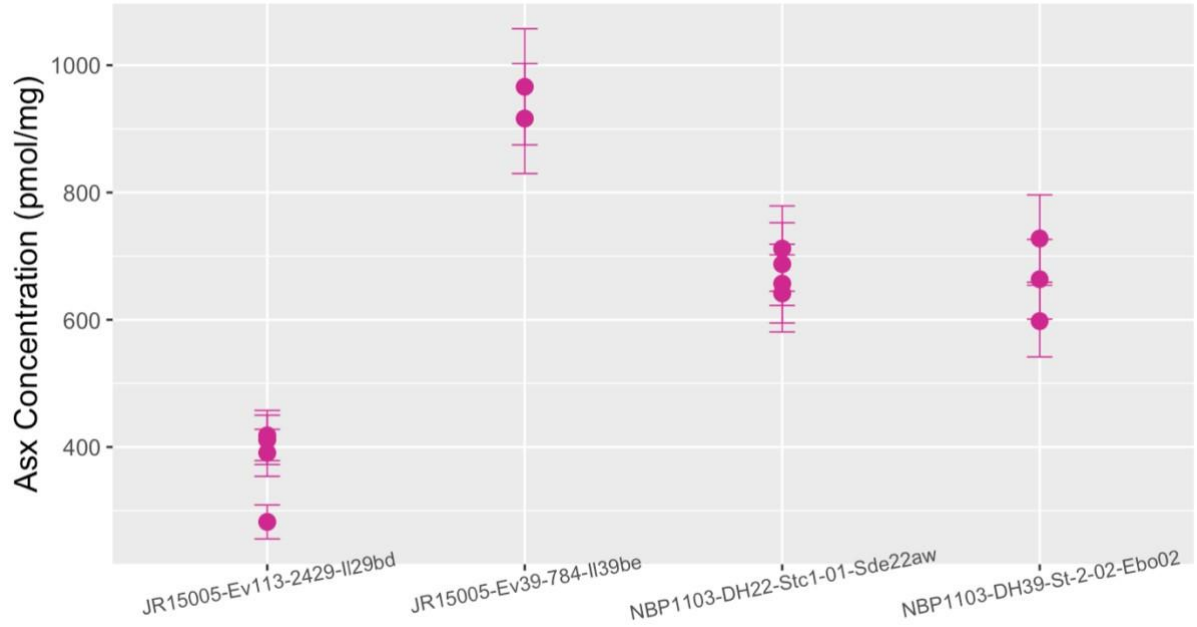

Figure 3.17, Internal Heterogeneity Asx concentration (pmol/mg) of linear Branches (all Stylasterids) with 7.5% preparative error bars

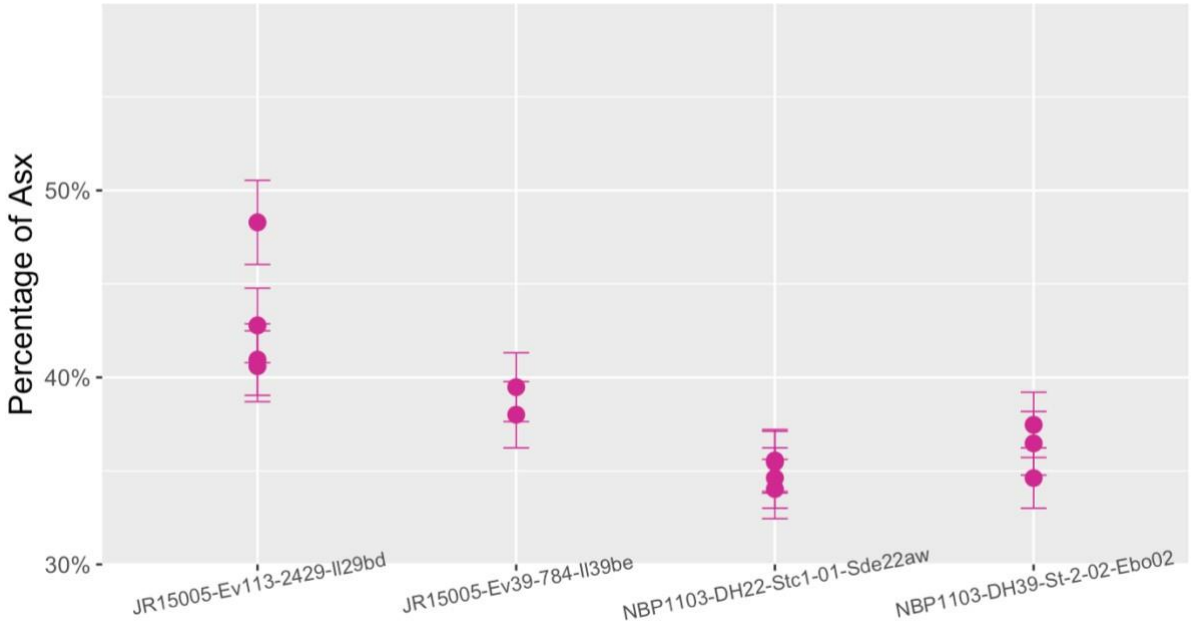

Figure 3.18, Internal Heterogeneity percentage of Asx of linear Branches (all Stylasterids) with 7.5% preparative error bars

There are clear differences between the amino acids within different sections of coral branches, leading to the question of what other variations there are between the different branch sections. Porosity of a branching scleractinian coral, *Acropora pulchra,* was studied by using 2D and 3D imagery. The imaging indicated that the corals are thicker further away from the tip of the coral;

however, the spacing of the skeletal elements did not change (Roche *et al*., 2010). This understanding of the thickening of material away from the tip could start to explain the small variation in the linear branch THAA (pmol/mg) and the tip-to-branch variation in THAA (pmol/mg) seen within the stylasterids analysed within this study.

Testing the internal heterogeneity showed that the range of total hydrolysed amino acid concentration variation within recorded sections of the coral is 10.87% more (average = 18.4%) variable within THAA than in the preparative replicates (average = 7.53%) and 14.33% more variable than analytical replicates (average = 4.07%).

Ampullae on stylasterid corals

Another factor that came into question when looking at the internal heterogeneity of the corals and the variation of amino acids within the skeletal material of stylasterid corals was the identification of ampullae. Ampullae in stylasterid corals are known to hold the gonophores (reproductive structures) of stylasterid corals, where it is thought the fertilised egg will crawl out of the ampullae and settle close to the original colony (Brooke and Stone, 2007). The ampullae also indicate the sexual dimorphism of the coral, with rounded external ampullae indicating the female colony; male ampullae are internal and often not visible until they are mature and small 'pits' develop or are much smaller and more numerous than female ampullae (Cairns, 2005). This visible distinct difference between male and female colonies could, therefore, have implications for the amino acids that are being used to form skeletal material, due to protein differences within the chromosomes. Ampullae in stylasterid coral cn be seen in figures 19-21, chapter 3, pages 52/53. Protein differences between the male and female sexes have been identified within the dental enamel protein amelogenin of multiple different taxa, although it is not identified if there are amino acid differences. Within the amelogenin X and Y proteins, it can be suggested that different proteins will use different amino acids (Cappellini *et al*., 2019). This is important for the ampullae of stylasterid corals as the identification of different sex proteins used within enamel could be a theory that could be applied to stylasterids, allowing them to change the skeletal morphology to develop the ampullae within the calcium carbonate.

Unfortunately, this identification and understanding of ampullae sex differences within the stylasterid coral was not discovered until towards the end of the lab work for this study. Therefore, the sexes and logging of ampullae were not reported and could not be identified in differences of amino acids. However, ampullae could account for the variation in some internal heterogeneity. Testing of the amino acids specifically within the ampullae is something that should be considered for future work. Remaining samples from this study have ampullae intact and therefore would be beneficial to look at in future studies.

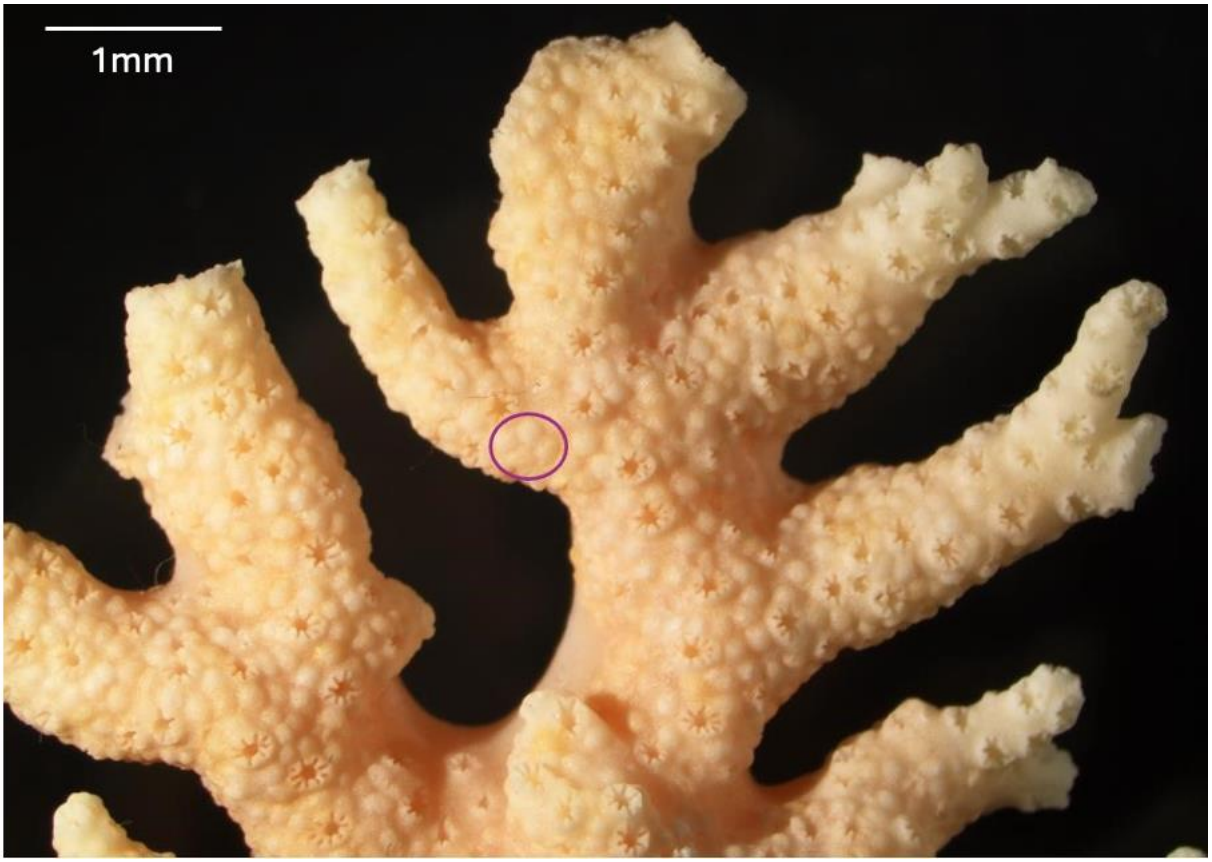

Figure 3.19: Microscope image of sample AT5009_B0246_Dive5161_Ev012_001, with purple circle indicating where ampullae can be seen. From the amount of ampullae it could be inferred that this sample is male.

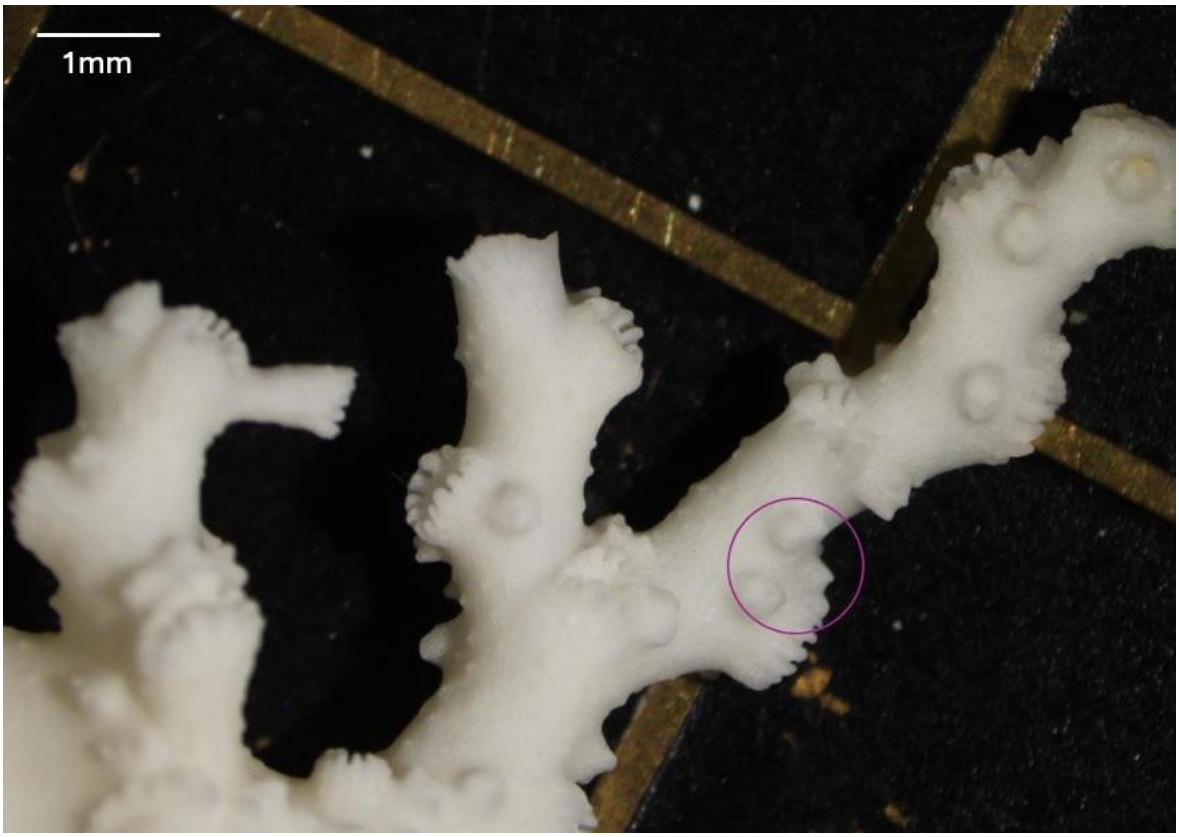

Figure 3.20, Microscope image of sample AT5009_B0193_Dive5172_Ev006_001, with purple circle indicating where ampullae can be seen. Fewer, larger ampullae could indicate a female coral

Figure 3.21, Microscope image of sample FKt230918_S0588_Ev14_01, with purple circle indicating where ampullae can be seen. Fewer ampullae could also infer female coral.

3.5.2 Scleractinian corals

Internal heterogeneity testing in scleractinian corals was more challenging for this experiment, as the structure of the scleractinian coral samples was not a full representation of the primary coral. Five scleractinian corals had internal heterogeneity examined on them. Most primary Scleractinia coral samples contained the septa; therefore, the internal heterogeneity analysis aimed to look at amino acid composition from the centre (where the growth of the coral started) to the ends of the septa. Sample DY081-031-ROV333-Ev033-201-570-Loph A, a cup coral, physically appeared to have a fuller growth range from the centre of the coral to the septa, forming better linearity of the analysis. Another factor that influenced the testing of the internal heterogeneity of scleractinian corals is the strength of the skeletal material in comparison to stylasterid corals. The material was much thicker and resistant to cutting, making it hard to select the particular pieces of the septa, (the septa is seen in Figure 3.22, chapter 3, page 55). This meant that most of the linearity, which was attempted to be tested in the stylasterid corals, was lost in the Scleractinia corals, and therefore was not tested for.

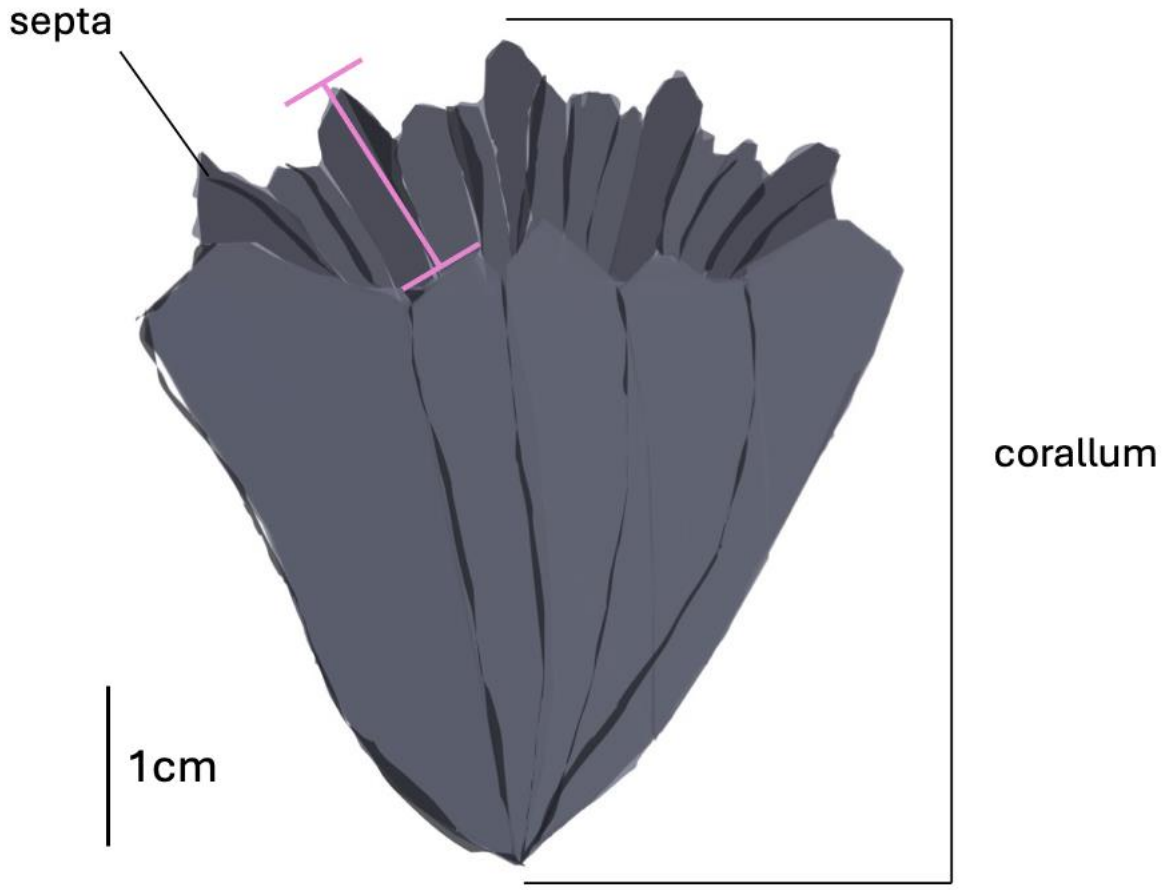

Figure 3.22: Diagram of Scleractinia solitary cup coral (Desmophyllum) with sections of the anatomy described. The pink section indicates the targeted section of initial Scleractinia samples.

The internal heterogeneity for [THAA] ranges from 3.9% - 46%, with an average of 21.6%, this is the most considerable variability seen within any of the tests completed within the replicability testing. The largest variation is seen within *JC094-15-EBA-ROV227-SLP46-B0018-Carlm-001,* belonging to the genus of *Caryophyllia.* This is the only sample of Caryophyllia tested within the internal heterogeneity of scleractinian corals. The error of Asx concentration for scleractinian internal heterogeneity had an average of 20% with a range of 4.7-45.3 and the percentage of Asx an average of 6.45 with a range of 1.04 - 22.2.

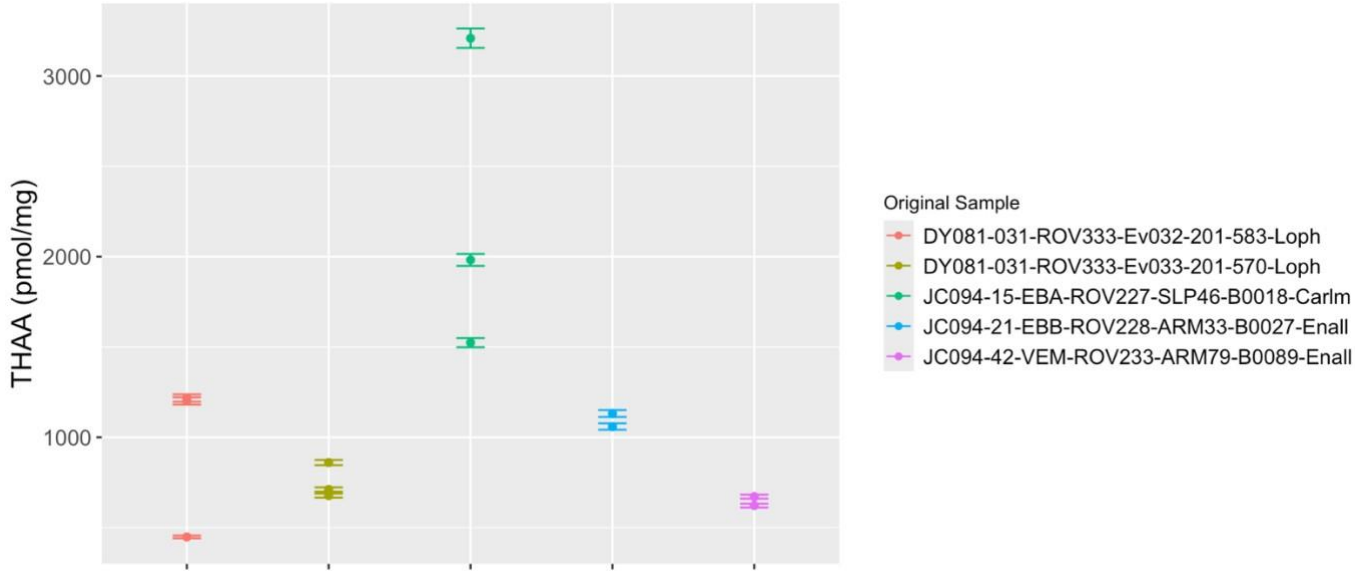

Figure 3.23, Scleractinian coral sample for the [THAA] internal heterogeneity with error bars of 1.67% representing the analytical variability.

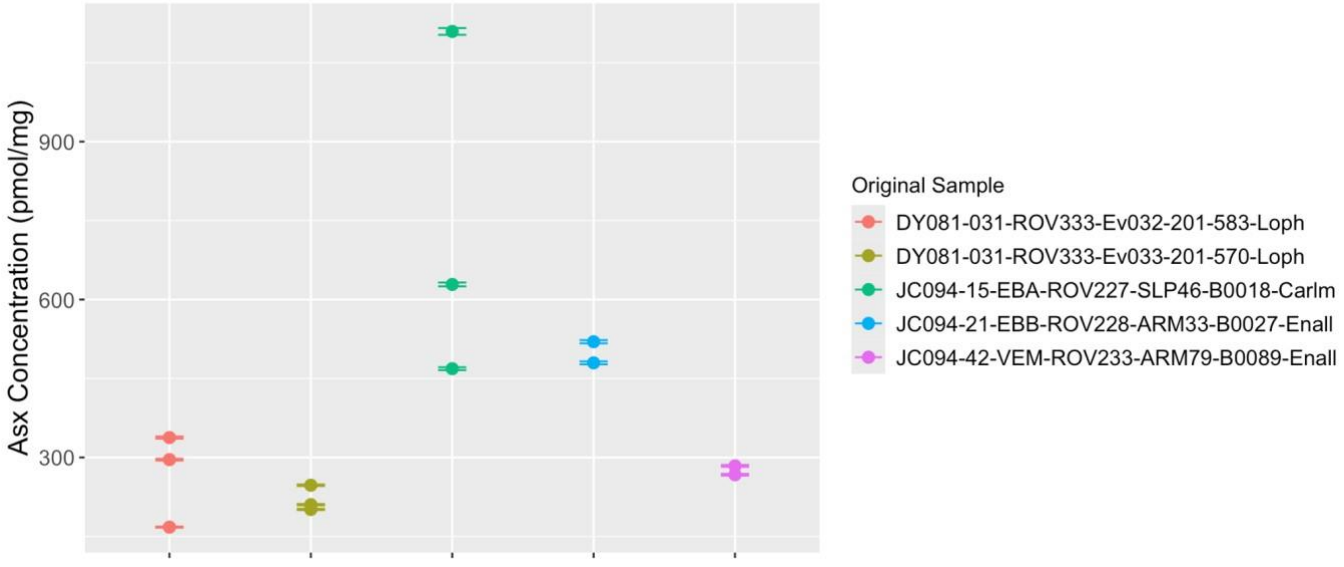

Figure 3.24, Scleractinian coral sample for the internal heterogeneity Asx concentration (pmol/mg) with error bars of 1.67% representing the analytical variability.

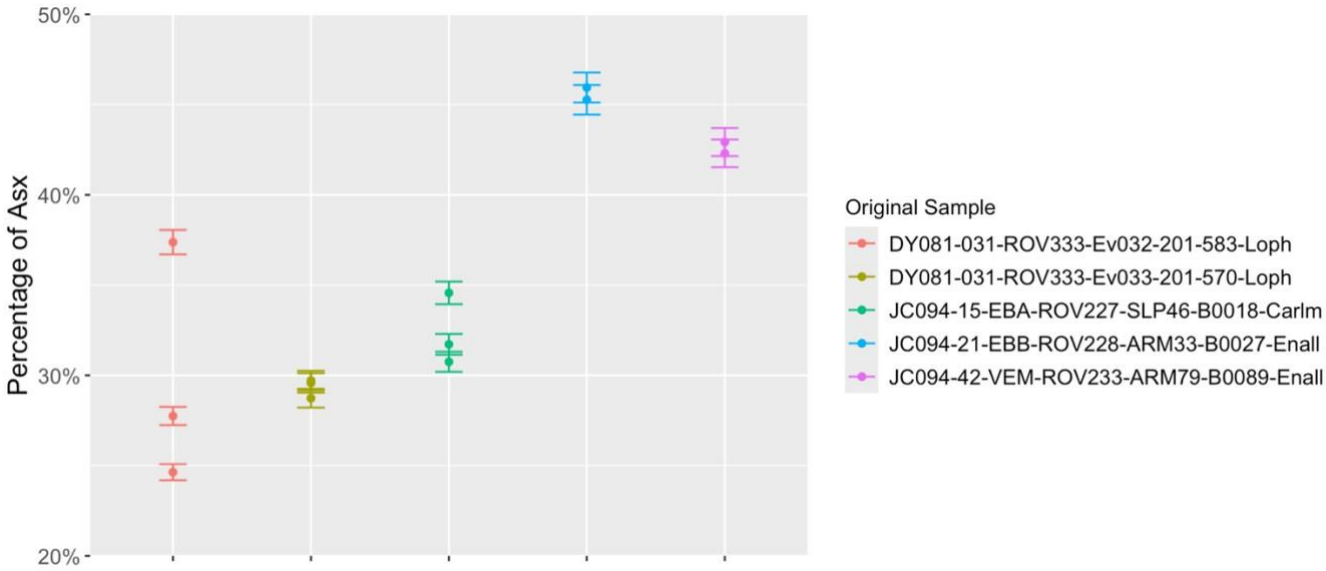

Figure 3.25: Scleractinian coral sample for the internal heterogeneity, percentage of Asx with error bars of 1.67% representing the analytical variability.

Although sampling of scleractinian corals was more challenging to follow a pattern, the large variation of [THAA] and Asx concentration indicates that there is variation within different parts of scleractinia coral skeletal material. Sampling in a more patterned way on a fuller coral sample would help to see if this is true for other samples. Using a whole coral and sampling from the base to the very end of the branches in a targeted sampling stratergy, would help cover questions raised from this smaller testing structure. Furthermore, analysis of branching Scleractinia would be beneficial to compare structural differences and determine if they, too, are following the same patterns as stylasterids tested within this study.

3.6 Comparison of replication

Stylasterid analytical replicates

	THAA (pmol/mg)		Asx Concentration		Percentage of Asx	
Sample	CoV (%)	Range	CoV (%)	Range	CoV (%)	Range
Stylasterid Analytical	4.07	1.12 – 8.57	3.02	0.25 – 6.13	4.41	1.25 – 11.4
Scleractinia Analytical	1.67	1.08 – 5.77	0.58	0.37 – 0.76	1.81	0.42 – 3.08
Preparative	7.53	1.23 – 8.85	9.43	4.74 – 22.2	4.66	1.25 – 13.9
Internal Heterogeneity (Tip-Branch)	18.4	5.33 – 29.2	19	6.21 – 31.6	6.19	1.99 - 16
Internal Heterogeneity (Linear branches)	11.6	4.53 – 22.6	8.76	3.75 – 16.9	4.25	2.09 – 8.24
Internal Heterogeneity (Scleractinia)	21.6	3.9 - 46	20	4.7 – 45.3	6.45	1.04 – 22.2

Table 7, Comparison of replication between total concentration, Asx concentration and percentage of Asx for the range and coefficient of variance.

The magnitude of analytical variability is the lowest of the replication hierarchies (Table 7, chapter 3 , page 58), followed by preparative replication and then internal heterogeneity. In StyBrcc the magnitude of analytical variability is much lower and similar to preparative replication results. StyBrcc internal heterogeneity analysis was focused on looking at only the tips of the skeletal material, rather than the tips and branches or longer linear material. This is an indication that the internal heterogeneity of samples has varied amino acids, dependent on the skeletal material position. The composition of the amino acids within the coral samples is also crucial to compare throughout the replicate analysis, as this shows the way amino acids are changing in each section within the corals.

Each of the samples tested has been shown to have a different concentration and percentage of amino acids. One specific genus that stands out is *Errinopora*, ErrNabi has a much higher THAA (pmol/mg) concentration than other samples tested, and this is confirmed within the replication results. *Errinopora* samples are also seen to have the largest variability through the replication tests

conducted for stylasterid corals. However, the internal variability within scleractinian corals is larger than in stylasterid corals; this large range is seen due to two samples (DY081-031-ROV333-Ev032-201-583Loph and JC094-15-EBA-ROV227-SLP46-B0018-Carlm). This range could be an indication that there is a change in the amino acids throughout the skeleton of scleractinian corals like the tip-to-branch stylasterid sample and should be studied in the future.

The THAA, Asx concentration and percentage of Asx variation are smaller in analytical replication (Table 7, chapter 3, page 58), in both stylasterid corals and Scleractinian corals (stylasterid averages: THAA = 4.07 pmol/mg, Asx concentration = 3.02 pmol/mg, percentage of Asx = 4.41%. Scleractinia averages: THAA = 1.67 pmol/mg, Asx concentration = 0.58 pmol/mg, percentage of Asx = 1.85%). This is an expected result as the sample is just a reinjection from the same homogenised powder that has been bleached, hydrolysed and then rehydrated.

The preparative replication method differs as the homogenised powder is separated after being ground in a pestle and mortar. Each vial with powder is then treated as a separate sample for further steps, including bleaching, hydrolysis and rehydration. The variability is increased as each step of the method introduces another level of uncertainty. The skeletal material taken from the initial sample to create the homogenous powder is also a larger piece of skeletal material, therefore introducing
skeletal material variability. This is seen to be important within the internal heterogeneity replication method.

The replication of internal heterogeneity within tip-to-toe branches and linear branches is more variable for THAA, Asx concentration and percentage of Asx compared to replication undertaken on analytical samples and preparative samples (figures 3.26 – 3.29, chapter 3, pages 60-63). The recording of which part of the initial sample has been taken and then had analysis completed has been crucial to understanding that variability could linked to skeletal material positioning. This would be why there is an increase in the variability from analytical replicates to preparative replicates and to internal heterogeneity replicates.

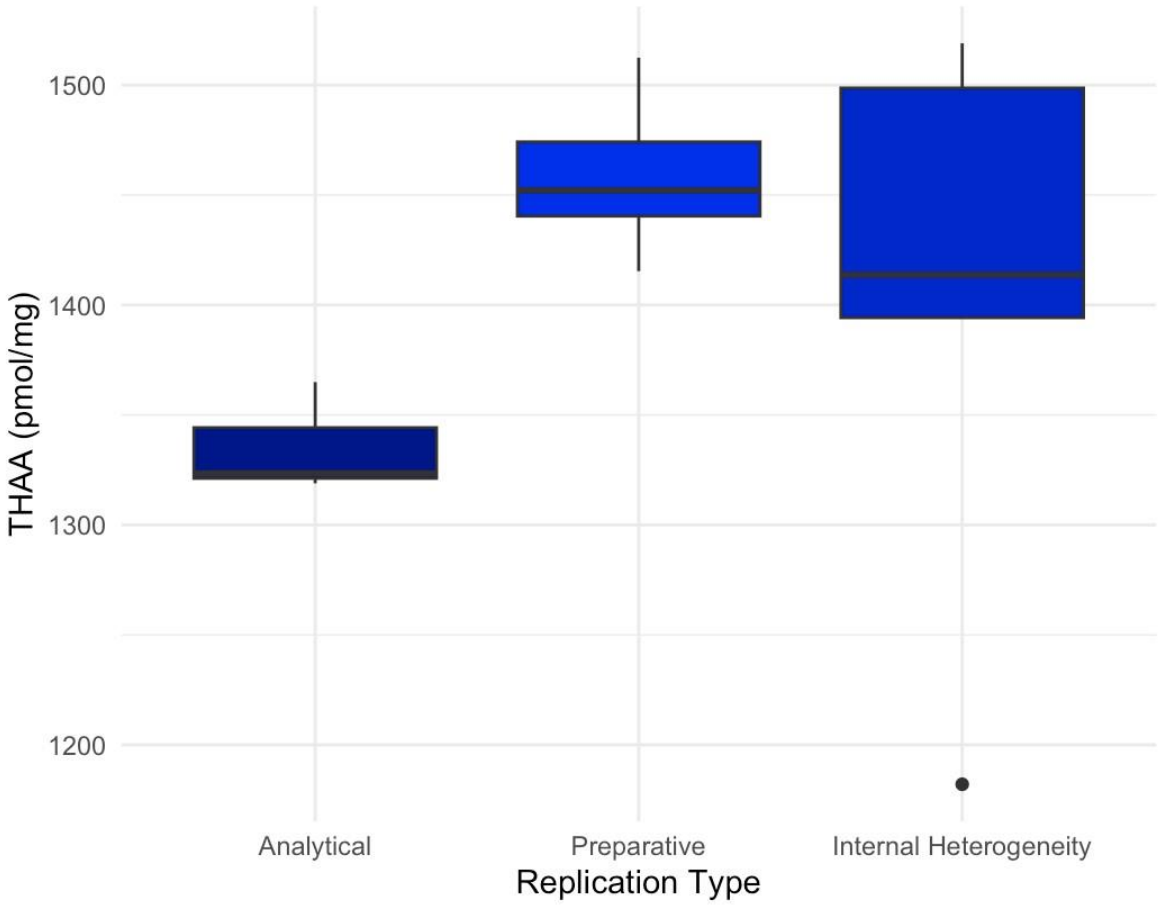

Figure 3.26: *Box plot of sample Fkt230918_SO588Ev14_01 comparing the THAA (total hydrolysed amino acid) concentration for analytical replicates, preparative replicates and internal heterogeneity. With the whiskers indicating the minimum and maximum of the data set, the interquartile range ranges from the 25th percentile to the 75th percentile. The bold line at the centre of the interquartile range indicates the median.*

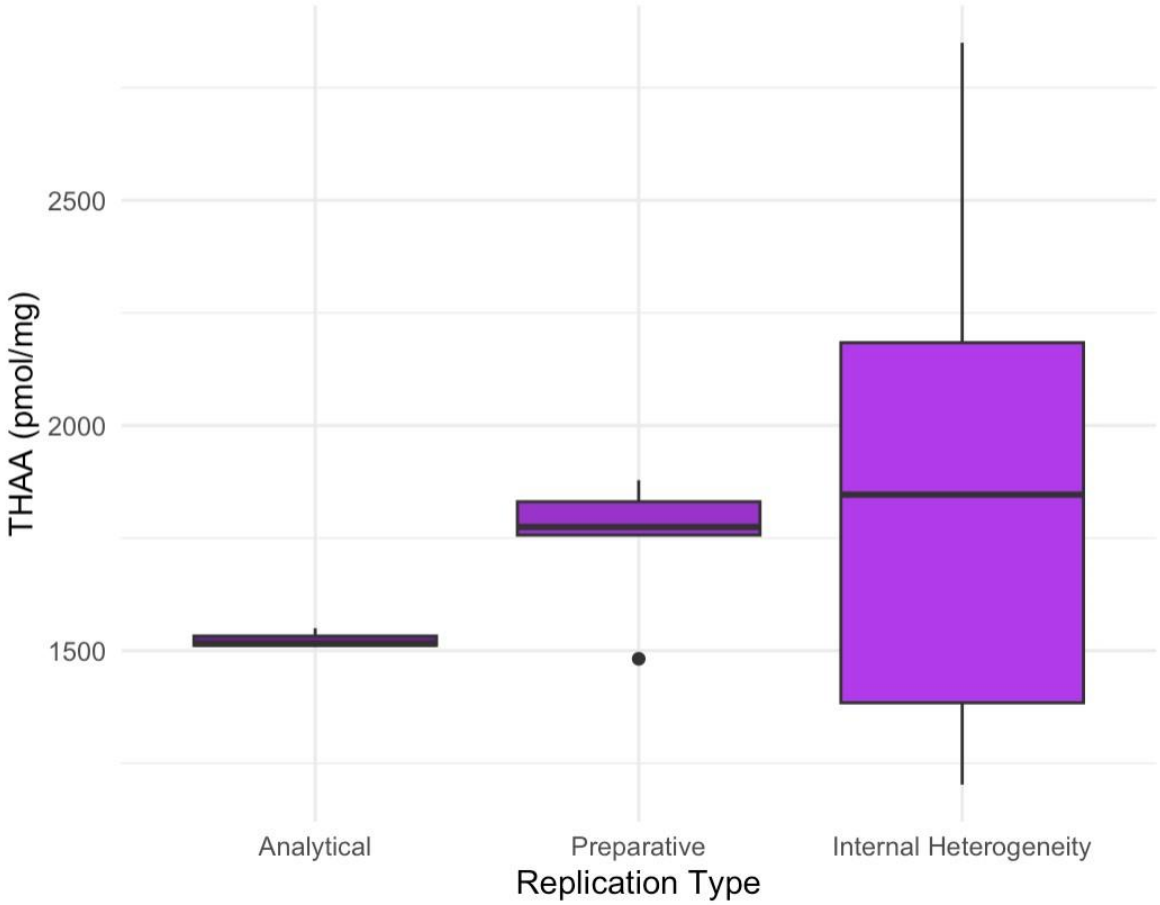

Figure 3.27, Box plot of sample Egr2426 comparing the THAA within analytical replication, preparation replication and internal heterogeneity. With the whiskers indicating the minimum and maximum of the data set, the interquartile range ranges from the 25th percentile to the 75th percentile. The bold line at the centre of the interquartile range indicates the median.

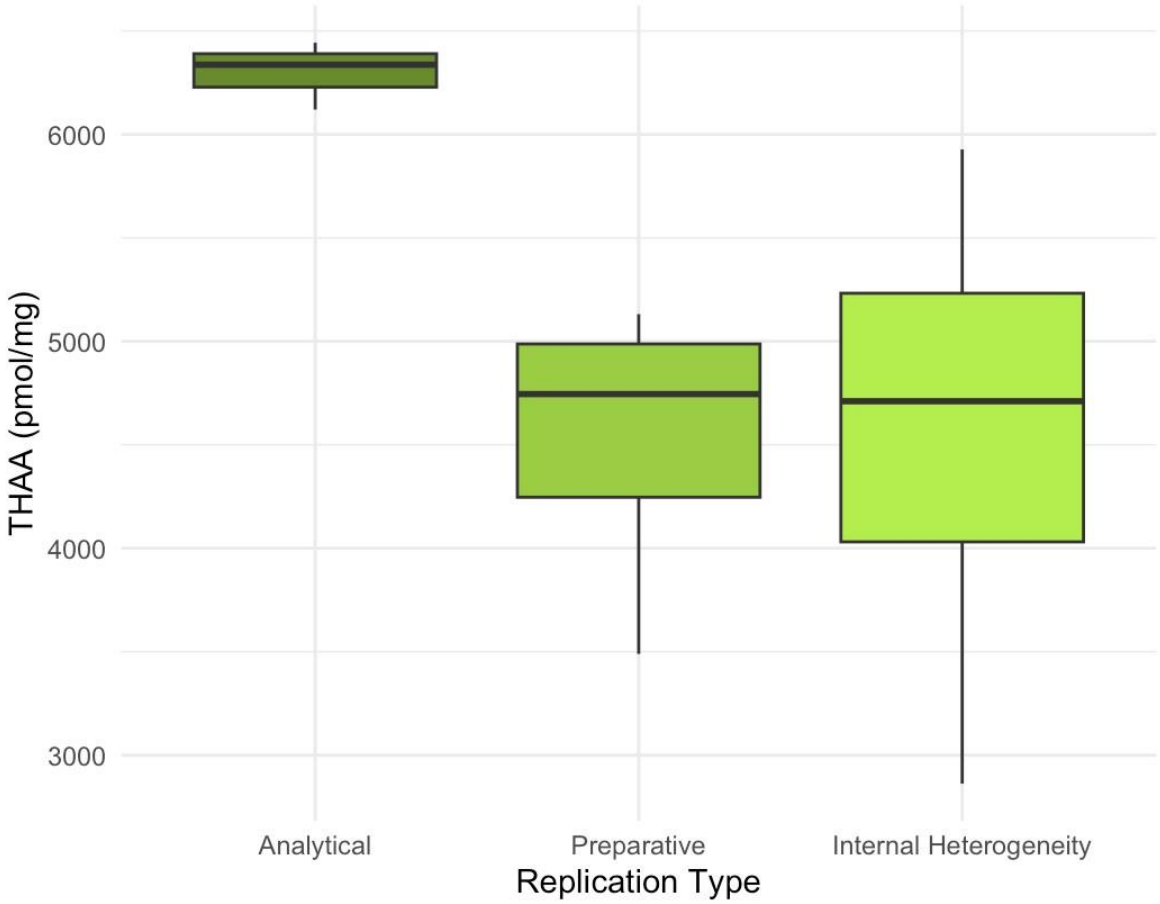

Figure 3.28, Box plot of sample ErrNabi comparing the THAA (Total hydrolysed amino acids) within analytical replication, preparation replication and internal heterogeneity. With the whiskers indicating the minimum and maximum of the data set, the interquartile range ranges from the 25th percentile to the 75th percentile. The bold line at the centre of the interquartile range indicates the median.

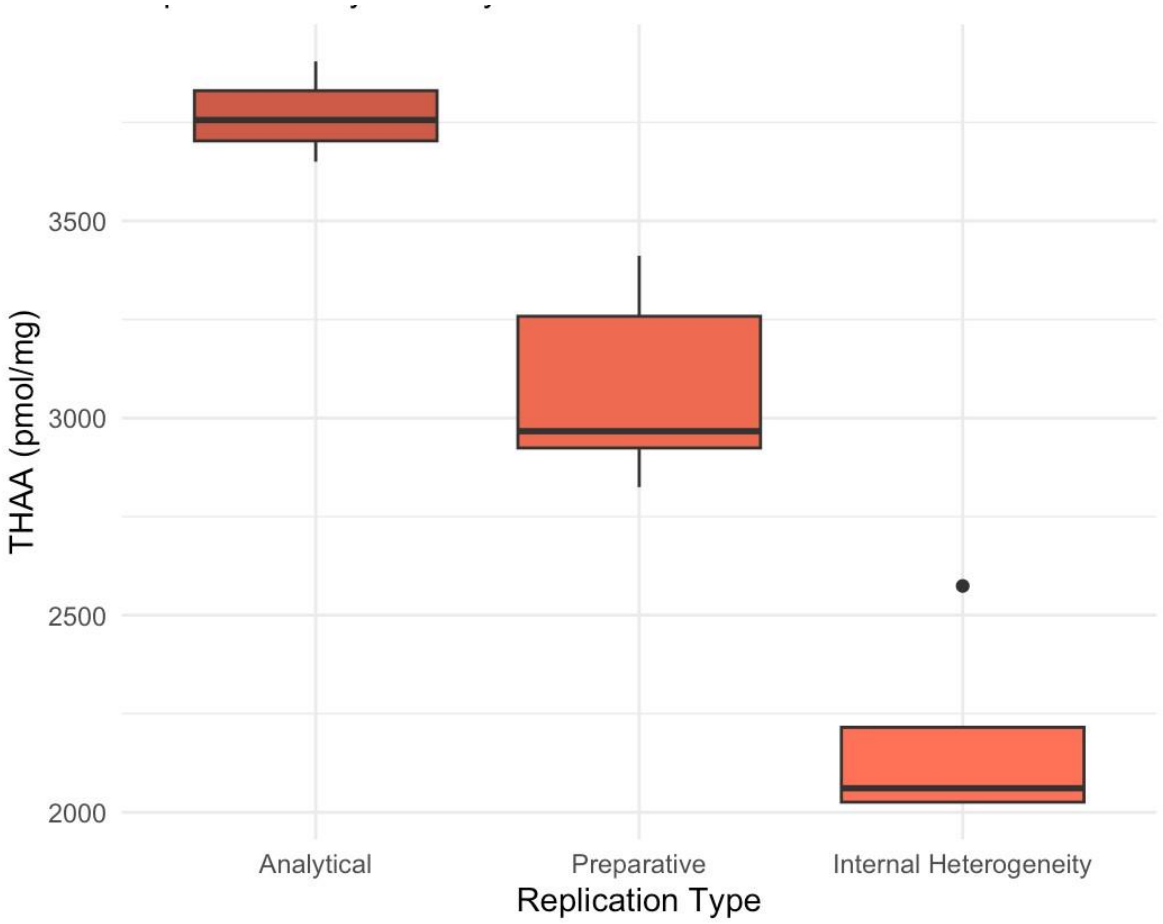

Figure 3.29, Box plot of sample StyBrcc comparing the THAA (Total hydrolysed amino acids) within analytical replication, preparation replication and internal heterogeneity. With the whiskers indicating the minimum and maximum of the data set, the interquartile range ranges from the 25th percentile to the 75th percentile. The bold line at the centre of the interquartile range indicates the median.

As expected, Figures 3.26-3.29, (chapter 3, pages 60-63) visualise that the preparation replicates have a large variation of results and a larger coefficient of variation than analytical replication (7.5% compared to 4%). This variation could come from a range of factors, for example, lab temperature, chemical reagents having slightly different concentrations or human error when measuring. But also from the skeletal variability, as seen within the internal heterogeneity.

3.7 Conclusions

It is clear that the analytical replicates have the least amount of variability, then the preparative replicates, with internal heterogeneity exhibiting the greatest variation. It is important to understand the inherent variability within and between samples in order to properly assess any differences related to taxa, environment, etc. The study of internal heterogeneity has also indicated a potential pattern between tips and other branches throughout the corals.

To confirm the pattern seen in the internal heterogeneity study, it would be helpful to observe where any of the original samples had been taken from compared to the primary coral and then undertake further internal heterogeneity testing from this. Further study should also focus on the most complete primary corals and measure the distance between each smaller sample taken from the coral.

It would also be beneficial to complete protein sequencing on the internal heterogeneity samples to see if there are any variations, especially between the tips where the THAA is lower than the branches. Like those within *Acropora millepora* and *Acropora palmata*, where it was seen that the corals are selecting proteins that would make them more resilient to environmental factors (Voolstra *et al.*, 2011). Two species of Caribbean Acropora tested indicated differences in the gene expression of the branch tips and bases (Hemond, Kaluziak and Vollmer, 2014). If there is variation in shallow corals, there is the possibility of gene expression between branch tips and bases in deep-sea corals. The variation between the tips and the branches could be from new skeletal material growing in different environmental conditions, to the material further in the main body of the coral. This could be an indication of resilience or vulnerability to climate change as discussed above with the evolution of decreasing THAA (pmol/mg) in scleractinian coral over the past 100 years (Nyberg *et al*, 2001).

4 Chapter 4 - Results: Is the composition of Amino Acids influenced by Taxa, Genus or mineralogy?

In this results chapter, the amino acid composition by genus between stylasterid corals and Scleractinia corals was observed. The first part of this chapter will cover the amino acids seen within Scleractinia and stylasterid corals, and the second will cover how amino acids vary within the mineralogy of corals.
Aims for the first half of this section:

1. To identify the amino acids within each genus tested of stylasterids
2. To identify the amino acids within each genus tested of Scleractinia

It has been hypothesised that there will be different amino acids within the genus and mineralogies of different corals. Therefore, all the amino acid data for all the samples tested within this study have been used to test these hypotheses, including the replicate data.

Lysine is not accounted for within the percentage of full amino acids as it is the most hydrophilic amino acid accounted for within the method used. Therefore, it comes out at the very end of the chromatograms and can be disguised with inorganic matter. The inclusion of inorganic matter being recorded around the same time as lysine means it can be hard to differentiate and therefore has not been accounted for (Figure 4.1, chapter 4, page 65).

Sample Info : JR15005-38-775-Egr775 - Species: Errina sp. mixed (arag.) Mineralogy: Mixed - Coral Colour: White Location: S. Orkney - Depth (m): 727 - Bleach info: Bleached 48h, hyd 24h at 110C - " Rehydration Volume (ml): 75 "NeARR No: 17491BH*

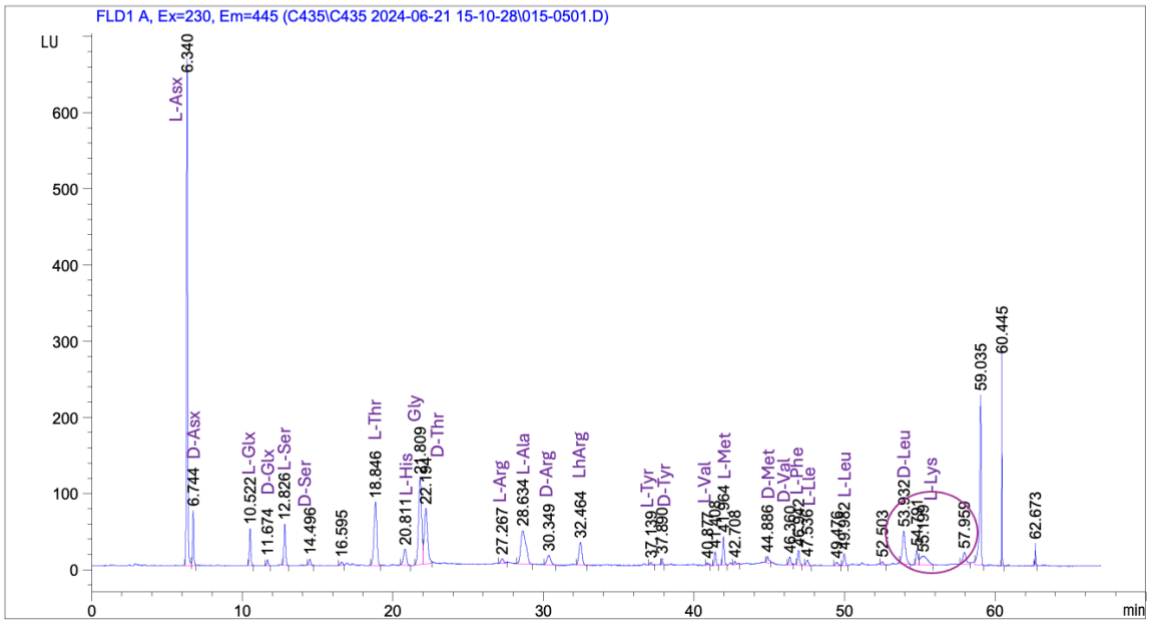

Figure 4.1, A Stylasterid chromatogram with the purple circle indicating a larger more uneven Lys peak than expected

4.1 Stylasterids

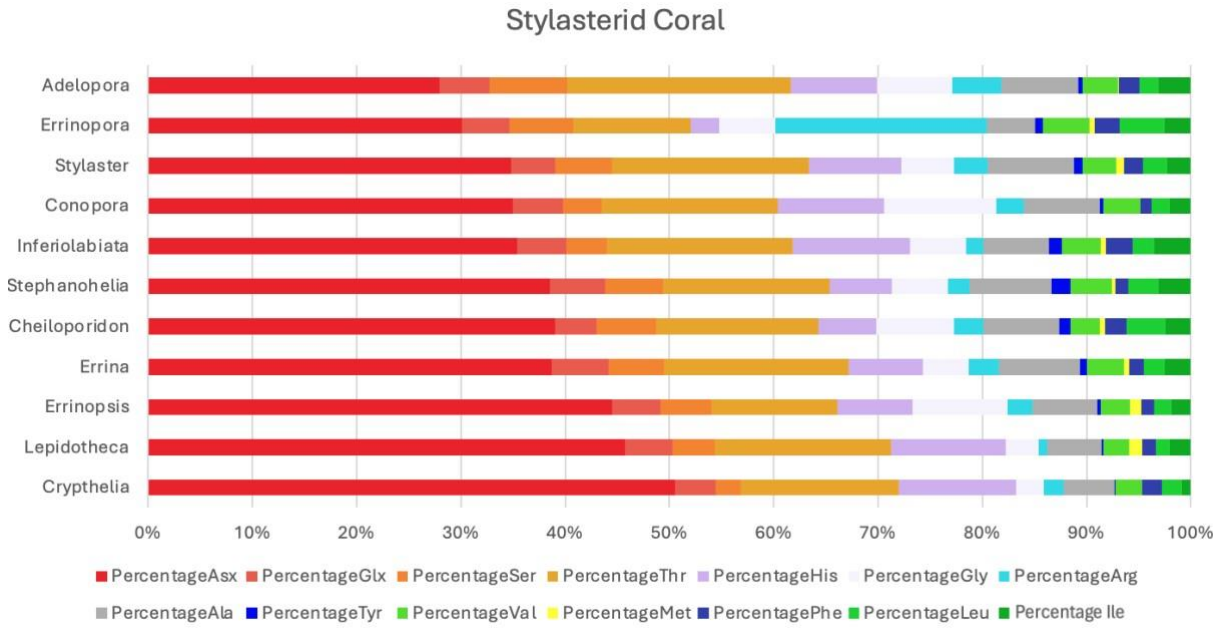

Figure 4.2, Amino acid composition of Stylasterids by genus(N=216, Adelopora =9, Errinopora =31, Stylaster =77, Conopora =2, Inferiolabiata =12, Stephanohelia =1, Cheiloporidion =3, Errina =41, Errinopsis =10, Lepidotheca =22, Crypthelia =7) . Found using the average percentage of each sample within the genus using all samples.

Colouration follows the descriptive variables of RasMol to indicate acidity change in amino acids.

Deep-sea stylasterid corals generally follow a similar composition pattern to each other. That of being very dominant in Asx, (between ~30% - 50%), a combination of aspartic acid and asparagine, and much lower in other amino acids (Figure 4.2, chapter 4, page 66). This dominance of aspartic acid is the same among the range of shallow-water corals (Rahman and Tamotsu Oomori, 2008). Threonine (Thr), is the second most dominant amino acid, between ~13% - 20%, seen within most stylasterid corals; however, *Errinopora* is the exception to this pattern, figure 4.1 (chapter 4, page 65).

Errinopora has much less Thr (~10%) and Asx (30%) than the other tested stylasterid corals within the study, with the exception of *Adelepora*. Instead, there is a much larger quantity of arginine (Arg) seen within the composition of the *Errinopora*. There is also much less Histidine within the composition of the *Errinopora*. Physically, *Errinopora* is different to other stylasterid corals too; the body of the coral is much flatter with fewer branch-like structures, which are also thicker and grow from the body of the main structure (Cairns and Lindner, 2011). The difference in the amino acid composition of *Errinopora* could indicate a difference in skeletal protein compared to other Stylasterids. The samples of *Errinopora* are also the shallowest samples within the study. When testing by genus, the average percentage of each amino acid was calculated.

Crypthelia found within the Galapagos presented the highest amount of Asx compared to other Stylasterid corals tested within this study. Again, the physical properties of *Crypthelia* are very different to other stylasterid corals, although the coral itself branches out with thin, intricate structures. The polyps of the coral are much larger in comparison to the body of the coral, and they often protrude from the branches of the coral, with small cover-like structures to protect the polyp from external threats.

4.2 Scleractinia

Scleractinia corals tested within this study are physiologically very different from stylasterid corals. They do not branch with polyps covering their body like stylasterid corals. They have one main structure and one main polyp. The testing of the material for the Scleractinia was focused on the septa (indicated in Figure 3.22, chapter 3, section 3.5.2, page 55), to keep the variation of the material used to a minimum. This is because it was predicted that the internal variation of heterogeneity could be seen in different parts of the Scleractinia corals.

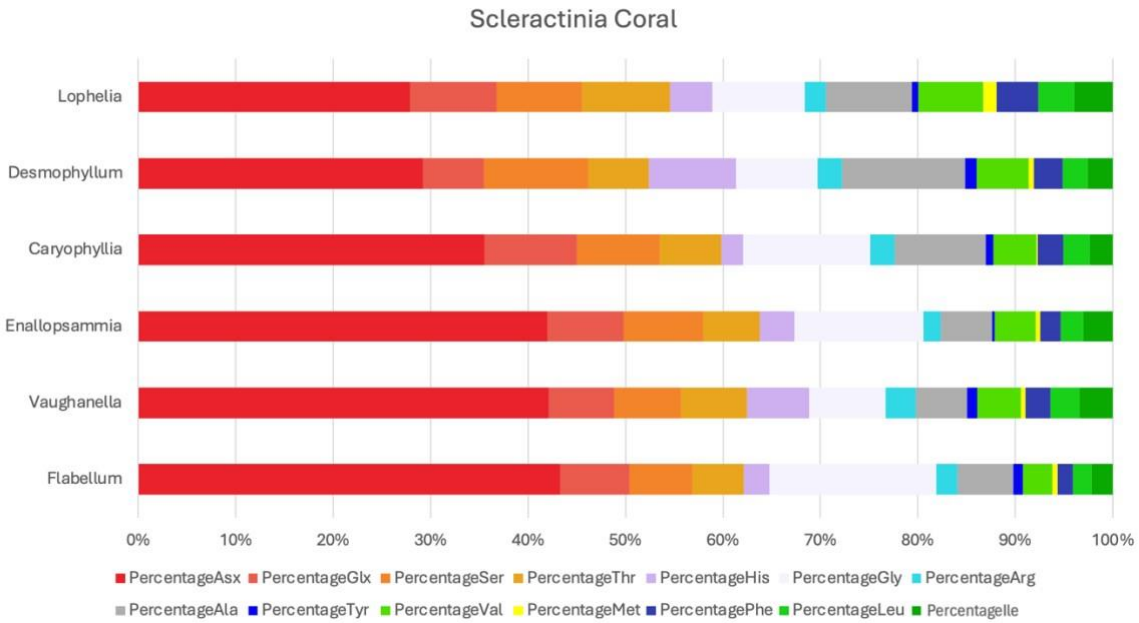

Figure 4.3, Amino acid composition of Scleractinia by genus, (n = 74, Lophelia =16, Desmophyllum = 7, Caryophyllia = 17, Enallopsammia =16, Vaughanella =3, Flabellum =15). Found using the average percentage of each sample within the genus using all samples only. Colouration follows the descriptive variables of RasMol to indicate acidity change in amino acids.

Lophelia is the lowest average percentage of Asx seen within and of the tested corals of the study. The percentage of methionine within Lophelia is the largest percentage seen within any coral tested within this study. Methionine is often lost from the method, as it oxidises during the hydrolysis process and therefore does not read strongly in chromatograms.

Flabellum contains the largest amount of Asx and glycine (Gly) among the other scleractinian corals tested. This shows a comparable decrease in histidine (His), indicating a variation of skeletal proteins being used to precipitate calcium carbonate from the matrix of the corals.

4.3 Discussion and conclusions for amino acids by genus

Asx dominates at an average of 37% (16.3 – 61.6) within all deep-sea coral samples tested within this study, both stylasterid and Scleractinia. Following patterns seen within shallow water corals that have been seen to use CARP and SAARPs. The amount of Asx used within each genus of coral varies, this could be influenced by biological controls or environmental controls. The proteins used within the process of biomineralisation could be influencing the physiological structure of the coral, indicating why some amino acids are much more abundant than others.

The composition of deep-sea scleractinian amino acids follows a pattern that many other shallow water scleractinia corals have (Gupta, Suzuki and Kawahata,

2006), with Asx, aspartic acids and asparagine dominating the composition of all the samples tested within this study, up to ~42%. On average, the amount of Asx within scleractinia is lower than in the Stylasterid corals sampled (stylasterids ~37.5% and scleractinia ~35.7%). The percentage of Threonine is lower than seen within Stylasterid corals, but Glycine is much larger. Glycine is a very stable amino acid and will preserve material better.

The variation in amino acid percentages within stylasterid corals ranges from 21.3 % compared to the amino acid percentages within scleractinia corals, 18.2%. There is also variation between genera of deep-sea corals. *Errinopora,* within the stylasterids, has the second-lowest amount of Asx out of all of the genus; however, it has the largest amount of Arg seen within any of the corals analysed as discussed above. *Errinopora* samples tested within this study are also high-Mg. Therefore, it is important to understand variation in amino acids by mineralogy.

4.3.1 Concentrations of amino acids by coral genus

The composition of amino acids had been averaged by genus; however, it is beneficial to see the relationship between the total concentration of amino acids to other specific amino acids. Asx was compared as it is the most abundant amino acid found within this study, Arg was compared due to the large quantity seen specifically in *Errinopora, and* Ala as there is roughly the same concentration between stylasterid corals and Scleractinia corals, around 5-10% (seen within Figures 4.4 and 4.3, chapter 4, pages 66/67).

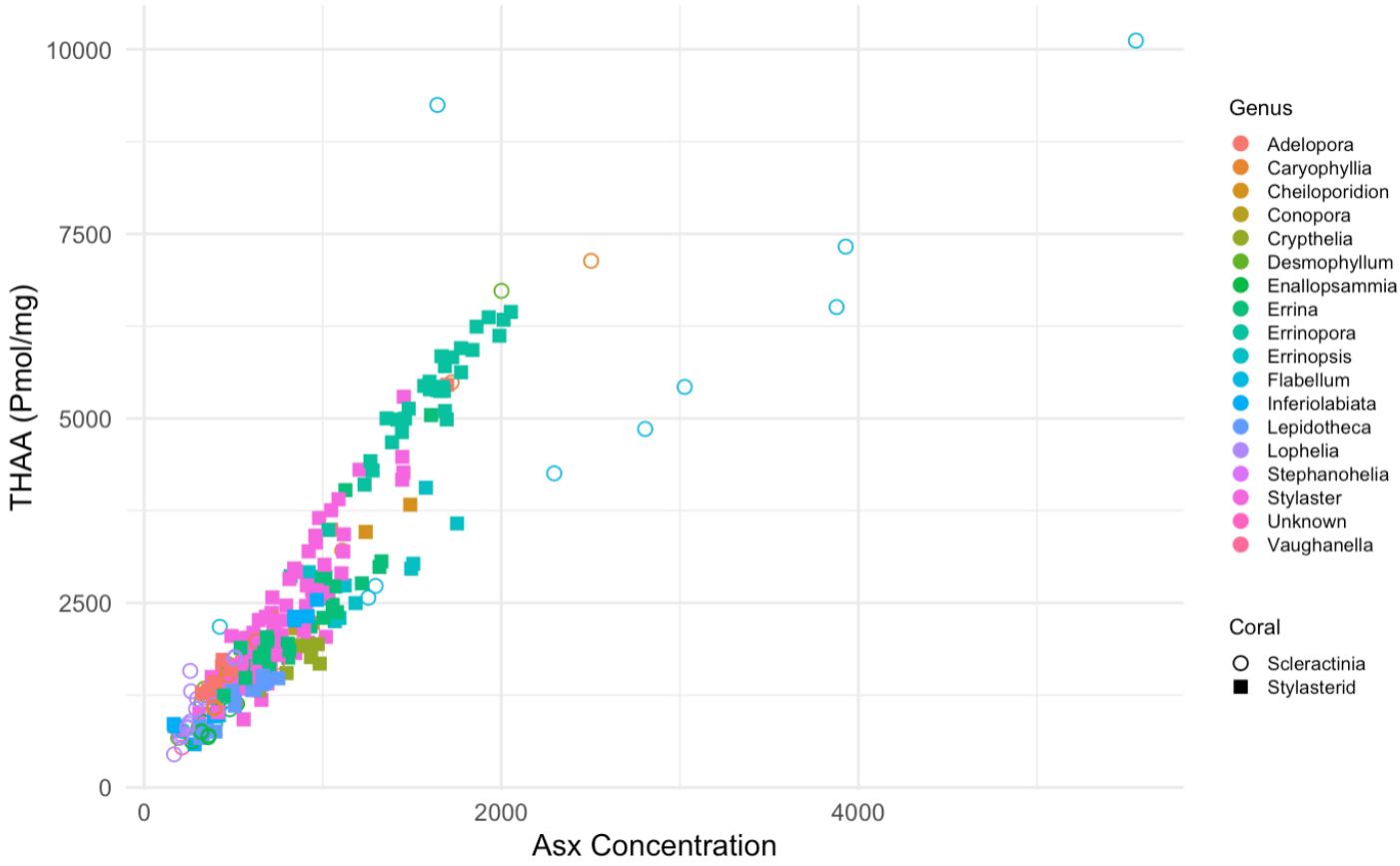

Figure 4.4, THAA (pmol/mg) and Asx concentration correlation, coloured by genus for all deep-sea corals using all samples.

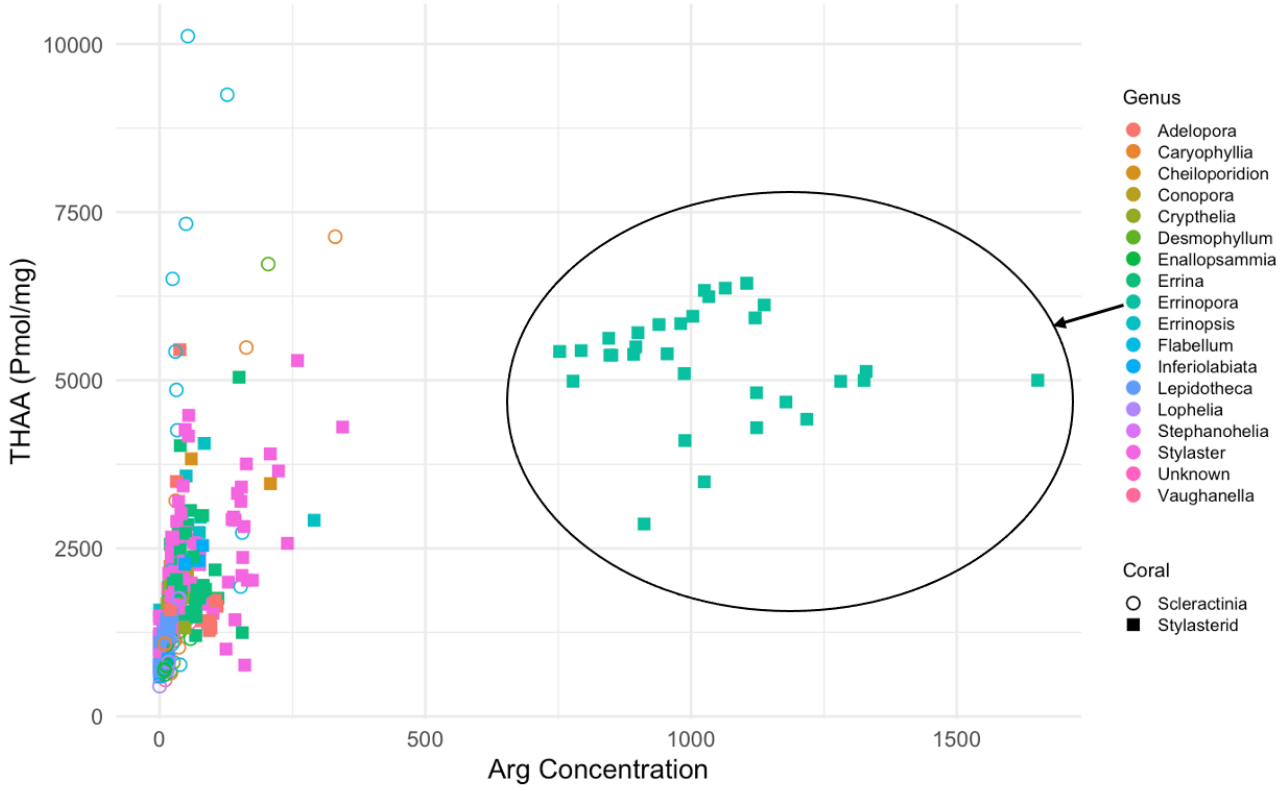

Figure 4.5, THAA (pmol/mg) and Arg concentration correlation, coloured by genus for all deep-sea corals using all samples. Circle indicates the unique Arg concentrations of Errinopora samples.

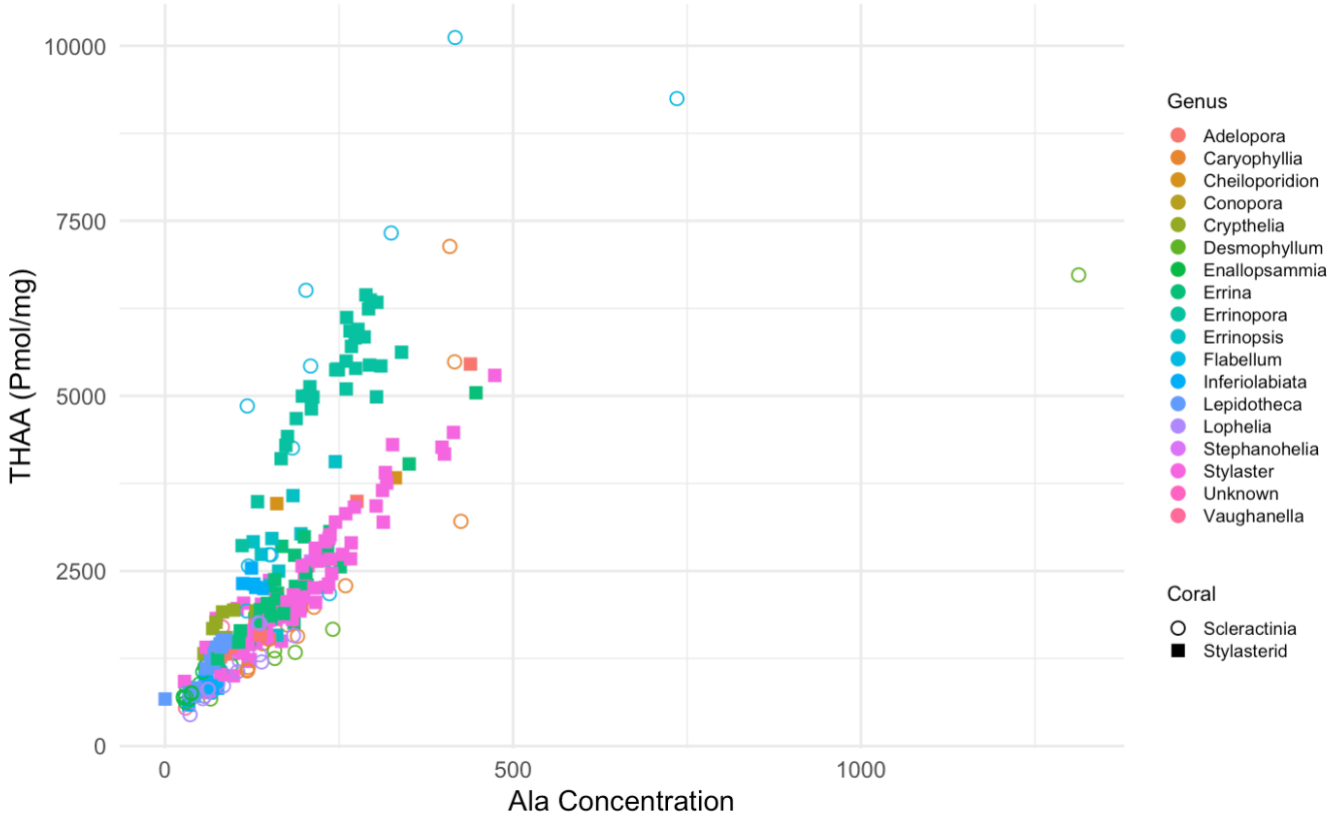

Figure 4.6, THAA (pmol/mg) and Ala concentration correlation, coloured by genus for all corals using all samples

Looking at the concentrations of these amino acids has identified a pattern of *Errinopora* behaving very differently from other stylasterid corals and Scleractinia corals. Partially highlighted in Figure 4.5 (chapter 4, page 69), where *Errinopora* has much larger concentrations of Arg than any other coral. There is also a strong correlation between the [THAA] and [Asx], although this does vary between genera (Figure 4.4, chapter 4, page 69).

4.4 Mineralogy amino acid differences

Aims for the second half of this section:

1. Identify amino acid concentration differences between Stylasterid coral mineralogies
2. Look at the differences between aragonite coral groups

The mineralogy of the samples used within this study was determined using XRD (x-ray diffraction) and element Ca (calcium)/ratios, completed by the team at Bristol university. Stylasterid corals can build their skeletons from aragonite, high-Mg calcite or a mix of both (Kershaw *et al.*, 2023). Scleractinia corals only use aragonite to biomineralise, with the exception of *Paraconotrochus antarcticus,* which has an internal skeletal composition of high-Mg calcite (Stolarski *et al.*, 2020); this species is not included in this study. Previous studies, such as Bostock et al. (2015) and Thresher et al. (2011) indicated that scleractinian species, such as those used within this study, are of aragonite mineralogy.

Genus	Number of samples	Mineralogy
Adelopora	3	Aragonite
Conopora	2	Aragonite
Unknown	1	Aragonite
Stylaster	41	Aragonite
Stephinohelia	1	Aragonite
Inferiolabiata	2	Aragonite
Crypthelia	7	Aragonite
Lepidotheca	4	Aragonite
Errina	6	Aragonite
	4	Mixed
	2	High-Mg Calcite
Cheiloporidion	3	High-Mg Calcite
Errinopora	2	High-Mg Calcite
Errinopsis	6	High-Mg Calcite
	1	Aragonite

Table 8: The samples used within the study and the mineralogy differences. Samples highlighted in pink indicate a genus with more than one mineralogy.

Four *stylasterid* samples had internal mixed mineralogy (Table 8, chapter 4, page 71), 13 were confirmed to be high-Mg calcite , through XRD spectra, and the rest of the stylasterid samples are aragonitic. Mixed stylasterid samples are rare and not easily available to analyse, which is why the sample quantity is so low.

4.4.1 Mineralogy variation of stylasterid corals

High-Mg calcite had a higher mean total concentration of amino acids than aragonitic Stylasterids (Fig. 4.8). The mean for the mixed samples sits between the THAA concentration of high-Mg calcite and aragonite; this may be because the high-Mg ratio within stylasterid corals is very small and mainly made from aragonite (Samperiz, 2018). It had been hypothesised that stylasterid corals using different mineralogies will use different proteins to biomineralise, which fits with the observed varience in total amino acid concentration.

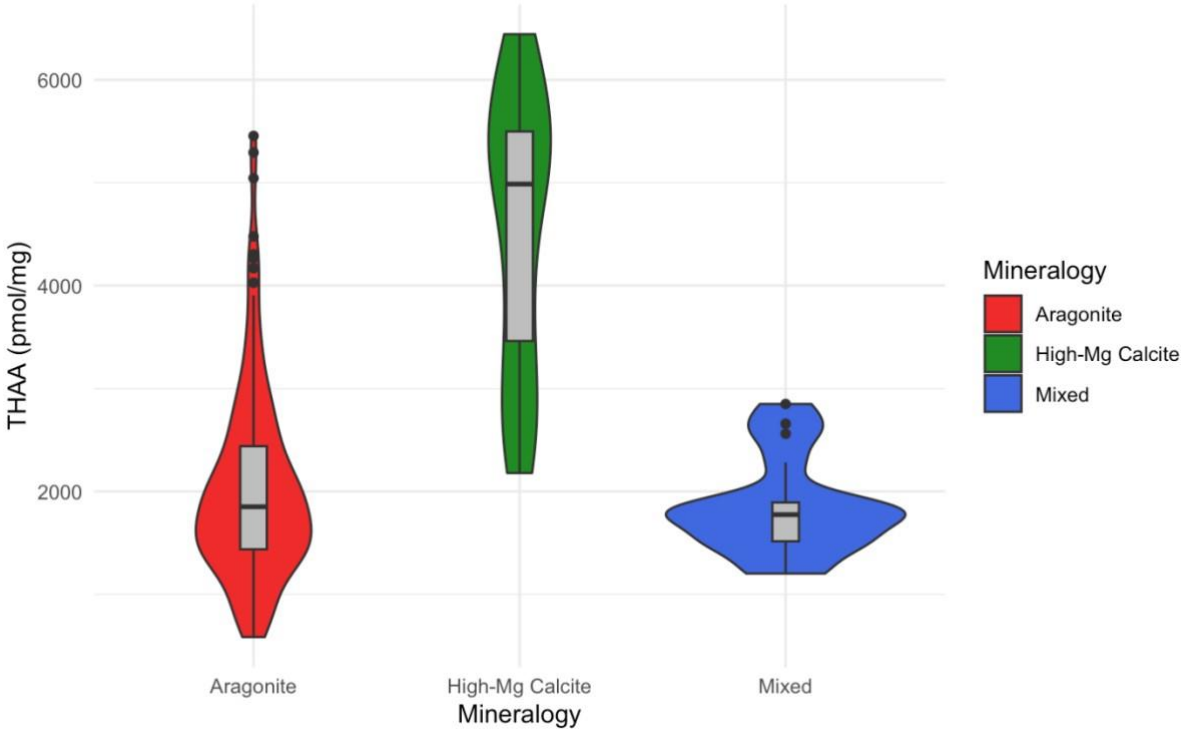

Figure 4.8 Violin and boxplot of stylasterid mineralogy THAA (pmol/mg) comparison using all samples. With the whiskers indicating the minimum and maximum of the data set, the interquartile range ranges from the 25th percentile to the 75th percentile. The bold line at the centre of the interquartile range indicates the median.

An unpaired, two-tailed, Mann-Whitney test was conducted on the comparison of aragonite stylasterid samples and the high-Mg calcite stylasterid samples. The test does not assume that both mineralogy groups have the same variants. The tests were Bonferroni corrected confidence intervals (number of tests = 3). P = 2.2e-16, indicating a strong statistical difference between the THAA (pmol/mg) of Aragonite stylasterid corals and high-Mg calcite stylasterid corals. The variance fof THAA of aragonitic corals is 856654 pmol/mg, for high-Mg calcite samples 1776760 pmol/mg and mixed samples 225554 pmol/mg.

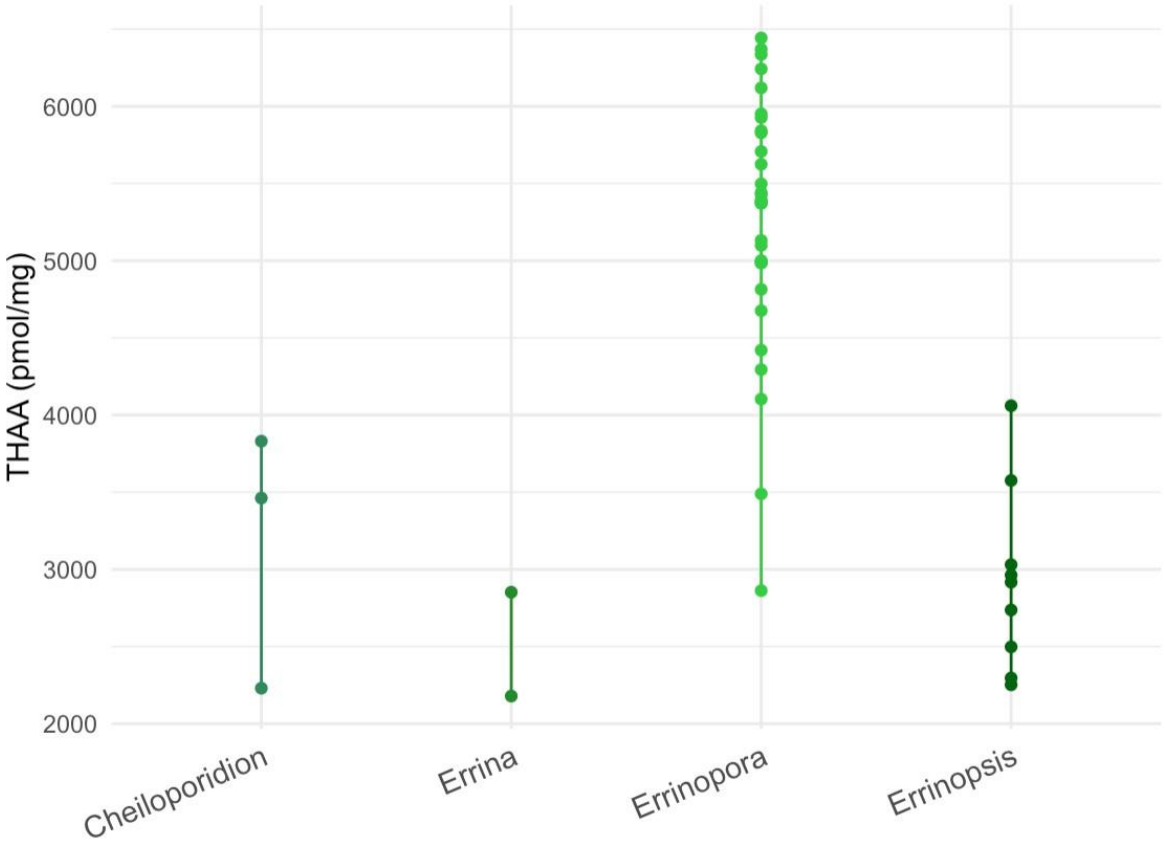

Figure 4.9, THAA (pmol/mg) range of high-Mg samples used within this study by genus. Cheiloporidion (n =3), Errina (n = 2), Errinopora (n = 31), Errinopsis (n = 9).

When the high-Mg samples are separated to identify if one genus is causing a shift of a higher concentration of THAA (pmol/mg), it can be identified from the samples tested that the genus of *Errinopora* has the samples with the largest concentration. The variance of *Cheiloporidion* is 702379 pmol/mg, *Errina* is 226336 pmol/mg, *Errinopora* is 677324 pmol/mg and *Errinopsis* is 348914 pmol/mg.

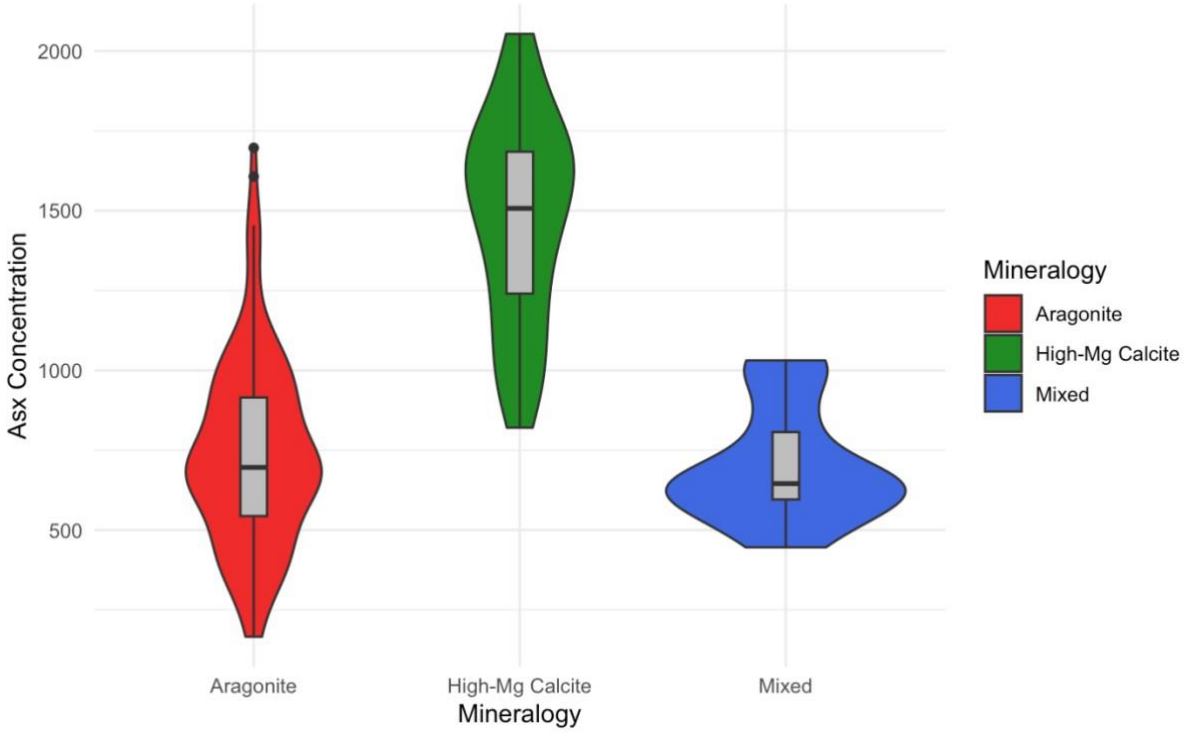

Figure 4.10 Violin and boxplot of Asx concentration (pmol/mg) of stylasterid mineralogies using all samples. With the whiskers indicating the minimum and maximum of the data set, the interquartile range ranges from the 25th percentile to the 75th percentile. The bold line at the centre of the interquartile range indicates the median.

An unpaired, two-tailed, Mann-Whitney test was conducted on the comparison of aragonite stylasterid samples and the high-Mg calcite stylasterid samples. The test does not assume that both mineralogy groups have the same variants. The tests were Bonferroni corrected confidence intervals (number of tests = 3). P = 2.2e-16, indicating a strong statistical difference between the Asx concentration (pmol/mg) of Aragonite stylasterid corals and high-Mg calcite stylasterid corals. The variance for Asx concentration of aragonitic corals is 83623 pmol/mg, for high-Mg calcite samples 103737 pmol/mg and mixed samples 32137 pmol/mg.

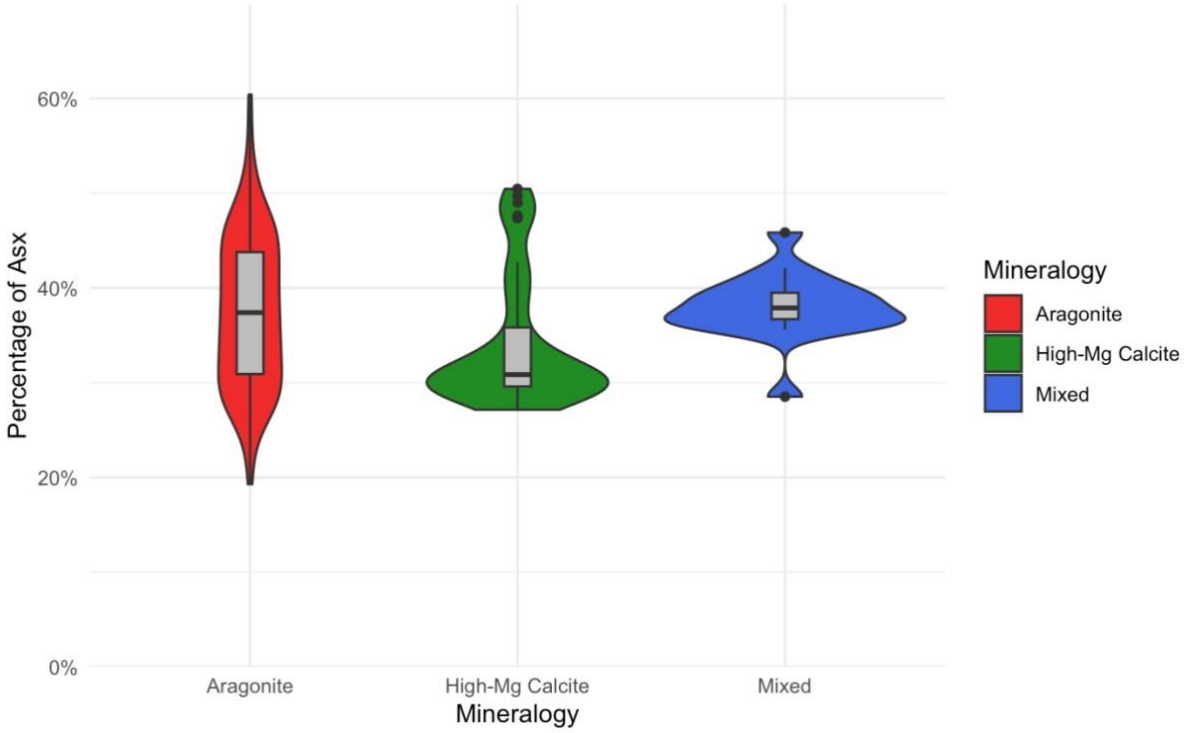

Figure 4.11 Violin and boxplot of the Percentage of Asx within the mineralogy groups of stylasterids, using all samples. With the whiskers indicating the minimum and maximum of the data set, the interquartile range ranges from the 25th percentile to the 75th percentile. The bold line at the centre of the interquartile range indicates the median.

An unpaired, two-tailed, Mann-Whitney test was conducted on the comparison of aragonite stylasterid samples and the high-Mg calcite stylasterid samples. The test does not assume that both mineralogy groups have the same variants. The tests were Bonferroni corrected confidence intervals (number of tests = 3). P = 0.008342, indicating there is a statistical difference between the percentage of Asx of Aragonite stylasterid corals and high-Mg calcite stylasterid corals. The variance for the percentage Asx of aragonitic corals is 0.0064%, for high-Mg calcite samples 0.0047% and mixed samples 0.013%.

4.4.2 Aragonite deep-sea corals

Aragonite is a commonly used form of calcium carbonate within a variety of corals. Three different coral taxa were analysed during this study, all of which use aragonite to biomineralise. The mean amount of THAA within all three corals (3 *Porites*, 54 scleractinia, 64 stylasterids) is similar (Fig. 4.12) : *Porites*: 1643 pmol/mg, Scleractinia*:* 2023 pmol/mg, stylasterid: 2031 pmol/mg. However, the Scleractinia corals have a much larger variation in THAA within the skeletal material than the other corals 448.5 – 10118.3µmol/g. This could be due to the variation in sample internal heterogeneity, as seen within the stylasterid corals (Section 3.3.3), but not tested in Scleractinia corals.

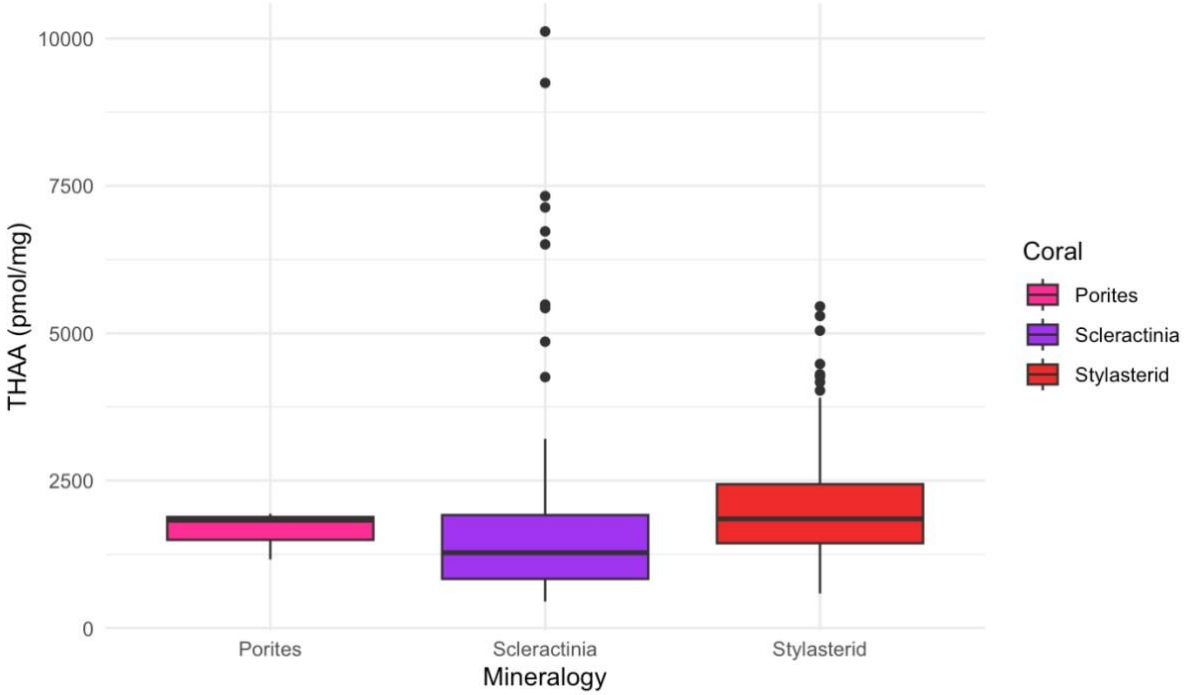

Figure 4.12, [THAA] (pmol/mg) within aragonite corals using all samples. With the whiskers indicating the minimum and maximum of the data set, the interquartile range ranges from the 25th percentile to the 75th percentile. The bold line at the centre of the interquartile range indicates the median. Points external to the boxplot could indicate outliers.

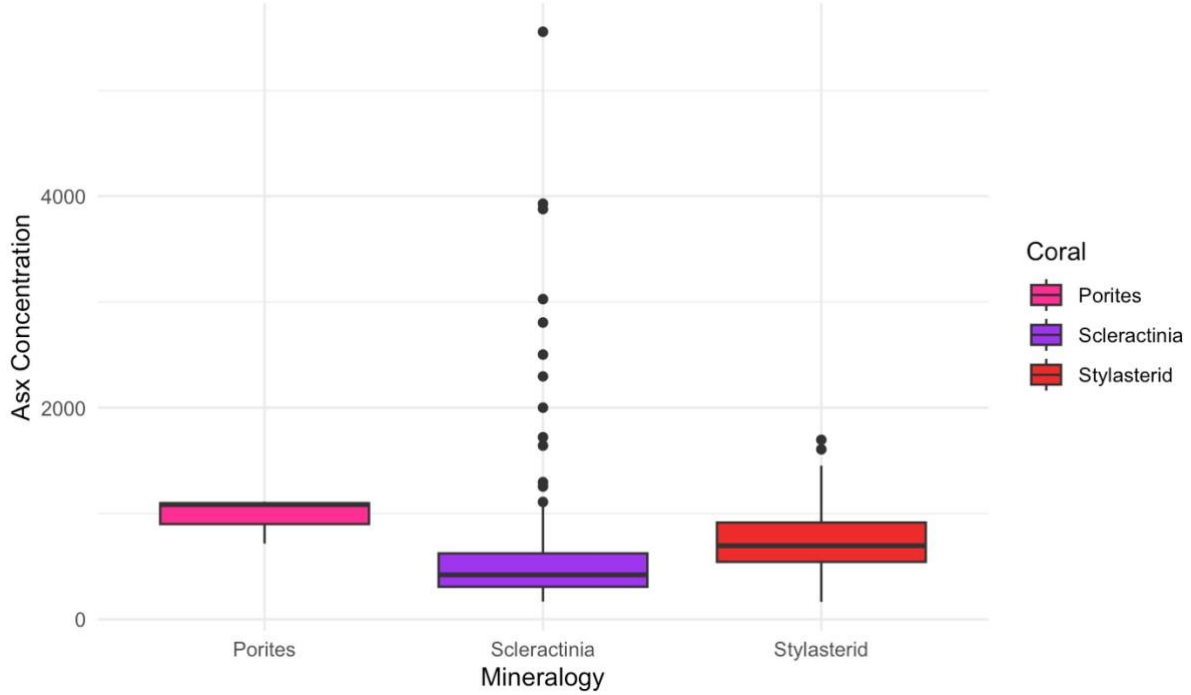

Figure 4.13: Asx concentration (pmol/mg) within aragonite corals using all samples. With the whiskers indicating the minimum and maximum of the data set, the interquartile

range ranges from the 25th percentile to the 75th percentile. The bold line at the centre of the interquartile range indicates the median. Points external to the boxplot could indicate outliers.

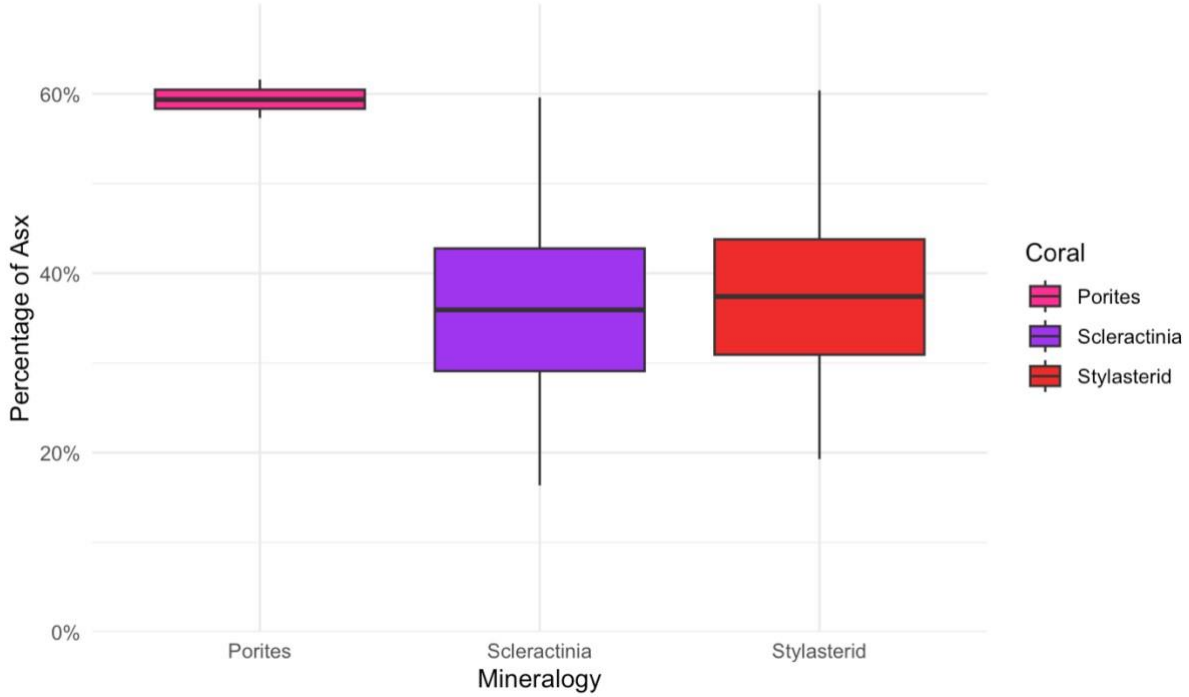

Figure 4.14: Percentage of Asx within aragonite corals using all samples. With the whiskers indicating the minimum and maximum of the data set, the interquartile range ranges from the 25th percentile to the 75th percentile. The bold line at the centre of the interquartile range indicates the median. Points external to the boxplot could indicate outliers.

4.4.3 Discussion and Conclusions

Mineralogy within stylasterids varies between THAA (pmol/mg), Asx concentration and the percentage of Asx. When the high-Mg samples were tested within this study, (separated by genus), it could be seen that *Errinopora* has the largest concentration of THAA (pmol/mg). It should also be considered that *Errinopora* is also the largest sample set of genera tested and therefore other high-Mg genera could potentially also have this results of a high THAA concentration, if they were tested the same quantity. This raises the question of if *Errinopora* is singularly skewing high-Mg samples (Figure 4.9, chapter 4, page 73). Other high-Mg calcite samples also have higher [THAA] than the average aragonite samples (4.9). Further testing on deep-sea corals with high-Mg calcite mineralogies is important to understanding if this is genus-related or mineralogy-related. Stylasterid and Scleractinia aragonite corals presented to be very similar averages of amino acids within the parameters tested, THAA, Asx concentration

and the percentage of Asx, indicating that aragonitic corals may have similar proteins for biomineralisation even within different corals.

5 Chapter 5 – Results: Does the external environment influence the organic composition of corals?

Environmental parameters are varied within the deep-sea and will interact with deep-sea corals in different ways. Prior studies evaluating environmental impacts on shallow water (Voolstra *et al*., 2011) and deep-sea corals (e.g. Stewart *et al.,* (2020), have been conducted to understand and make predictions for corals for the future. Stewart *et al*. (2020) show that stylasterid corals build aragonite skeletons in undersaturated water despite low pH at the site of calcification. This study identified that although stylasterid corals and Scleractinia corals live within the same boundaries, they do not have the same biomineralisation techniques. This is important, as both taxa can live within low pH and aragonite saturation zones. The aragonite saturation state is an important factor for aragonitic corals being able to biomineralise skeletal material. Aragonite is used to form calcium carbonate crystals within the process of biomineralisation. The lower the aragonite saturation state, the harder it is for marine calcifying organisms to produce skeletal material (Venn *et al*., 2012), and they will also become prone to dissolution (Ries, Cohen and McCorkle, 2009). This is due to the lack of availability of carbonate ions needed for corals to biomineralise (Mollica *et al.,* 2018). However, stylasterid and scleractinian corals can live in undersaturated water, as they have strategies to contend with the environmental parameters of undersaturated aragonite conditions. Scleractinian corals can change the pH levels within their calcifying fluid, which is thought to assist with the biomineralisation of their skeletons (McCulloch *et al.,* 2012). Understanding if amino acid profiles may change alongside the inorganic, physical oceanographic data will further help us understand how resilient the different corals are to climate change.

Within the unpublished data from the PhD thesis of Tomiak (2013), it was seen within a controlled pH setting that *Stylophora pistillata* was increasing the [THAA] within lower, more acidic pH levels (Figure 5.1, chapter 5, page 79). A study conducted by Kellock *et al*, (2020) also indicated that shallow water corals could be responding to environmental changes by inversely correlating the concentrations of [THAA], Asx, glutamic acid and alanine in response to seawater pH. This was tested on the skeletal material of growing *Porites* corals, in different aragonite saturation states and pH concentrations. Deep-sea corals may be responding in the same or in a similar way to shallow-water corals within these environmental parameters. This change in amino acids with different pHs could

be a sign of adaptability and response to ocean acidification. The resilience and adaptability of deep-sea corals have been previously studied within another scleractinian coral, *Flabellidae,* in response to the external acidified seawater. This indicated an increase of AAR1, an aspartic acid-rich protein thought to be crucial to the biomineralisation precipitation of aragonite (Li *et al*, 2023).

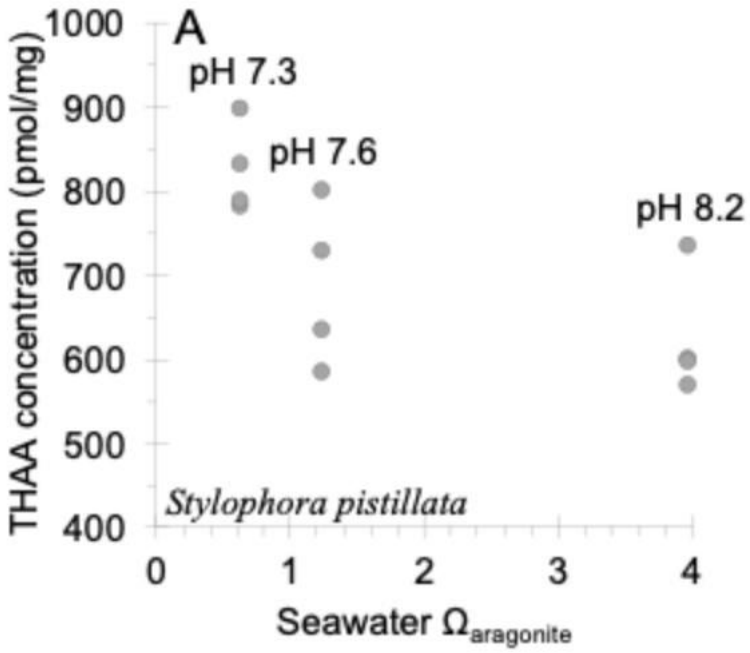

Figure 5.1 [THAA] of Stylophora pistillata (Tomiak, P. 2013). Unpublished data of shallow water branching scleractinian coral (Stylophora pistillata) revealed an increase in THAA in the intra-crystalline fraction of the skeleton with a decrease in aragonite saturation state and pH increase.

It was hypothesised at the beginning of this study that environmental parameters such as aragonite saturation state could therefore impact the protein concentration and composition in a wider group of corals, including deep-water scleractinian corals and stylasterid corals.

To test the hypothesis that hydrographic environmental parameters impact the amino acid concentrations within coral skeletons, I compared the amino acids of all the corals (and their replicates) measured in this study to the environment in which they grew. The two main amino acid data sets compared to the hydrological data are:

- **[THAA] (pmol/mg),** as this was the parameter shown to increase with pH in the preliminary data set seen in the proposal. There is also a direct correlation with Asx concentration; therefore, if there are any increases or decreases in [THAA] this would also be the same for Asx concentration. It has been seen by Allison *et al*. (2024), that THAA concentrations in *Porites* are higher in warmer seawater temperatures, although warmer temperatures have the opposite correlation to what has been seen above for the aragonite saturation state it does indicate a potential

environmental modifier to amino acids. Therefore, has still been addressed.

- **Asx,** as this is the most dominant amino acid thus far found within coral skeletons analysed and is known to be part of the main group of proteins that are thought to control the precipitation of calcium carbonate within the process of biomineralisation (Kellock *et al*., 2020). As concentration was being tested, percentage was also tested, as a second option to see if any variation was taking place within the percentage factor of amino acids. Furthermore, Gupta et al,.(2006) identified that the mole%Asx, seen as the percentage of Asx within this thesis, had a lower concentration during winter and high content during summer, indicating that growth, and therefore biomineralisation, of shallow water *Porites* coral could be being impacted by external environmental conditions.

To explore the controls on amino acids in the corals, the samples were split in two ways: by location and by taxa. The taxa were further split to determine if environmental factors could influence taxa differently. Stylasterid corals and Scleractinia corals are very different from one another. The amino acid composition seen in chapter 4 highlighted this, and therefore, when looking at the environmental parameters against amino acids, they were examined separately. This split in groups included:

- **All samples**
- **Stylasterid corals**
- **Aragonite-only stylasterid** corals (to exclude mineralogy effects)
- Stylasterid corals within the genus of ***Stylaster*** (to assess one genus only)
- All **scleractinian** corals
- Scleractinia coral within the genus of ***Caryophyllia*** (to assess one genus only)

Stylaster (n = 77) and *Caryophyllia* (n = 17) were selected to be analysed, as they both represent the largest genus within the stylastrid and scleractinian corals respectively.

The hydrographic data used within this study followed the protocol used in Stewart *et al*. (2020). Water column data are either from GLODAP and GLODAP 2 (Lauvset, S *at al*., 2021) or directly from the relevant expedition, if available. The corals were matched to the hydrographic data by longitude, latitude and depth, within the closest proximal radius. For cruises DY081, JC094 and NBP1103, this is a radius of 30 km and 30 m depth, from the coral sampling site (Stewart *et al*, 2020). As discussed in Kershaw (2023), aragonite saturation and seawater pH were calculated using a SEACARB package within R (Gattuso *et al*., 2021). Parameters for this calculation included dissolved inorganic carbon (DIC), dissociation constants of carbonate, and alkalinity, all acquired from Lueker *et al*. (2000).

Within Kershaw (2023), hydrographic parameters including temperature, salinity, aragonite saturation and pH were used to compare the distribution coefficient of barium. Barium (Ba) is important within cold-water corals as it can be used to

understand past ocean circulations, especially previous Ba cycles (Hemsing *et al.*, 2018). The knowledge this study provided for deep-sea corals' responses to past ocean circulations has been incredibly important to not only this study but other studies. Therefore, the selection of environmental factors that were compared to Ba have also been selected to compare to the amino acid data In this study. Including, including, temperature, salinity, aragonite saturation and pH.

Temperature within the warm summer months has previously been identified as a control for the calcification of shallow water corals. Miller (1995), saw that the calcification rates of shallow water scleractinian coral (*Oculina arbuscula*) increased with warmer seawater temperatures (summer). Furthermore, as previously discussed the [THAA] increased for another shallow water coral (*Porites*) when exposed to warmer water temperatures (Allison *et al.*, 2024). Although these experiments have been conducted on shallow-water corals, it is important to test these results for deep-sea corals, as temperature change is something that will occur in the deep sea with global warming.

In the shallow water coral (*Montipora verrucosa*) it is seen that low salinity increases the vulnerability of corals when exposed to warmer temperatures, even in short periods of time (Coles and Jokiel, 1978). However, the main effects of salinity of shallow water corals are seen in their symbiotic relationships to zooxanthellae relating to photosynthesis (Kerswell and Jones, 2003, Muthiga and Szmant, 1987). The little understanding of how deep-sea corals will react to salinity is why salinity has been selected to observe. Although salinity is mostly stable in the deep-sea, it is important to observe quasi-consistent variables for comparison and salinity has been compared to other inorganic variables like Ba, (Kershaw, 2023).

It is known that scleractinian corals use calcification fluid to biomineralise, they are also known to be able to change the pH of the calcification fluid. Allison *et al.* (2014), through the use of boron geochemistry, saw that scleractinian corals are also concentrating DIC at the site of calcification, above the values of the seawater around them. This is important as DIC is directly correlated to ocean acidification, as it will increase with more dissolved carbon dioxide (Xue and Cai, 2020); therefore, it is important to understand what impact DIC is having on deep-sea coral.

Assessing prior studies identified the environmental parameters for examination in this study, which are:

- Location
- Temperature
- Salinity
- pH
- Aragonite saturation

- Dissolved inorganic carbon (DIC)

5.1 Location

As location directly relates to the environmental parameters that have been individually assessed within this study, it was important to assess if the location as a whole was an important factor for the [THAA] (pmol/mg) and % Asx of samples. This could occur if, for example, the dominant food source for the corals was different in different locations, as they will go through periods of starvation and feasting in the deep sea (Maier *et al.*, 2023)

When looking at locations, some were grouped together due to their proximity; e.g. Burwood Bank/Falklands islands were combined with the other Drake passage samples. The Aleutian Islands (Alaska) were also combined into the North Pacific/Alaska location group.

All Coral

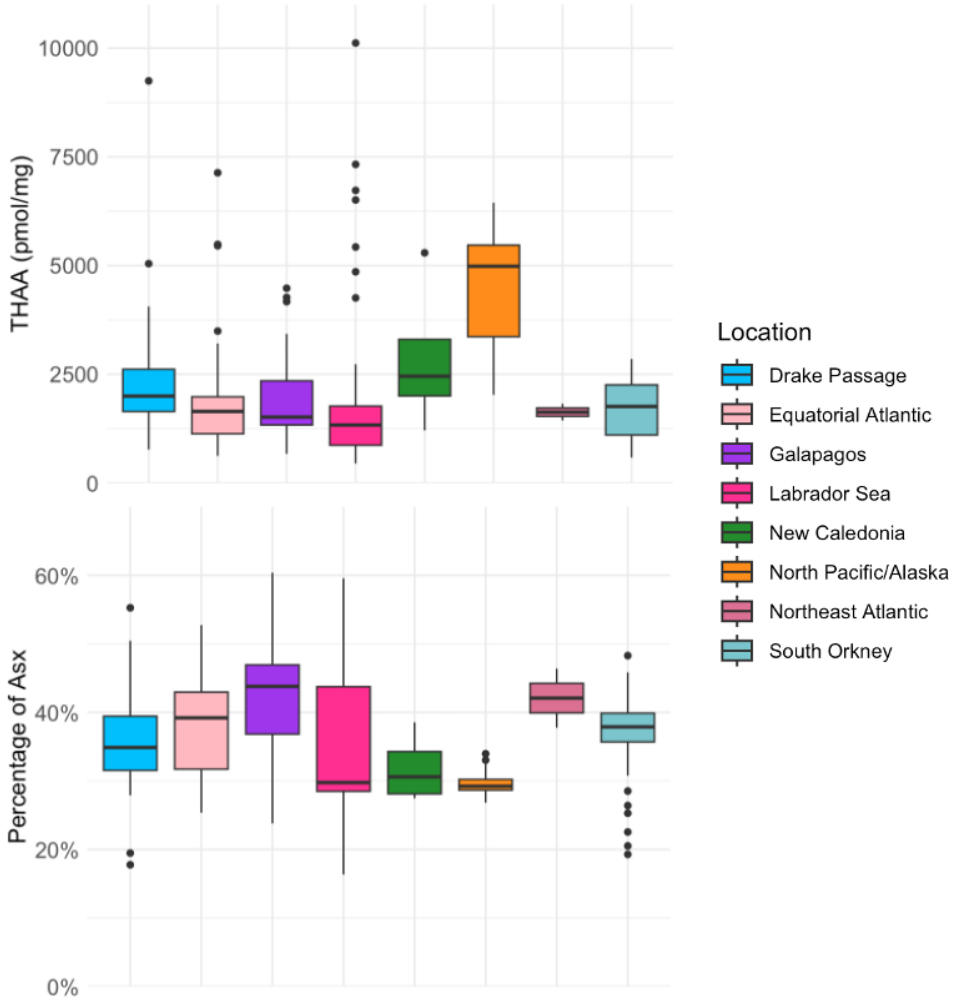

Figures 5.2 a and b, boxplot of the [THAA] (top) and % Asx (bottom) against the location for *all corals. With the whiskers indicating the minimum and maximum of the data set,*

the interquartile range ranges from the 25th percentile to the 75th percentile. The bold line at the centre of the interquartile range indicates the median. With a 95% confidence interval.

Stylasterid corals

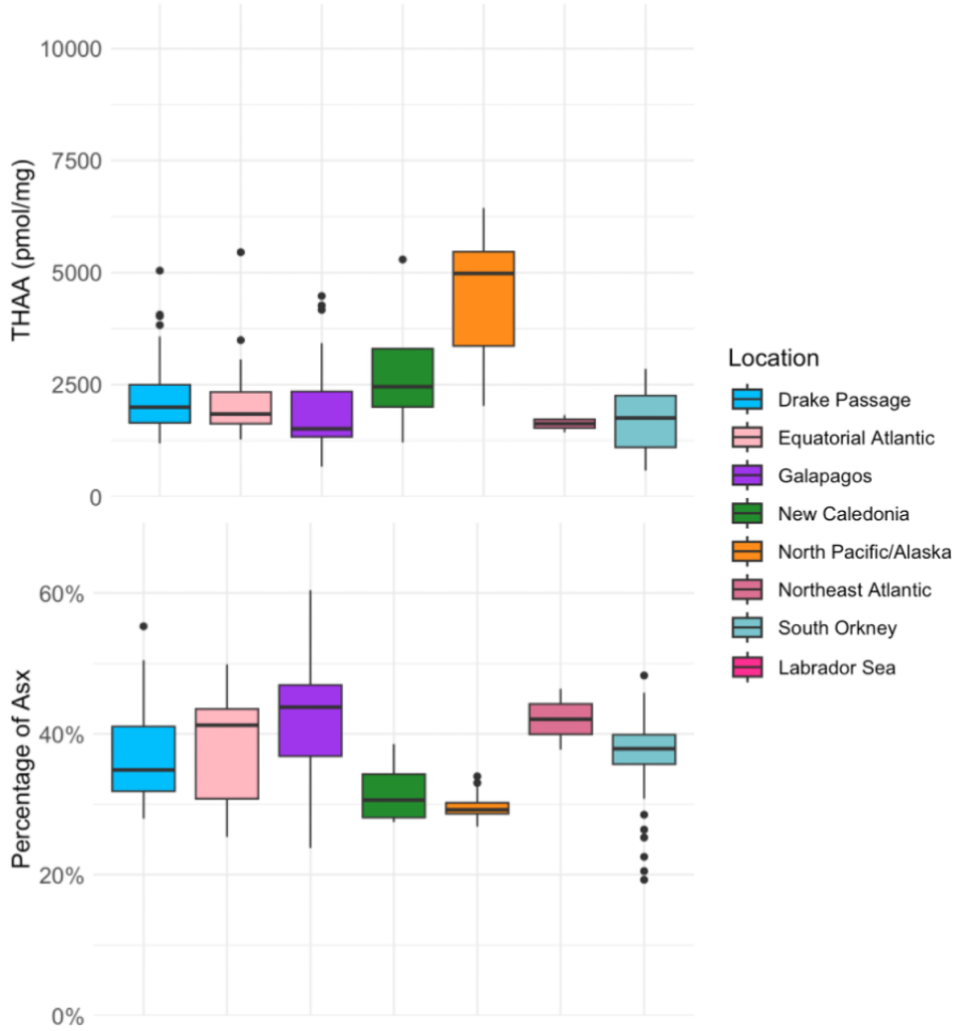

Figures 5.3 a and b: *boxplot of the [THAA] (top) and % Asx (bottom) against the location* for *stylasterid corals. With the whiskers indicating the minimum and maximum of the data set, the interquartile range ranges from the 25th percentile to the 75th percentile. The bold line at the centre of the interquartile range indicates the median. With a 95% confidence interval.*

Aragonite stylasterid

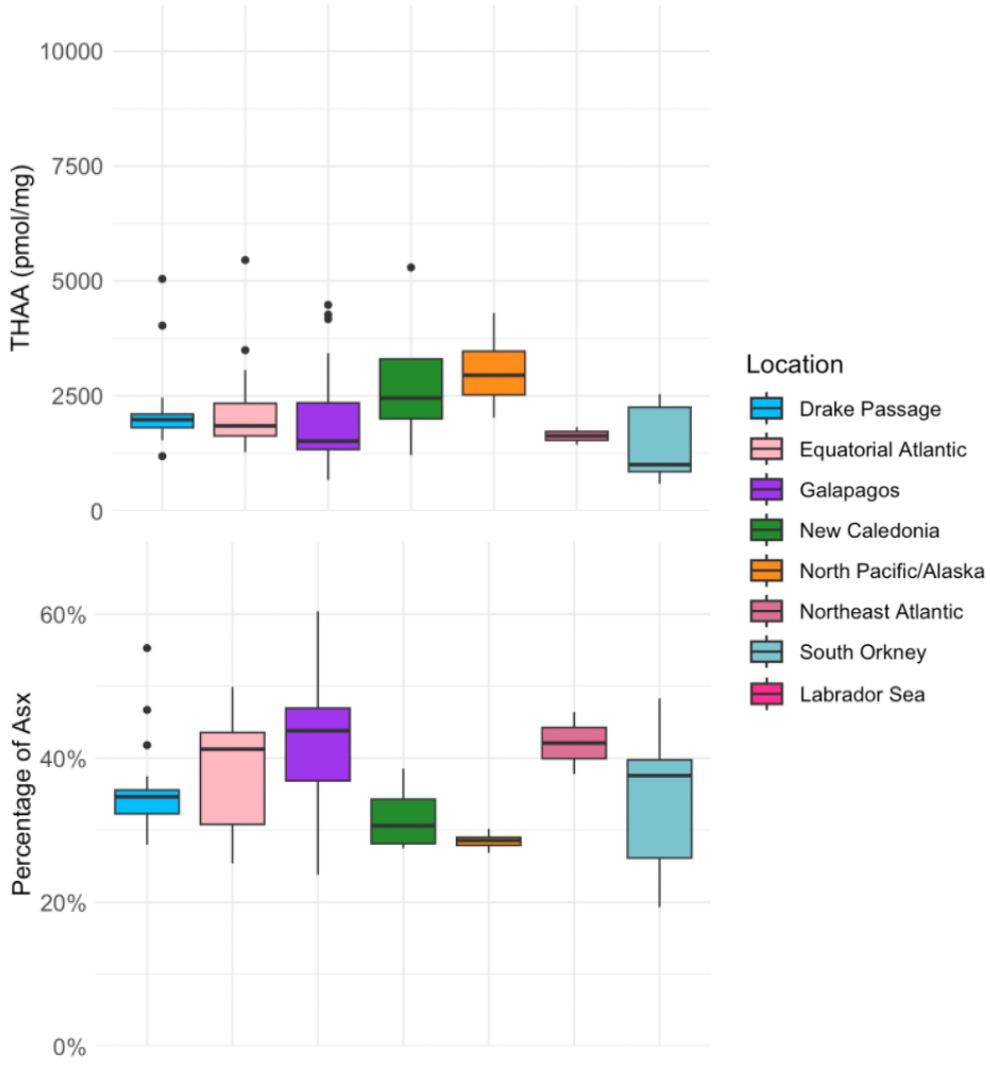

Figure 5.4 a and b: *boxplot of the [THAA] (top) and % Asx (bottom) against the location for aragonite stylasterid corals. With the whiskers indicating the minimum and maximum of the data set, the interquartile range ranges from the 25th percentile to the 75th*

percentile. The bold line at the centre of the interquartile range indicates the median. With a 95% confidence interval.

Stylaster

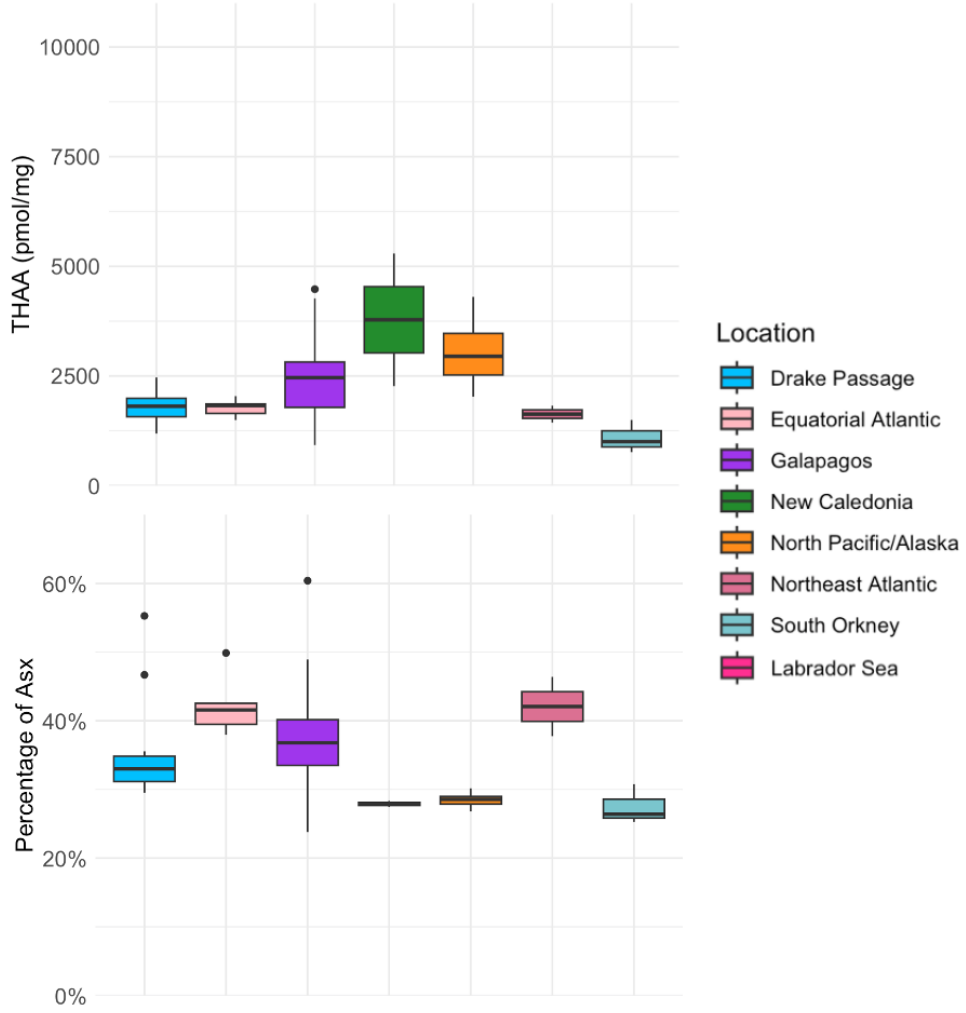

Figure 5.5 a and b: *boxplot of the [THAA] (top) and % Asx (bottom) against the location* for *Stylaster corals. With the whiskers indicating the minimum and maximum of the data set, the interquartile range ranges from the 25th percentile to the 75th percentile. The bold*

line at the centre of the interquartile range indicates the median. With a 95% confidence interval.

Scleractinia

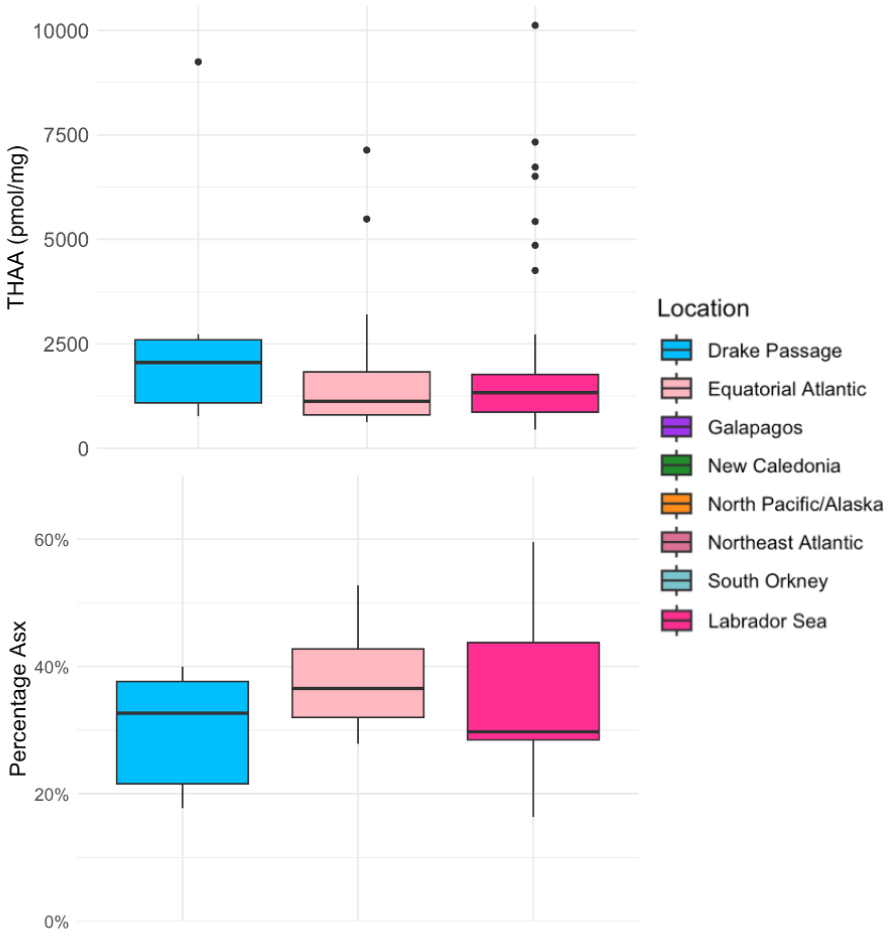

Figures 5.6 a and b: *boxplot of the [THAA] (top) and % Asx (bottom) against the location for scleractinian corals. With the whiskers indicating the minimum and maximum of the data set, the interquartile range ranges from the 25th percentile to the 75th percentile. The*

bold line at the centre of the interquartile range indicates the median. With a 95% confidence interval.

Caryophyllia

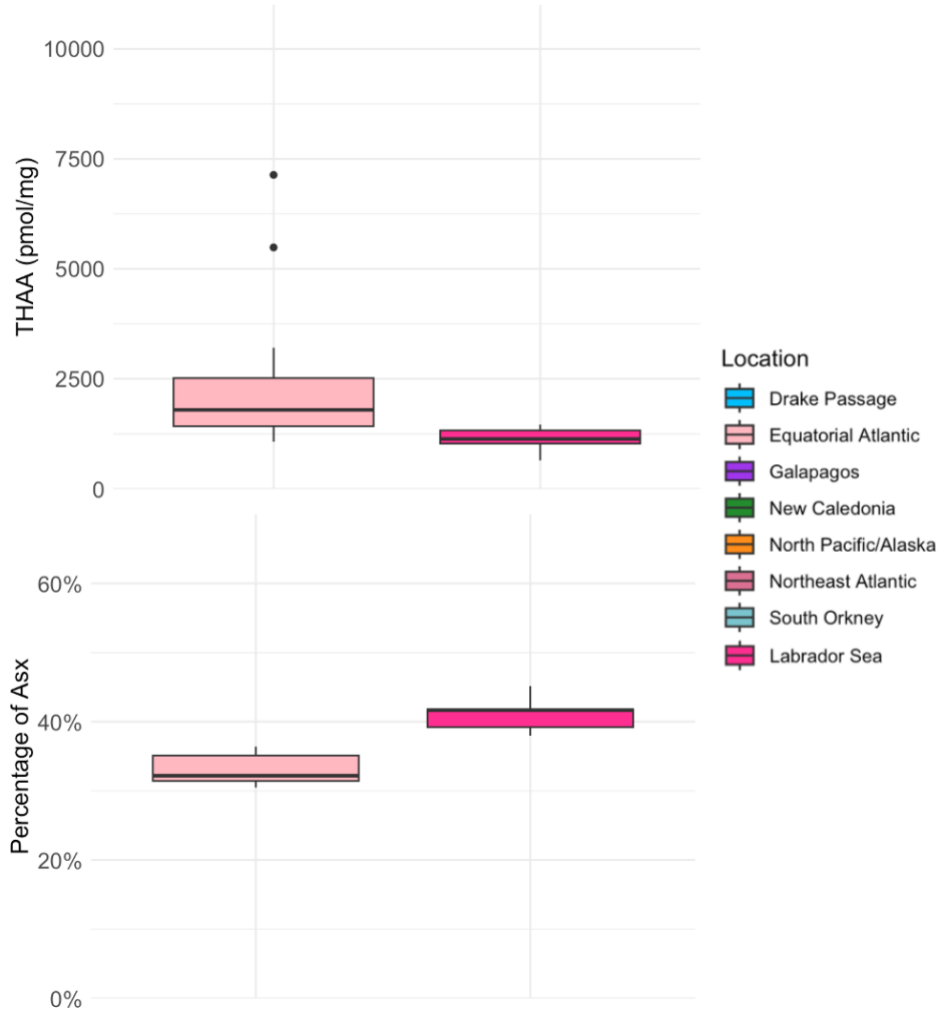

Figure 5.7 a and b: *boxplot of the [THAA] (top) and % Asx (bottom) against the location* for *Caryophyllia genus corals. With the whiskers indicating the minimum and maximum*

of the data set, the interquartile range ranges from the 25th percentile to the 75th percentile. The bold line at the centre of the interquartile range indicates the median. With a 95% confidence interval.

Location	Median		Mean	
	[THAA]	% Asx	[THAA]	% Asx
North Pacific / Alaska	4985	0.29	4502	0.30
Drake Passage	2102	0.35	2507	0.36
South Orkney	1767	0.38	1824	0.36
New Caledonia	2454	0.31	2853	0.32
Labrador Sea	1333	0.30	2203	0.36
Northeast Atlantic	1629	0.42	1629	0.42
Equatorial Atlantic	1645	0.39	1856	0.38
Galapagos	1516	0.44	1863	0.42

Table 9, The median and mean [THAA] and % Asx of each location tested.

As always in oceanographic data sets, there are multiple variables for each sample, so it is hard to determine if one parameter is controlling amino acids. The North Pacific/Alaska boxplot has much higher [THAA] (Fig. 5.2a and table 9, chapter 5, page 88) than the other locations. The North Pacific/Alaska sampling location contains *Errinopora* samples, which in this study are only high-Mg, shown in chapter 4 (section 4.4.1) to have a larger amount of [THAA] than any other genus seen in this study. It is therefore difficult to determine if increases are location-related or genus related. All further plots therefore have location colour-coded, to show the variation for each location and the potential influence for each environmental parameter.

5.2 Temperature

Samples within this study have been taken from around the world's oceans, with a water temperature range of 0.1 ºC – 20.1 ºC. Hydrographic temperature data was taken from GLODAP and GLODAP 2 (Lauvset, S *at al.*, 2021). Seawater temperature will increase with rising global temperatures, even in the deep-sea, (Yasuhara and Danovaro, 2014) and therefore it is important we can understand if there is any correlation between amino acids and temperature.

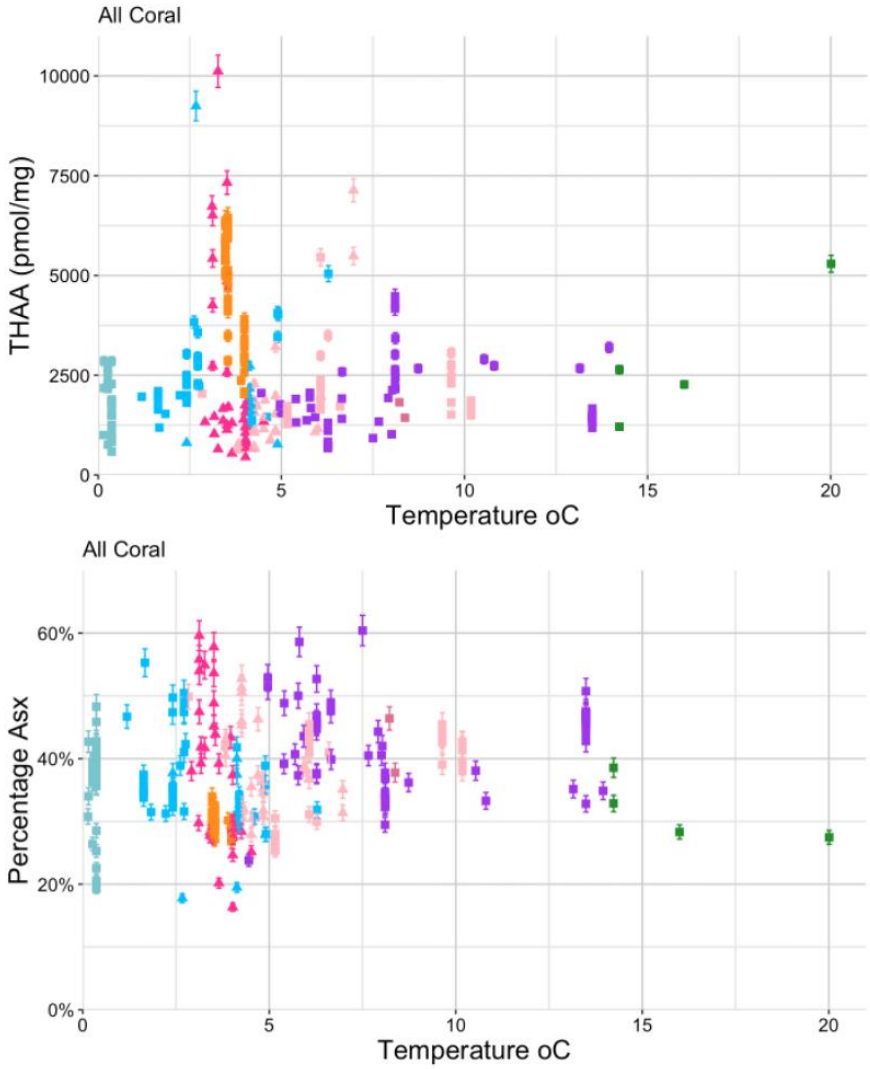

Figure 5.8 a and b: All coral [THAA] (top) and % Asx (bottom) for all coral samples against temperature (^{O}C). Colour responds to the location of where the sample was taken. Error bars are 4%, representing the analytical replicate error.

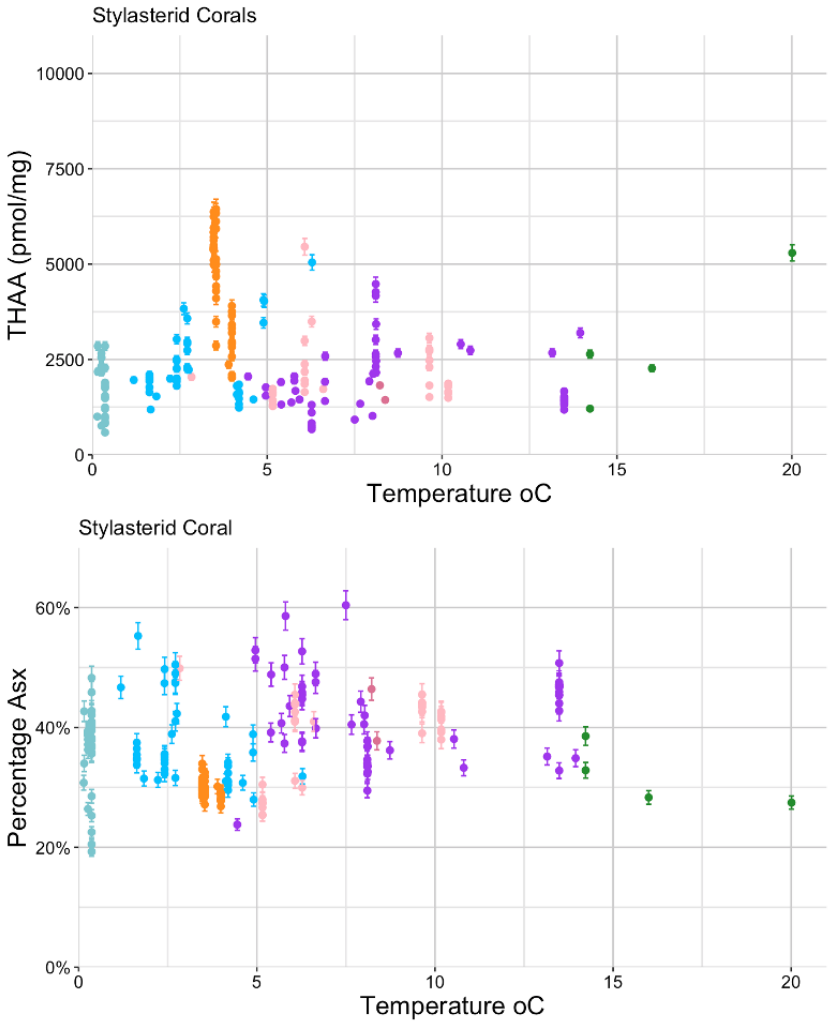

Figure 5.9 a and b: *stylasterid coral [THAA] (top) and % Asx (bottom) for all coral samples against temperature (ºC). Colour responds to the location of where the sample was taken. Error bars are 4%, representing the analytical replicate error.*

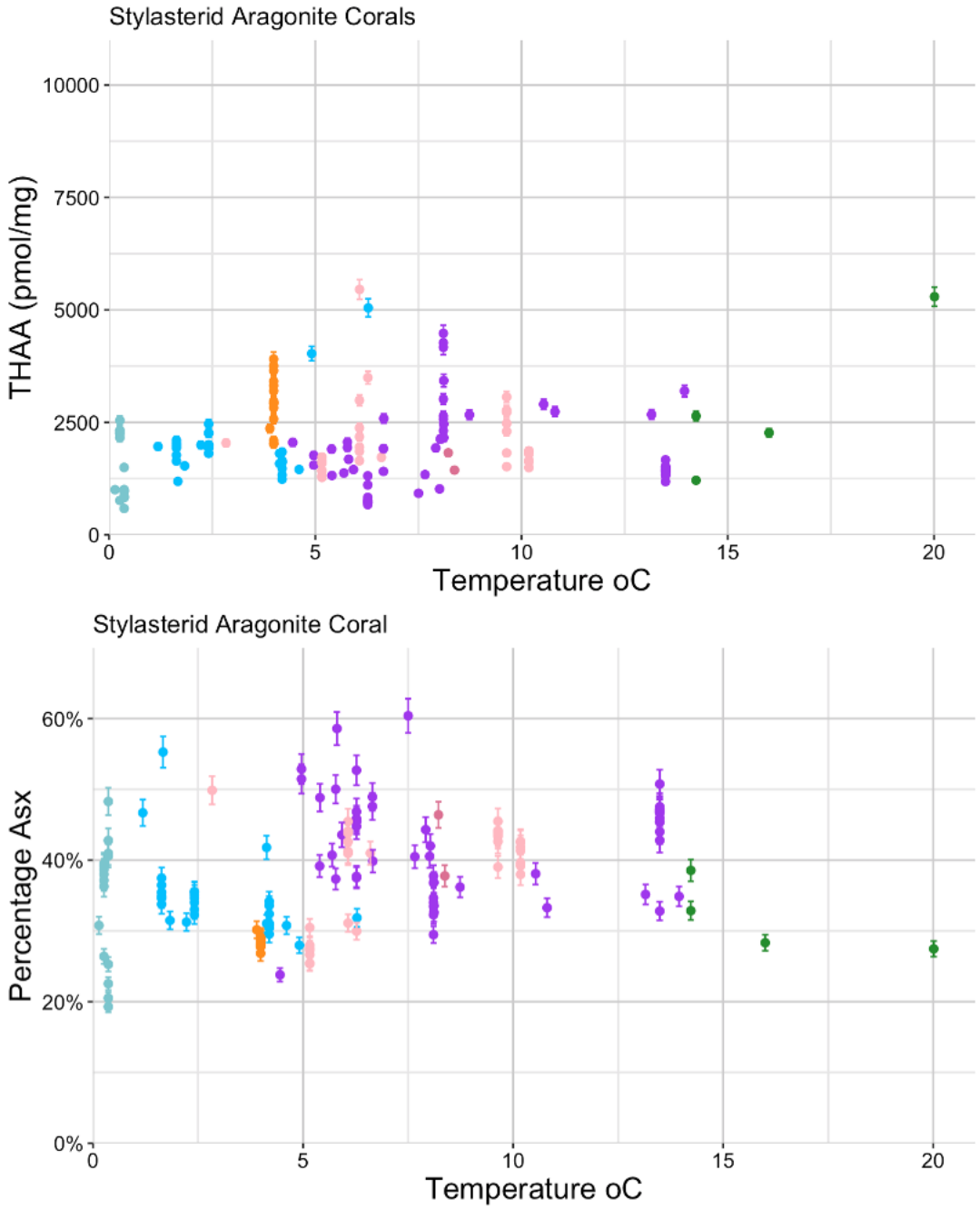

Figure 5.10 a and b: Aragonite stylasterid [THAA] (top) and % Asx (bottom) for all coral samples against temperature (ºC). Colour responds to the location of where the sample was taken. Error bars are 4%, representing the analytical replicate error.

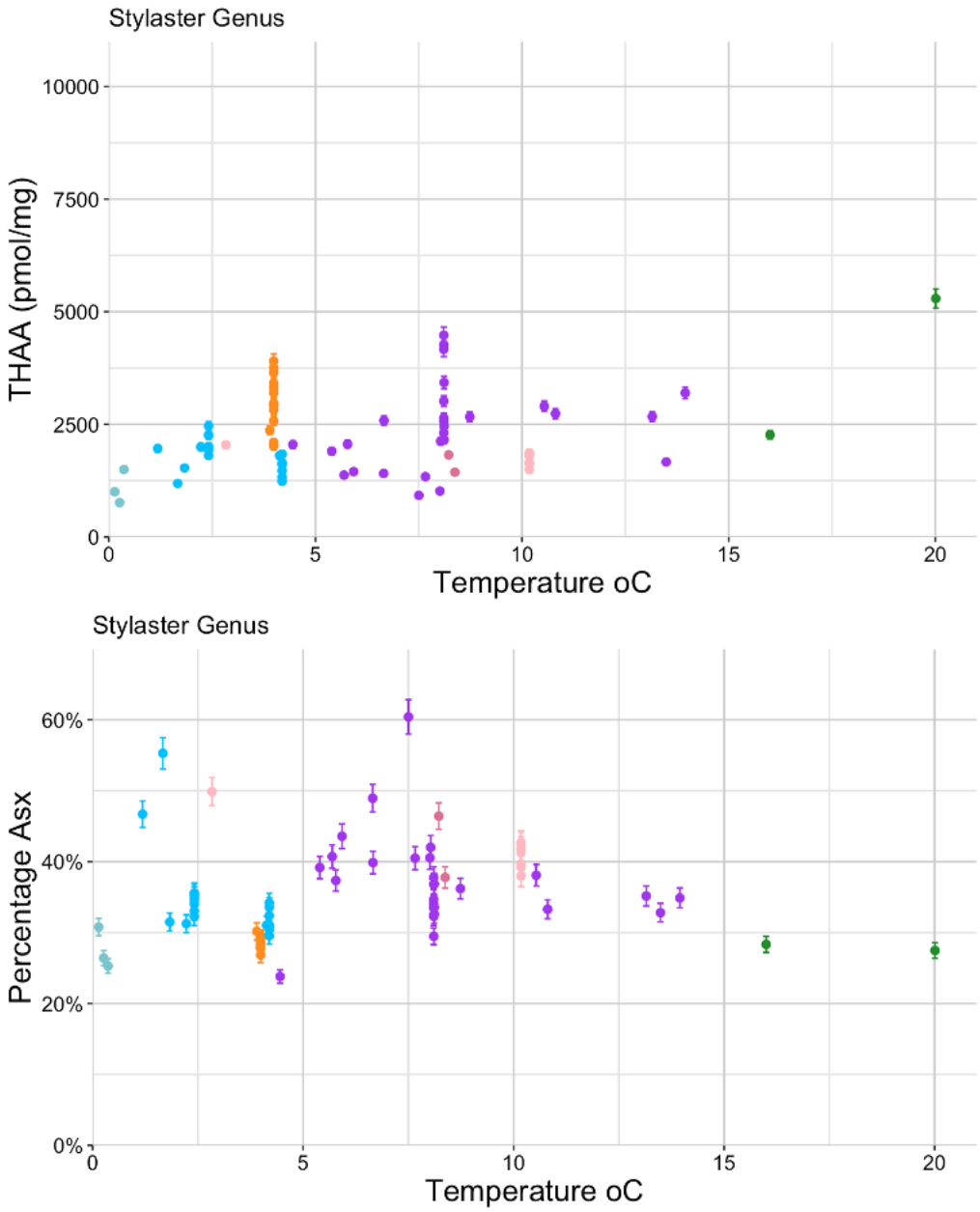

Figure 5.11 a and b: *Stylaster* genus coral samples [THAA] (top) and % Asx (bottom) against Temperature ^{o}C. Colour responds to the location of where the sample was taken. Error bars are 4%, following the analytical replicate error of THAA (pmol/mg) and analytical replicate error of % Asx.

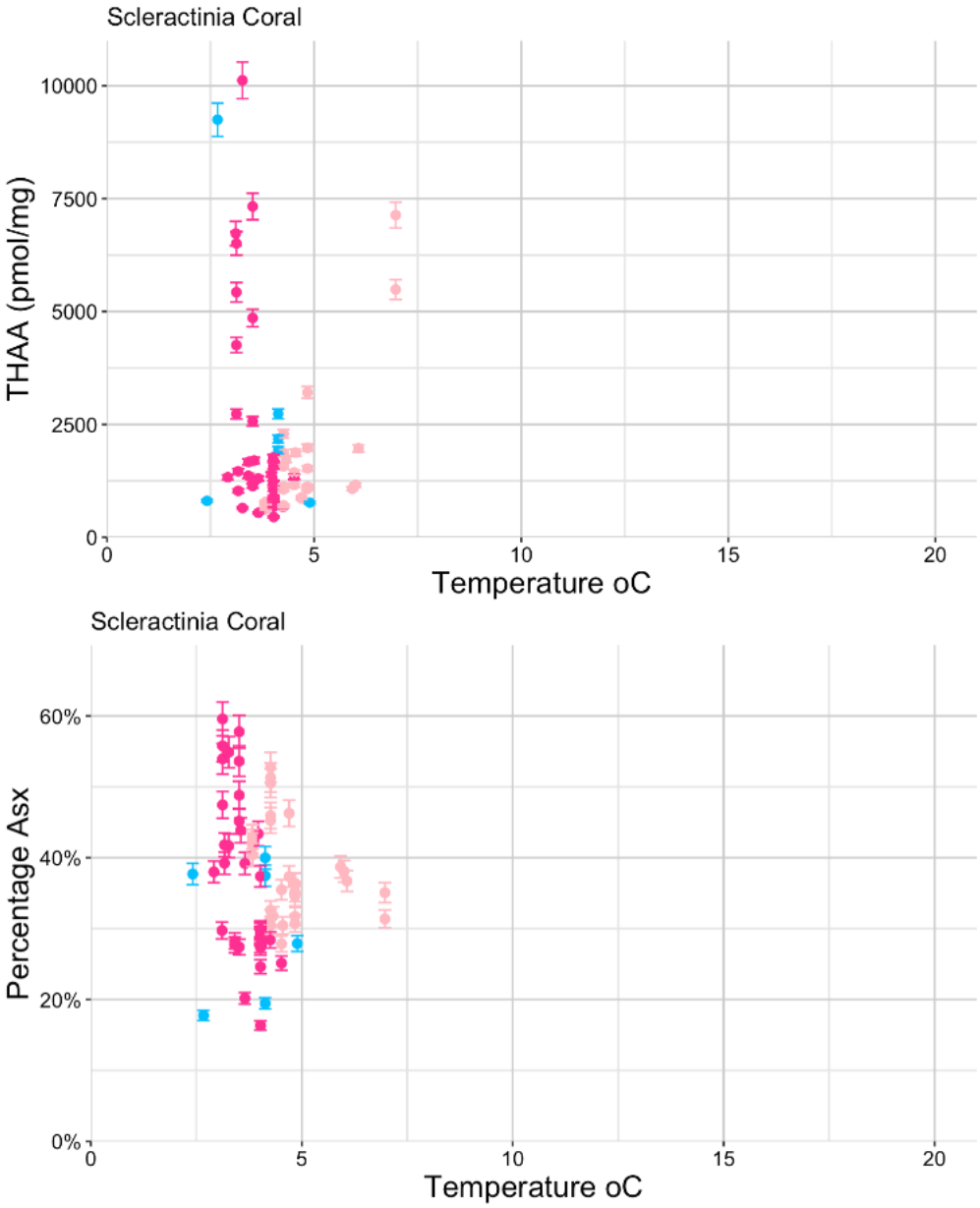

Figure 5.12 a and b: *scleractinian coral [THAA] (top) and % Asx (bottom) for all coral samples against temperature (ºC). Colour responds to the location of where the sample was taken. Error bars are 4%, representing the analytical replicate error.*

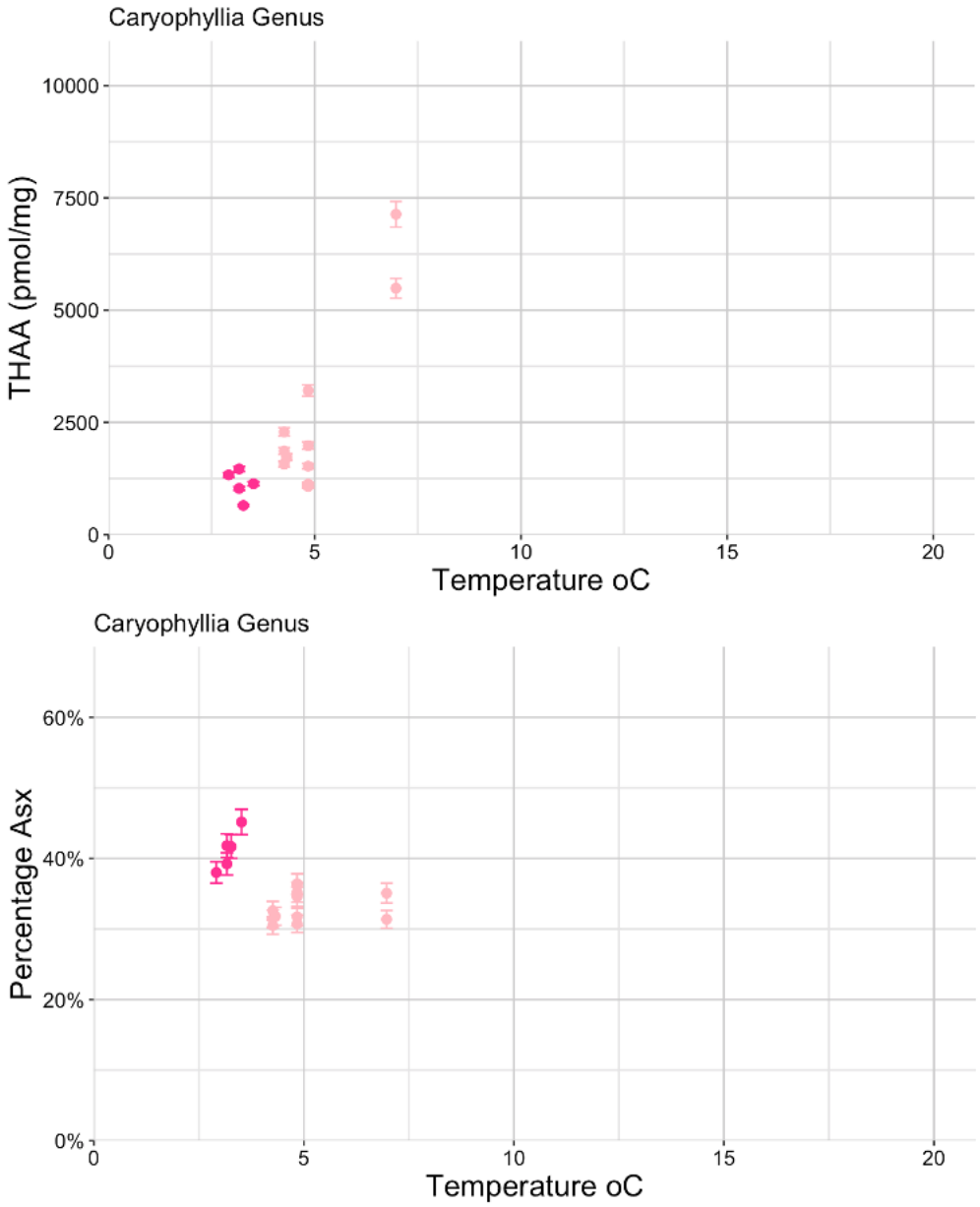

Figure 5.13 a and b: *Caryophyllia* genus [THAA] (top) and % Asx (bottom) for all coral samples against temperature (°C). Colour responds to the location of where the sample was taken. Error bars are 4%, representing the analytical replicate error.

5.2.1 Summary of findings for temperature

Temperature (°C)									
Taxa	Subset	Residual Std Error		F-statistic		R - Squared		P value	
		[THAA]	% Asx	[THAA]	% Asx	[THAA]	% Asx	[THAA]	% Asx
All Coral		1622	0.08	1.168	12.34	0.0006	0.04	0.2807	0.0005
Stylasterid	All	1424	0.07	2.223	16.95	0.0057	0.07	0.1374	0.0005
	Aragonite only	925	0.08	1.298	14.56	0.0021	0.09	0.2564	0.0002
	Stylaster	852	0.07	7.104	2.18	0.0753	0.02	0.0094	0.1444
Scleractinia	All	2059	0.10	0.576	2.54	-0.0059	0.02	0.4506	0.1157
	Caryophyllia	1001	0.04	32.08	6.38	0.6602	0.25	0.00004	0.0233

Table 10, *Regression analysis of temperature ºC for THAA (pmol/mg) and % Asx for the six groups tested, showing the residual error, F-statistic, R-squared and p-value. Pink shading indicates p-values of < 0.05, which are therefore statistically significant. The residual standard error has been shown as it quantifies the interval between data points and the regression line. The F-statistic indicates the overall significance of the regression model and the r-squared value the strength of the correlation between the data points and the regression line. The p-value offers insight into the statistical significance of if the independent variable has a meaningful relationship with the dependent variable.*

Within the tests conducted, there is no correlation between the [THAA] for temperature and the full coral data set (Fig. 5., Table 10, chapter 5 page 95); however, once the corals have been broken down into genera, there is a significant correlation (p-value of less than 0.05) between the [THAA] for temperature for *Stylaster* and *Caryophyllia*. Although *Stylaster* had a low R-squared value, indicating a poor fit of the trend. However, for *Caryophyllia* R^2 = 0.66, indicating a better fit to the trend. There are not many samples available within the *Caryophyllia* genus, so this may be biasing the data.

The statistical analysis of temperature and [THAA] and % Asx further indicates there are some relationships between temperature and the amino acid

parameters measured here. The linear regression tested for the % Asx and temperature has four groups with statistically significant results: all coral, stylasterid, aragonite stylasterid and *Caryophyllia* genus, although all with low correlation to the regression line (R^2<0.26). Indicating that there is a relationship between the independent variable and dependent variable, but the variation in the data points from the regression is very large and therefore, neither temperature nor [THAA] or % Asx can be used to directly infer the other. *Caryophyllia* has a stronger trend than the other corals. It could be inferred that although the temperature is seen to have a limited impact on the % Asx within stylasterid corals, the correlation with this Scleractinia genus is much more predominant.

Although there is a statistical significance within groups for both [THAA] and % Asx, other than for *Caryophyllia,* the split groups indicate low R-squared values throughout and therefore, although there are significant p values, there is a large variation of data within the temperature parameter. It is difficult to determine if temperature is controlling the [THAA] within this analysis due to the low fit ranges. The statistical significance in all corals, stylasterid coral and aragonite stylasterid coral does indicate that it could be impacting the % Asx and proteins within *Caryophyllia*; this is something that would need further exploration, especially in a larger range of samples within the *Stylaster* genus.

5.3 Salinity:

The salinity of the water used in this study ranges from 33.2 to 35.7, and hydrographic salinity data from GLODAP and GLODAP 2 (Lauvset, S *at al.*, 2021). Salinity and temperature, when factored together, are seen within shallow-water corals to potentially make the animal more vulnerable (Coles and Jokiel, 1978). Within deep-sea corals, there is little understanding of whether salinity has any impact on deep-sea corals and their amino acids.

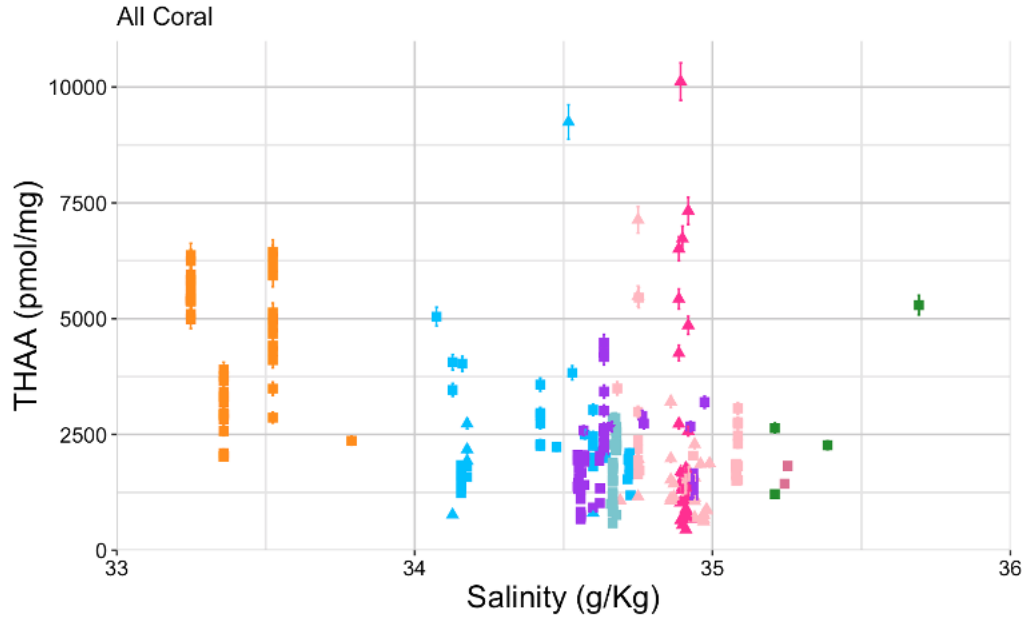

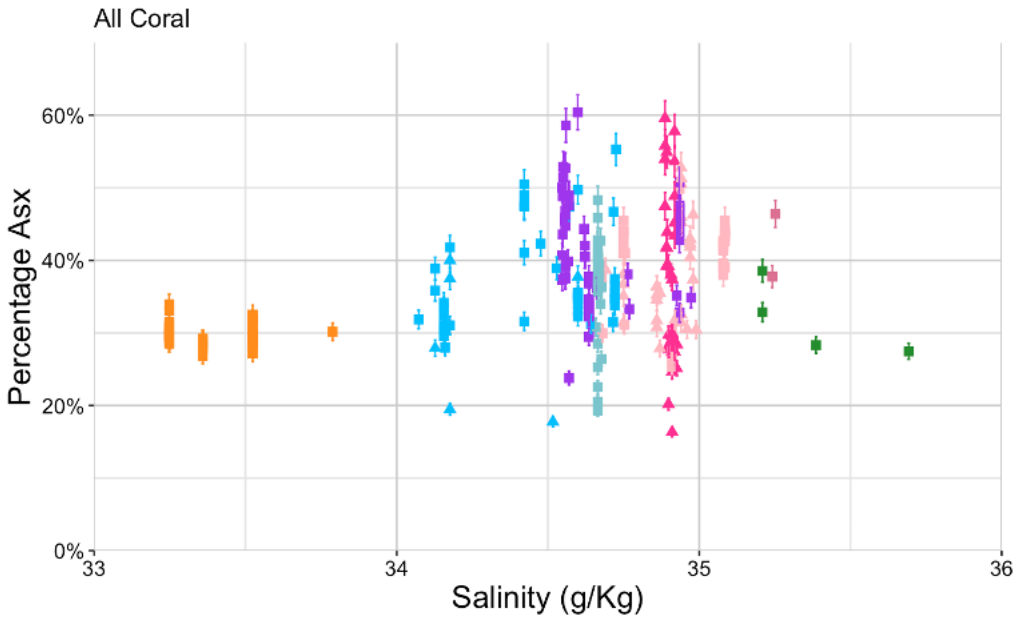

Figure 5.14 a and b: *All coral, [THAA] (top) and % Asx (bottom) for all corals against salinity (g/kg). Colour responds to the location of where the sample was taken. Error bars are 4%, representing the analytical replicate error.*

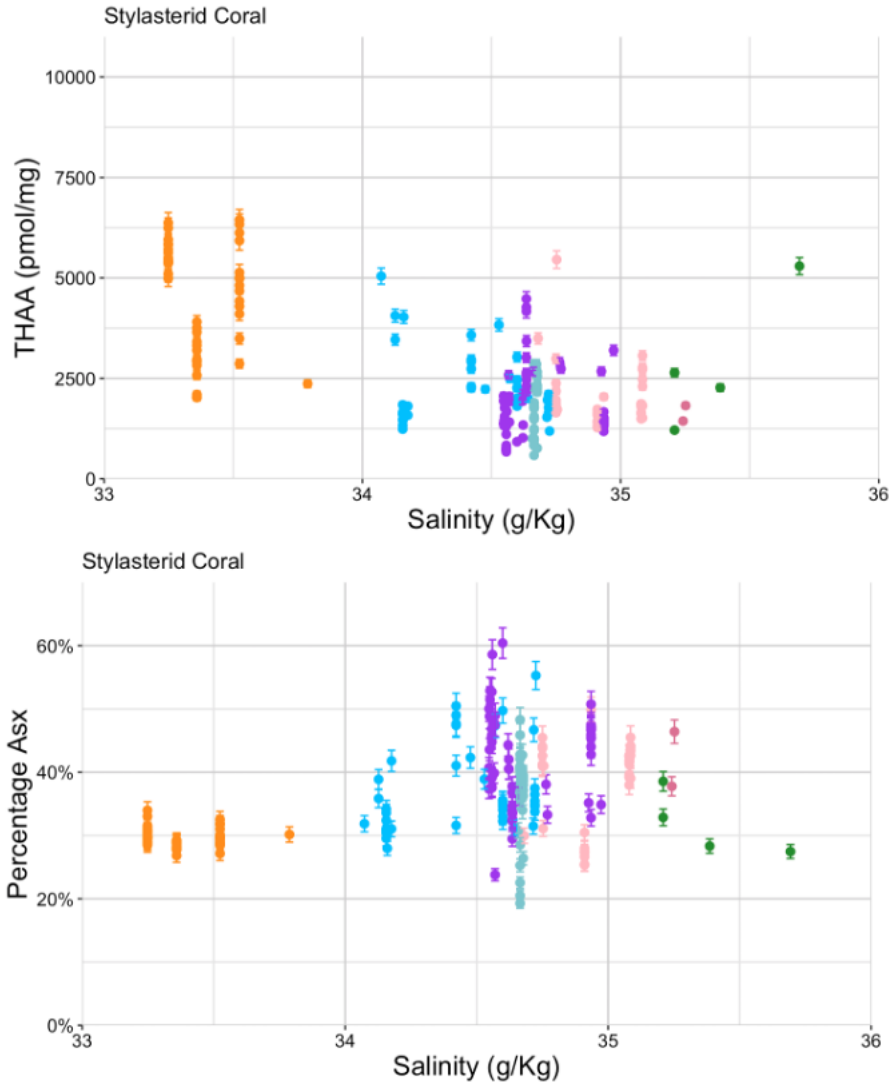

Figure 5.15 a and b: Stylasterid *coral [THAA] (top) and % Asx (bottom) for all corals against salinity (g/kg). Colour responds to the location of where the sample was taken. Error bars are 4%, representing the analytical replicate error.*

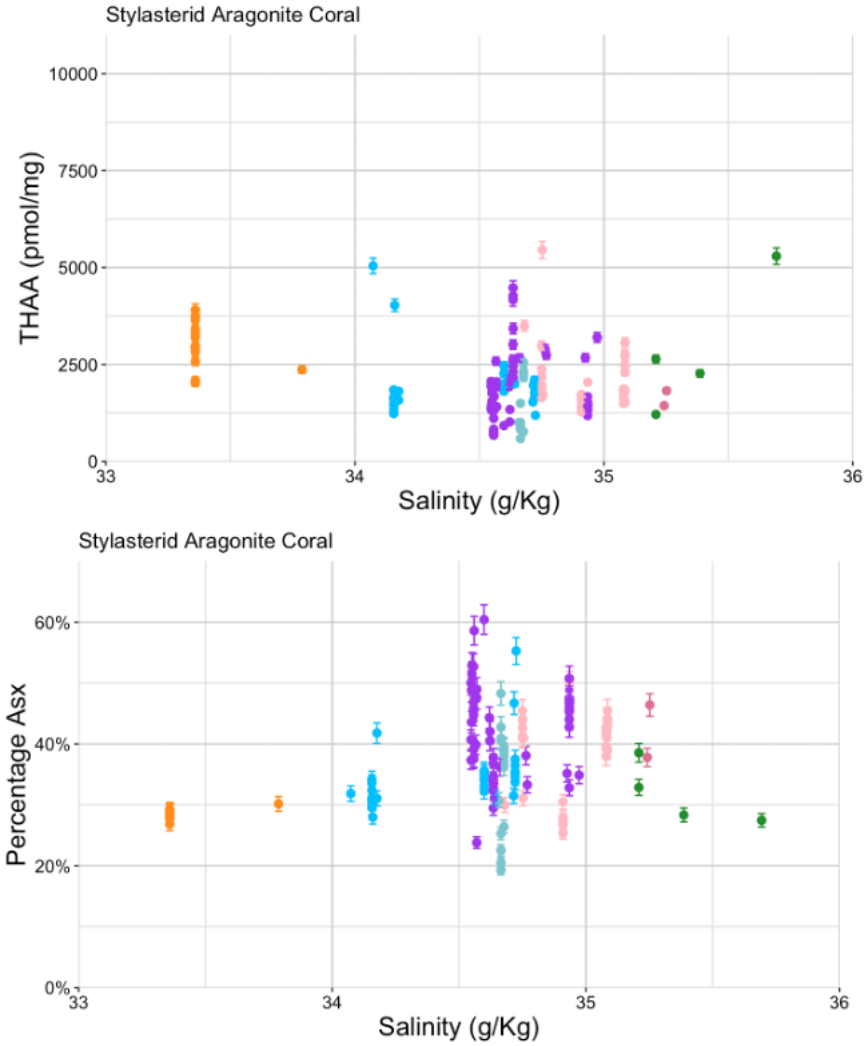

Figure 5.16 a and b: Aragonite stylasterid *coral. [THAA] (top) and % Asx (bottom) for all corals against salinity (g/kg). Colour responds to the location of where the sample was taken. Error bars are 4%, representing the analytical replicate error.*

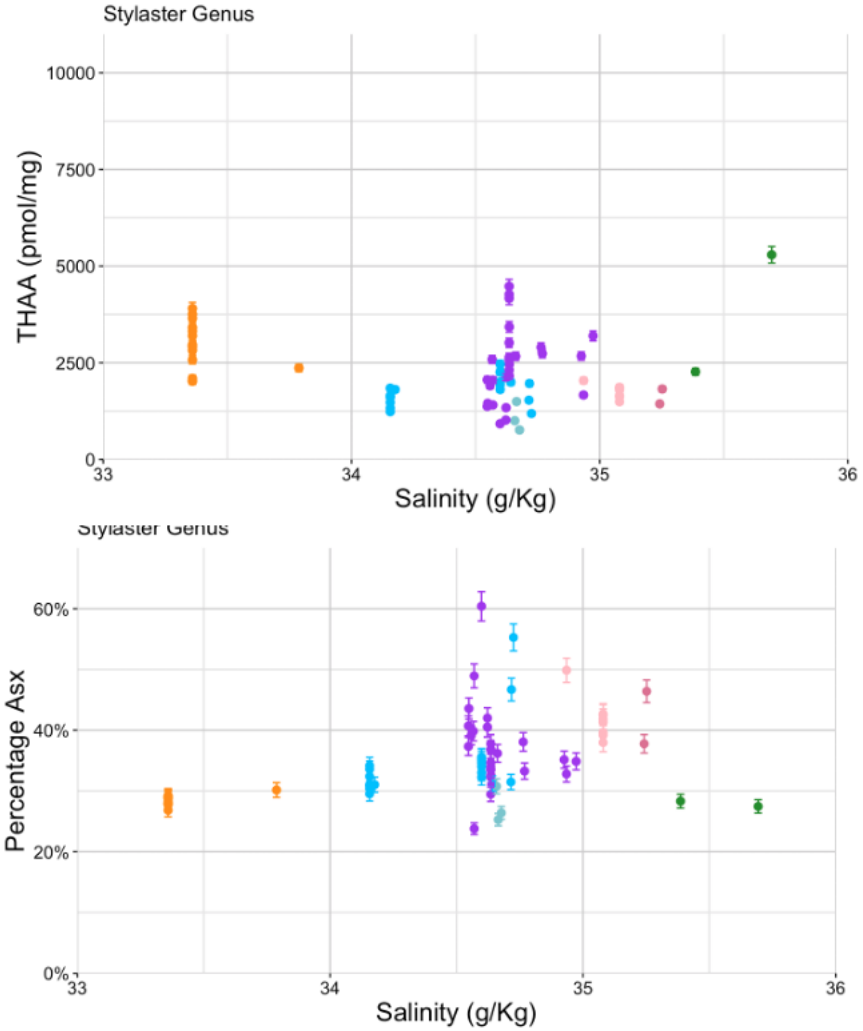

Figure 5.17 a and b: *Stylaster [THAA] (top) and % Asx (bottom) for all corals against salinity (g/kg). Colour responds to the location of where the sample was taken. Error bars are 4%, representing the analytical replicate error.*

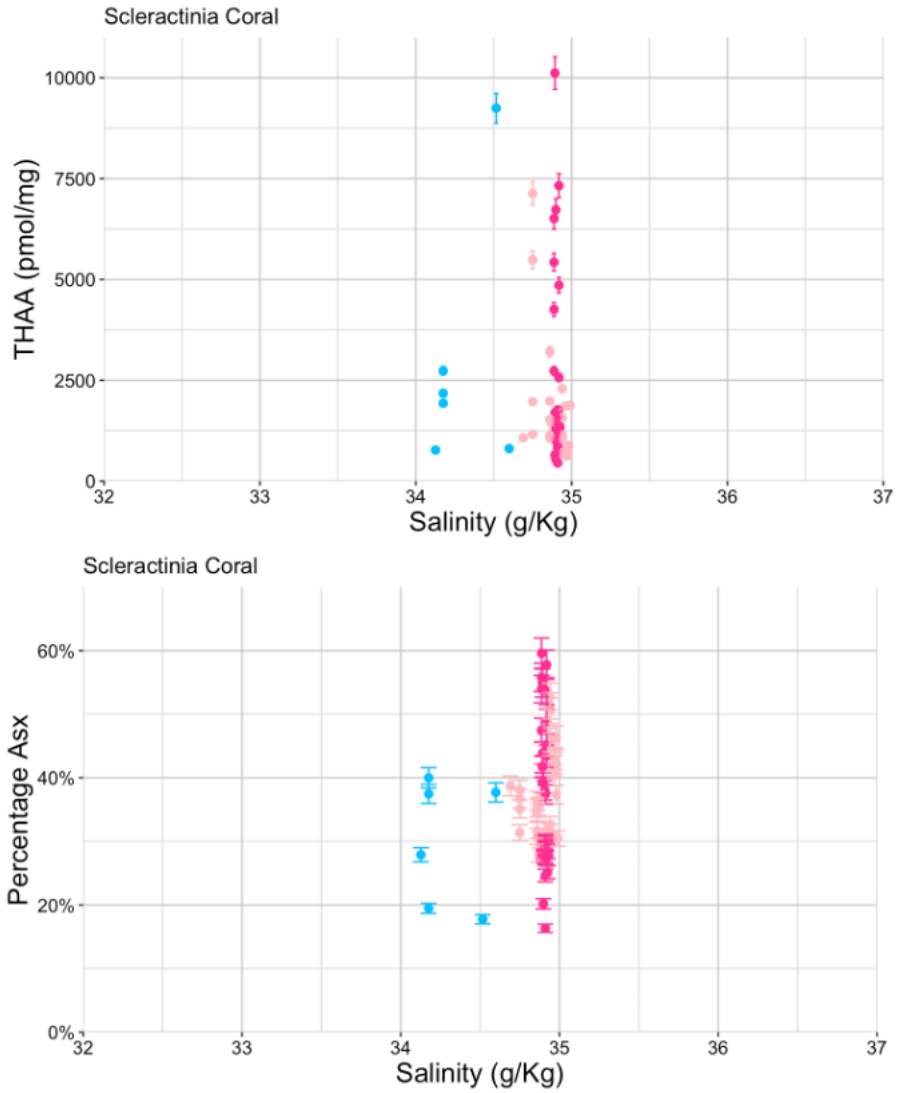

Figure 5.18 a and b: *[THAA] (top) and % Asx (bottom) for all corals against salinity (g/kg). Colour responds to the location of where the sample was taken. Error bars are 4%, representing the analytical replicate error.*

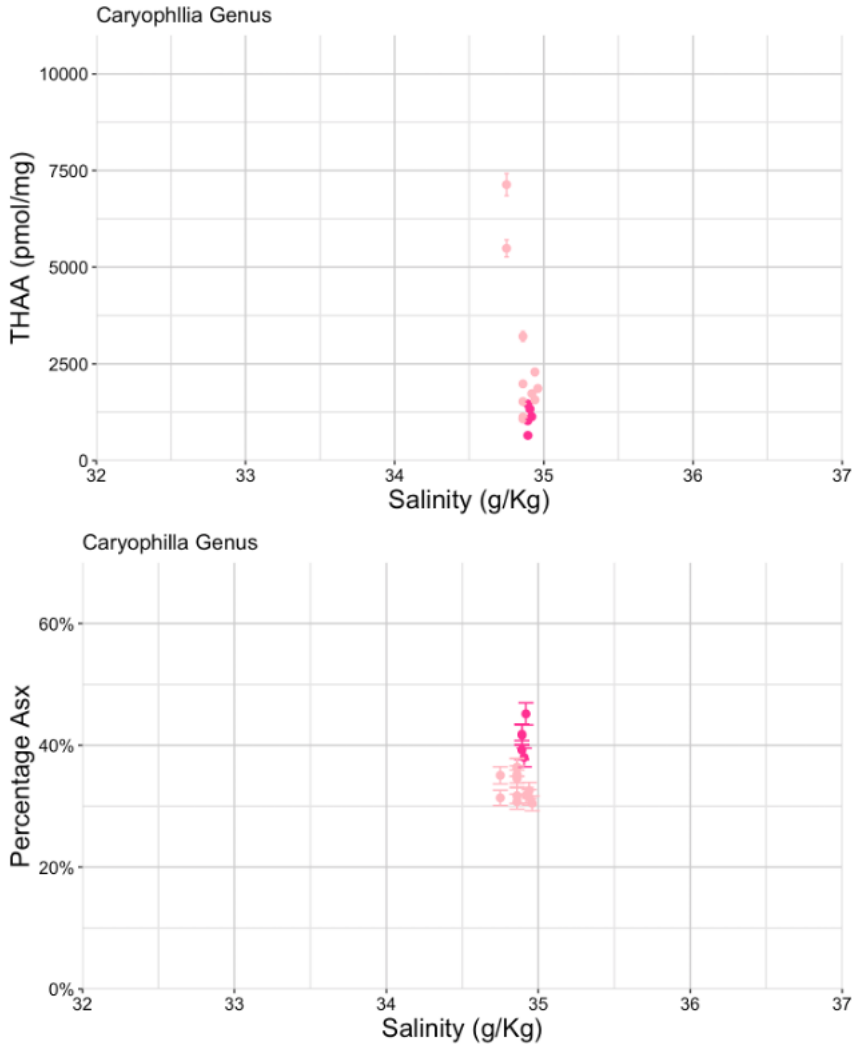

Figure 5.19 a and b: *Caryophyllia [THAA] (top) and % Asx (bottom) for all corals against salinity (g/kg). Colour responds to the location of where the sample was taken. Error bars are 4%, representing the analytical replicate error.*

5.3.1 Summary of findings for Salinity

Salinity g/kg									
Taxa	Group	Residual Std. Error		F - statistic		R - Squared		P value	
		[THAA]	% Asx	[THAA]	% Asx	[THAA]	% Asx	[THAA]	% Asx
All Coral		1369	0.14	117.6	46.0	0.288	0.14	2.2e-16	6.758e-11
Stylasterid	All	1049	0.07	183.3	65.1	0.463	0.23	2.2e-16	5.119e-14
	Aragonite only	892	0.08	12.4	21.4	0.074	0.12	0.0005	8.128e-06
	Stylaster only	869	0.06	4.0	23.0	0.038	0.23	0.0494	8.271e-06
Scleractinia	All	2045	0.10	1.5	3.0	0.007	0.03	0.2174	0.09
	Caryophyllia only	1175	0.05	19.2	0.2	0.532	-0.06	0.0005	0.69

Table 11, Regression analysis of salinity (g/kg) for THAA (pmol/mg) and % Asx for the six groups tested. Showing the residual error, F-statistic, R-squared and p-value. Pink shading indicates p-values of < 0.05, and therefore statistically significant.

The linear regression undertaken for the salinity vs [THAA] indicated that all groups other than *scleractinian* coral have some level of being statistically significant.
Caryophyllia, again, has the strongest linear regression within the groups (R^2 = 0.53), with stylasterid corals having the second strongest linear regression (R^2 =0.46).

Five out of six groups showed statistical significance within [THAA], this is important to identify, as this trend is especially strong within the stylasterid groupings. Indicating there could be impacts on the [THAA] within stylasterid coral skeletons from the salinity of the water they are growing in. This trend is also seen within *Caryophyllia* but not scleractinian corals, indicating that the variation within the Scleractinia could be missed when the whole group is analysed together.

Within the linear regression of salinity (g/kg) and % Asx, statistically, all coral, stylasterid coral, aragonite stylasterids and *Stylaster* genus had some level of significance, but not Scleractinia coral or *Caryophyllia* genus. The correlation between the % Asx, only seen within stylasterid coral groups, could be due to the large number of stylasterid samples. This is likely why the "all coral" group is also statistically significant. There is no correlation between the % Asx and scleractinian corals or in the *Caryophyllia* genus. Of the groups that had a p-value less than 0.05, the R-squared values are low (< 0.23), indicating the spread of data in the dependent value (% Asx) is very widely distributed. Therefore, generally, salinity is not a good predictor of % Asx.

[THAA] and % Asx tests found that stylasterid corals (stylasterid corals, aragonite stylasterid corals and *Stylaster* corals) all shared some statistical significance. This is a stronger trend when high-Mg calcite samples are included (Figure 5.15 a and b, page 98, Table 11, chapter 5, page 103), as they are the largest sample range included within the lower salinities. However, this trend still exists within the groupings that don't have high-Mg samples, and therefore, salinity could have an impact (low) on the [THAA] and % Asx within stylasterid corals. A correlation is also seen within *Caryophyllia* for [THAA], but the salinity range is very low (34.75-34.96). A larger sample range of both Scleractinian corals and *Caryophyllia* would need to be analysed to confirm these relationships.

5.4 pH

The pH data reported were measured from the surrounding water of the coral (either at the time of collection or based on previously collected data and ranged from 7.58 – 8.09 (Lauvset, S *at al.*, 2021). The range of surface ocean pH globally is 7.9 – 8.4, although this differs in the deep-sea, as it is naturally lower, although is getting worse with climate change (Harris *et al.*, 2023). The data within this study is in a lower variation of global pH parameters (Owens, 2009). pH has been calculated using a SEACARB package within R (Gattuso *et al.*, 2021). Parameters used in this calculation included DIC, dissociation constants of carbonate and alkalinity, all acquired from Lueker *et al.* (2000).

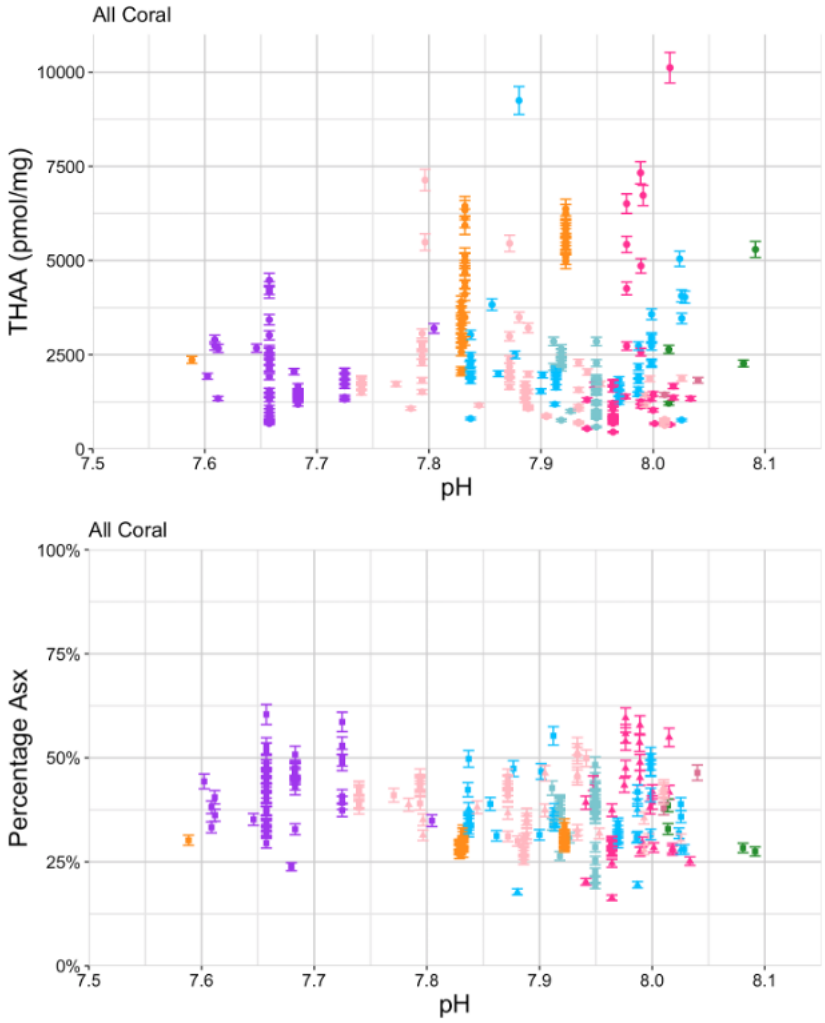

Figure 5.20 a and b *All coral [THAA] (top) and % Asx (bottom) against pH. Colour responds to the location of where the sample was taken. Error bars are 4%, representing the analytical replicate error.*

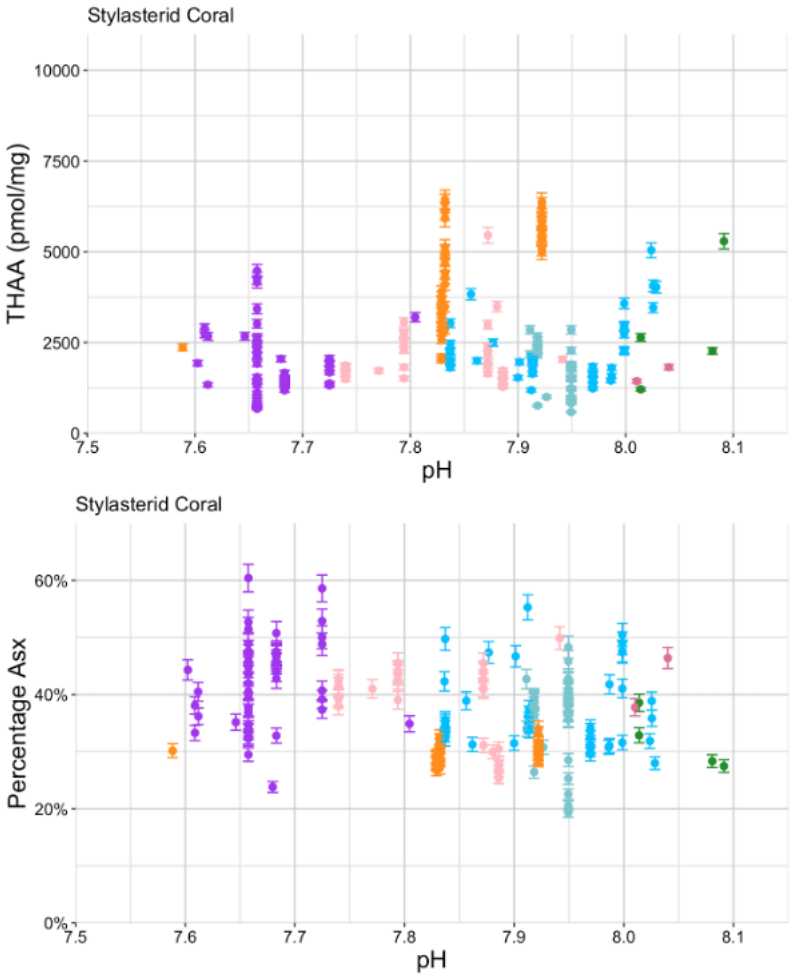

Figure 5.21 a and b: Stylasterid *[THAA] (top) and % Asx (bottom) against pH. Colour responds to the location of where the sample was taken. Error bars are 4%, representing the analytical replicate error.*

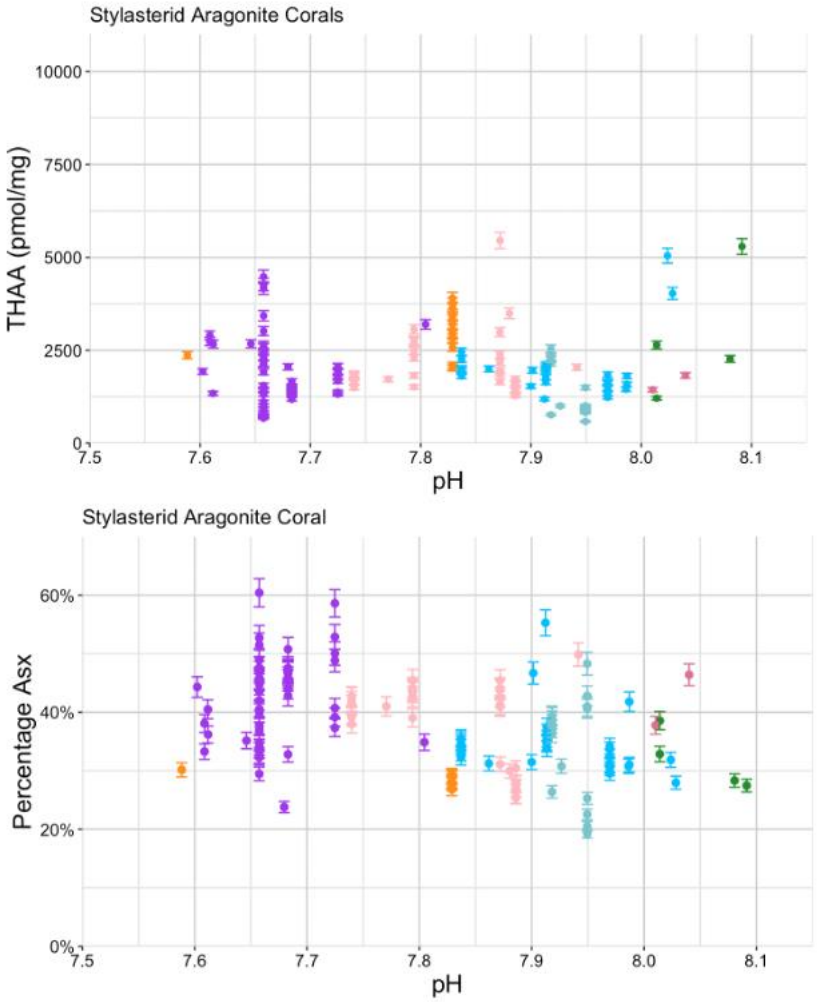

Figure 5.22 a and b: *Aragonite [THAA] (top) and % Asx (bottom) against pH. Colour responds to the location of where the sample was taken. Error bars are 4%, representing the analytical replicate error.*

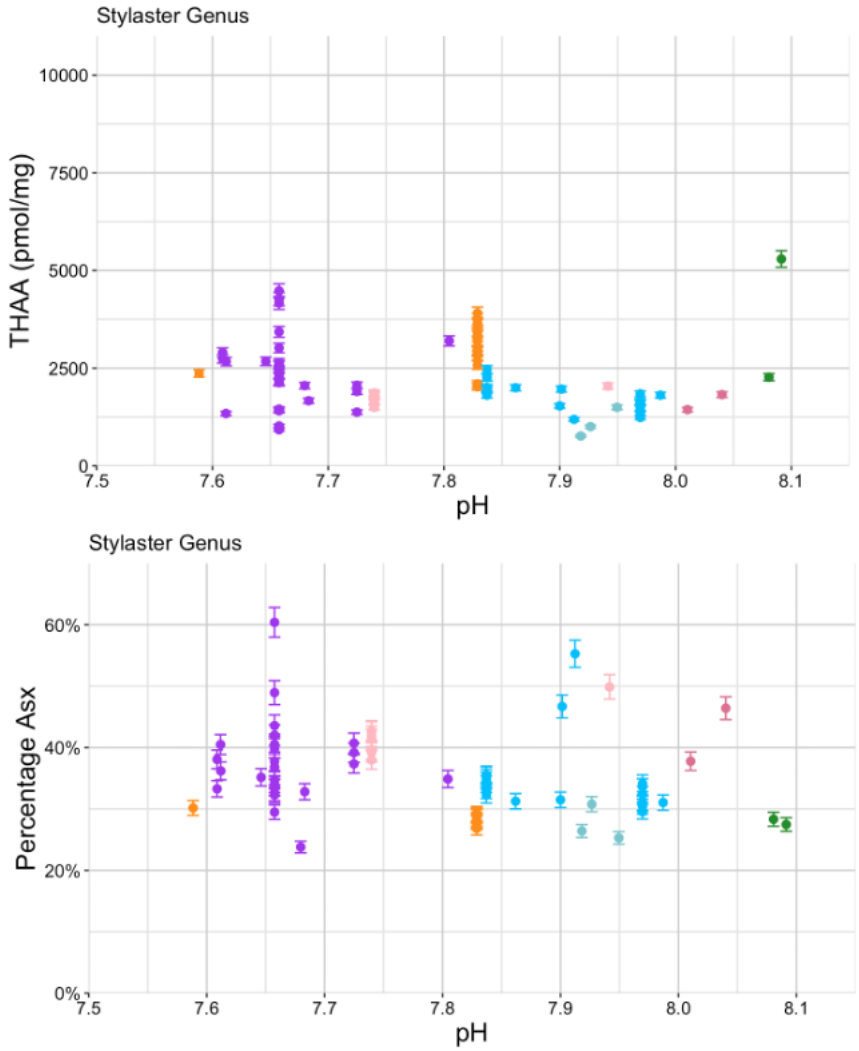

Figure 5.23a and b: *Stylaster [THAA] (top) and % Asx (bottom) against pH. Colour responds to the location of where the sample was taken. Error bars are 4%, representing the analytical replicate error.*

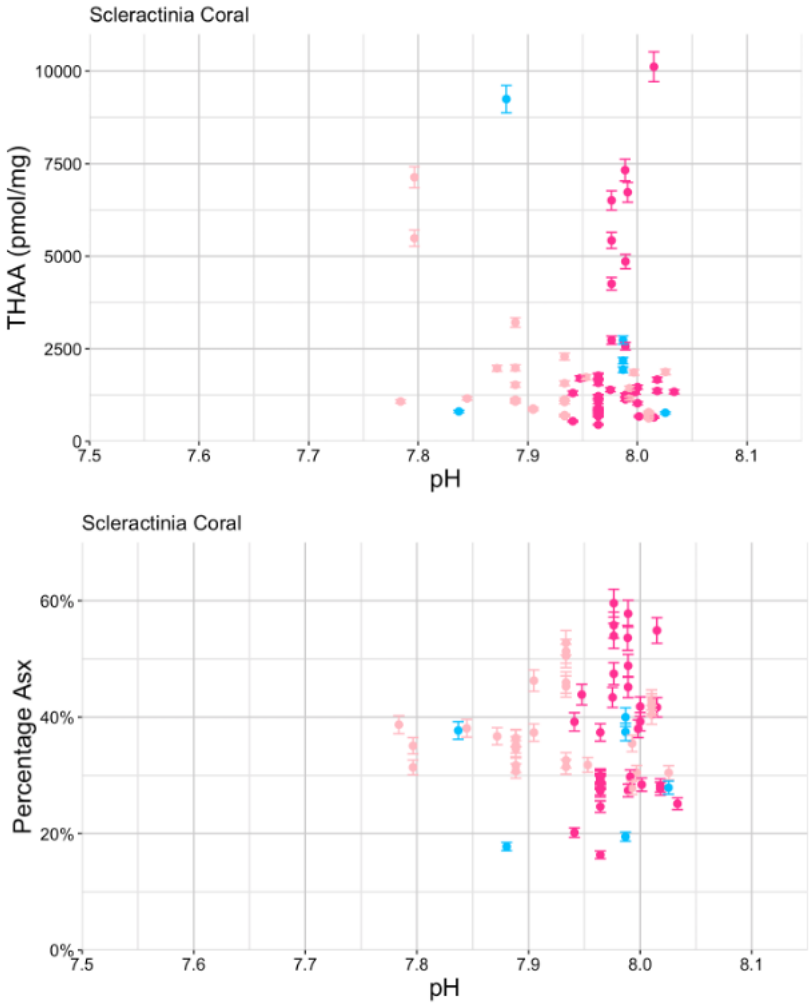

Figure 5.24 a and b: Scleractinia *[THAA] (top) and % Asx (bottom) against pH. Colour responds to the location of where the sample was taken. Error bars are 4%, representing the analytical replicate error.*

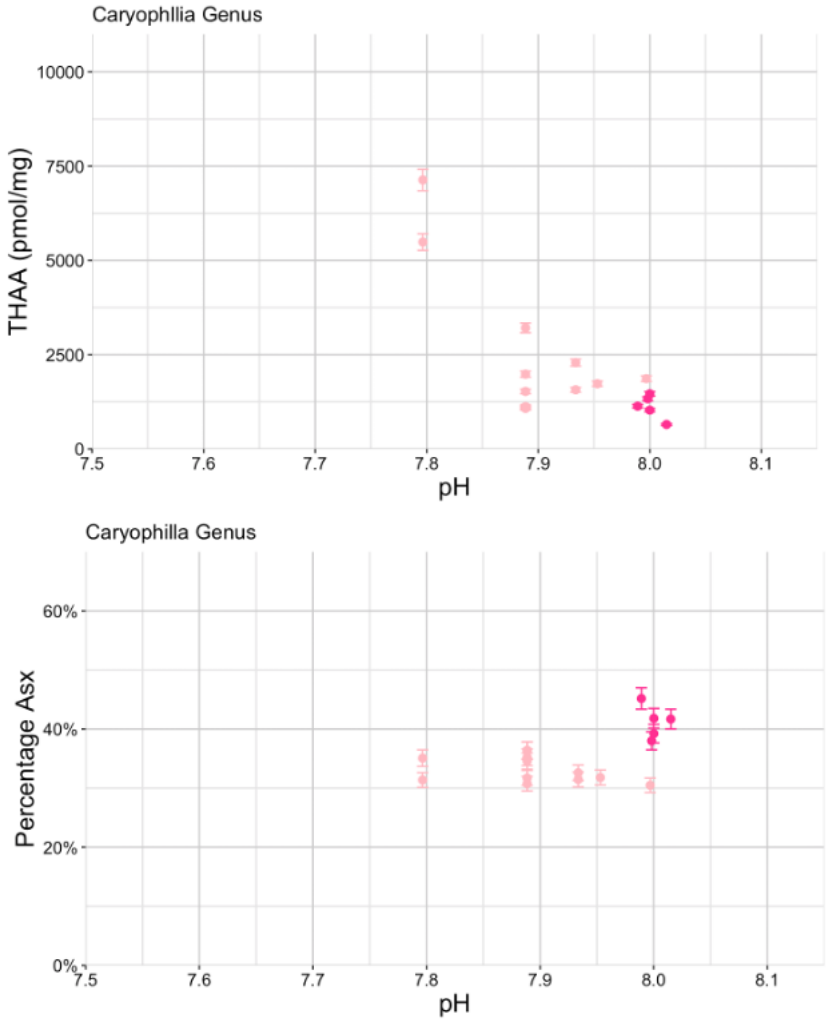

Figure 5.25 a and b: *Caryophillia [THAA] (top) and % Asx (bottom) against pH. Colour responds to the location of where the sample was taken. Error bars are 4%, representing the analytical replicate error.*

5.4.1 Summary of findings for pH

pH									
Taxa	Group	Residual Std. Error		F - statistic		R - Squared		P value	
		[THAA]	% Asx	[THAA]	% Asx	[THAA]	% Asx	[THAA]	% Asx
All Coral		1623	0.080	0.69	15.8	-0.0010	0.05	0.4082	8.907e-05
Stylasterid	All	1405	0.072	8.02	25.7	0.0318	0.10	0.0051	8.792e-07
	Aragonite only	924	0.067	1.76	24.9	0.0052	0.14	0.1872	1.721e-06
	Stylaster only	882	0.067	1.68	5.0	0.0090	0.05	0.1987	0.03
Scleractinia	All	2054	0.003	0.95	0.2	-0.0007	-0.01	0.3339	0.70
	Caryophyllia only	1197	0.040	17.90	5.2	0.5137	0.21	0.0007	0.04

Table 12: Regression analysis of pH for [THAA] and % Asx for the six groups tested, showing the residual error, F-statistic, R-squared and p-value. Pink shading indicates p-values of < 0.05, and therefore statistically significant.

Linear regression was undertaken on [THAA] for pH (Table 12, chapter 5, page 114); the groups that showed statistical significance were stylasterid coral and *Caryophyllia*. The low F-statistic, R-squared value and p-value of stylasterid corals show that although samples do follow a trend, the data is largely spread within the linear regression. The *Caryophyllia* genus has a large F-statistic, R-squared value (0.51) and low p-value, indicating a stronger trend to the line of best fit within the linear regression. In this analysis, a correlation with pH is seen for the stylasterids and for the *Caryophyllia* genus within the scleractinian coral, but not within the combined genus group of Scleractinia coral.

Although Scleractinia corals, as a combined taxa group, do not have a significant relationship between [THAA] and pH, *Caryophyllia* does. This follows the same trend as the shallow-water coral *Stylophora pistillata* (Tomiak, 2013). Both have higher [THAA] at lower pHs, although the magnitudes are different (Figure 5.26, chapter 5, page 112).

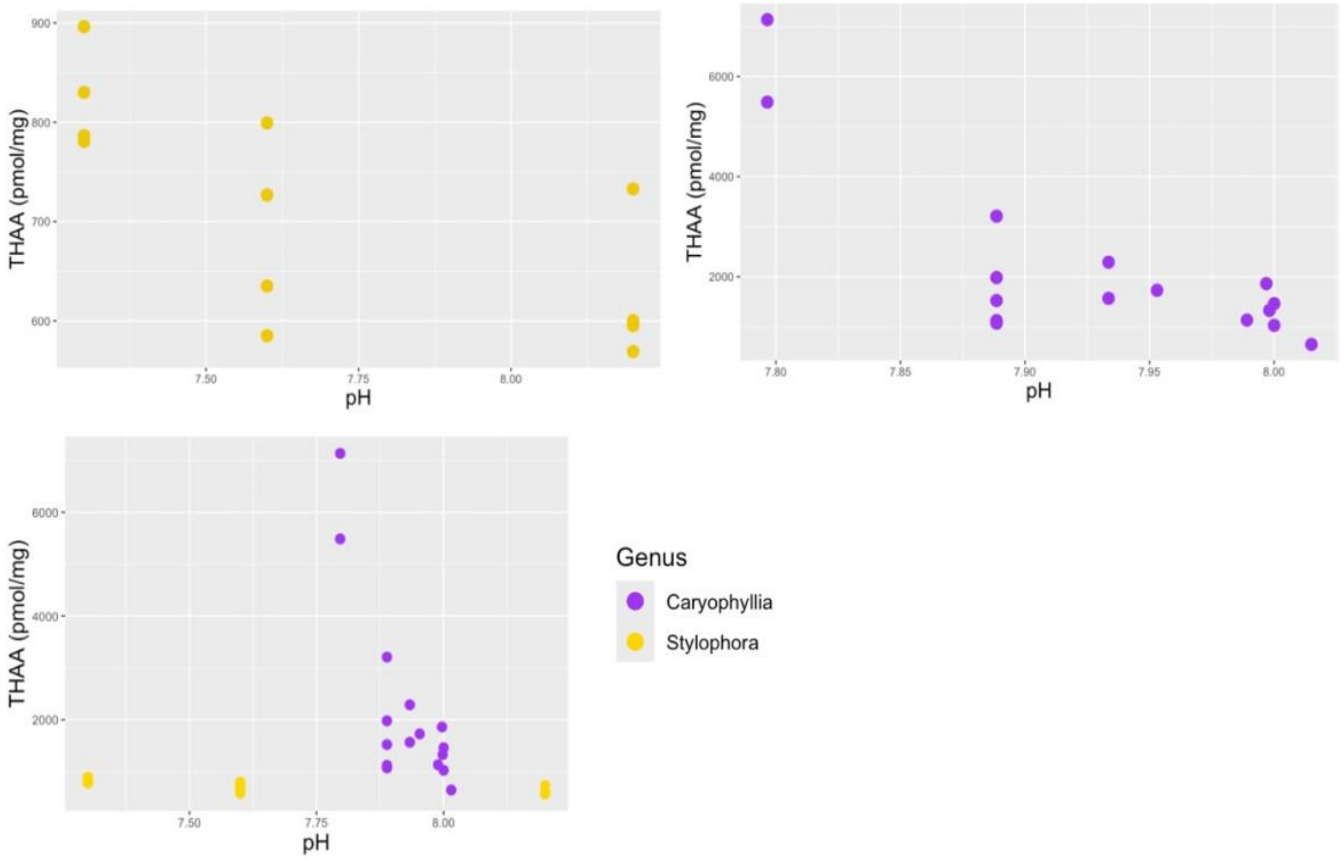

Figure 5.26: [THAA] of shallow coral data from (Tomiak, 2013) and Caryophyllia against pH.

The linear regression undertaken for the % Asx revealed a larger quantity of groups with a level of statistical significance than for the [THAA]. All groups other than Scleractinia showed a p-value less than 0.05 but low R-squared values (R^2 > 14). *Caryophyllia* was the exception to this with an R-squared value of 0.51 indicating samples fit within the trend of increased [THAA] at low pH. pH overall seems, to have more of an impact on the % Asx than on the [THAA]. The % Asx gradually decreases with increasing pH (Fig.
5.20b / table 12, chapter 5, page 114)

5.5 Aragonite saturation state

The aragonite saturation state (Ω) within the samples tested is mainly concentrated between 0.5 and 1.5. Within this study anything falling below the aragonite saturation state of 1 is considered to be undersaturated and therefore prone to dissolution as suggested by Harris, DeGrandpre and Hales, (2013). However, with rapid environmental changes, many deep-sea corals live on the 1Ω boundary and it is important to notice environmental change could mean 1Ω would in future not be a suitable medium for saturated or undersaturated water. The samples are therefore divided and tested (T-test) between the two factors of undersaturated and saturated. Aragonite saturation was calculated using a

SEACARB package within R (Gattuso *et al*., 2021). Parameters for this calculation include DIC, dissociation constants of carbonate and alkalinity acquired from Lueker *et al*. (2000).

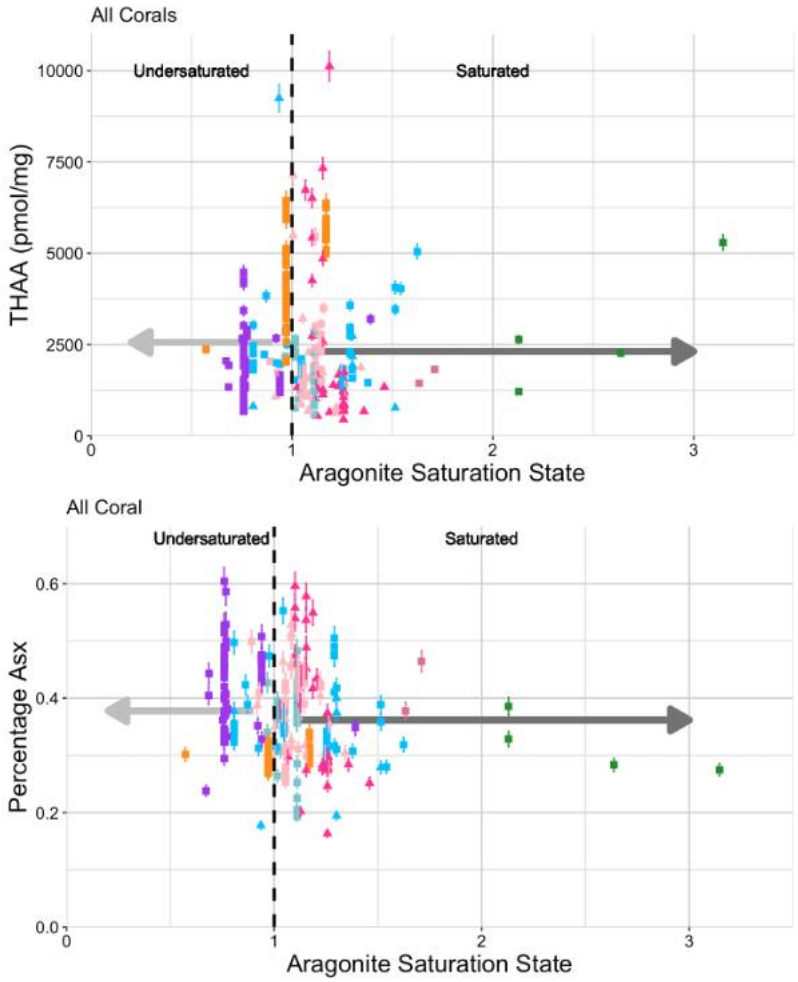

Figure 5.27 a and b: *All coral [THAA] (top) and % Asx (bottom) against aragonite saturation. Colour responds to the location of where the sample was taken. Error bars are 4%, representing the analytical replicate error. Arrows point to the direction of more undersaturated or more saturated water and are located at the mean of the samples on either side of the saturation divide on the y-axis.*

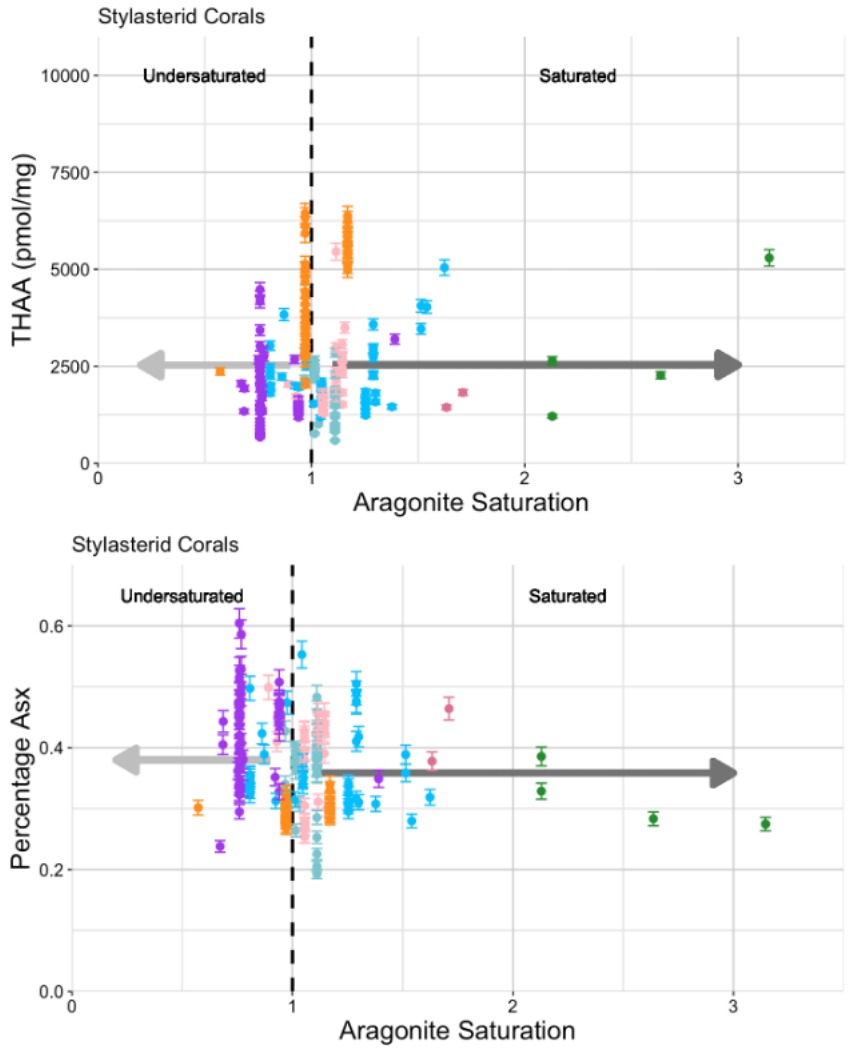

Figure 5.28 a and b: Stylasterid *coral [THAA] (top) and % Asx (bottom) against aragonite saturation. Colour responds to the location of where the sample was taken. Error bars are 4%, representing the analytical replicate error. Arrows point to the direction of more undersaturated or more saturated water and are located at the mean of the samples on either side of the saturation divide on the y-axis.*

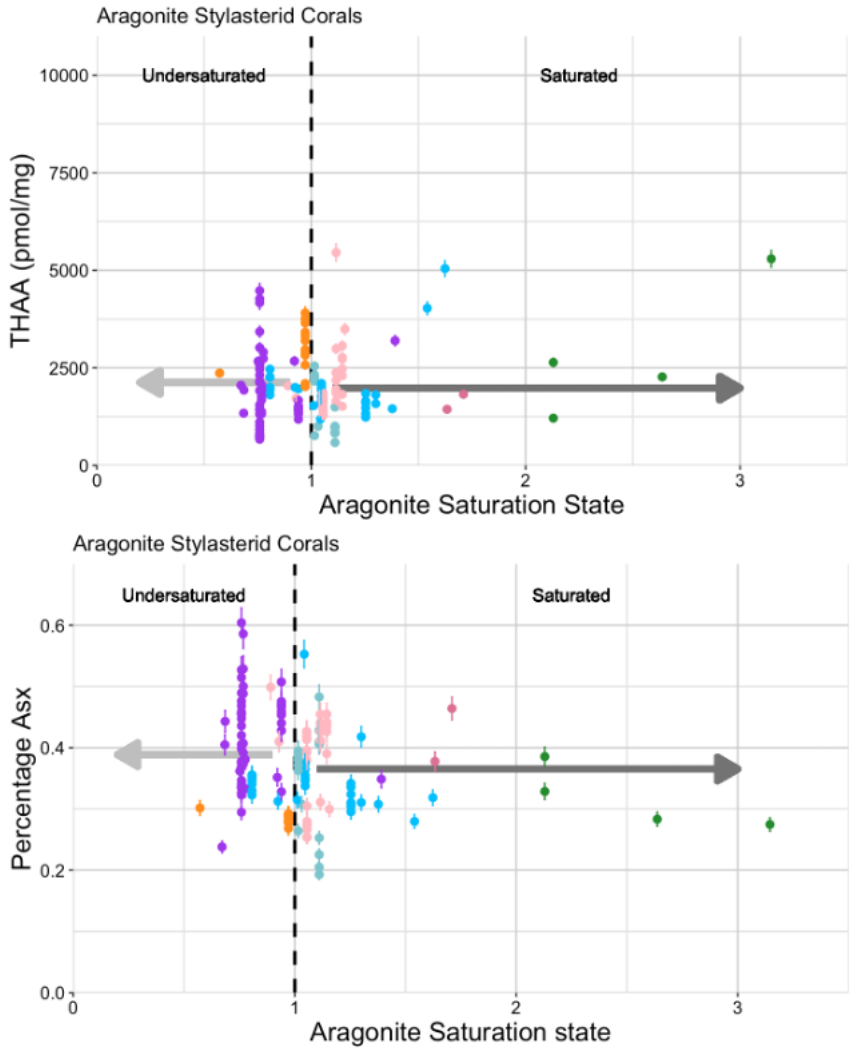

Figure 5.29 a and b: *Aragonite stylasterid [THAA] (top) and % Asx (bottom) against aragonite saturation. Colour responds to the location of where the sample was taken. Error bars are 4%, representing the analytical replicate error. Arrows point to the direction of more undersaturated or more saturated water and are located at the mean of the samples on either side of the saturation divide on the y-axis.*

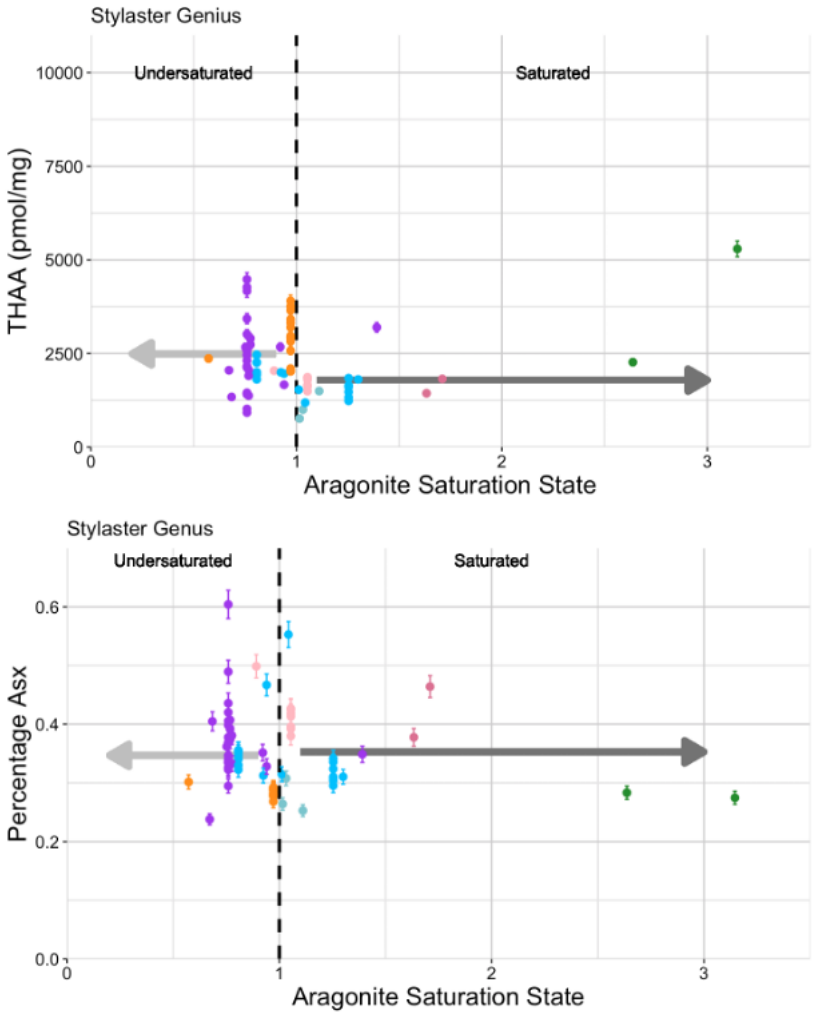

Figure 5.30 a and b: *Stylaster [THAA] (top) and % Asx (bottom) against aragonite saturation. Colour responds to the location of where the sample was taken. Error bars are 4%, representing the analytical replicate error. Arrows point to the direction of more undersaturated or more saturated water and are located at the mean of the samples on either side of the saturation divide on the y-axis.24a - Statistical significance*

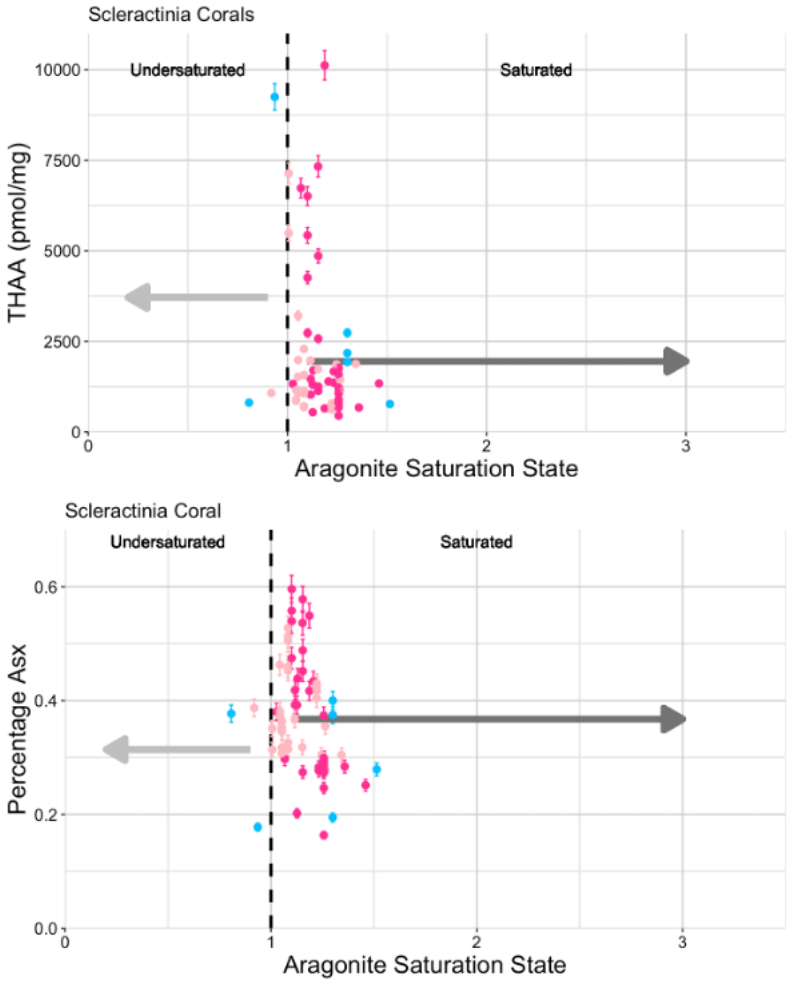

Figure 5.31 a and b: Scleractinia *[THAA] (top) and % Asx (bottom) against aragonite saturation. Colour responds to the location of where the sample was taken. Error bars are 4%, representing the analytical replicate error. Arrows point to the direction of more undersaturated or more saturated water and are located at the mean of the samples on either side of the saturation divide on the y-axis.*

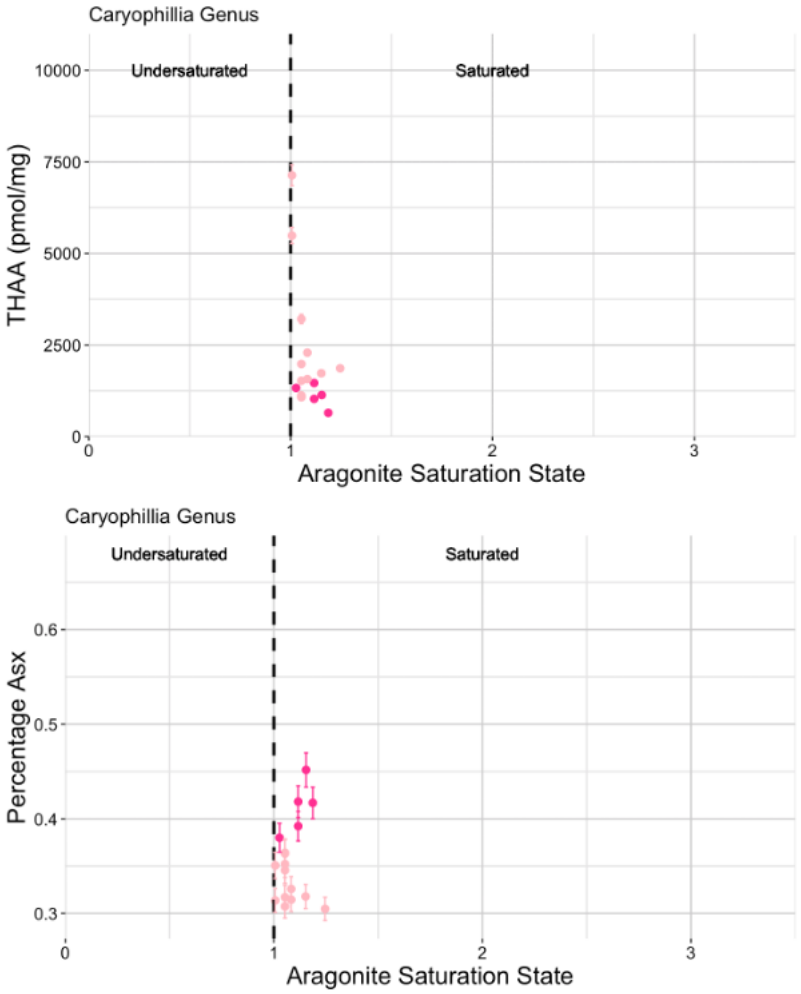

Figure 5.32 a and b: *Caryophyllia [THAA] (top) and % Asx (bottom) against aragonite saturation. Colour responds to the location of where the sample was taken. Error bars are 4%, representing the analytical replicate error. Arrows point to the direction of more undersaturated or more saturated water and are located at the mean of the samples on either side of the saturation divide on the y-axis.*

5.5.1 Summary of findings for aragonite saturation

T-tests were conducted on the aragonite saturation against [THAA] for the samples taken in undersaturated water and the samples taken in saturated water. This is to understand if corals in undersaturated water are reacting differently to saturated water. The *Caryophyllia* samples have not had a t-test conducted on the group, as there are no samples below the aragonite saturation state of 1 within this study.

Aragonite Saturation State										
Group	Mean		SD		T.test result					
					T		df		p-value	
	[THAA]	% Asx	[THAA]	% Asx	[THAA]	% Asx	[THAA]	% Asx	[THAA]	% Asx
All corals (Undersaturated)	2561	0.38	1488	0.084	1.3123	1.5841	239.79	207.64	0.1907	0.1147
All Corals (Saturated)	2310	0.36	1692	0.080						
Stylasterid Corals (Undersaturated)	2527	0.38	1336	0.083	0.036612	2.0533	212.91	195.39	0.9708	0.04137
Stylasterid Corals (Saturated)	2534	0.36	1512	0.068						
Aragonite Stylasterid Corals (Undersaturated)	2127	0.39	1179	0.085	0.79333	1.9724	207.34	178.55	0.4285	0.05011
Aragonite Stylasterid Corals (Saturated)	1981	0.37	1533	0.087						
Stylaster Genus (Undersaturated)	2491	0.35	812	0.068	3.4192	-0.3474	45.504	46.214	0.001335	0.7299
Stylaster Genus (Saturated)	1788	0.35	858	0.071						
Scleractinia Corals (Undersaturated)	3709	0.31	4797	0.119	0.63221	-0.77202	2.0266	2.1151	0.5911	0.517
Scleractinia Corals (Saturated)	1952	0.37	1900	0.097						

Table 13, T-test analysis of aragonite saturation, undersaturated and saturated saturation states for the six tested groups for THAA (pmol/mg) and % Asx. Pink shading indicates p-values of < 0.05, and therefore statistically significant.

The T-test results showed that only one group had a statistical difference between the [THAA] in undersaturated and saturated water: *Stylaster* genus, p = 0.001.

T-tests were also conducted for the % Asx within the samples for the undersaturated and saturated states. The results showed that two groups have some statistical differences between the undersaturated water and saturated: stylasterid corals and aragonite stylasterid corals (Table 13, chapter 5, page 122). The distribution of samples within the aragonite saturation parameter is concentrated within the range of 0.4-3.2, indicating that many deep-sea corals can live within low saturation states (Stewart *et al.*, 2022). The statistical significance seen within the analysis between both [THAA] and the % Asx is seen within only stylasterid groupings. Stylaster [THAA] is increased in the undersaturated water (mean = 2491) compared to saturated (mean = 1788). The % Asx is also higher in undersaturated water for stylasterid corals (undersaturated mean = 38% saturated mean = 36%) and stylasterid aragonite corals (undersaturated = 39%, saturated = 37%).

The two groups of stylasterid corals that are statistically significant for the % Asx are stylasterids, which include the high-Mg samples and aragonite stylasterids. This means there could be a link between the mineralogy, as this is the differentiating factor between those groups in undersaturated water and saturated. Therefore, the mineralogies within undersaturated and saturated water have been tested. (Figures 5.33 -5.35, chapter 5, pages 123-125).

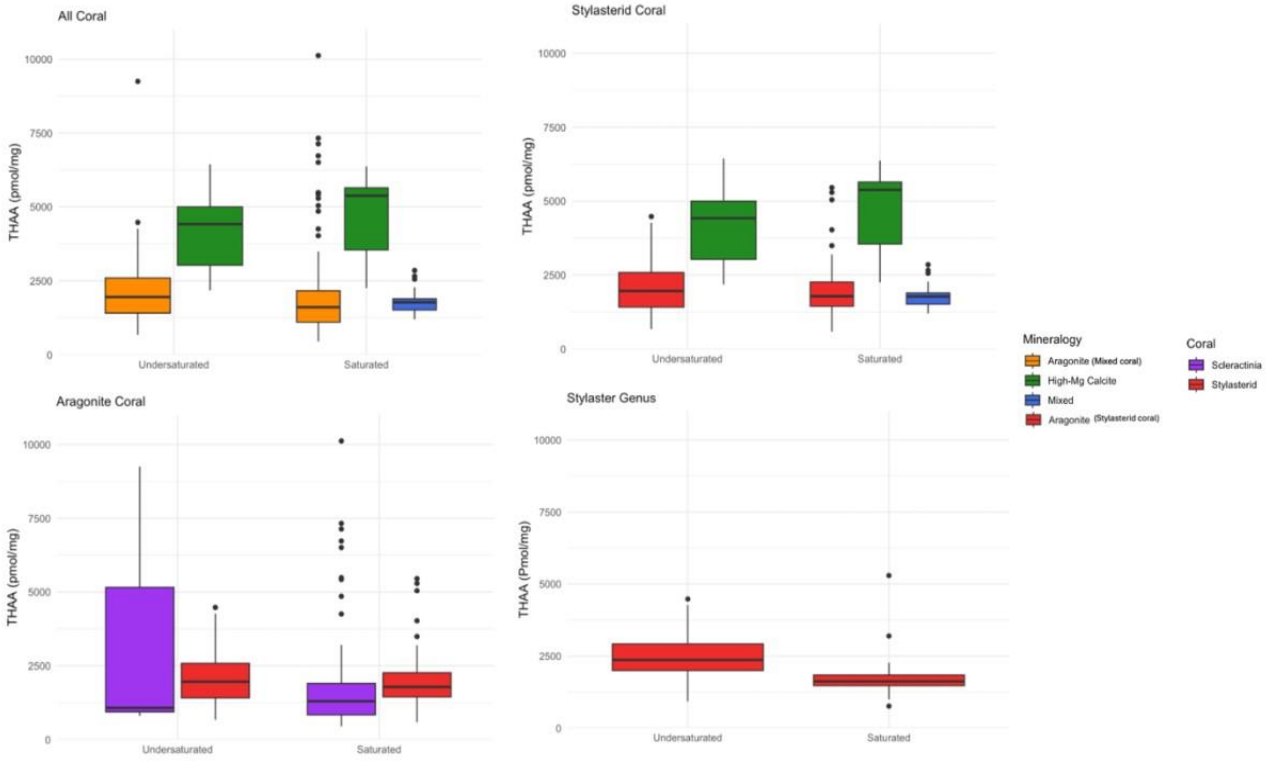

Figure 5.33: *Box plots indicating the [THAA] against undersaturated and saturated water and the mineralogy of the corals within the saturation states.*

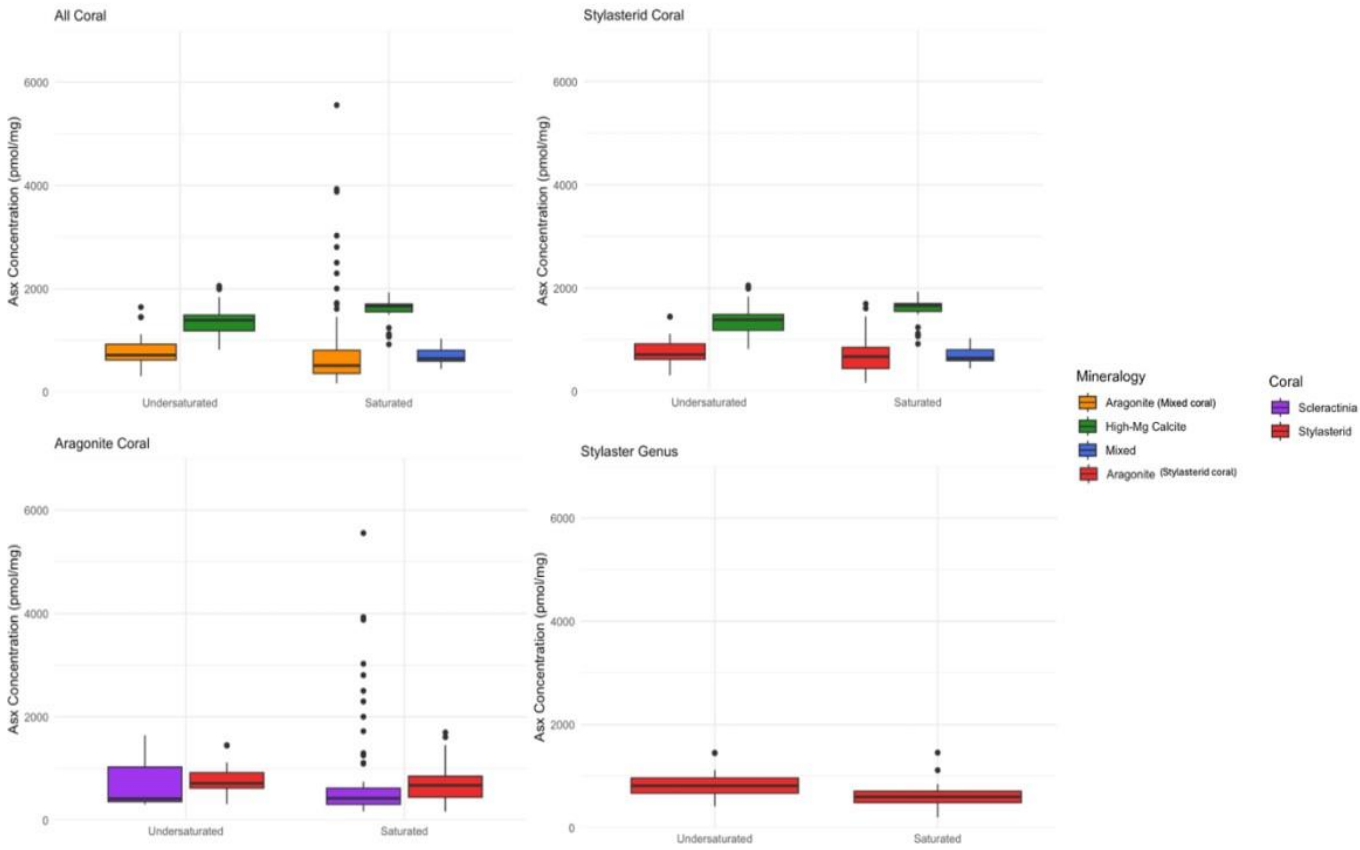

Figure 5.34: *Box plots indicating the Asx concentration in undersaturated and saturated water and the mineralogy of the corals within the saturation states.*

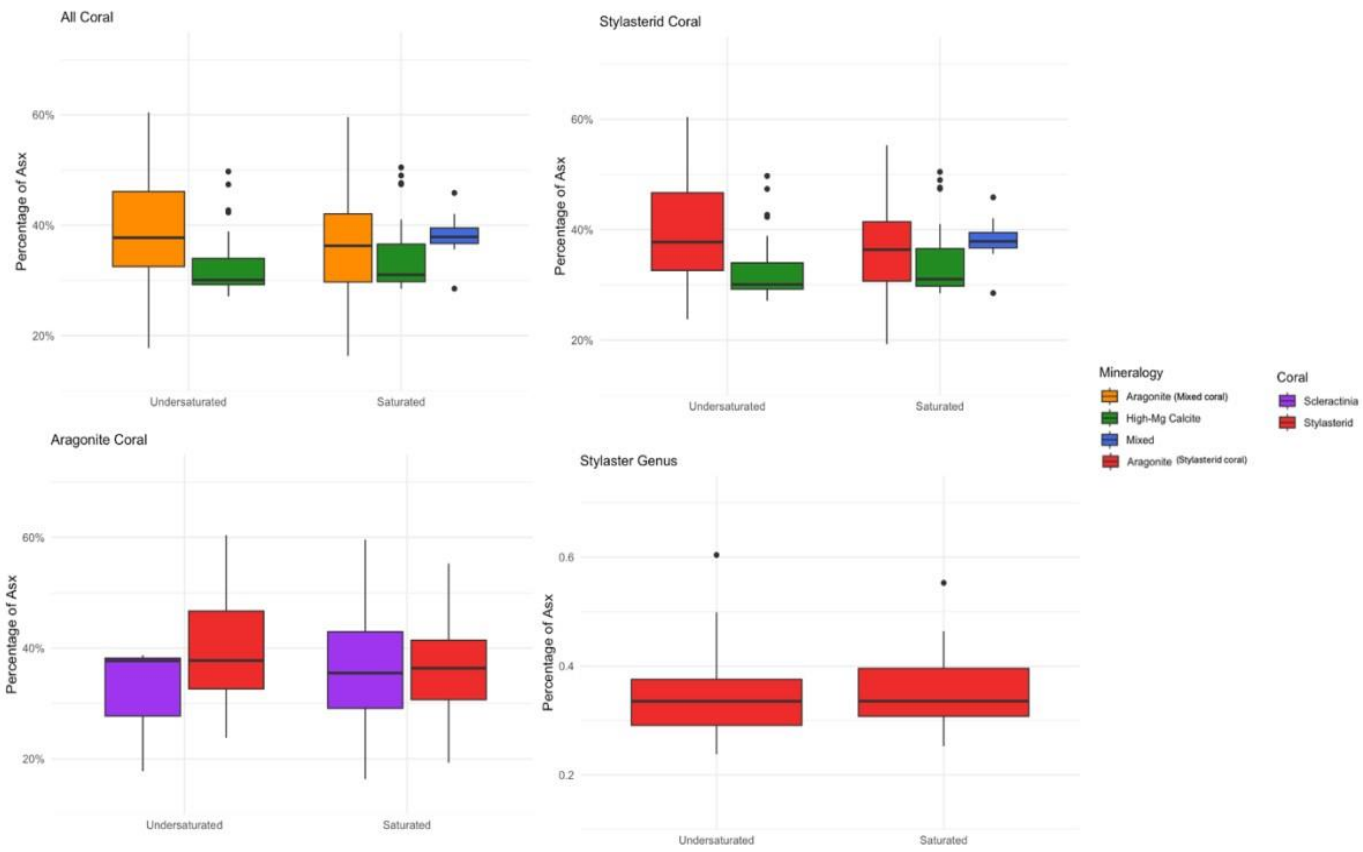

***Figure 5.35**, Box plots indicating the percentage of Asx in undersaturated and saturated water and the mineralogy of the corals within the saturation states.*

High-Mg samples are always higher in [THAA] (Section 4.4.1), and Asx % compared to aragonite mixed coral and aragonite stylasterid groups (Table 13, chapter 5, page 122). Unfortunately, it was not possible to compare the mineralogy of *Stylaster as they are all* aragonite samples within this study. However, the variation of [THAA] and % Asx between undersaturated and saturated water has been visualised in the boxplots (Figures 5.33 – 5.35, chapter 5, pages 123-125).

5.6 Dissolved inorganic carbon (DIC)

When DIC is readily available in the form of carbonate ions, it allows for corals to be able to build their skeletal material more easily and therefore is a positive for them (Tambutté *et al.*, 2011). However, as a result of climate change the concentration of carbonate ions in the ocean decreases. As explained in section 1.5, the CO_2 within the atmosphere is in equilibrium with other reactions in the ocean. If the equilibrium in Eq. 5.1 shifts in favour of the formation of bicarbonate (HCO_3^-), there are fewer carbonate ions available for the formation of coral skeletal material (Erez *et al.*, 2010).

$$H^+(aq) + {CO_3}^-(aq) \rightleftharpoons {HCO_3}^-(aq) \text{ (Equation 5.1)}$$

DIC hydrographic data is from GLODAP and GLODAP 2 (Lauvset, S *at al.*, 2021).

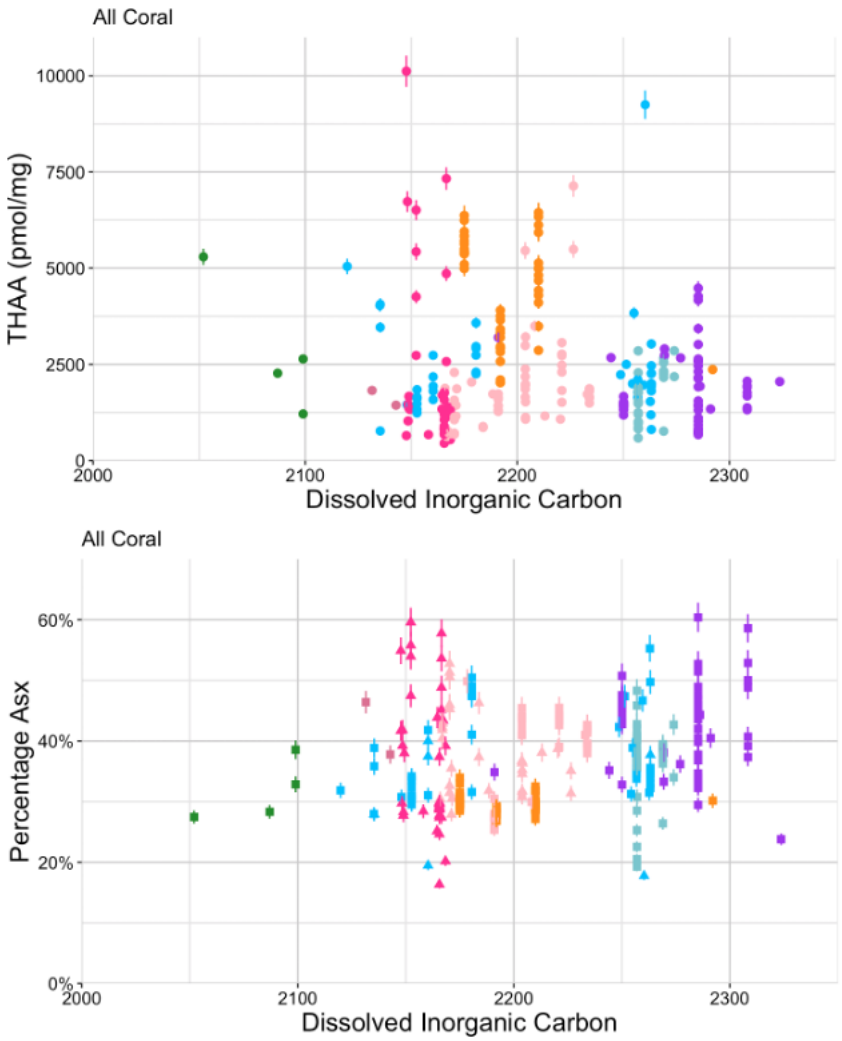

Figure 5.36 a and b: *All coral [THAA] (top) and % Asx (bottom) against dissolved inorganic carbon (µmol/kg) for all coral samples. Colour responds to the location of where the sample was taken. Error bars are 4%, representing the analytical replicate error.*

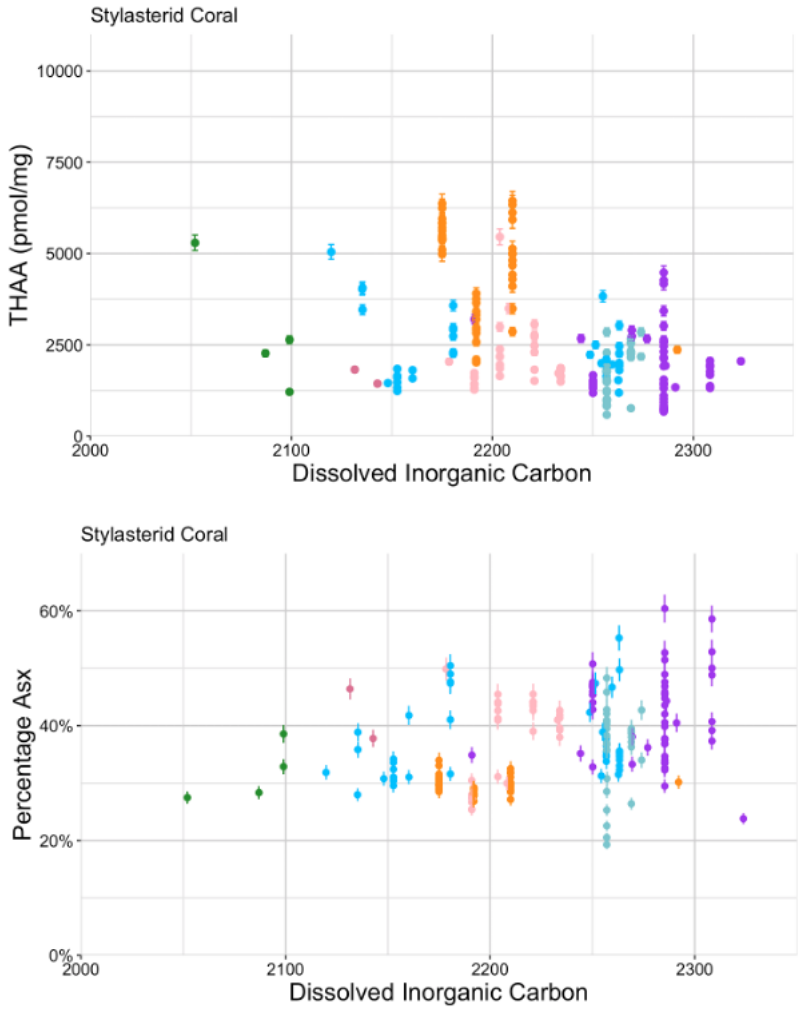

Figure 5.37 a and b: Stylasterid *[THAA] (top) and % Asx (bottom) against dissolved inorganic carbon (µmol/kg) for all coral samples. Colour responds to the location of where the sample was taken. Error bars are 4%, representing the analytical replicate error.*

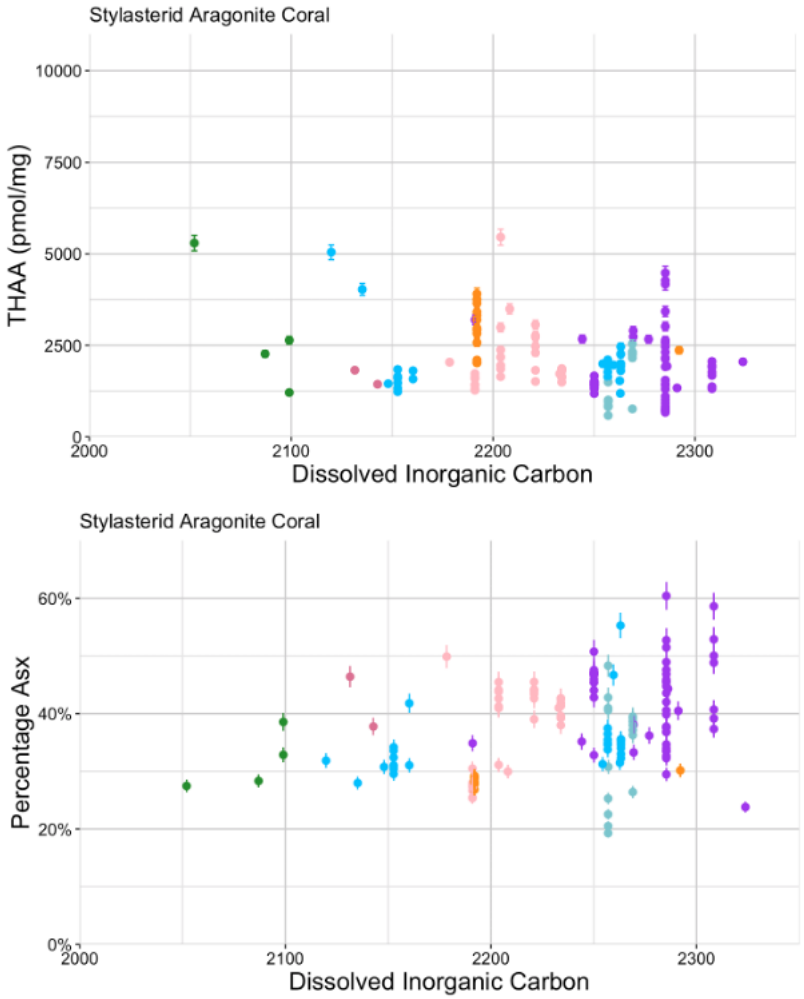

Figure 5.38a and b: *Aragonite* stylasterid *[THAA] (top) and % Asx (bottom) against dissolved inorganic carbon (µmol/kg) for all coral samples. Colour responds to the location of where the sample was taken. Error bars are 4%, representing the analytical replicate error.*

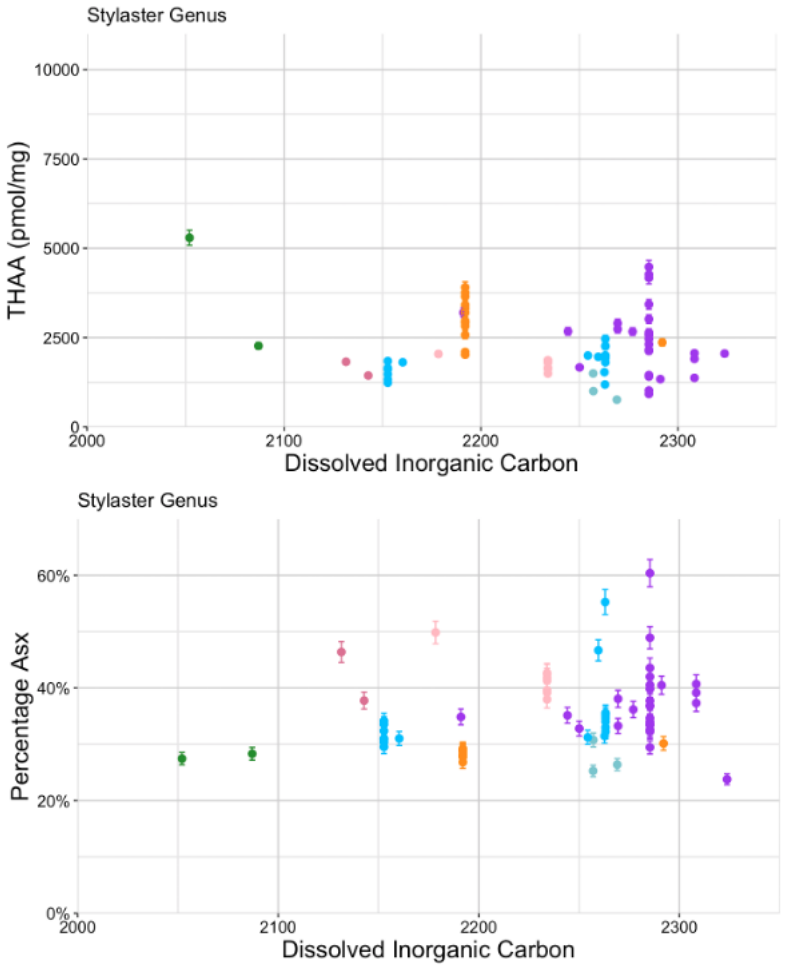

Figure 5.39a and b: *Stylaster [THAA] (top) and % Asx (bottom) against dissolved inorganic carbon (µmol/kg) for all coral samples. Colour responds to the location of where the sample was taken. Error bars are 4%, representing the analytical replicate error.*

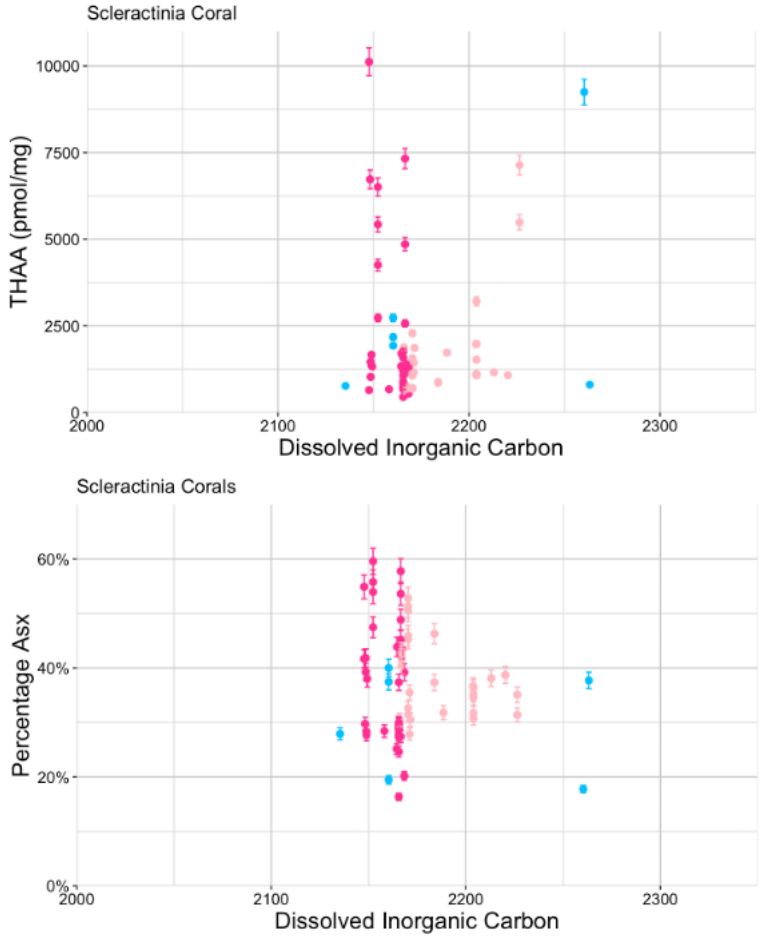

Figure 5.40a and b: Scleractinia *[THAA] (top) and % Asx (bottom) against dissolved inorganic carbon (µmol/kg) for all coral samples. Colour responds to the location of where the sample was taken. Error bars are 4%, representing the analytical replicate error.*

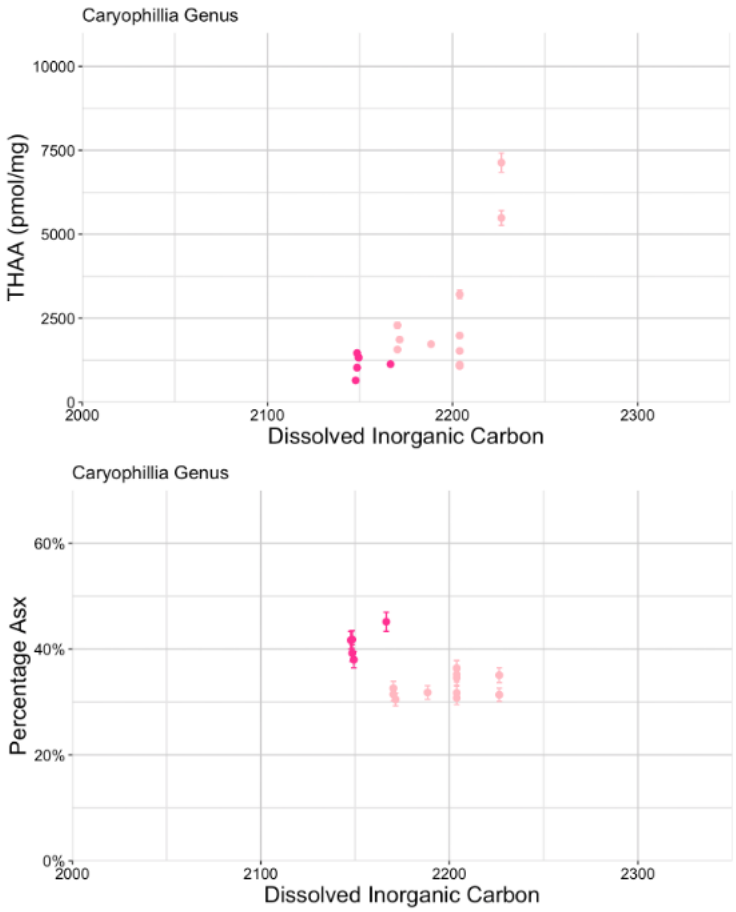

Figure 5.41 a and b: *Caryophyllia [THAA] (top) and % Asx (bottom) against dissolved inorganic carbon (µmol/kg) for all coral samples. Colour responds to the location of where the sample was taken. Error bars are 4%, representing the analytical replicate error.*

5.6.1 Summary of dissolved inorganic carbon (DIC)

DIC (µmol/kg)									
Taxa	Group	Residual Std. Error		F - Statistic		R - Squared		P value	
		[THAA]	% Asx	[THAA]	% Asx	[THAA]	% Asx	[THAA]	% Asx
All Coral		1600	0.08	9.3	18.6	0.028	0.06	0.003	2.273e-05
Stylasterid	All	1299	0.07	45.7	37.9	0.173	0.15	1.332e-10	3.703e-09
	Aragonite only	874	0.08	18.8	18.9	0.110	0.11	2.706e-05	2.627e-05
	Stylaster only	884	0.70	1.3	7.7	0.004	0.08	0.254	0.007
Scleractinia	All	2041	0.10	1.8	2.0	0.011	0.01	0.181	0.164
	Caryophyllia only	1381	0.04	9.7	6.3	0.352	0.25	0.007	0.024

Table 14, Regression analysis of dissolved inorganic carbon (DIC) for THAA (pmol/mg) and % Asx for the six groups tested. Showing the residual error, F-statistic, R-squared and p-value. Pink shading indicates p-values of < 0.05, and therefore statistically significant.

Regression analysis has been undertaken on the [THAA] against DIC. The results indicate that there are four out of the six groups with some statistical significance for regression analysis: all coral, stylasterid coral, aragonite stylasterid coral and the *Caryophyllia* genus. Although the R-squared values are very low for the majority of the groups tested (< 0.35), the F-statistic for stylasterid coral is high, once again indicating a wide variation in [THAA]. DIC could be directly related to the [THAA].

Although there is no significance for the stylasterid genus of *Stylaster,* the significance for the stylasterid and aragonite stylasterid samples suggests that DIC is loosely correlated with [THAA] for stylasterid corals. The samples within the *Stylaster* genus are condensed towards the DIC level of 2200 (µmol/kg), so the lack of samples with lower DIC could be the reason there is no significance. There is no significance for Scleractinia corals either.

Regression analysis for DIC for the % Asx showed that five of the six groups indicated statistical significance; only the Scleractinia coral had no statistical

significance, although all R^2 were low (≤0.25). The p-values indicate there is a relationship between the DIC and the % Asx, however, the independent variable of DIC cannot accurately predict the dependent variable due to the variability of the data.

Statistical significance is seen within the same groups for THAA (pmol/mg) as it is in the Asx % for p-values >0.05. Yet *Stylaster* is also significant within the % Asx for DIC. Scleractinia coral however, does not show statistical significance with DIC for either parameter. *Caryophyllia* has the highest R^2 value, but the sample size is small and would need to be looked at on a larger scale.

5.7 Discussion and Conclusions

After completing regression analysis on each group for each environmental parameter, it can be seen from the statistical significance that there may be some environmental impacts on the [THAA] and % Asx within the deep-sea coral skeletons analysed (Table 15, chapter 5, page 134). However, the range in amino acid data should be taken into account. % Asx has greater statistical significance and better correlation than THAA (pmol/mg) against the environmental parameters examined. 14 / 30 groups tested for [THAA] had statistically significant relationships with the chosen environmental parameters, versus 20/30 for % Asx. Salinity is the only environmental parameter where more groups have statistically significant relationships for [THAA] than % Asx.

Taxa	Subset	Temperature		Salinity		pH		Aragonite saturation state		DIC	
		THAA	% Asx	THAA	% Asx	THAA	% Asx	THAA	% Asx	THAA	% Asx
	All Coral (n = 290)										
Stylasterid	All (n = 216)										
	Aragonite (n = 146)										
	Stylaster (n = 77)										
Scleractinia	All (n = 74)										
	Caryophyllia (n = 17)							ND	ND		

Table 15: Visual representation summarising the regression analysis for correlation of environmental factors and [THAA] & % Asx. Pink-shaded squares correspond to statistically significant relationships between the AA parameter and the environmental parameter. Darker shades of pink indicate a lower p-value than lighter shades, and therefore greater statistical significance. ND indicates where no data was possible to test, because there were no samples from Caryophyllia that are Ω<1. Therefore, for this parameter, n= 273 for "All corals" and n= 57 for scleractinia corals.

From Table 15 it can be seen that when the Scleractinia are grouped together, there are no apparent relationships with environmental hydrographic parameters, but for individual Scleractinia genera, there may be (e.g. *Caryophyllia*).

The correlation found of decreasing [THAA] with increasing pH for *Caryophyllia* follows the pattern of the decreasing Asx concentration with increasing pH (pCO_2 increases) in *Porites* by Kellock *et al* (2020), as [THAA] and [Asx] are correlated within this study (Chapter 4, Figure 4.4, page 71). This is important, as one experiment was undertaken on shallow-water *Porites* and the other on deep-sea *Caryophyllia*. Therefore, the implications of understanding what is happening to the skeletal amino acid variability of shallow-water corals may be applicable to our further understanding of deep-water corals, although not all taxa will respond in the same way. This study does indicate a trend of increasing % Asx with decreasing pH within the stylasterid grouping but not in the scleractinian group.

However, it must be noted that the relatively small sample group size and pH range could be influencing results.

The understanding of deep-sea corals living in the undersaturated aragonite saturation zone gained through inorganic data explained that at least some scleractinian corals are able to upregulate the pH of their calcifying fluid to live in water with increased pCO_2 (Wall *et al.*, 2015). However, this process is apparently not used for stylasterid corals, and it was thought that organic molecules could play a much larger part in the process of biomineralisation (Stewart *et al.*, 2022). From this new amino acid data, there is a difference in the % Asx between corals growing in undersaturated compared with saturated conditions for stylasterid and aragonite stylasterids, and the [THAA] of *Stylaster*. Although it is not known exactly which proteins are used by the corals in biomineralisation, the high amounts of acidic amino acids and the increase of % Asx in undersaturated aragonite (Ω) could imply that larger quantities of CARPs being used for biomineralisation in undersaturated conditions (Mass *et al.*, 2013).

Throughout this chapter, it has become apparent that it is crucial to split the coral groups further than just by order/family (Scleractinia and stylasterid). The relationships can differ down to the genus level; this is seen within *Stylaster* and *Caryophyllia* (Table 15). Scleractinian corals as a whole have no correlation to environmental factors; however, when they are split to a specific genus level, there are trends seen, for example, in *Caryophyllia* (e.g. Fig 5.41, 5.25). Within the stylasterid groups, this is also crucial, as there are more correlations that are statistically significant with environmental trends in the stylasterid group when high-Mg samples are included. However, it should be noted that the high-Mg group includes some samples that happen to come from narrow ranges (e.g. *Errinopora* was only sampled from a salinity range of 33.2-33.5 g/kg).

Factors other than the environmental parameters selected here might be impacting the results, e.g. location (Section 5.1), mineralogy (Section 4.4.1) and taxa (Sections 4.1 and 4.2). It is important to understand that amino acid variations may be impacted by environmental factors, but the control by other aspects may be more dominant.

5.7.1 Location

Identifying patterns within/between locations was important to consider first, as environmental parameters will be related to locality (Section 5.1). However, the samples tested in this study are tied to a range of factors that could be having an impact on each other. Therefore, aspects such as genus (Sec. 4.1 and 4.2) could appear to affect the relationships with location, as some genera in the study are from only one location. In general, there was no clear relationship between each location for [THAA] and % Asx.

5.7.2 Mineralogy

The mineralogy is also important to consider with stylasterid corals (chapter 4, section 4.41), as the high-Mg calcite samples are the highest in [THAA] and therefore could be influencing patterns within stylasterid corals (e.g. in Figures 5.15a and 5.16a, chapter 5, pages 101/102). Within the stylasterid group, while the p-values were both statistically significant for salinity with and without the high-Mg samples included (Table 11, chapter 5, page 106), the R^2 value showed a large difference: 0.46 for high-Mg samples, and 0.07 without the high-Mg calcite samples. Therefore, this study has shown that it is important to split the mineralogies of the stylasterid corals for comparison with other studies.

5.7.3 Taxonomic effects

Errinopora has the highest [THAA] of all the corals in this study (chapter 4, section 4.1). Being able to separate the groups down to one genus provides better insight into how environmental parameters are impacting specific corals more directly. Looking at *Stylaster* and *Caryophyllia* individually has often identified the patterns that were hidden behind the taxonomic variation within larger groupings. The *Caryophyllia* genus has a correlation with a wide range of environmental factors, yet scleractinian corals as a whole showed no significant correlation with the environmental parameters chosen within the study. Scleractinian corals may be behaving differently to each other, as they are such a large collective group (Budd *et al*., 2010) and therefore grouping them together for data analysis is not a reliable way to test if environmental parameters are impacting particular corals.

However, some of the significant results may be due to the sample sizes, where groups are particularly small (e.g. *Caryophyllia* n = 17, *Stylaster* n = 77), this could cause bias. When the aragonite *Stylaster* is considered, with a sample size (n = 77) 7/10 tests were statistically significant. This means that to determine if an environmental parameter has an impact on the [THAA] or % of the Asx, ideally, a large number of each genera should be used to understand the full picture.

5.7.4 Other factors

Environmental parameters are shown to correlate with some amino acid parameters within this study. However, other parameters that are likely to have importance have not been considered within this study, including the availability of food. Deep-sea corals are also affected by bottom water hydrodynamics, strong velocity's allow for good food availability for deep-sea corals (Dierk Hebbeln, David Van Rooij and Wienberg, 2016). It is known that the availability of food within the deep sea is limited, yet the variability of food availability has only been tested on a solitary Scleractinia coral, which showed no change in skeletal growth rate with food availability (Thierry Baussant *et al*., 2017).

The variety of locations of the corals means that it is highly likely that the corals in this study will have had different nutrient availability. Although the skeletal growth rates of the coral may not vary with food availability, it may still have an impact on skeletal amino acid concentrations and, therefore, should be considered in the future.

$\delta^{18}O$ should also be compared to amino acid data, as $\delta^{18}O$ within the skeletal material of corals has been shown to provide paleotemperature information from the water in which corals have grown (Samperiz *et al.*, 2020). This past understanding of the temperatures that corals were able to grow in, combined with new amino acid data giving a small insight into skeletal proteins, could further unlock the ability to make predictions for these corals when facing climate change in the future. Furthermore, oxygen concentrations as another form of environmental data, compared to amino acid data found within this study would be beneficial as variation in oxygen concentrations can lead to hypoxia or hyperoxia. High stress from too much oxygen or not enough oxygen may impact deep-sea corals when combined with other environmental stressors, as suggested by a hypoxia study conducted on *L.Pertusa* by Hebbeln et al. (2020).

Previous biogeochemical variables, like ocean acidification, deoxygenation and temperature increases, classed as a tipping point for mass dying of deep-sea corals could be a beneficial way of selecting dated fossilised samples available. The dated fossil amino acid data compared to known paleoclimate biogeochemistry variables could be a beneficial way of understanding more what the modern deep-sea coral data could help to predict.

Conclusions and future work

6.1 Measuring Amino Acids in Deep-sea corals

The initial focus of this study was to identify whether intra-crystalline amino acids could be extracted and measured within deep-sea coral skeletons.

In order to this this, three shallow water *Porites* corals and one hundred and thirty-six deep-sea corals were tested as the initial study. The shallow water corals were used to provide for verification as a standard to previous unpublished HPLC data of shallow water *Porites* corals (Hewitt, T. 2018. Amino acids in biomineralisation of coral: investigating and comparing the artificial protein

degradation of *Pocillopora eydouxi* with *Porites* sp. fossil data. Unpublished BSc dissertation, University of York) the method used in this thesis was conducted using a UHPLC.

Unfortunately, in the first instance, the method did not provide resolvable data. Samples were run multiple times on the UHPLC and HPLC and still provided blank data. Efforts were made to identify the cause of the method failure by retesting each part of the process. Whilst the cause was not determined, a thorough review including remaking all samples again and refreshing all reagents This provided an effective solution, and data was then acquired. The data generated from the shallow water *Porites* data were similar to the previous data collected by HPLC, providing confidence in the new method.

The study further showed that the UHPLC method is well-suited to analysis of amino acids from deep-sea corals. Including total hydrolysable amino acid concentration, the concentration of individual amino acid chiral pairs and the percentage of amino acids.

6.2 Amino acid composition and variability

Asx was found to dominate the amino acid composition in all the samples tested within the study and, therefore, was used as the main parameter in subsequent data analysis as well as [THAA].

Testing the variability of the data obtained across different hierarchies (Chapter 3) allowed assessment of analytical and preparative reproducibility, as well as within coral heterogeneity. Analytical replication [THAA] was found to be at 4% error for stylasterid corals and 1.6% for scleractinia corals, calculated by the coefficient of variance. Preparative replicate [THAA] was found to be at 7% calculated by the coefficient of variance. The internal heterogeneity was tested within both stylasterid corals and scleractinian corals. Scleractinia corals resulted in the highest variability within all the tests, at 21.6% for [THAA], although due to sampling constraints of very resistant material, it was hard to keep to a systematic subsampling pattern. Stylasterid corals also had a large amount of variability within the internal heterogeneity, with an average coefficient of variance of 18.4% within tip-to-branch samples.

From the branches of stylasterid corals, the tips in eight out of 12 samples had lower [THAA] and [Asx] than some parts or all of the branch material (Section 3.5.1, Figures 3.13 and 3.14, chapter 3, pages 49/50). The percentage of Asx is lower in the tips with 10/12 of the samples than in some or all of the branch sections (Fig. 3.15). The branches that are not diverging (linear) were also tested for amino acid variance; the average variability was always lower than the linear branch sections. It would be beneficial to see if this pattern of decreasing concentration in the tips is happening across the whole body of stylasterid

corals. It would also be helpful to more selectively test parts of scleractinia corals, working from the base of the cup to the very end of the septa.

6.3 Testing hypothesis 1 - Corals of different Genera will have different amino acids.

Results from the extraction of intra-crystalline skeletal amino acids within both stylasterid corals and scleractinian corals showed differences between genera and mineralogy, answering the first and second hypotheses of the study (Chapter 4). It was observed that scleractinian corals have a considerably smaller percentage of threonine than stylasterid corals, but more glycine (Fig. 4.2). Scleractinia corals have less % of Asx than stylasterid corals. Within the genus, *Errinopora* also presented the largest % of Arg than any other stylasterid genus, *Adelopora* corals had the lowest % of Asx for stylasterid corals, and *Crypthelia* had the highest. This was the first instance of *Errinopora* standing out from other corals in terms of amino acid data, unfortunately there is no current genetic data for most stylasterid corals including *Errinopora*. Furthermore, the Errinopora samples in this study were taken from the same area of the North Pacific / Alaska, and therefore there had no variation in location like other samples, which could alter the amino acids range.

6.4 Testing hypothesis 2 - Corals with different mineralogies will have different amino acids due to protein differences.

When the data from stylasterid corals were analysed further to look at the genus, it became apparent that there was a much larger concentration of total amino acids within high-Mg calcite samples, although this was dominated by the genus of *Errinopora*. *Errinopora* also had an unusually high concentration and percentage of arginine compared to other stylasterid corals, which may relate to a different evolutionary lineage of this genus. Further testing on *Errinopora* from different locations and mineralogies (Fisher, 1931) will help identify if this is a pattern seen throughout that genus or just the samples within this study. Furthermore, it would also be helpful to select more samples with high-Mg calcite mineralogy and more mixed mineralogy to better understand the amino acid concentration differences.

6.5 Testing hypothesis 3 -The environment will have an impact on amino acid levels, particularly in stressful conditions

To understand if amino acids were variable against environmental parameters, [THAA] and % Asx were compared against hydrographic data. This could help us to understand potential threats of changing environmental parameters for deep-

sea corals, which could lead to vulnerability. The variation in [THAA] and %Asx was explored for five hydrographic parameters (temperature, salinity, pH, aragonite saturation and dissolved inorganic carbon). Relationships between these AA variables and specific environmental parameters were statistically significant in 34/60 tests (Chapter 5; Table 15, page 134). Results showed that overall, the variation in the % of Asx was more closely related to the change in environmental parameters than [THAA] was.

These tests showed the importance of dividing coral groups up to explore the relationships down to the genus level. Groupings should be identified by mineralogy or genus, as often the larger pooled data masked patterns evident within these smaller groups. This was particularly highlighted when the genus of *Caryophyllia* was split from the general group of scleractinia. *Caryophyllia* had a particularly interesting relationship with pH, with increased [THAA] at lower pH (Fig. 5.26) This had been previously seen within from unpublished data within the shallow water branching scleractinian coral *Stylophora pistillata* (Tomiak, 2013) and therefore indicates a potential mechanism whereby corals are strengthening their skeletons under lower pH conditions (shown from increased pCO_2 levels) as seen in shallow water corals (Kellock *et al*, (2020).

It is hard to determine if environmental factors are uniquely controlling changes in amino acids or if biological controls dominate. As discussed, within all environmental parameters split between genus and mineralogy are crucial to understanding this. The *Caryophyllia* genus has shown to have amino acid variation against multiple parameters, and this should be explored with a wider range of samples. This study has indicated a number of interesting areas to explore; a diversified sample range of corals, including, where possible, samples in undersaturated aragonite zones ($\Omega < 1$), samples within the pH range of 7.25 – 7.5. Branched scleractinia samples and other taxa, including octocorals and bamboo corals, would also help to discover if there are similar amino acids throughout multiple deep-sea corals.

6.6 Further work

6.6.1 Mass spectrometry

Knowing that amino acids can be extracted from deep-sea corals opens the door to future work to understand this better. Amino acid data is most powerful when paired with mass spectrometry work to identify proteins. This would especially be useful when looking at the internal heterogeneity of both stylasterid and scleractinia corals.

As discussed above, expanding the data set for specific samples, including *Errinopora* and *Caryophyllia,* would help us understand what makes them

different. These samples would also benefit from mass spectrometry work, especially the *Errinopora*, to help us understand why they are so different from other stylasterid corals within their amino acids.

6.6.2 Genome sequencing

Current work is being conducted on constructing and sequencing the genomes of *Stylasteridae*. When this new information is available it should be compared to any amino acid data extracted for this study, especially in highlighted corals like *Errinopora*. The pairing of genome sequencing with amino acid data will create indication of where biological controls in skeletal biomineralisation are correlated between genus.

6.6.3 Sample selection

Further expanding the internal heterogeneity throughout coral genera and in particular, samples would also be advantageous. It would be suggested that looking at a full stylasterid coral from the base to the tips, following the growth direction, is the best way to do this. For scleractinia corals, working from the base to the septa in the same way would better describe the internal heterogeneity.

Larger amino acid data sets on deep-sea corals should also include looking at octocorals and bamboo corals, where possible.
Expansion of samples should include looking at species and genus from a range of locations. As discussed, *Errinopora* for example, has been seen to be unique in its amino acid composition, yet is only found in one location. Looking at Errinopora samples from a range of other locations will help determine if these differences are genus-based or impacted by environmental factors.

6.6.4 Covariates of oceanographic parameters

Although looking at the effects of environmental parameters against amino acids revealed some correlations, It is a really good idea for future work should include how multiple environmental parameters impact amino acids together. Especially as environmental parameters like DIC, aragonite saturation, temperature and pH are all covariant of each other. Statistical testing using a multivariate statistical testing like RDA redundancy analysis or principal component analysis, would be beneficial as it combines multi-response variables and analyses the relationship between them, indicating the variation that could be potentially seen between multiple environmental factors and amino acid data. Permanova could also be a good statistical way of comparing the amino acid data to the multidimensional environmental parameter data. Different environmental parameters to those used within this study should also be used, such as pressure, nutrient availability and oxygen levels.

7 Reference list

Adkins, J.F., Henderson, G.M., Wang, S.-L., O'Shea, S. and Mokadem, F. (2004). Growth rates of the deep-sea scleractinia Desmophyllum cristagalli and Enallopsammia rostrata. *Earth and Planetary Science Letters*, 227(3-4), pp.481–490. doi:https://doi.org/10.1016/j.epsl.2004.08.022.

Aguilar, C., Raina, J.-B., Fôret, S., Hayward, D.C., Lapeyre, B., Bourne, D.G. and Miller, D.J. (2019). Transcriptomic analysis reveals protein homeostasis breakdown in the coral Acropora millepora during hypo-saline stress. *BMC Genomics*, 20(1). doi:https://doi.org/10.1186/s12864-019-5527-2.

Allison, N., Cohen, I., Finch, A.A., Erez, J. and Tudhope, A.W. (2014). Corals concentrate dissolved inorganic carbon to facilitate calcification. *Nature Communications*, [online] 5(1), p.5741. doi:https://doi.org/10.1038/ncomms6741.

Allison, N., Ross, P., Castillo Alvarez, C., Penkman, K., Kröger, R., Kellock, C., Cole, C., Clog, M., Evans, D., Hintz, C., Hintz, K. and Finch, A.A. (2024). The influence of seawater pCO2 and temperature on the amino acid composition and aragonite CO3 disorder of coral skeletons. *Coral Reefs*, 43(5), pp.1317–1329. doi:https://doi.org/10.1007/s00338-024-02539-z.

Anagnostou, E., Sherrell, R.M., Gagnon, A., LaVigne, M., Field, M.P. and McDonough, W.F. (2011). Seawater nutrient and carbonate ion concentrations recorded as P/Ca, Ba/Ca, and U/Ca in the deep-sea coral Desmophyllum dianthus. *Geochimica et Cosmochimica Acta*, 75(9), pp.2529–2543. doi:https://doi.org/10.1016/j.gca.2011.02.019.

Anderson, O.F., Stephenson, F., Behrens, E. and Rowden, A.A. (2022). Predicting the effects of climate change on deep-water coral distribution around New Zealand—Will there be suitable refuges for

protection at the end of the 21st century? *Global Change Biology*, 28(22), pp.6556–6576. doi:https://doi.org/10.1111/gcb.16389.

Andersson, A.J. and Gledhill, D. (2013). Ocean Acidification and Coral Reefs: Effects on Breakdown, Dissolution, and Net Ecosystem Calcification. *Annual Review of Marine Science*, 5(1), pp.321–348. doi:https://doi.org/10.1146/annurev-marine-121211-172241.

Anteco, S. (n.d.). *RRS James Clark Ross JR15005 Cruise Report South Orkneys -State of the Antarctic Ecosystem Huw Griffiths & the scientists of SO-AntEco*. [online] Available at: https://www.bodc.ac.uk/resources/inventories/cruise_inventory/reports/jr15005.pdf [Accessed 10 Mar. 2025].

ANTHONY, K.R.N., MAYNARD, J.A., DIAZ-PULIDO, G., MUMBY, P.J., MARSHALL, P.A., CAO, L. and HOEGH-GULDBERG, O. (2011). Ocean acidification and warming will lower coral reef resilience. *Global Change Biology*, [online] 17(5), pp.1798–1808. doi:https://doi.org/10.1111/j.1365-2486.2010.02364.x.

Armstrong, A.A. and Masetti, G. (2016). *CRUISE REPORT*. [online] Available at: https://ccom.unh.edu/sites/default/files/publications/Arnstrong-2016-marianas-FS1601-Cruise-Report-fugro.pdf [Accessed 10 Mar. 2025].

Baco, A.R., Morgan, N., Roark, E.B., Silva, M., Shamberger, K.E.F. and Miller, K. (2017). Defying Dissolution: Discovery of Deep-Sea Scleractinian Coral Reefs in the North Pacific. *Scientific Reports*, 7(1). doi:https://doi.org/10.1038/s41598-017-05492-w.

Bo, M., Bavestrello, G., Angiolillo, M., Calcagnile, L., Canese, S., Cannas, R., Cau, A., D'Elia, M., D'Oriano, F., Follesa, M.C., Quarta, G. and Cau, A. (2015). Persistence of Pristine Deep-Sea Coral Gardens in the Mediterranean Sea (SW Sardinia). *PLOS ONE*, [online] 10(3), p.e0119393. doi:https://doi.org/10.1371/journal.pone.0119393.

Bostock, H.C., Tracey, D.M., Currie, K.I., Dunbar, G.B., Handler, M.R., Mikaloff Fletcher, S.E., Smith, A.M. and Williams, M.J.M. (2015). The carbonate mineralogy and distribution of habitat-forming deep-sea corals in the southwest pacific region. *Deep Sea Research Part I: Oceanographic Research Papers*, 100, pp.88–104. doi:https://doi.org/10.1016/j.dsr.2015.02.008.

British Oceanographic Data Centre. (2013). *Cruise inventory - RV Nathaniel B. Palmer NBP1103 - cruise summary report*. [online] Available at: https://www.bodc.ac.uk/resources/inventories/cruise_inventory/report/15005/ [Accessed 10 Mar. 2025].

British Oceanographic Data Centre. (2025). *Cruise inventory - RRS James Cook JC094 - cruise summary report*. [online] Available at: https://www.bodc.ac.uk/resources/inventories/cruise_inventory/report/13397/ [Accessed 10 Mar. 2025].

Brooke, S., Ross, S.W., Bane, J.M., Seim, H.E. and Young, C.M. (2013). Temperature tolerance of the deep-sea coral Lophelia pertusa from the southeastern United States. *Deep Sea Research Part II: Topical Studies in Oceanography*, 92, pp.240–248. doi:https://doi.org/10.1016/j.dsr2.2012.12.001.

Brooke, S. and Stone, R. (2007). Reproduction of deep-water hydrocorals (family Stylasteridae) from the Aleutian Islands, Alaska. *Bulletin of Marine Science*, 81(3), pp.519–532.

Bruckner, A.W. (2001). Tracking the Trade in Ornamental Coral Reef Organisms: The Importance of CITES and its Limitations. *Aquarium Sciences and Conservation*, 3(1/3), pp.79–94. doi:https://doi.org/10.1023/a:1011369015080.

Budd, A.F., Romano, S.L., Smith, N.D. and Barbeitos, M.S. (2010). Rethinking the Phylogeny of Scleractinian Corals: A Review of Morphological and Molecular Data. *Integrative and Comparative Biology*, 50(3), pp.411–427. doi:https://doi.org/10.1093/icb/icq062.

Cairns, S.D. (1992). Worldwide distribution of the Stylasteridae (Cnidaria: Hydrozoa). *Oceanographic literature review*, 40(10), pp.860–860. doi:https://doi.org/10.1016/0967-0653(93)91433-d.

Cairns, S.D. (Stephen D. (2005). Revision of the Hawaiian Stylasteridae (Cnidaria: Hydrozoa: Athecata). *Pacific Science*, 59(3), pp.439–451. doi:https://doi.org/10.1353/psc.2005.0034.

Cairns, S.D. and Lindner, A. (2011). A Revision of the Stylasteridae (Cnidaria, Hydrozoa, Filifera) from Alaska and Adjacent Waters. *ZooKeys*, 158, pp.1–88. doi:https://doi.org/10.3897/zookeys.158.1910.

Cairns, S.D. and Macintyre, I.G. (1992). Phylogenetic Implications of Calcium Carbonate Mineralogy in the Stylasteridae (Cnidaria: Hydrozoa). *PALAIOS*, 7(1), p.96. doi:https://doi.org/10.2307/3514799.

Cappellini, E., Welker, F., Pandolfi, L., Ramos-Madrigal, J., Samodova, D., Rüther, P.L., Fotakis, A.K., Lyon, D., Moreno-Mayar, J.V., Bukhsianidze, M., Rakownikow Jersie-Christensen, R., Mackie, M., Ginolhac, A., Ferring, R., Tappen, M., Palkopoulou, E., Dickinson, M.R., Stafford, T.W., Chan, Y.L. and Götherström, A. (2019). Early Pleistocene enamel proteome from Dmanisi resolves Stephanorhinus phylogeny. *Nature*, [online] 574(7776), pp.103–107. doi:https://doi.org/10.1038/s41586-019-1555-y.

Carricart-Ganivet, J.P. (2004). Sea surface temperature and the growth of the West Atlantic reef-building coral Montastraea annularis. *Journal of Experimental Marine Biology and Ecology*, 302(2), pp.249–260. doi:https://doi.org/10.1016/j.jembe.2003.10.015.

Coles, S.L. and Jokiel, P.L. (1978). Synergistic effects of temperature, salinity and light on the hermatypic coral Montipora verrucosa. *Marine Biology*, 49(3), pp.187–195. doi:https://doi.org/10.1007/bf00391130.

Conci, N., Lehmann, M., Vargas, S. and Wörheide, G. (2020). Comparative proteomics of octocoral and scleractinian skeletomes and the evolution of coral calcification. *Genome Biology and Evolution*. doi:https://doi.org/10.1093/gbe/evaa162.

Cristina Castillo Alvarez, Kirsty Penkman, Kröger, R., Finch, A.A., Matthieu Clog, Brasier, A.T., Still, J. and Allison, N. (2024). Insights into the response of coral biomineralisation to environmental change from aragonite precipitations in vitro. *Geochimica et Cosmochimica Acta*, 364, pp.184–194. doi:https://doi.org/10.1016/j.gca.2023.10.032.

Cuif, J.-P. and Dauphin, Y. (2005). The two-step mode of growth in the scleractinian coral skeletons from the micrometre to the overall scale. *Journal of Structural Biology*, 150(3), pp.319–331. doi:https://doi.org/10.1016/j.jsb.2005.03.004.

Dalziel, I., et al (2025). *NBP0805 - Marine Geoscience Data System*. [online] Marine-geo.org. Available at: https://www.marine-geo.org/tools/entry/NBP0805#documents [Accessed 10 Mar. 2025].

Dierk Hebbeln, David Van Rooij and Wienberg, C. (2016). Good neighbours shaped by vigorous currents: Cold-water coral mounds and contourites in the North Atlantic. *Marine Geology*, 378, pp.171–185. doi:https://doi.org/10.1016/j.margeo.2016.01.014.

EMILIANI, C., HUDSON, J.H., SHINN, E.A. and GEORGE, R.Y. (1978). Oxygen and Carbon Isotopic Growth Record in a Reef Coral from the Florida Keys and a Deep-Sea Coral from Blake Plateau. *Science*, 202(4368), pp.627–629. doi:https://doi.org/10.1126/science.202.4368.627.

Erez, J., Reynaud, S., Silverman, J., Schneider, K. and Allemand, D. (2010). Coral Calcification Under Ocean Acidification and Global Change. *Coral Reefs: An Ecosystem in Transition*, pp.151–176. doi:https://doi.org/10.1007/978-94-007-0114-4_10.

Falini, G., Fermani, S. and Goffredo, S. (2015). Coral biomineralization: A focus on intra-skeletal organic matrix and calcification. *Seminars in Cell & Developmental Biology*, 46, pp.17–26. doi:https://doi.org/10.1016/j.semcdb.2015.09.005.

Fallon, S.J., Thresher, R.E. and Adkins, J. (2013). Age and growth of the cold-water scleractinian Solenosmilia variabilis and its reef on SW Pacific seamounts. *Coral Reefs*, 33(1), pp.31–38. doi:https://doi.org/10.1007/s00338-013-1097-y.

Farfan, G.A., Cordes, E.E., Waller, R.G., DeCarlo, T.M. and Hansel, C.M. (2018). Mineralogy of Deep-Sea Coral Aragonites as a Function of Aragonite Saturation State. *Frontiers in Marine Science*, 5. doi:https://doi.org/10.3389/fmars.2018.00473.

Feely, R.A. and Doney, S.C. (2011). Ocean Acidification: the Other CO2 Problem. *Limnology and Oceanography e-Lectures*, [online] 1(1). doi:https://doi.org/10.4319/lol.2011.rfeely_sdoney.5.

Findlay, H.S. and Turley, C. (2021). Ocean acidification and climate change. *Climate Change*, 3, pp.251–279. doi:https://doi.org/10.1016/b978-0-12-821575-3.00013-x.

Fischer, C.S.J. and Fischer, J., (2001). *Crusie report*.

Fisher, W.K. (1931). L.—*Californian Hydrocorals*. *Annals and Magazine of Natural History*, 8(46), pp.391–399. doi:https://doi.org/10.1080/00222933108673409.

FITZGERALD, L.M. and SZMANT, A.M. (1997). Biosynthesis of 'essential' amino acids by scleractinian corals. *Biochemical Journal*, 322(1), pp.213–221. doi:https://doi.org/10.1042/bj3220213.

Gagnon, A.C., Gothmann, A.M., Branson, O., Rae, J.W.B. and Stewart, J.A. (2021). Controls on boron isotopes in a cold-water coral and the cost of resilience to ocean acidification. *Earth and Planetary Science Letters*, 554, p.116662. doi:https://doi.org/10.1016/j.epsl.2020.116662.

Gattuso, J.-P., Williamson, P., Duarte, C.M. and Magnan, A.K. (2021). The Potential for Ocean-Based Climate Action: Negative Emissions Technologies and Beyond. *Frontiers in Climate*, 2. doi:https://doi.org/10.3389/fclim.2020.575716.

Geoscience, M. (2025). *Underway Hydrographic, Weather and Ship-state Data (JGOFS) from Laurence M. Gould expedition LMG0802 (2008)*. [online] Marine-geo.org. Available at: https://www.marine-geo.org/tools/search/Files.php?data_set_uid=8291#documents [Accessed 10 Mar. 2025].

Guinotte, J.M., Orr, J., Cairns, S., Freiwald, A., Morgan, L. and George, R. (2006). Will human-induced changes in seawater chemistry alter the distribution of deep-sea scleractinian corals? *Frontiers in Ecology and the Environment*, 4(3), pp.141–146. doi:https://doi.org/10.1890/1540-9295(2006)004[0141:whcisc]2.0.co;2.

Gupta, L.P., Suzuki, A. and Kawahata, H. (2006). Aspartic acid concentrations in coral skeletons as recorders of past disturbances of metabolic rates. *Coral Reefs*, 25(4), pp.599–606. doi:https://doi.org/10.1007/s00338-006-0152-3.

Hansen, G. and Stone, D. (2015). Assessing the observed impact of anthropogenic climate change. *Nature Climate Change*, [online] 6(5), pp.532–537. doi:https://doi.org/10.1038/nclimate2896.

Harris, K.E., DeGrandpre, M.D. and Hales, B. (2013). Aragonite saturation state dynamics in a coastal upwelling zone. *Geophysical Research Letters*, 40(11), pp.2720–2725. doi:https://doi.org/10.1002/grl.50460.

Harris, P.T., Westerveld, L., Zhao, Q. and Costello, M.J. (2023). Rising snow line: Ocean acidification and the submergence of seafloor geomorphic features beneath a rising carbonate compensation depth. *Marine Geology*, [online] 463, p.107121. doi:https://doi.org/10.1016/j.margeo.2023.107121.

Hauri, C., Friedrich, T. and Timmermann, A. (2015). Abrupt onset and prolongation of aragonite undersaturation events in the Southern Ocean. *Nature Climate Change*, 6(2), pp.172–176. doi:https://doi.org/10.1038/nclimate2844.

Hebbeln, D., Wienberg, C., Dullo, W.-C., Freiwald, A., Mienis, F., Orejas, C. and Titschack, J. (2020). Cold-water coral reefs thriving under hypoxia. *Coral Reefs*. doi:https://doi.org/10.1007/s00338-020-01934-6.

Hemond, E.M., Kaluziak, S.T. and Vollmer, S.V. (2014). The genetics of colony form and function in Caribbean Acropora corals. *BMC Genomics*, 15(1), p.1133. doi:https://doi.org/10.1186/1471-2164-15-1133.

Hemsing, F., Hsieh, Y.-T., Bridgestock, L., Spooner, P.T., Robinson, L.F., Frank, N. and Henderson, G.M. (2018). Barium isotopes in cold-water corals. *Earth and Planetary Science Letters*, 491, pp.183–192. doi:https://doi.org/10.1016/j.epsl.2018.03.040.

Hendry, K., et al (2017). *RRS Discovery Cruise DY081, July 6 th -August 8 th 2017 ICY-LAB Isotope CYcling in the LABrador Sea Cruise Report*. [online] Available at: https://www.bodc.ac.uk/resources/inventories/cruise_inventory/reports/dy081.pdf [Accessed 10 Mar. 2025].

Hendy, E., Tomiak, P.J., Collins, M.J., Hellstrom, J., Tudhope, A.W., Lough, J. and Kirsty Penkman (2012). Assessing amino acid racemization variability in coral intra-crystalline protein for geochronological applications. *Geochimica et Cosmochimica Acta*, 86, pp.338–353. doi:https://doi.org/10.1016/j.gca.2012.02.020.

Hennige, S.J., Wicks, L.C., Kamenos, N.A., Bakker, D.C.E., Findlay, H.S., Dumousseaud, C. and Roberts, J.M. (2014). Short-term metabolic and growth responses of the cold-water coral Lophelia pertusa to ocean acidification. *Deep Sea Research Part II: Topical Studies in Oceanography*, [online] 99, pp.27–35. doi:https://doi.org/10.1016/j.dsr2.2013.07.005.

Hennige, S.J., Wicks, L.C., Kamenos, N.A., Perna, G., Findlay, H.S. and Roberts, J.M. (2015). Hidden impacts of ocean acidification to live and dead coral framework. *Proceedings of the Royal Society B: Biological Sciences*, 282(1813), p.20150990. doi:https://doi.org/10.1098/rspb.2015.0990.

Hicks, T.L., Shamberger, F., Roark, E.B., Baco, A.R., Watling, L. and Feely, R.A. (2025). Seawater Carbonate Chemistry Along the Hawaiian-Emperor Seamount Chain in the North Pacific. *Journal of Geophysical Research Oceans*, 130(5). doi:https://doi.org/10.1029/2024jc021750.

Hill, R.L. (1965). Hydrolysis of Proteins. *Advances in Protein Chemistry*, pp.37–107. doi:https://doi.org/10.1016/s0065-3233(08)60388-5.

Hoegh-Guldberg, O., Mumby, P.J., Hooten, A.J., Steneck, R.S., Greenfield, P., Gomez, E., Harvell, C.D., Sale, P.F., Edwards, A.J., Caldeira, K., Knowlton, N., Eakin, C.M., Iglesias-Prieto, R., Muthiga, N., Bradbury, R.H., Dubi, A. and Hatziolos, M.E. (2007). Coral reefs under rapid climate change and ocean acidification. *Science*, 318(5857), pp.1737–1742.

Höök, M. and Tang, X. (2013). Depletion of Fossil Fuels and Anthropogenic Climate change—A Review. *Energy Policy*, [online] 52(1), pp.797–809. doi:https://doi.org/10.1016/j.enpol.2012.10.046.

Howell, K.L., et al (2016). *DEEP LINKS PROJECT*. [online] Available at: https://www.bodc.ac.uk/resources/inventories/cruise_inventory/reports/jc136.pdf [Accessed 10 Mar. 2025].

Hu, W., Zheng, X., Li, Y., Du, J., Lv, Y., Su, S., Xiao, B., Ye, X., Jiang, Q., Tan, H., Liao, B. and Chen, B. (2022). High vulnerability and a big conservation gap: Mapping the vulnerability of coastal scleractinian corals in South China. *Science of The Total Environment*, 847, p.157363. doi:https://doi.org/10.1016/j.scitotenv.2022.157363.

Hubbard, D. and Scaturo, D. (1985). *GROWTH RATES OF SEVEN SPECIES OF SCLERACTINEAN CORALS FROM CANE BAY AND SALT RIVER, ST. CROIX, USVI*. [online] Available at: https://www.aoml.noaa.gov/general/lib/CREWS/Cleo/St.%20Croix/salt_river3.pdf?utm_source=chatgpt.com [Accessed 27 Mar. 2025].

IPCC (2019). *Impacts of 1.5°C Global Warming on Natural and Human Systems*. [online] Ipcc.ch. Available at: https://www.ipcc.ch/sr15/chapter/chapter-3/.

IPCC (2021). *Climate Change 2021: The Physical Science Basis*. [online] IPCC. Available at: https://www.ipcc.ch/report/ar6/wg1/.

Johnson, B.M. and Miller, G.H. (1997). ARCHAEOLOGICAL APPLICATIONS OF AMINO ACID RACEMIZATION. *Archaeometry*, 39(2), pp.265–287. doi:https://doi.org/10.1111/j.1475-4754.1997.tb00806.x.

Kaufman, D.S. and Manley, W.F. (1998). A new procedure for determining dl amino acid ratios in fossils using reverse phase liquid chromatography. 17(11), pp.987–1000. doi:https://doi.org/10.1016/s0277-3791(97)00086-3.

Kellock, C., Cole, C., Penkman, K., Evans, D., Kröger, R., Hintz, C., Hintz, K., Finch, A. and Allison, N. (2020). The role of aspartic acid in reducing coral calcification under ocean acidification conditions. *Scientific Reports*, 10(1). doi:https://doi.org/10.1038/s41598-020-69556-0.

Kershaw, J. (2023). *Stylasterid coral geochemistry: a novel approach for oceanographic reconstruction*.

Kershaw, J., Stewart, J.A., Strawson, I., de Carvalho Ferreira, M.L., Robinson, L.F., Hendry, K.R., Samperiz, A., Burke, A., Rae, J.W.B., Day, R.D., Etnoyer, P.J., Williams, B. and Häussermann, V. (2023). Ba/Ca of stylasterid coral skeletons records dissolved seawater barium concentrations. *Chemical Geology*, [online] 622, p.121355. doi:https://doi.org/10.1016/j.chemgeo.2023.121355.

Kerswell, A. and Jones, R. (2003). Effects of hypo-osmosis on the coral Stylophora pistillata: nature and cause of 'low-salinity bleaching'. *Marine Ecology Progress Series*, 253, pp.145–154. doi:https://doi.org/10.3354/meps253145.

King, T.M., Rosenheim, B.E. and James, N.P. (2024). Deep-sea stylasterid $\delta^{18}O$ and $\delta^{13}C$ maps inform sampling scheme for paleotemperature reconstructions. *Biogeosciences*, [online] 21(22), pp.5361–5379. doi:https://doi.org/10.5194/bg-21-5361-2024.

Laipnik, R., Bissi, V., Sun, C.-Y., Falini, G., Gilbert, P.U.P.A. and Mass, T. (2020). Coral acid rich protein selects vaterite polymorph in vitro. *Journal of Structural Biology*, 209(2), p.107431. doi:https://doi.org/10.1016/j.jsb.2019.107431.

Leung, J.Y.S., Zhang, S. and Connell, S.D. (2022). Is ocean acidification really a threat to marine calcifiers? A systematic review and meta-analysis of 980+ studies spanning two decades. *Small*, [online] 18(35), p.2107407. doi:https://doi.org/10.1002/smll.202107407.

Li, J., Zhou, T., Li, Y. and Xu, K. (2023). Adaptive mechanisms of the deep-sea coral Polymyces wellsi (Flabellidae, Scleractinia) illuminate strategies for global climate change. *Ecological Indicators*, 154, pp.110502–110502. doi:https://doi.org/10.1016/j.ecolind.2023.110502.

Lueker, T.J., Dickson, A.G. and Keeling, C.D. (2000). Ocean pCO2 calculated from dissolved inorganic carbon, alkalinity, and equations for K1 and K2: validation based on laboratory measurements of CO2 in gas and seawater at equilibrium. *Marine Chemistry*, 70(1-3), pp.105–119. doi:https://doi.org/10.1016/s0304-4203(00)00022-0.

Luo, Z., Chen, L. and Jia, G. (2024). Bulk and amino acid isotope evidence of supplementary food sources besides euphotic production for a deep-sea coral community in the South China Sea. *Frontiers in Marine Science*, 11. doi:https://doi.org/10.3389/fmars.2024.1399814.

Maier, S.R., Brooke, S., De, L.H., Evert de Froe, van, Kutti, T., Furu Mienis and Dick van Oevelen (2023). On the paradox of thriving cold-water coral reefs in the food-limited deep sea. *Biological Reviews*, 98(5), pp.1768–1795. doi:https://doi.org/10.1111/brv.12976.

Marine-geo.org. (2023). *AT50-09BC - Marine Geoscience Data System*. [online] Available at: https://www.marine-geo.org/tools/search/entry.php?id=AT50-09BC#documents [Accessed 10 Mar. 2025].

Martinez, L.H. (2005). POST INDUSTRIAL REVOLUTION HUMAN ACTIVITY AND CLIMATE CHANGE: WHY THE UNITED STATES MUST IMPLEMENT MANDATORY LIMITS ON INDUSTRIAL GREENHOUSE GAS EMMISSIONS. *Journal of Land Use & Environmental Law*, [online] 20(2), pp.403–421. doi:https://doi.org/10.2307/42842978.

Mass, T., Drake, Jeana L., Haramaty, L., Kim, J. Dongun, Zelzion, E., Bhattacharya, D. and Falkowski, Paul G. (2013). Cloning and Characterization of Four Novel Coral Acid-Rich Proteins that Precipitate Carbonates In Vitro. *Current Biology*, 23(12), pp.1126–1131. doi:https://doi.org/10.1016/j.cub.2013.05.007.

McCulloch, M., Trotter, J., Montagna, P., Falter, J., Dunbar, R., Freiwald, A., Försterra, G., López Correa, M., Maier, C., Rüggeberg, A. and Taviani, M. (2012). Resilience of cold-water scleractinian corals to ocean acidification: Boron isotopic systematics of pH and saturation state up-regulation. *Geochimica et Cosmochimica Acta*, 87, pp.21–34. doi:https://doi.org/10.1016/j.gca.2012.03.027.

Miller, M. (1995). Growth of a temperate coral:effects of temperature, light, depth, and heterotrophy. *Marine Ecology Progress Series*, 122, pp.217–225. doi:https://doi.org/10.3354/meps122217.

Mitterer, R.M. (1976). *AMINO ACID COMPOSITION AND METAL BINDING CAPABILITY OF THE SKELETAL PROTEIN OF CORALS*. [online] Available at: https://www.researchgate.net/profile/Richard-Mitterer/publication/233665050_Amino_Acid_Composition_and_Metal_Binding_Capability_of_the_Skeletal_Protein_of_Corals/links/546ced220cf2a7492c55ae37/Amino-Acid-Composition-and-Metal-Binding-Capability-of-the-Skeletal-Protein-of-Corals.pdf [Accessed 10 Mar. 2025].

Mollica, N.R., Guo, W., Cohen, A.L., Huang, K.-F., Foster, G.L., Donald, H.K. and Solow, A.R. (2018). Ocean acidification affects coral growth by reducing skeletal density. *Proceedings of the National Academy of Sciences*, [online] 115(8), pp.1754–1759. doi:https://doi.org/10.1073/pnas.1712806115.

Mummadisetti, M.P., Drake, J.L. and Falkowski, P.G. (2021). The spatial network of skeletal proteins in a stony coral. *Journal of The Royal Society Interface*, 18(175), p.20200859. doi:https://doi.org/10.1098/rsif.2020.0859.

MUTHIGA, N.A. and SZMANT, A.M. (1987). THE EFFECTS OF SALINITY STRESS ON THE RATES OF AEROBIC RESPIRATION AND PHOTOSYNTHESIS IN THE HERMATYPIC CORAL SIDERASTREA SIDEREA. *The Biological Bulletin*, 173(3), pp.539–551. doi:https://doi.org/10.2307/1541699.

Negrete-García, G., Lovenduski, N.S., Hauri, C., Krumhardt, K.M. and Lauvset, S.K. (2019). Sudden emergence of a shallow aragonite saturation horizon in the Southern Ocean. *Nature Climate Change*, [online] 9(4), pp.313–317. doi:https://doi.org/10.1038/s41558-019-0418-8.

Nyberg, J., Csapó, J., Malmgren, B.A. and Winter, A. (2001). Changes in the D- and L-content of aspartic acid, glutamic acid, and alanine in a scleractinian coral over the last 300 years. *Organic Geochemistry*, 32(5), pp.623–632. doi:https://doi.org/10.1016/s0146-6380(01)00020-1.

Orr, J.C., Fabry, V.J., Aumont, O., Bopp, L., Doney, S.C., Feely, R.A., Gnanadesikan, A., Gruber, N., Ishida, A., Joos, F., Key, R.M., Lindsay, K., Maier-Reimer, E., Matear, R., Monfray, P., Mouchet, A., Najjar, R.G., Plattner, G.-K., Rodgers, K.B. and Sabine, C.L. (2005). Anthropogenic Ocean Acidification over the Twenty-First Century and Its Impact on Calcifying Organisms. *Nature*, 437(7059), pp.681–686. doi:https://doi.org/10.1038/nature04095.

Owens, N.J.P. (2009). *Ocean acidification - RGS*. [online] www.rgs.org. Available at: https://www.rgs.org/schools/resources-for-schools/ocean-acidification.

Parker, S., Penney, A. and Clark, M. (2009). Detection criteria for managing trawl impacts on vulnerable marine ecosystems in high seas fisheries of the South Pacific Ocean. *Marine Ecology Progress Series*, 397, pp.309–317. doi:https://doi.org/10.3354/meps08115.

Penkman, K.E.H., Kaufman, D.S., Maddy, D. and Collins, M.J. (2008). Closed-system behaviour of the intra-crystalline fraction of amino acids in mollusc shells. *Quaternary Geochronology*, 3(1-2), pp.2–25. doi:https://doi.org/10.1016/j.quageo.2007.07.001.

Puce, S., Pica, D., Stefano Schiaparelli and Enrico Negrisolo (2016). Integration of Morphological Data into Molecular Phylogenetic Analysis: Toward the Identikit of the Stylasterid Ancestor. *PLoS ONE*, 11(8), pp.e0161423–e0161423. doi:https://doi.org/10.1371/journal.pone.0161423.

Puverel, S., Tambutté, E., Pereira-Mouriès, L., Zoccola, D., Allemand, D. and Tambutté, S. (2005). Soluble organic matrix of two Scleractinian corals: Partial and comparative analysis. *Comparative Biochemistry and Physiology Part B: Biochemistry and Molecular Biology*, 141(4), pp.480–487. doi:https://doi.org/10.1016/j.cbpc.2005.05.013.

Rahman, M.A. and Tamotsu Oomori (2008). Aspartic Acid-rich Proteins in Insoluble Organic Matrix Play a Key Role in the Growth of Calcitic Sclerites in Alcyonarian Coral. *Chinese journal of biotechnology/Shengwu gongcheng xuebao*, 24(12), pp.2127–2128. doi:https://doi.org/10.1016/s1872-2075(09)60003-0.

Ramos-Silva, P., Kaandorp, J., Huisman, L., Marie, B., Zanella-Cléon, I., Guichard, N., Miller, D.J. and Marin, F. (2013). The Skeletal Proteome of the Coral Acropora millepora: The Evolution of Calcification by Co-Option and Domain Shuffling. *Molecular Biology and Evolution*, [online] 30(9), pp.2099–2112. doi:https://doi.org/10.1093/molbev/mst109.

Ries, J.B., Cohen, A.L. and McCorkle, D.C. (2009). Marine calcifiers exhibit mixed responses to CO2-induced ocean acidification. *Geology*, [online] 37(12), pp.1131–1134. doi:https://doi.org/10.1130/g30210a.1.

Risk, M.J., Heikoop, J.M., Snow, M.G. and R.P. Beukens (2002). Lifespans and growth patterns of two deep-sea corals: Primnoa resedaeformis and Desmophyllum cristagalli. *Hydrobiologia*, 471(1/3), pp.125–131. doi:https://doi.org/10.1023/a:1016557405185.

Robert, K., et al (2023). *FKt230918 Cruise Report FKt230918 Cruise Report*. [online] Available at: https://research.library.mun.ca/16501/1/FKt230918%20-%20CruiseReport_Final.pdf [Accessed 10 Mar. 2025].

Robinson, L.F., Adkins, J.F., Frank, N., Gagnon, A.C., Prouty, N.G., Brendan Roark, E. and de Flierdt, T. van (2014). The geochemistry of deep-sea coral skeletons: A review of vital effects and applications for palaeoceanography. *Deep Sea Research Part II: Topical Studies in Oceanography*, [online] 99, pp.184–198. doi:https://doi.org/10.1016/j.dsr2.2013.06.005.

Roche, R.C., Abel, R.L., Johnson, K.G. and Perry, C.T. (2010). Spatial variation in porosity and skeletal element characteristics in apical tips of the branching coral Acropora pulchra (Brook 1891). *Coral Reefs*, 30(1), pp.195–201. doi:https://doi.org/10.1007/s00338-010-0679-1.

Romano, S.L. and Palumbi, S.R. (1996). Evolution of Scleractinian Corals Inferred from Molecular Systematics. *Science*, 271(5249), pp.640–642. doi:https://doi.org/10.1126/science.271.5249.640.

Rosenthal, Y., Lear, C.H., Oppo, D.W. and Linsley, B.K. (2006). Temperature and carbonate ion effects on Mg/Ca and Sr/Ca ratios in benthic foraminifera: Aragonitic speciesHoeglundina elegans. *Paleoceanography*, 21(1), p.n/a-n/a. doi:https://doi.org/10.1029/2005pa001158.

SAMADI, S. (2021). *SPANBIOS 2021*. [online] Flotteoceanographique.fr. Available at: https://campagnes.flotteoceanographique.fr/campagnes/18000701/ [Accessed 10 Mar. 2025].

Samperiz, A., Robinson, L.F., Stewart, J.A., Strawson, I., Leng, M.J., Rosenheim, B.E., Ciscato, E.R., Hendry, K.R. and Santodomingo, N. (2020). Stylasterid corals: A new paleotemperature archive. *Earth and Planetary Science Letters*, [online] 545, p.116407. doi:https://doi.org/10.1016/j.epsl.2020.116407.

Sands, C. et al (2018). *JR18003 Cruise Report*. [online] Available at: https://www.bodc.ac.uk/resources/inventories/cruise_inventory/reports/jr18003.pdf [Accessed 10 Mar. 2025].

Sanger, F. (1952). The Arrangement of Amino Acids in Proteins. *Advances in Protein Chemistry*, pp.1–67. doi:https://doi.org/10.1016/s0065-3233(08)60017-0.

Shen, Y., Guilderson, T.P., Sherwood, O.A., Castro, C.G., Chavez, F.P. and McCarthy, M.D. (2021). Amino acid δ13C and δ15N patterns from sediment trap time series and deep-sea corals: Implications for biogeochemical and ecological reconstructions in paleoarchives. *Geochimica et Cosmochimica Acta*, 297, pp.288–307. doi:https://doi.org/10.1016/j.gca.2020.12.012.

Shinn, E.A. (1966). Coral GrowthRate, an Environmental Indicator. *Journal of Paleontology*, [online] 40(2), pp.233–240. doi:https://doi.org/10.2307/1301658.

Sogin, E.M., Putnam, H.M., Anderson, P.E. and Gates, R.D. (2016). Metabolomic signatures of increases in temperature and ocean acidification from the reef-building coral, Pocillopora damicornis. *Metabolomics*, 12(4). doi:https://doi.org/10.1007/s11306-016-0987-8.

Sridevi, B. and Sarma, V.V.S.S. (2024). Rapid shoaling of aragonite saturation horizon in the northern Indian Ocean. *Environmental Research Communications*, 6(5), p.051006. doi:https://doi.org/10.1088/2515-7620/ad45c1.

Stewart, J.A., Li, T., Spooner, P.T., Burke, A., Chen, T., Roberts, J., Rae, J.W.B., Peck, V., Kender, S., Liu, Q. and Robinson, L.F. (2021). Productivity and Dissolved Oxygen Controls on the Southern Ocean Deep-Sea Benthos During the Antarctic Cold Reversal. *Paleoceanography and Paleoclimatology*, 36(10). doi:https://doi.org/10.1029/2021pa004288.

Stewart, J.A., Robinson, L.F., Day, R.D., Ivo Strawson, Burke, A., Rae, J.W.B., Spooner, P.T., Samperiz, A., Etnoyer, P.J., Williams, B., Paytan, A., Leng, M.J., Vreni Häussermann, Wickes, L.N., Bratt, R. and Pryer, H. (2020). Refining trace metal temperature proxies in cold-water scleractinian and

stylasterid corals. *Earth and Planetary Science Letters*, 545, pp.116412–116412. doi:https://doi.org/10.1016/j.epsl.2020.116412.

Stewart, J.A., Strawson, I., Kershaw, J. and Robinson, L.F. (2022). Stylasterid corals build aragonite skeletons in undersaturated water despite low pH at the site of calcification. *Scientific Reports*, 12(1). doi:https://doi.org/10.1038/s41598-022-16787-y.

Stolarski, J., Coronado, I., Murphy, J.G., Kitahara, M.V., Katarzyna Janiszewska, Mazur, M., Gothmann, A.M., Bouvier, A.-S., Marin-Carbonne, J., Taylor, M.L., Quattrini, A.M., McFadden, C.S., Higgins, J.A., Robinson, L.F. and Anders Meibom (2020). A modern scleractinian coral with a two-component calcite–aragonite skeleton. *Proceedings of the National Academy of Sciences*, 118(3). doi:https://doi.org/10.1073/pnas.2013316117.

Stolarski, J., Kitahara, M.V., Miller, D.J., Cairns, S.D., Mazur, M. and Meibom, A. (2011). The ancient evolutionary origins of Scleractinia revealed by azooxanthellate corals. *BMC Evolutionary Biology*, 11(1), p.316. doi:https://doi.org/10.1186/1471-2148-11-316.

Sun, H., Gao, Z.-Y., Zhao, D.-R., Sun, X.-W. and Chen, L.-Q. (2021). Spatial variability of summertime aragonite saturation states and its influencing factor in the Bering Sea. *Advances in Climate Change Research*, 12(4), pp.508–516. doi:https://doi.org/10.1016/j.accre.2021.04.001.

Takeuchi, T., Yamada, L., Shinzato, C., Sawada, H. and Satoh, N. (2016). Stepwise Evolution of Coral Biomineralization Revealed with Genome-Wide Proteomics and Transcriptomics. *PLOS ONE*, 11(6), p.e0156424. doi:https://doi.org/10.1371/journal.pone.0156424.

Tambutté, S., Holcomb, M., Ferrier-Pagès, C., Reynaud, S., Tambutté, É., Zoccola, D. and Allemand, D. (2011). Coral biomineralization: From the gene to the environment. *Journal of Experimental Marine Biology and Ecology*, 408(1-2), pp.58–78. doi:https://doi.org/10.1016/j.jembe.2011.07.026.

Tambutté, S., Tambutté, E., Zoccola, D. and Allemand, D. (2007). Organic Matrix and Biomineralization of Scleractinian Corals. pp.243–259. doi:https://doi.org/10.1002/9783527619443.ch14.

Thierry Baussant, Nilsen, M., Ravagnan, E., Westerlund, S. and Sreerekha Ramanand (2017). Physiological responses and lipid storage of the coral *Lophelia pertusa* at varying food density. 80(5), pp.266–284. doi:https://doi.org/10.1080/15287394.2017.1297274.

Thresher, R., Tilbrook, B., Fallon, S., Wilson, N. and Adkins, J. (2011). Effects of chronic low carbonate saturation levels on the distribution, growth and skeletal chemistry of deep-sea corals and other seamount megabenthos. *Marine Ecology Progress Series*, 442, pp.87–99. doi:https://doi.org/10.3354/meps09400.

Tracey, D.M., Marriott, P., Hitt, N., Neil, H. and Clark, M.R. (2024). Age and growth of a habitat-forming deep-sea coral *Solenosmilia variabilis* in the New Zealand region: implications for fisheries management. *New Zealand Journal of Marine and Freshwater Research*, pp.1–23. doi:https://doi.org/10.1080/00288330.2024.2398779.

Turley, C.M., Roberts, J.M. and Guinotte, J.M. (2007). Corals in deep-water: will the unseen hand of ocean acidification destroy cold-water ecosystems? *Coral Reefs*, 26(3), pp.445–448. doi:https://doi.org/10.1007/s00338-007-0247-5.

Us-ocb.org. (2024). *Upwelling and solubility drive global surface dissolved inorganic carbon (DIC) distribution :: Ocean Carbon & Biogeochemistry*. [online] Available at: https://www.us-ocb.org/upwelling-and-solubility-drive-global-surface-dic-distribution/.

Venn, A.A., Tambutte, E., Holcomb, M., Laurent, J., Allemand, D. and Tambutte, S. (2012). Impact of seawater acidification on pH at the tissue-skeleton interface and calcification in reef corals. *Proceedings of the National Academy of Sciences*, 110(5), pp.1634–1639. doi:https://doi.org/10.1073/pnas.1216153110.

Voolstra, C.R., Shinichi Sunagawa, Matz, M.V., Bayer, T., Aranda, M., Buschiazzo, E., DeSalvo, M.K., Lindquist, E., Szmant, A.M., Mary Alice Coffroth and Medina, M. (2011). Rapid Evolution of Coral Proteins Responsible for Interaction with the Environment. *PLOS ONE*, 6(5), pp.e20392–e20392. doi:https://doi.org/10.1371/journal.pone.0020392.

Wall, M., Ragazzola, F., Foster, L.C., Form, A. and Schmidt, D.N. (2015). pH up-regulation as a potential mechanism for the cold-water coral *Lophelia pertusa* to sustain growth in aragonite undersaturated conditions. *Biogeosciences*, 12(23), pp.6869–6880. doi:https://doi.org/10.5194/bg-12-6869-2015.

Wigley, T.M.L. and Raper, S.C.B. (1987). Thermal expansion of sea water associated with global warming. *Nature*, [online] 330(6144), pp.127–131. doi:https://doi.org/10.1038/330127a0.

Xue, L. and Cai, W.-J. (2020). Total alkalinity minus dissolved inorganic carbon as a proxy for deciphering ocean acidification mechanisms. *Marine Chemistry*, 222, p.103791. doi:https://doi.org/10.1016/j.marchem.2020.103791.

Yasuhara, M. and Danovaro, R. (2014). Temperature impacts on deep-sea biodiversity. *Biological Reviews*, 91(2), pp.275–287. doi:https://doi.org/10.1111/brv.12169.

Zaquin, T., Malik, A., Drake, J.L., Putnam, H.M. and Mass, T. (2021). Evolution of Protein-Mediated Biomineralization in Scleractinian Corals. *Frontiers in Genetics*, 12. doi:https://doi.org/10.3389/fgene.2021.618517.

Zheng, M.-D. and Cao, L. (2014). Simulation of global ocean acidification and chemical habitats of shallow- and cold-water coral reefs. *Advances in Climate Change Research*, 5(4), pp.189–196. doi:https://doi.org/10.1016/j.accre.2015.05.002.

8 Appendix

8.1 Replicate data tables:

8.1.1 Analytical

Analytical replicates Stylasterids (THAA)

Sample	Genus	Coefficient of Variance (%)
JR15005-Ev39-784-Il39be	*Inferiolabiata*	1.49
JC094-B0480-Hydls(f)-001Sty80an	*Stylaster*	1.80
Adp88	*Adelopora*	4.25
JC094-F0184-Hydlm-001Eal001	*Errina*	8.37
Egr2426	*Errina*	1.47
StyBrcc	*Stylaster*	3.39
Sdefg	*Stylaster*	1.12
ErrNabi	*Errinopora*	2.61
JC094-B0548-Hydls/m-001 to 019-Eal48aq	*Errina*	8.57
JR15005-Ev113-2429-Il29bd	*Inferiolabiata*	2.18
NBP1103-DH22-Stc1-01Sde22aw	*Stylaster*	5.03
NBP1103-DH39-St-2-02-Ebo02	*Errina*	2.66
ErrNabk	*Errinopora*	5.04
AT5009_B0246_Dive5161_Ev012_001	*Stylaster*	3.66

AT5009_B1616_Dive5174_Ev008_001	*Lepidotheca*	1.12
FKt230918_S0588_Ev14_01	*Lepidotheca*	1.90
	Mean	4.07%

Table A.1, The coefficient of variance for Stylasterid corals using analytical data only. This is the coefficient of variance of THAA (Pmol/mg).

Analytical replicates

Scleractinia (THAA)

Sample	Genus	Coefficient of Variance (%)
DY081-031-ROV333-Ev032-201-583Loph	*Lophelia*	5.77
JC094-42-VEM-ROV233-ARM79B0089-Enall-00	*Enallopsammia*	2.33
DY081-031-ROV333-Ev033-201-570Loph	*Lophelia*	1.08
JC094-21-EBB-ROV228-ARM33B0027-Enall-001	*Enallopsammia*	2.09
JC094-15-EBA-ROV227-SLP46-B0018Carlm-00	*Caryophyllia*	2.30
	Mean	1.67%

Table A.2, The coefficient of Variance of THAA (Pmol/mg) for scleractinia corals using analytical data only.

Analytical replicates

Asx Concentration

Stylasterids

Sample	Genus	Coefficient of Variance
JR15005-Ev39-784-Il39be	*Inferiolabiata*	1.94
JC094-B0480-Hydls(f)-001-Sty80an	*Stylaster*	2.44
Adp88	*Adelopora*	5.96
JC094-F0184-Hydlm-001-Eal001	*Errina*	5.85
Egr2426	*Errina*	2.45
StyBrcc	*Stylaster*	5.31
Sdefg	*Stylaster*	1.45
ErrNabi	*Errinopora*	1.61
JC094-B0548-Hydls/m-001 to 019-Eal48aq	*Errina*	3.06
JR15005-Ev113-2429-Il29bd	*Inferiolabiata*	6.13
NBP1103-DH22-Stc1-01-Sde22aw	*Stylaster*	3.70
NBP1103-DH39-St-2-02-Ebo02	*Errina*	4.82
ErrNabk	*Errinopora*	5.07
AT5009_B0246_Dive5161_Ev012_001	*Stylaster*	0.25
AT5009_B1616_Dive5174_Ev008_001	*Lepidotheca*	1.31
FKt230918_S0588_Ev14_01	*Lepidotheca*	1.24
	Mean %	3.02

Table A.3, The coefficient of Variance of Asx concentration (Pmol/mg) for stylasterid corals using analytical data only.

Asx Concentration

Scleractinia

Sample	Genus	Coefficient of Variance
DY081-031-ROV333-Ev032-201-583-Loph	*Lophelia*	0.65
JC094-42-VEM-ROV233-ARM79-B0089-Enall-00	*Enallopsammia*	0.76
DY081-031-ROV333-Ev033-201-570-Loph	*Lophelia*	0.52

JC094-21-EBB-ROV228-ARM33-B0027-Enall001	*Enallopsammia*	0.37
JC094-15-EBA-ROV227-SLP46-B0018-Carlm-00	*Caryophyllia*	0.62
	Mean %	0.58

Table A.4, The coefficient of Variance of THAA (Pmol/mg) for scleractinia corals using analytical data only.

Percentage Asx

Stylasterids

Sample	Genus	Coefficient of Variance
JR15005-Ev39-784-Il39be	*Inferiolabiata*	3.20
JC094-B0480-Hydls(f)-001-Sty80an	*Stylaster*	2.87
Adp88	*Adelopora*	9.57
JC094-F0184-Hydlm-001-Eal001	*Errina*	3.76
Egr2426	*Errina*	1.63
StyBrcc	*Stylaster*	2.20
Sdefg	*Stylaster*	2.23
ErrNabi	*Errinopora*	1.25
JC094-B0548-Hydls/m-001 to 019-Eal48aq	*Errina*	5.87
JR15005-Ev113-2429-Il29bd	*Inferiolabiata*	7.93
NBP1103-DH22-Stc1-01-Sde22aw	*Stylaster*	4.34
NBP1103-DH39-St-2-02-Ebo02	*Errina*	2.47
ErrNabk	*Errinopora*	6.80
AT5009_B0246_Dive5161_Ev012_001	*Stylaster*	3.65
AT5009_B1616_Dive5174_Ev008_001	*Lepidotheca*	11.4
FKt230918_S0588_Ev14_01	*Lepidotheca*	1.41
	Mean %	4.41

Table A.5, The coefficient of Variance of the percentage of Asx for stylasterid corals using analytical data only.

Analytical replicates

Percentage Asx

Scleractinia

Sample	Genus	Coefficient of Variance
DY081-031-ROV333-Ev032-201-583-Loph	*Lophelia*	0.42
JC094-42-VEM-ROV233-ARM79-B0089-Enall-00	*Enallopsammia*	3.08
DY081-031-ROV333-Ev033-201-570-Loph	*Lophelia*	1.51
JC094-21-EBB-ROV228-ARM33-B0027-Enall001	*Enallopsammia*	2.20
JC094-15-EBA-ROV227-SLP46-B0018Carlm-00	*Caryophyllia*	1.85
	Average	1.81

Table A.6, The coefficient of Variance of the percentage of Asx for scleractinia corals using analytical data only.

8.1.2 Preparative

Preparative replicate

THAA (pmol/mg)

Sample	Number of samples	Genus	Coefficient of variance (%)
FKt230918_S0588_Ev14_01	*6*	*Lepidotheca*	2.33
Egr2426	*5*	*Errina*	8.85
StyBrcc	*7*	*Stylaster*	7.35
ErrNabi	*8*	*Errinopora*	1.23
ErrNabk	*12*	*Errinopora*	6.82
		Mean	7.53%

Table A.7, The THAA coefficient of variance of stylasterid corals for the preparative replicates.

Asx Concentration			
Preparative replicate			
Sample	Number of samples	Genus	Coefficient of variance
FKt230918_S0588_Ev14_01	*6*	*Lepidotheca*	4.74
Egr2426	*5*	*Errina*	7.35
StyBrcc	*7*	*Stylaster*	6.93
ErrNabi	*8*	*Errinopora*	11.4
ErrNabk	*12*	*Errinopora*	5.90
		Average	7.26

Table A.8, The Asx concentration (pmol/mg) coefficient of variance of stylasterid corals for the preparative replicates.

Percentage Asx		
Preparative replicate		
Sample	Coefficient of variance	%
FKt230918_S0588_Ev14_01		4.60
Egr2426		1.81
StyBrcc		1.25
ErrNabi		1.93
ErrNabk		3.90
	Average	2.69

Table A.9, The percentage of Asx coefficient of variance of stylasterid corals for the preparative replicates.

8.1.3 Internal Heterogeneity **Internal**

Heterogeneity

Tip to Branch Samples

[THAA]

Sample		Genus	Coefficient of variance (%)
AT5009_B0246_Dive5161_Ev012_001	*A*	*Stylaster*	11.03
AT5009_B1616_Dive5174_Ev008_001	*B*	*Lepidotheca*	22.6
FKt230918_S0588_Ev14_01	*C*	*Lepidotheca*	9.54
JC094-B0480-Hydls(f)-001-Sty80an	*D*	*Stylaster*	5.33
Adp88	*E*	*Adelopora*	5.54
Egr2426 (Test 1)	*F*	*Errina*	34.5
Egr2426 (Test 2)	*G*	*Errina*	29.2
JC094-F0184-Hydlm-001-Eal001	*H*	*Errina*	28.8
StyBrcc	*I*	*Stylaster*	12.1
Sdefg	*J*	*Stylaster*	18.2
ErrNabi	*K*	*Errinopora*	12.00
JC094-B0548-Hydls/m-001 to 019Eal48aq	*L*	*Errina*	32.4
		Average	18.4%

Table A.10, The percentage of Asx coefficient of variance of stylasterid corals for the Internal heterogeneity of tip-to-branch samples.

Internal Heterogeneity

Linear Branches

[THAA]		
Sample	Genus	Coefficient of Variance
JR15005-Ev113-2429-Il29bd	*Inferiolabiata*	22.6
NBP1103-DH22-Stc1-01-Sde22aw	*Stylaster*	4.53
NBP1103-DH39-St-2-02-Ebo02	*Errina*	13.00
JR15005-Ev39-784-Il39be	*Inferiolabiata*	6.44
	Average	11.6%

Table A.11 The coefficient of variance for the [THAA] for the internal heterogeneity of linear stylasterid branches

Asx Concentration		
Internal Heterogeneity Tip to Branch Samples		
Sample	Genus	Coefficient of variance
AT5009_B0246_Dive5161_Ev012_001	*Stylaster*	16.9
AT5009_B1616_Dive5174_Ev008_001	*Lepidotheca*	19.1
FKt230918_S0588_Ev14_01	*Lepidotheca*	12.4
JC094-B0480-Hydls(f)-001-Sty80an	*Stylaster*	6.21
Adp88	*Adelopora*	9.30
Egr2426 (Test 1)	*Errina*	29.9
Egr2426 (Test 2)	*Errina*	12.1
JC094-F0184-Hydlm-001-Eal001	*Errina*	30.1
StyBrcc	*Stylaster*	10.9
Sdefg	*Stylaster*	18.8
ErrNabi	*Errinopora*	31.6
JC094-B0548-Hydls/m-001 to 019Eal48aq	*Errina*	30.8
	Average	19.0

Table A.12, The Asx concentration coefficient of variance of stylasterid corals for the Internal heterogeneity of the tip-to-branch samples.

Asx Concentration
Internal Heterogeneity Linear Branches

Sample	Genus	Coefficient of variance
JR15005-Ev113-2429-Il29bd	*Inferiolabiata*	16.9
NBP1103-DH22-Stc1-01-Sde22aw	*Stylaster*	4.66
NBP1103-DH39-St-2-02-Ebo02	*Errina*	9.79
JR15005-Ev39-784-Il39be	*Inferiolabiata*	3.75
	Average	8.76

Table A.13, The Asx concentration coefficient of variance of stylasterid corals for the Internal heterogeneity of the linear branch samples.

Percentage Asx Internal Heterogeneity Tip to Branch Samples		
AT5009_B0246_Dive5161_Ev012_001	*Stylaster*	10.9
AT5009_B1616_Dive5174_Ev008_001	*Lepidotheca*	8.40
FKt230918_S0588_Ev14_01	*Lepidotheca*	4.21
JC094-B0480-Hydls(f)-001-Sty80an	*Stylaster*	4.71
Adp88	*Adelopora*	4.26
Egr2426 (Test 1)	*Errina*	7.95
Egr2426 (Test 2)	*Errina*	16.0
JC094-F0184-Hydlm-001-Eal001	*Errina*	3.24
StyBrcc	*Stylaster*	2.81
Sdefg	*Stylaster*	4.22
ErrNabi	*Errinopora*	5.55
JC094-B0548-Hydls/m-001 to 019Eal48aq	*Errina*	1.99
	Average	6.19

Table A.14, The percentage of Asx coefficient of variance of stylasterid corals for the Internal heterogeneity of the tip-to-branch samples.

Percentage Asx		
Internal Heterogeneity Linear Branches		
Sample	Genus	Coefficient of variance
JR15005-Ev113-2429-Il29bd	*Inferiolabiata*	8.24
NBP1103-DH22-Stc1-01-Sde22aw	*Stylaster*	2.09
NBP1103-DH39-St-2-02-Ebo02	*Errina*	4.00
JR15005-Ev39-784-Il39be	*Inferiolabiata*	2.70
	Average	4.25

Table A.15, The percentage of Asx coefficient of variance of stylasterid corals for the Internal heterogeneity of the linear branch samples.

[THAA]	
Internal Heterogeneity Scleractinia	
Sample	Coefficient of variance %
DY081-031-ROV333-Ev032-201-583-Loph	46.0
JC094-42-VEM-ROV233-ARM79-B0089-Enall-00	5.4
DY081-031-ROV333-Ev033-201-570-Loph	13.0
JC094-21-EBB-ROV228-ARM33-B0027-Enall-001	4.6
JC094-15-EBA-ROV227-SLP46-B0018-Carlm-00	39.0
Average	21.6

Table A.16 Coefficient of variance [THAA] of internal heterogeneity of scleractinia corals

Asx Concentration
Internal Heterogeneity Scleractinia

Sample	Coefficient of variance %
DY081-031-ROV333-Ev032-201-583-Loph	33.2
JC094-42-VEM-ROV233-ARM79-B0089-Enall-00	4.7
DY081-031-ROV333-Ev033-201-570-Loph	11.1
JC094-21-EBB-ROV228-ARM33-B0027-Enall-001	5.7
JC094-15-EBA-ROV227-SLP46-B0018-Carlm-00	45.3
	Average 20.0

Table A.17 Coefficient of variance [THAA] of internal heterogeneity of scleractinia corals

Percentage of Asx	
Internal Heterogeneity Scleractinia	
Sample	Coefficient of variance %
DY081-031-ROV333-Ev032-201-583-Loph	22.2
JC094-42-VEM-ROV233-ARM79-B0089-Enall-00	1.04
DY081-031-ROV333-Ev033-201-570-Loph	1.81
JC094-21-EBB-ROV228-ARM33-B0027-Enall-001	1.05
JC094-15-EBA-ROV227-SLP46-B0018-Carlm-00	6.14
Average	6.45

Table A.18 Coefficient of variance [THAA] of internal heterogeneity of scleractinia corals

8.2 Replicate data graphs

8.2.1 Analytical

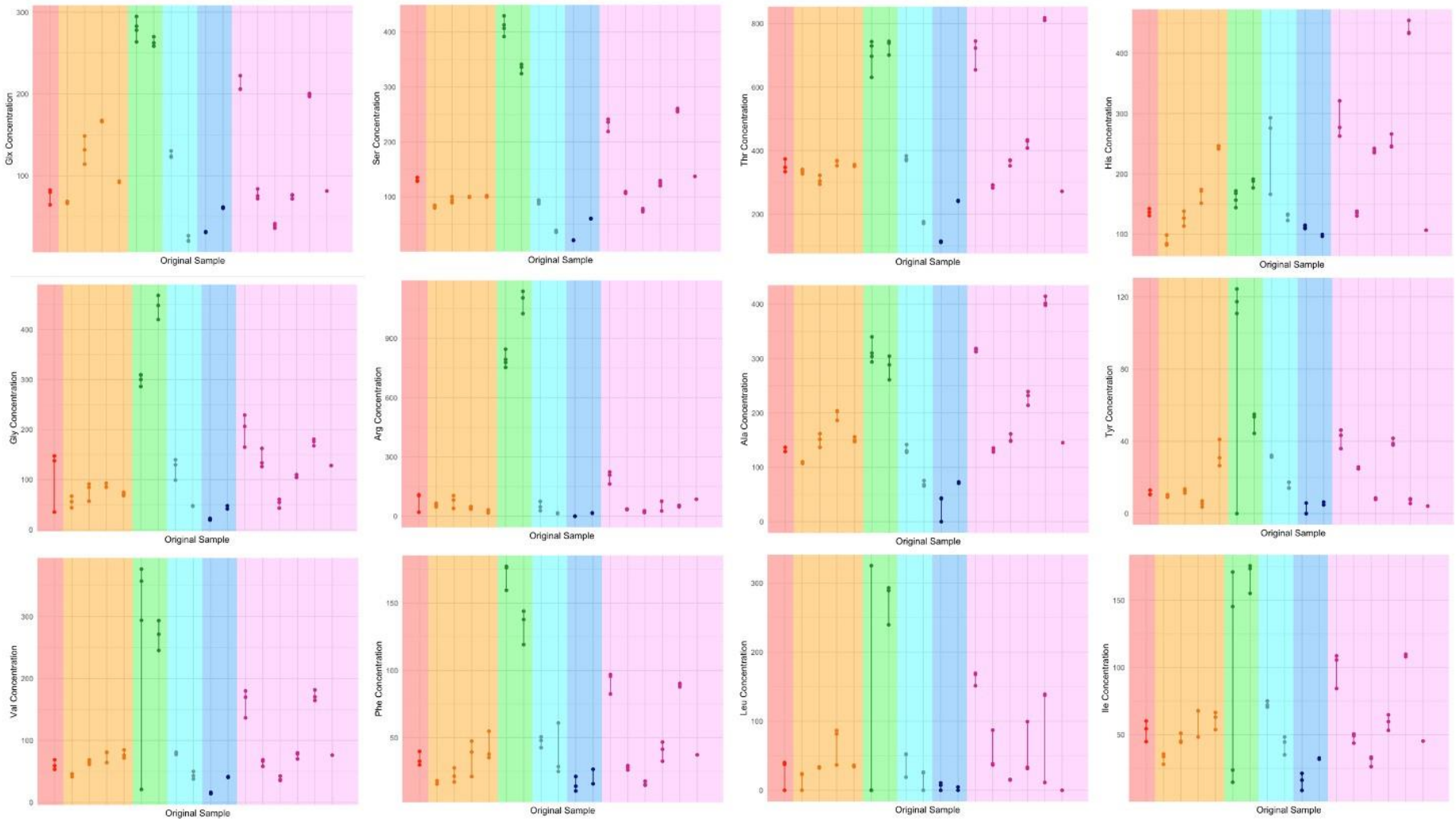

Figure 7.1 Concentration of amino acids for stylasterid analytical replicate data, colour corresponds to the genus and sample found in section 3.3

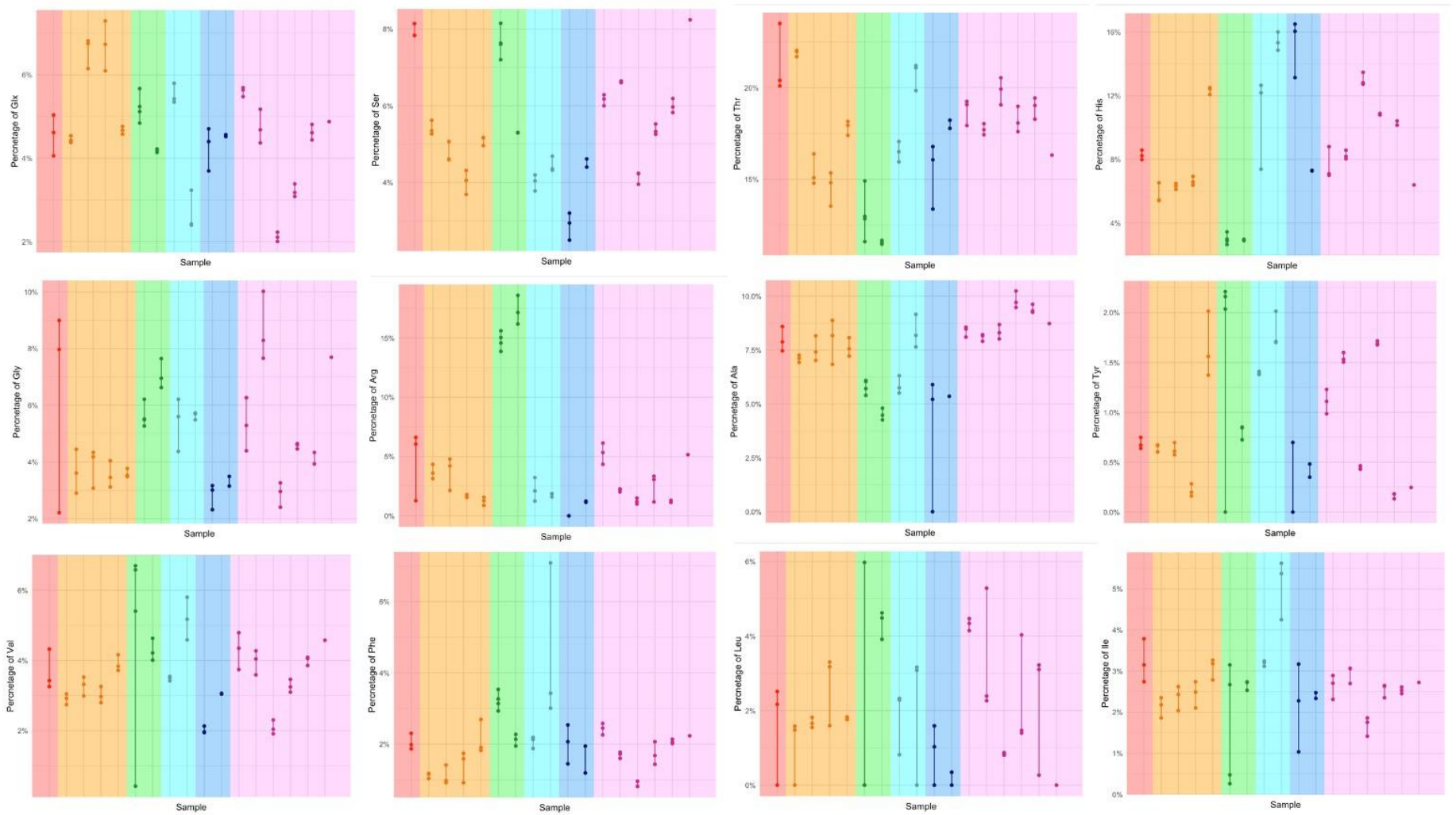

Figure 7.2 Percentage composition of amino acids for stylasterid analytical replicate data, colour corresponds to the genus and sample found in section 3.3

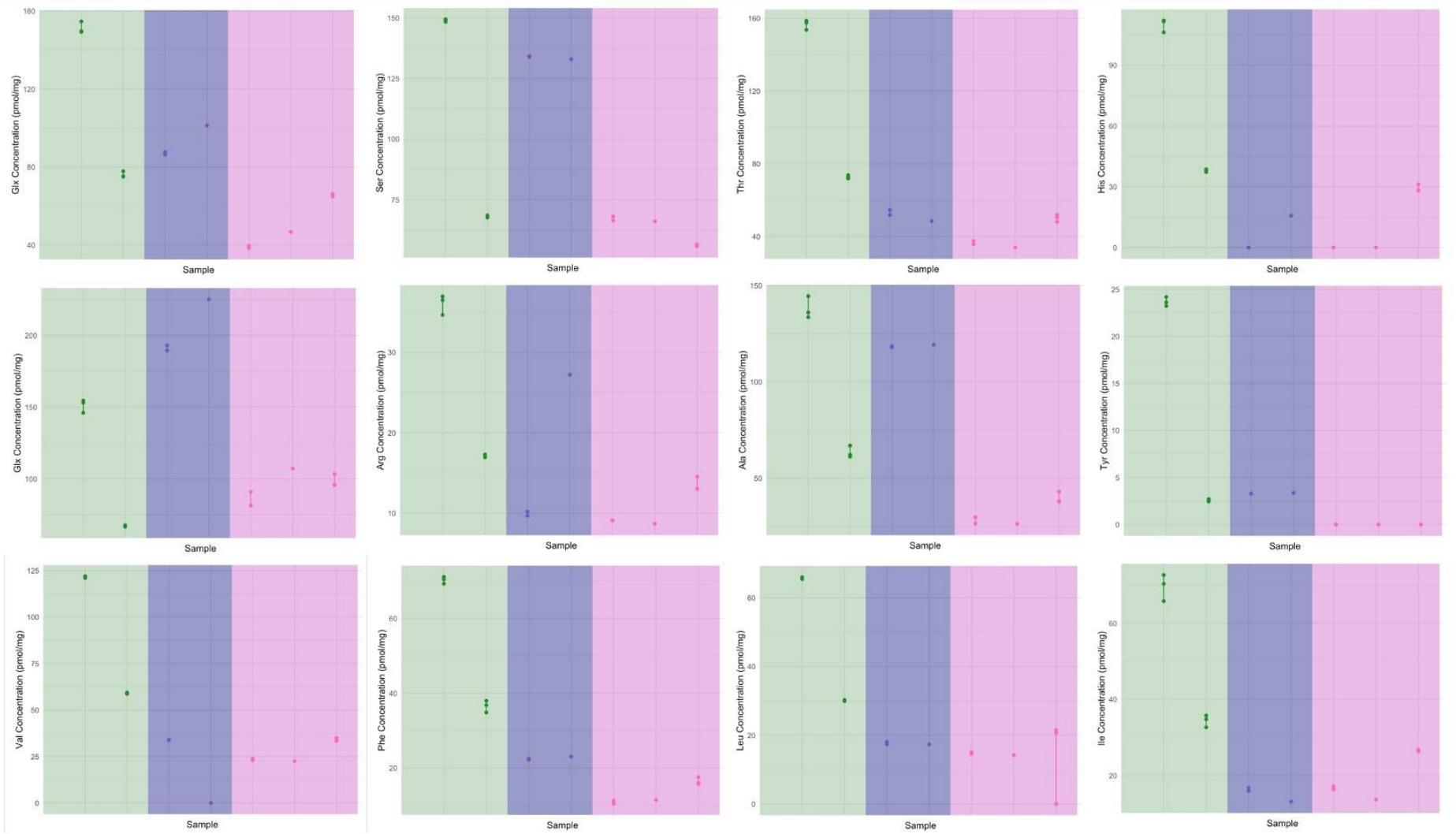

Figure 7.3 Concentration of amino acids for scleractinia analytical replicate data, colour corresponds to the genus and sample found in section 3.3

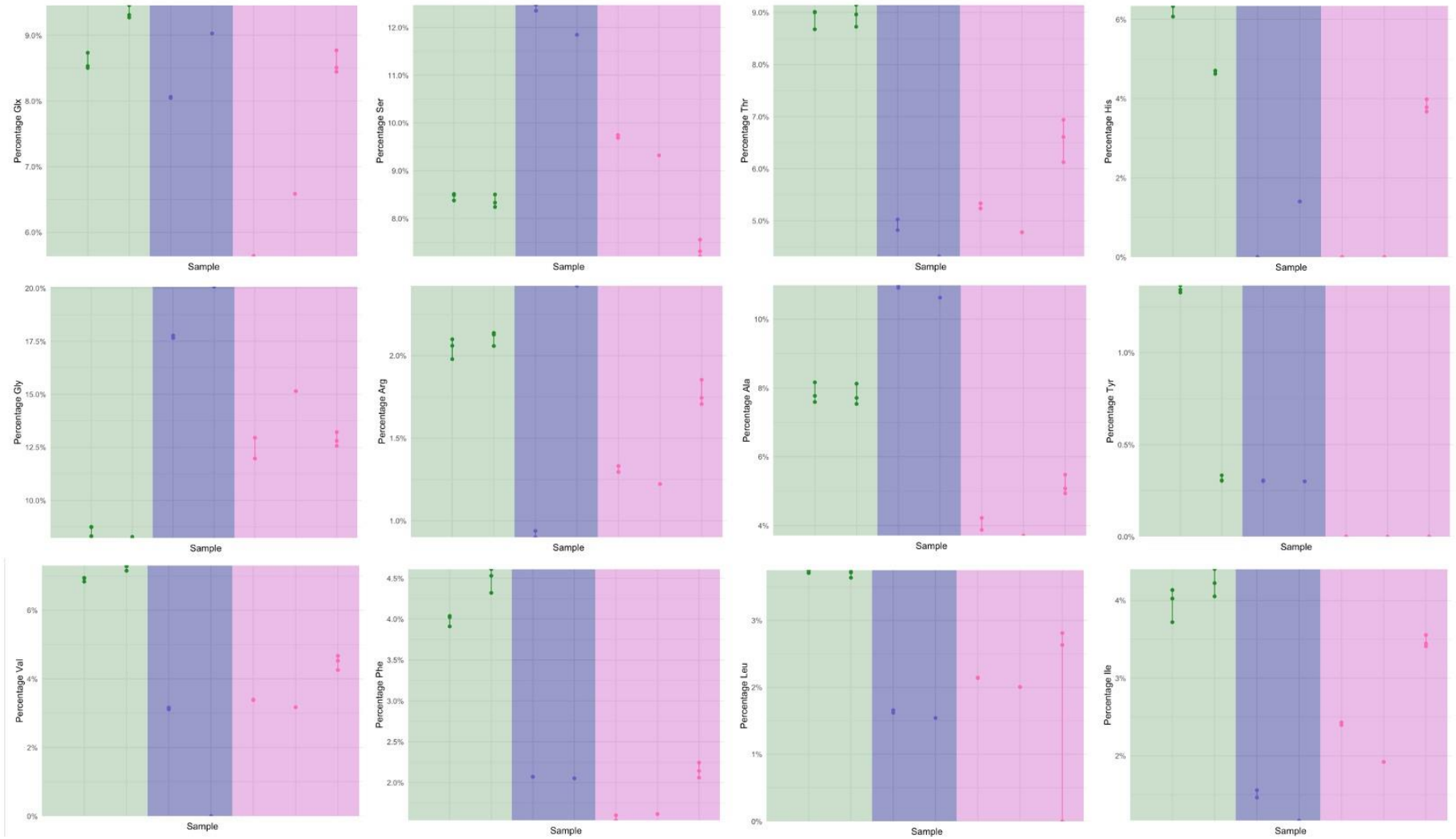

Figure 7.4 Percentage composition of amino acids for scleractinia analytical replicate data, colour corresponds to the genus and sample found in section 3.3

8.2.2 Preperative

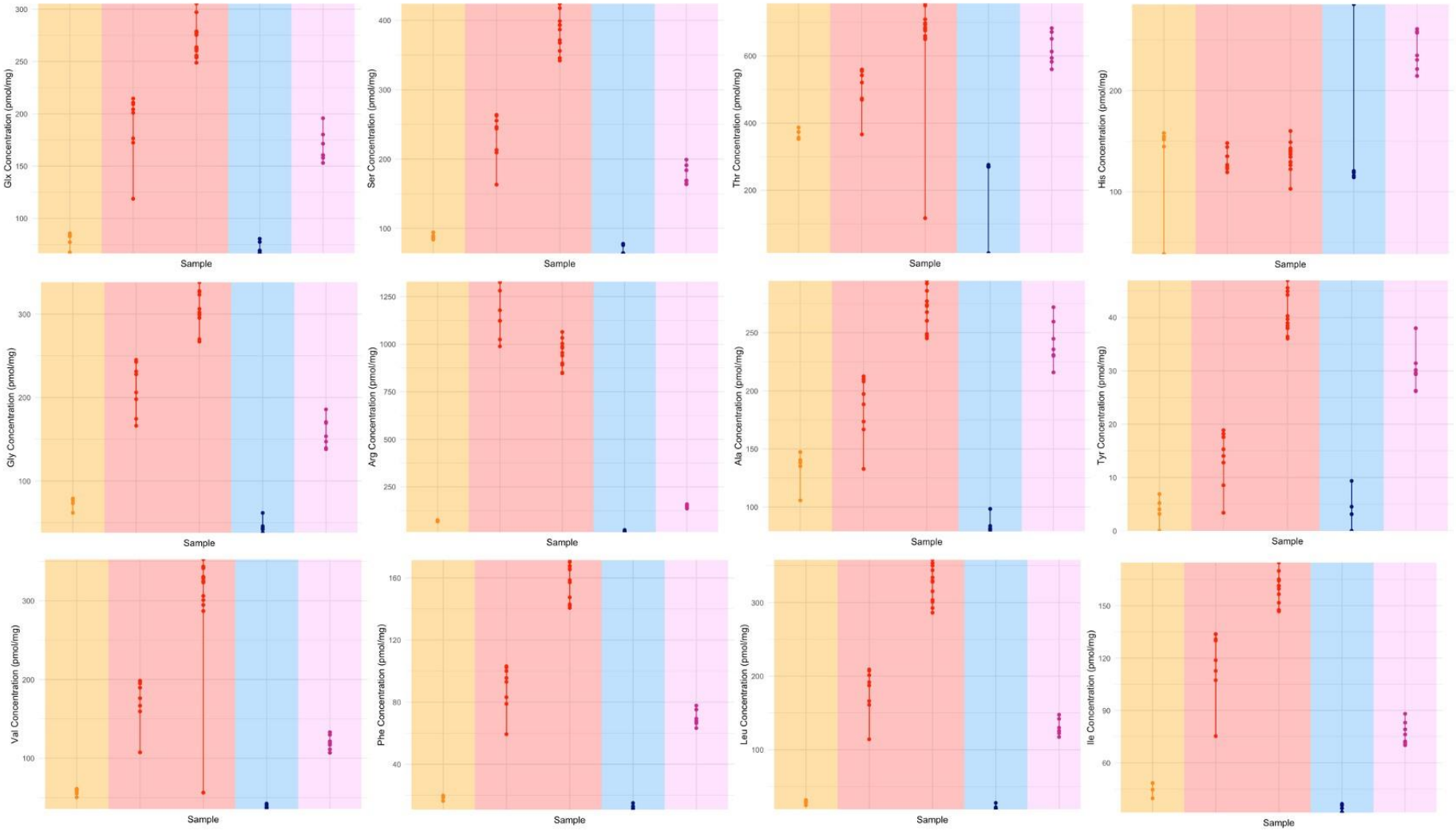

Figure 7.5 Concentration of amino acids for stylasterid preparative replicate data, colour corresponds to the genus and sample found in section 3.4

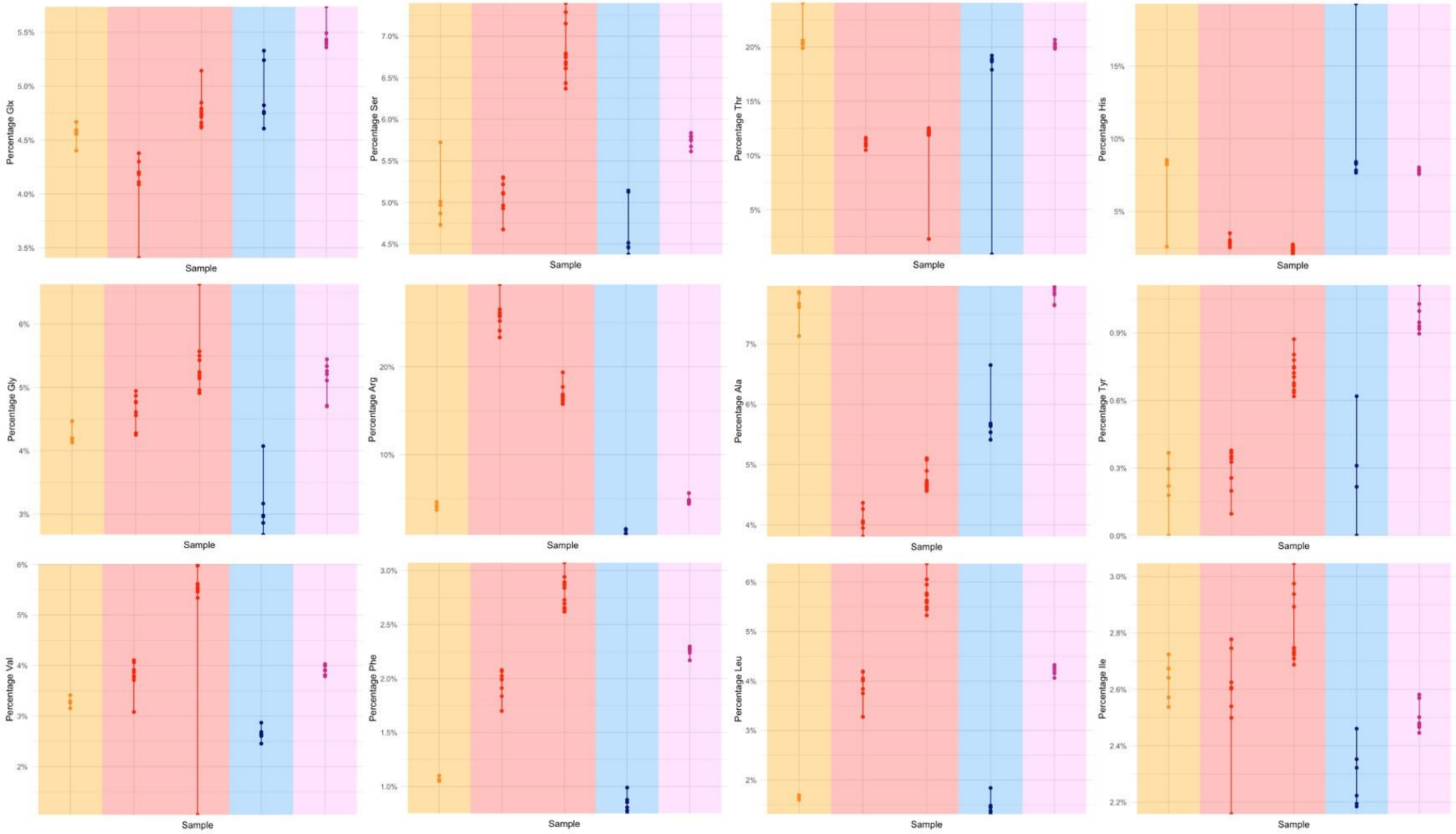

Figure 7.6 Percentage composition of amino acids for stylasterid preparative replicate data, colour corresponds to the genus and sample found in section 3.4

8.2.3 Internal heterogeneity

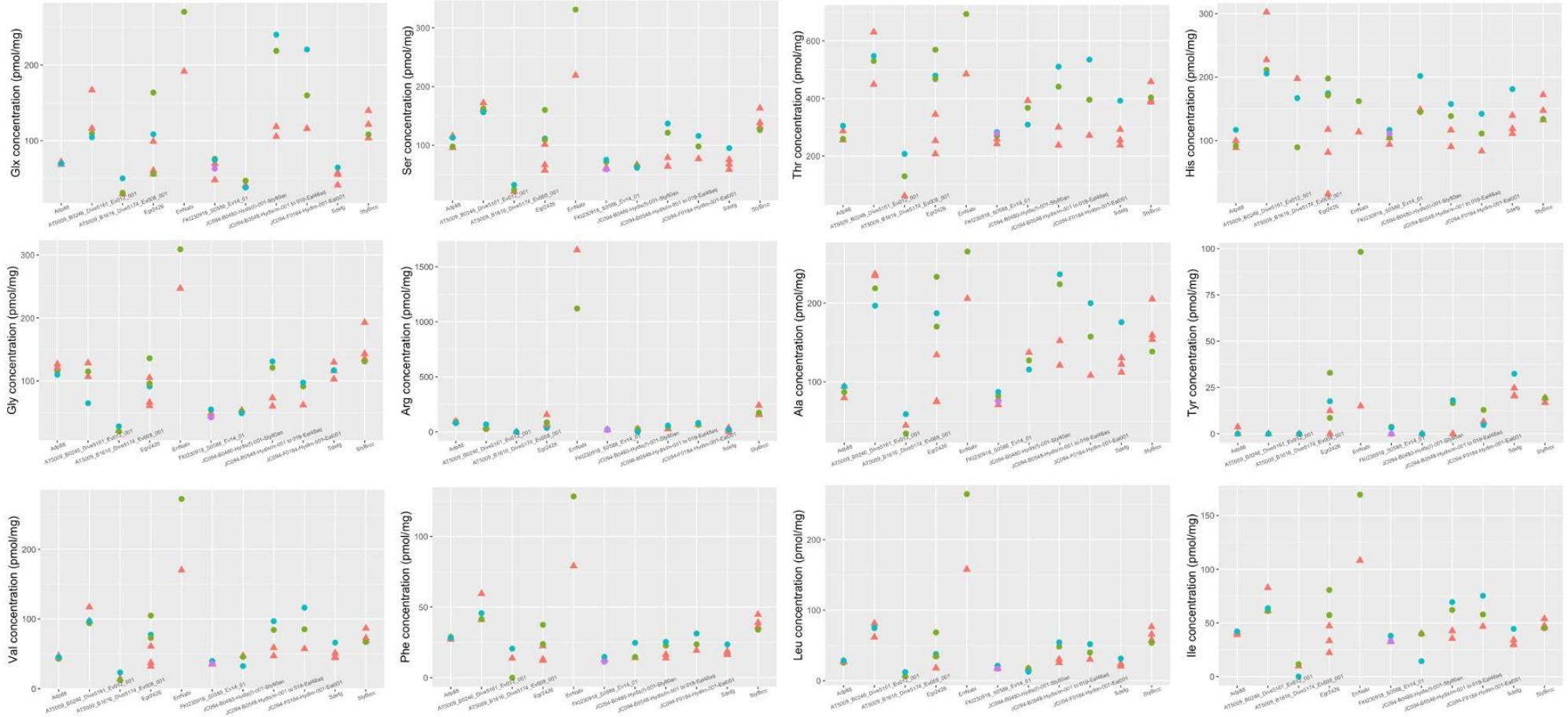

Figure 7.7 Concentration of amino acids for stylasterid internal heterogeneity tip-to-branch replicate data, colour corresponds to the section of the branch found in section 3.5.1

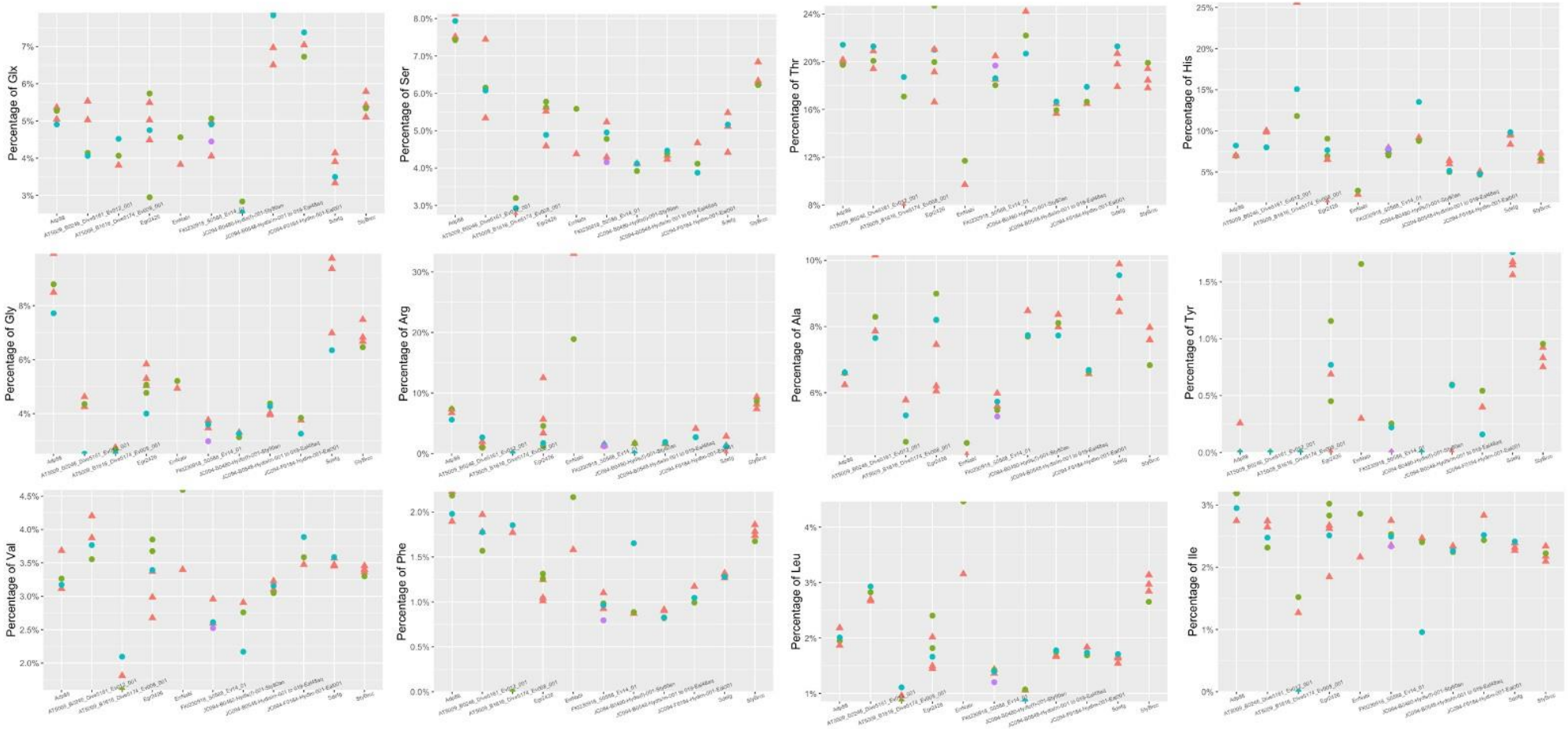

Figure 7.8 Percentage composition of amino acids for stylasterid internal heterogeneity tip-to-branch replicate data, colour corresponds to the section of the branch found in section 3.5.1

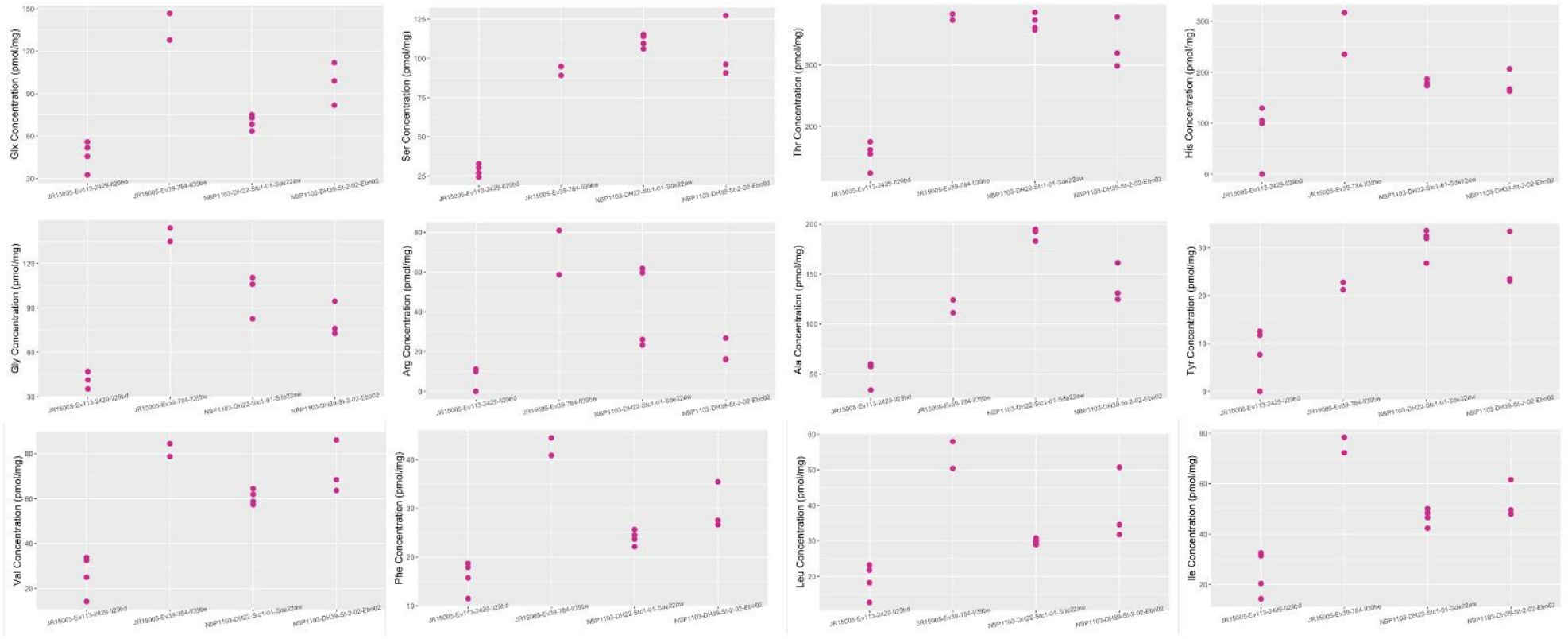

Figure 7.8 Concentration of amino acids for stylasterid internal heterogeneity linear branch replicate data

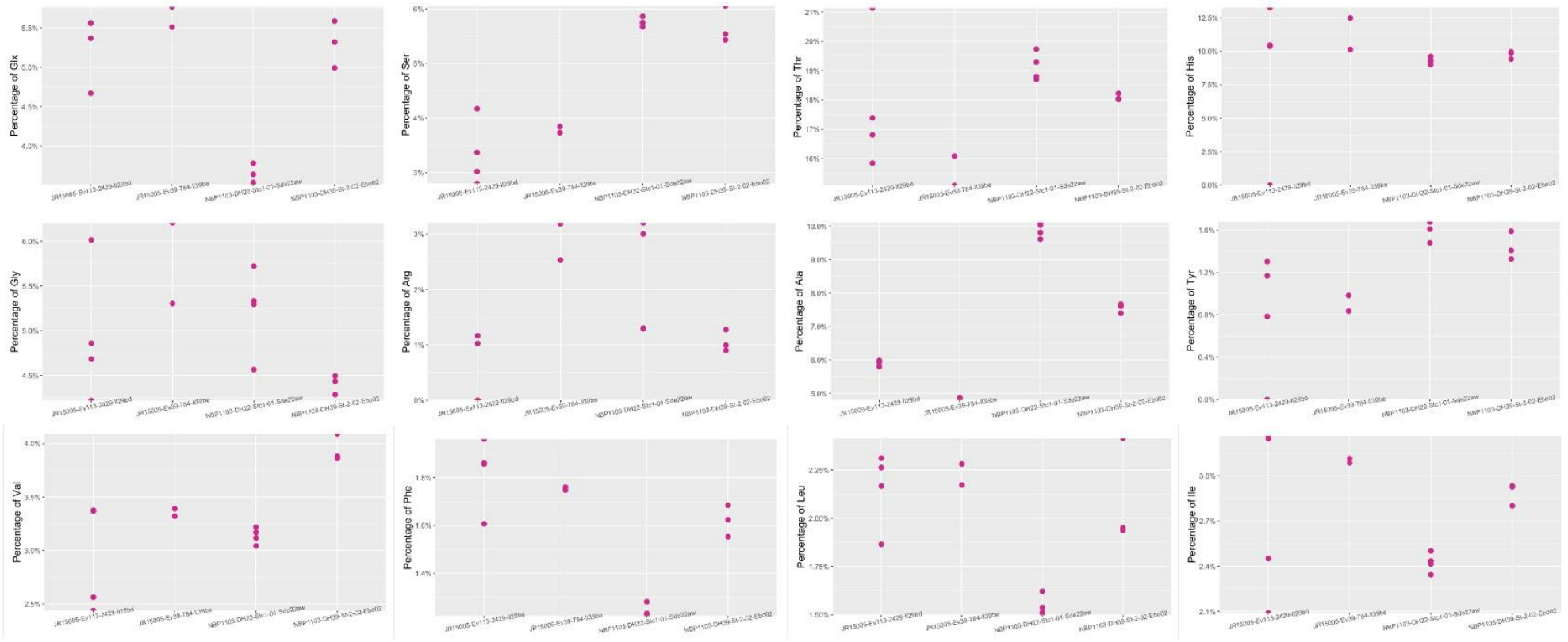

Figure 7.9 Percentage composition of amino acids for stylasterid internal heterogeneity linear branch replicate data

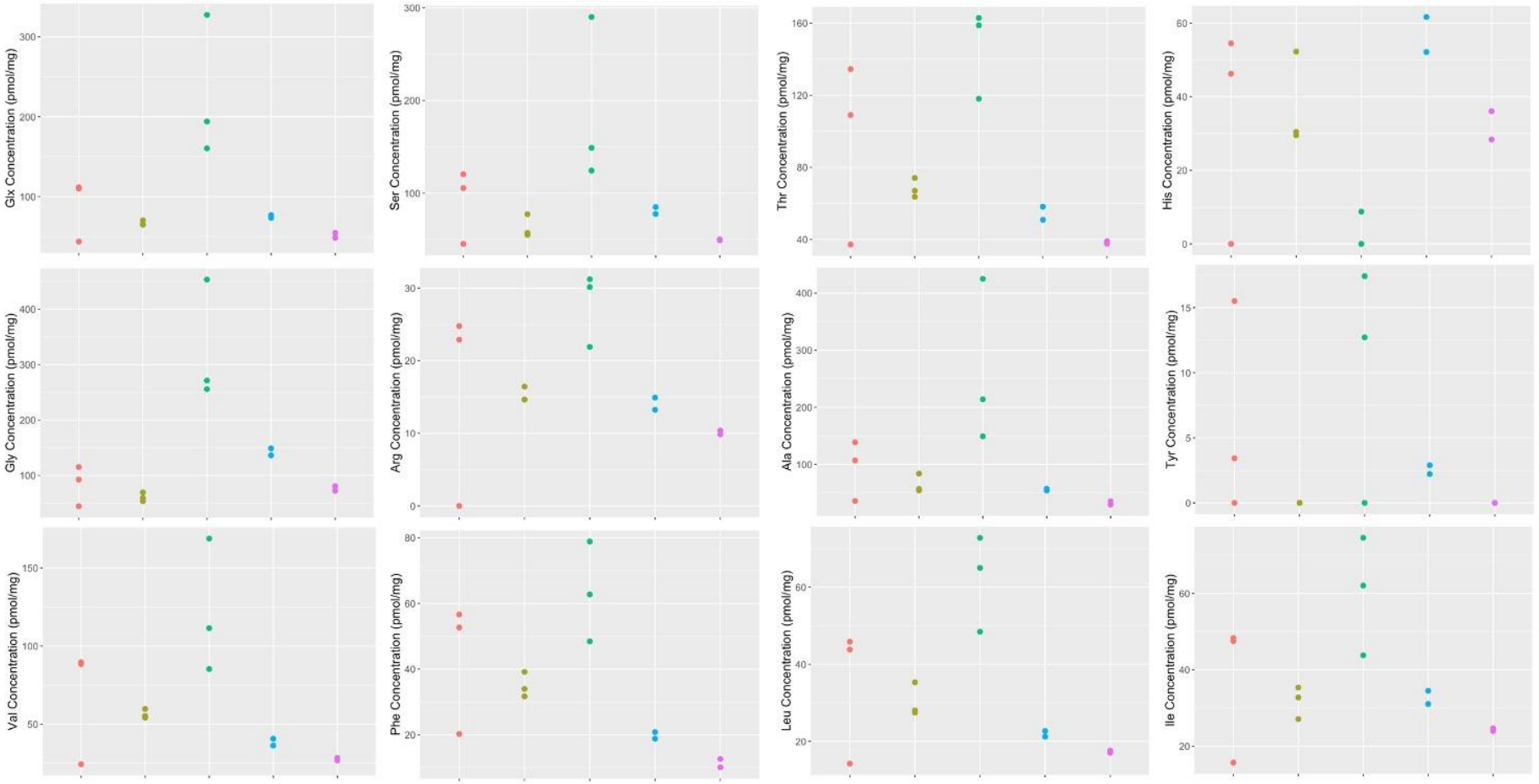
Glx Concentration (pmol/mg)
Ser Concentration (pmol/mg)
Thr Concentration (pmol/mg)
His Concentration (pmol/mg)
Gly Concentration (pmol/mg)
Arg Concentration (pmol/mg)
Ala Concentration (pmol/mg)
Tyr Concentration (pmol/mg)
Val Concentration (pmol/mg)
Phe Concentration (pmol/mg)
Leu Concentration (pmol/mg)
Ile Concentration (pmol/mg)

Figure 7.10 Concentration of amino acids for scleractinia internal heterogeneity replicate data, colour corresponds to the sample found within section 3.5.2

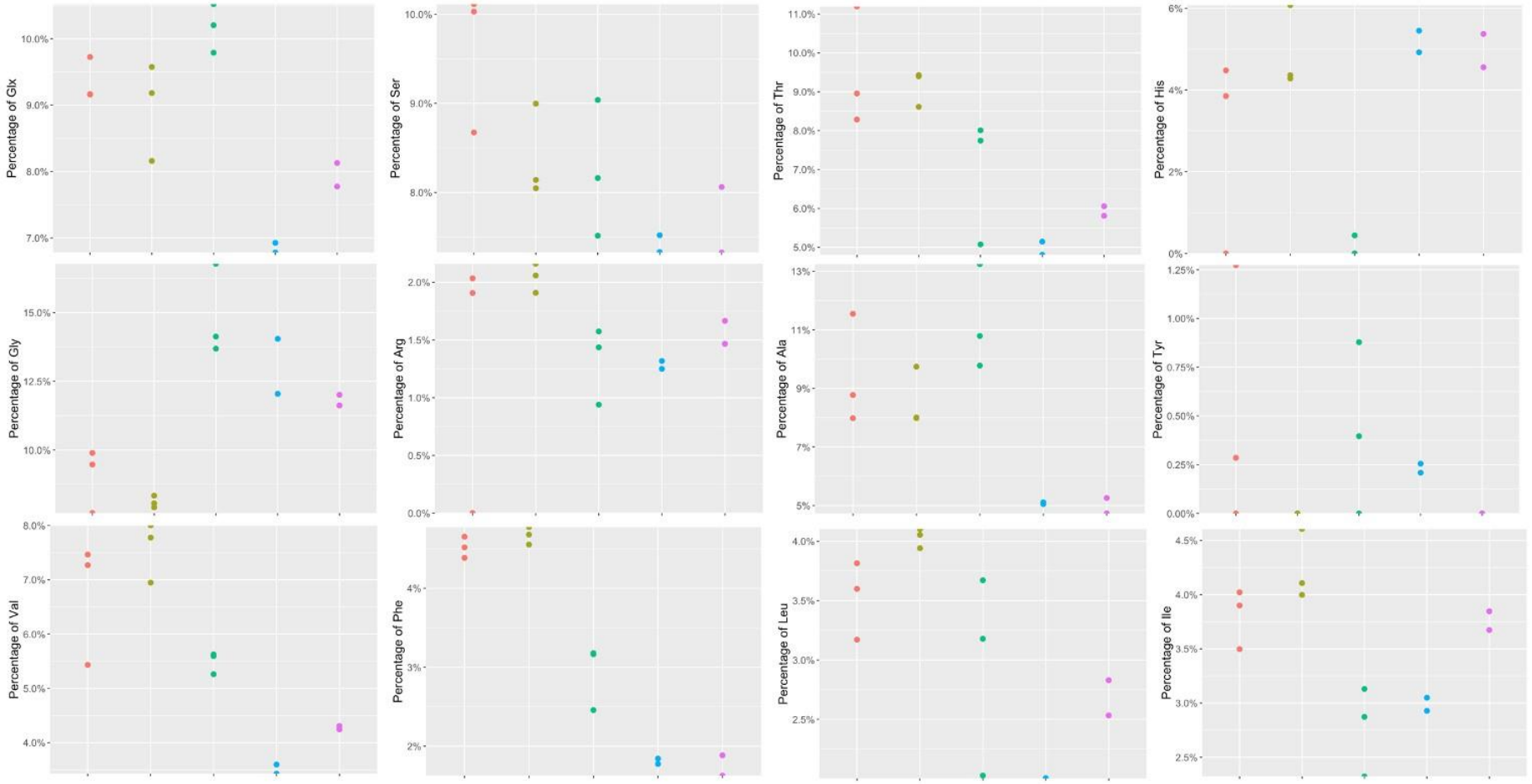

Figure 7.10 Concentration of amino acids for scleractinia internal heterogeneity replicate data, colour corresponds to the sample found within section 3.5.2